

EFFECT OF 1,2-DIPALMITOYL-SN-GLYCERO-3-
PHOSPHOETHANOLAMINE (DPPE)-PEG2000 AND 1,2-
DIPALMITOYL-SN-GLYCERO-3-PHOSPHOETHANOLAMINE
(DPPE)-PEG5000 ON FATTY ACID NANOLIPOSOMES AND
THEIR LANGMUIR MONOLAYER

TEO YIN YIN

FACULTY OF SCIENCE
UNIVERSITY OF MALAYA
KUALA LUMPUR

2012

EFFECT OF 1,2-DIPALMITOYL-SN-GLYCERO-3-
PHOSPHOETHANOLAMINE (DPPE)-PEG2000 AND 1,2-
DIPALMITOYL-SN-GLYCERO-3-PHOSPHOETHANOLAMINE
(DPPE)-PEG5000 ON FATTY ACID NANOLIPOSOMES AND
THEIR LANGMUIR MONOLAYER

TEO YIN YIN

THESIS SUBMITTED IN FULFILLMENT OF
THE REQUIREMENT FOR THE DEGREE
OF DOCTOR OF PHILOSOPHY

DEPARTMENT OF CHEMISTRY
FACULTY OF SCIENCE
UNIVERSITY OF MALAYA
KUALA LUMPUR

2012

UNIVERSITI MALAYA

ORIGINAL LITERARY WORK DECLARATION

Name of Candidate: **TEO YIN YIN**

(I.C/Passport No: **790721-14-5576**)

Registration/Matric No: **SHC 060034**

Name of Degree: **DOCTOR OF PHILOSOPHY**

Title of Project Paper/Research Report/Dissertation/Thesis ("this Work"):

EFFECT OF 1,2-DIPALMITOYL-SN-GLYCERO-3-PHOSPHO-ETHANOLAMINE (DPPE)-PEG2000 AND 1,2-DIPALMITOYL-SN-GLYCERO-3-PHOSPHOETHANOLAMINE (DPPE)-PEG5000 ON FATTY ACID NANOLIPOSOMES AND THEIR LANGMUIR MONOLAYER

Field of Study: **BIOCOLLOID**

I do solemnly and sincerely declare that:

- (1) I am the sole author/writer of this Work;
- (2) This Work is original;
- (3) Any use of any work in which copyright exists was done by way of fair dealing and for permitted purposes and any except or extract from, or reference to or reproduction of any copyright work has been disclosed expressly and sufficiently and the title of the Work and its authorship have been acknowledged in this Work;
- (4) I do not have any actual knowledge nor do I ought reasonably to know that the making of this work constitutes an infringement of any copyright work;
- (5) I hereby assign all and every rights in the copyright to this Work to the University of Malaya ("UM"), who henceforth shall be owner of the copyright in this Work and that any reproduction or use in any form or by any means whatsoever is prohibited without the written consent of UM having been first had and obtained;
- (6) I am fully aware that if in the course of making this Work I have infringed any copyright whether intentionally or otherwise, I may be subject to legal action or any other action as may be determined by UM.

Candidate's Signature

Date: **30 JULY 2012**

Subscribed and solemnly declared before,

Witness's Signature

Date: **30 JULY 2012**

Name: **PROF. DR. MISNI MISRAN**

Designation: **LECTURER**

ABSTRACT

Liposome is an artificial colloidal particle that formed from convolution of bilayer structure from amphiphilic molecules into a spherical particle. At certain pH, the presence of both ionized and non-ionized fatty acid molecules in the solution leads to the formation of dimers that can be an analog to the double chain phospholipids. Fatty acid liposomes provide both hydrophilic and hydrophobic compartments that make them suitable candidates as a carrier for water soluble and liposoluble substances that have potential for medicinal or cosmetic applications. Unmodified fatty acid liposome suspensions are normally unstable and it needs to be addressed so that it is more viable for useful applications. The widely applied method in stabilizing of liposome is through steric stabilization. In this study, polyethoxylated groups with different polymerization degree grafted to phospholipids namely 1,2-dipalmitoyl-*sn*-glycero-3-phosphoethanolamine-N-[methoxy(polyethylene glycol)2000] and 1,2-dipalmitoyl-*sn*-glycero-3-phosphoethanolamine-N-[methoxy(polyethylene glycol)5000] were incorporated in fatty acid liposome to improve their stability. The stability of fatty acid/PEGylated lipid liposomes was characterized by their critical vesiculation concentration, mean particle size and zeta potential for a period of 30 days. The presence of liposomes was identified by transmission electron micrograph. It was found that the stability of fatty acid liposomes can be enhanced with incorporation of PEGylated lipid. Langmuir monolayer isotherm was used for the intermolecular interaction study, and the most compatible mixture proportion of fatty acid to PEGylated lipid for the formation of a stable liposome suspension was proposed accordingly. The energetically favorable composition of a resulting mixture was found varied slightly depending on the type of PEGylated lipid. The loading efficiencies of these liposomes were assessed by both water soluble calcein as well as water insoluble α -tocopherol acetate. Certain amount of these compounds could be successfully loaded into the resulting liposomes under this experimental condition. As for a fixed fatty acid concentration, the loading efficiency was found to be affected by the type of fatty acid, bilayer composition and the amount of calcein and α -tocopherol acetate.

Keywords: fatty acid liposome, PEGylated lipid, monolayer

ABSTRAK

Liposome ialah sejenis zarah koloid buatan yang dihasilkan oleh molekul-molekul amphiphilic yang menyusun menjadi dua lapisan dan seterusnya membelit menjadi zarah sfera. Pada pH tertentu, kehadiran kedua-dua jenis molekul asid lemak terion dan bukan terion dalam satu larutan menyebabkan pembentukan dimer yang menjadi analog kepada molekul phospholipid yang mempunyai dua rantai hidrokarbon. Liposome yang diperbuat daripada asid lemak juga mempunyai dua ruangan yang menjadikannya berpotensi sebagai pengangkut kepada bahan larut air dan larut minyak untuk aplikasi perubatan atau kosmetik. Biasanya liposome asid lemak adalah tidak stabil dalam suatu larutan. Masalah ini perlu diatasi agar menjadikannya lebih sesuai untuk pelbagai kegunaan. Kaedah yang digunakan secara meluas untuk menstabilkan liposome dalam suatu larutan ialah melalui penstabilan steric. Dalam kajian ini, kumpulan polyethoxylated yang mempunyai darjah pempolimeran yang berlainan dan dicantumkan kepada phospholipid iaitu 1,2-dipalmitoyl-*sn*-glycero-3-phosphoethanolamine-N-[methoxy(polyethylene glycol)2000] and 1,2-dipalmitoyl-*sn*-glycero-3-phosphoethanolamine-N-[methoxy(polyethylene glycol)5000] telah digunakan dalam penghasilan liposome asid lemak agar meningkatkan kestabilannya. Kestabilan liposome asid lemak yang mempunyai PEGylated lipid telah dikaji dengan melalui kepekatan kritikal pembentukan liposome, min saiz zarah dan keupayaan zeta selama 30 hari. Kehadiran liposome dalam larutan telah dikenal pasti oleh transmisi elektron mikroskop. Daripada hasil kajian, kestabilan liposome asid lemak boleh dipertingkatkan dengan kehadiran PEGylated lipid. Isotherm Langmuir satu lapisan molekul telah digunakan untuk kajian interaksi antara molekul. Campuran asid lemak dan PEGylated lipid yang paling sesuai untuk pembentukan liposome telah dicadangkan. Komposisi yang mempunyai tenaga bebas yang paling negatif didapati bergantung kepada jenis PEGylated lipid yang digunakan. Keberkesanan muatan liposome telah dikaji dengan memasukkan calcein dan α -tocopherol acetate. Sejumlah tertentu bahan tersebut telah berjaya dimasukkan ke dalam liposome di bawah keadaan kajian ini. Bagi kepekatan asid lemak yang tetap, keberkesanan muatan didapati bergantung kepada jenis asid lemak yang digunakan, komposisi dua lapisan yang menghasilkan liposome dan jumlah calcein atau α -tocopherol acetate yang digunakan.

Kata kunci: liposome asid lemak, PEGylated lipid, molekul satu lapisan

ACKNOWLEDGEMENT

I wish to express my highest gratitude to my supervisor, Professor Dr. Misni Misran for his support, guidance and encouragement throughout my studies. I would also like to thank him for his patience in correcting and improving the previous draft of this thesis. He is always available when I needed his advice.

I am deeply grateful to the fellowship sponsored by both Ministry of Higher Education Malaysia and University Malaya. Special thanks to Ministry of Science, Technology and Innovation, Malaysia for the financial support and funding this project. I would also extend my gratitude to all my labmates who have been cheered me up throughout this study.

Since this acknowledgement section is too brief to adequately express my gratitude to everybody, I hope that those not mentioned here will be able to forgive me and trust that the lack of mention should not be translated into lack of gratitude.

I would like to convey my special thanks to my family for having rendered me enormous support during the whole tenure of my research. My parents never pressured me about school and yet they managed to instill in me the need to become a well-educated person. Last but not least, I would like to express my deepest appreciation to my husband Mr. Low Kah Hin for being there whenever I need help. Without them none of this would be possible.

TABLE OF CONTENTS	Page
ABSTRACT (English)	ii
ABSTRAK (Malay)	iii
ACKNOWLEDGEMENTS	iv
TABLE OF CONTENTS	v
LIST OF FIGURES	viii
LIST OF TABLES	xvi
LIST OF SYMBOLS AND ABBREVIATIONS	xvii
LIST OF PUBLICATIONS	xix

Chapter 1: INTRODUCTION TO LIPOSOME

1.1	Background of liposome	1
1.2	Structure and shape of aggregates	3
1.3	Morphology and liposome size	5
1.4	Similarities between fatty acid liposomes and phospholipid liposomes	6
1.5	Differences between fatty acid liposomes and phospholipid liposomes	7
1.6	Preparation of fatty acid liposome	8
1.7	Stability of fatty acid liposomes	10
1.7.1	Sterically stabilized liposomes	12
1.7.2	Langmuir monolayer	15
1.8	Effect of fatty acid on human health	16
1.9	Applications of liposomes	17
1.10	Objectives of research	19
1.11	References	20

Chapter 2: LITERATURE REVIEW

2.1	Fatty acid liposomes	25
2.2	Aggregation number of fatty acid liposomes	26
2.3	Characterization fatty acid liposomes	30
2.3.1	pH equilibrium plot	30
2.2.2	Determination of critical vesiculation concentration (CVC)	32
2.2.3	Transmission electron micrograph	33

	Page
2.2.4	Stability of fatty acid liposomes 34
2.3	Characterization of stability in fatty acid liposomes 37
2.4	Encapsulation of hydrophilic and hydrophobic materials in fatty acid liposomes 43
2.5	Separation of encapsulated substance in liposomes from non-encapsulated substance 46
2.6	References 48

Chapter 3: MATERIALS AND METHODS

3.1	Materials 54
3.1.1	Introduction 54
3.1.2	Surfactants 54
3.1.3	Chemicals 55
3.1.4	Solvents 56
3.2	Instrumentation 56
3.2.1	Particle size 56
3.2.1.1	Dynamic light scattering 56
3.2.1.2	Operation of DLS for size measurement 59
3.2.2	Zeta potential 59
3.2.2.1	Electrophoretic mobility 60
3.2.2.2	Operation of zetasizer for zeta potential measurement 61
3.2.3	Langmuir monolayer 63
3.2.3.1	Π -A isotherm 64
3.3	Methods 67
3.3.1	Preparation of 0.25 M borate buffer pH 8.5 67
3.3.2	Preparation of 0.50 M phosphate buffer buffer pH 7.0 67
3.3.3	Preparation of stock solution 68
3.3.4	Titration of the stock solution with HCl 68
3.3.5	Transmission electron microscopy 69
3.3.6	Determinations of critical vesiculation concentration (CVC) 69
3.3.7	Particle size measurement 70
3.3.8	Zeta potential measurement 70
3.3.9	Langmuir monolayer analysis 71

	Page
3.3.9.1 Analysis of Langmuir monolayer isotherm	73
3.3.10 Loading efficiency of liposome	76
3.3.10.1 Encapsulation of calcein	76
3.3.10.2 Encapsulation of DL- α -tocopherol acetate (VE)	76
3.3.10.3 Separation method	77
3.3.10.4 Determination of loading efficiency	80
3.4 References	81
 Chapter 4: RESULTS AND DISCUSSION	
4.1 Titration curve	82
4.2 Critical vesiculation concentration (CVC)	91
4.3 Stability of fatty acid liposomes	98
4.3.1 Particle size	98
4.3.2 Zeta potential	106
4.4 Transmission electron micrographs	111
4.5 Encapsulation of calcein and DL- α -tocopherol acetate (VE)	115
4.5.1 Separation method by size exclusion chromatography vs ultrafiltration	115
4.5.2 Encapsulation of calcein	118
4.5.4 Encapsulation of VE	124
4.6 Langmuir monolayer analysis	130
4.6.1 Langmuir monolayer for mixture of fatty acid and PEGylated lipids	130
4.6.2 Langmuir monolayer for mixture of fatty acid PEGylated lipids VE	162
4.6.3 Application of monolayer studies in liposome formulation	196
4.7 References	197
 Chapter 5: Conclusion	
5.0 Conclusions	200
5.1 Future works	205
 Appendix	

LIST OF FIGURES

Figure	Title	Page
1.1	A schematic illustration of different types of liposomes. The lines represent the bilayers of the liposomes which are not drawn to scale.	6
2.1	A 3-D bar chart of total fatty acid monomer in a liposome with respect to their particle size and effective area per head group with $l_b = 3.5$ nm.	29
2.2	A proposed pathway of liposome formation by hydration method.	45
3.1	Molecular structure of (a) DPPE-PEG2000 and (b) DPPE-PEG5000.	55
3.2	Schematic representation of zeta potential.	60
3.3	Schematic of zeta potential measurement route.	63
3.4	A schematic representing partially Wilhelmy plate immersed in subphase.	64
3.5	A schematic representing Π - A isotherm.	66
3.6	Transformation of molecular orientation upon compression of Langmuir monolayer.	67
3.7	Langmuir monolayer isotherm of stearic acid on deionized water as the subphase at 25.0 °C.	72
3.8	Separation of calcein by using (a) size exclusion chromatography and (b) ultrafiltration methods.	79
4.1	Equilibrium titration curve for (12.50 ± 0.05) mM (a) palmitoleic acid and (b) oleic acid with their mixture solutions at 28 °C. ■ pure fatty acid, ■ FA+Lecinol S-10, ◇ FA + DPPE-PEG2000, △ FA + DPPE-PEG2000 + Lecinol S-10, ○ FA + DPPE-PEG5000, ☆ FA+ DPPE-PEG5000 + Lecinol S-10.	85
4.2	Equilibrium titration curve for (12.50 ± 0.05) mM (a) linoleic acid and (b) linolenic acid with their mixture solutions at 28 °C. ■ pure fatty acid, ■ FA+Lecinol S-10, ◇ FA + DPPE-PEG2000, △ FA + DPPE-PEG2000 + Lecinol S-10, ○ FA + DPPE-PEG5000, ☆ FA+ DPPE-PEG5000 + Lecinol S-10.	86
4.3	Changes of mean particle size with respect to pH for (a) palmitoleic acid and (b) oleic acid with their mixture solutions at 30 °C. ■ pure fatty acid, ■ FA+Lecinol S-10, ◇ FA + DPPE-PEG2000, △ FA + DPPE-PEG2000 + Lecinol S-10, ○ FA + DPPE-PEG5000, ☆ FA+ DPPE-PEG5000 + Lecinol S-10.	87

Figure	Title	Page
4.4	Changes of mean particle size with respect to pH for (a) linoleic acid and (b) linolenic acid with their mixture solutions at 30 °C. ■ pure fatty acid, ▣ FA+Lecinol S-10, ◇ FA + DPPE-PEG2000, △ FA + DPPE-PEG2000 + Lecinol S-10, ○ FA + DPPE-PEG5000, ☆ FA+DPPE-PEG5000 + Lecinol S-10.	88
4.5	Changes of mean zeta potential for (a) palmitoleic acid and (b) oleic acid with their mixture solutions as a fuction of pH at 30 °C. ■ pure fatty acid, ▣ FA+Lecinol S-10, ◇ FA + DPPE-PEG2000, △ FA + DPPE-PEG2000 + Lecinol S-10, ○ FA + DPPE-PEG5000, ☆ FA+DPPE-PEG5000 + Lecinol S-10.	89
4.6	Changes of mean zeta potential for (a) linoleic acid and (b) linolenic acid with their mixture solution as a function of pH at 30 °C. ■ pure fatty acid, ▣ FA+Lecinol S-10, ◇ FA + DPPE-PEG2000, △ FA + DPPE-PEG2000 + Lecinol S-10, ○ FA + DPPE-PEG5000, ☆ FA+DPPE-PEG5000 + Lecinol S-10.	90
4.7	Variation in mean surface tension for different concentration of (a) palmitoleic acid solution and their mixtures with (b) Lecinol S-10, (c) DPPE-PEG2000, (d) DPPE-PEG2000-Lecinol S-10, (e) DPPE-PEG5000 and (f) DPPE-PEG5000-Lecinol S-10 at 20.0 °C to 40.0 °C. ■ = 20 °C, ▣ = 25 °C, ◇ = 30 °C, △ = 35 °C and ☆ = 40 °C. Error bars indicate S.D. for $N = 5$.	92
4.8	Variation in mean surface tension for different concentration of (a) oleic acid solution and their mixtures with (b) Lecinol S-10, (c) DPPE-PEG2000, (d) DPPE-PEG2000-Lecinol S-10, (e) DPPE-PEG5000 and (f) DPPE-PEG5000-Lecinol S-10 at 20.0 °C to 40.0 °C. ■ = 20 °C, ▣ = 25 °C, ◇ = 30 °C, △ = 35 °C and ☆ = 40 °C. Error bars indicate S.D. for $N = 5$.	93
4.9	Variation in mean surface tension for different concentration of (a) linoleic acid solution and their mixtures with (b) Lecinol S-10, (c) DPPE-PEG2000, (d) DPPE-PEG2000-Lecinol S-10, (e) DPPE-PEG5000 and (f) DPPE-PEG5000-Lecinol S-10 at 20.0 °C to 40.0 °C. ■ = 20 °C, ▣ = 25 °C, ◇ = 30 °C, △ = 35 °C and ☆ = 40 °C. Error bars indicate S.D. for $N = 5$.	94
4.10	Variation in mean surface tension for different concentration of (a) linolenic acid solution and their mixtures with (b) Lecinol S-10, (c) DPPE-PEG2000, (d) DPPE-PEG2000-Lecinol S-10, (e) DPPE-PEG5000 and (f) DPPE-PEG5000-Lecinol S-10 at 20.0 °C to 40.0 °C. ■ = 20 °C, ▣ = 25 °C, ◇ = 30 °C, △ = 35 °C and ☆ = 40 °C. Error bars indicate S.D. for $N = 5$.	95

Figure	Title	Page
4.11	CVC at 30 °C as a function of C18 fatty acid mixtures. ■ pure fatty acid, ▣ FA+Lecinol S-10, ◇ FA + DPPE-PEG2000, △ FA + DPPE-PEG2000 + Lecinol S-10, ○ FA + DPPE-PEG5000, ☆ FA+ DPPE-PEG5000 + Lecinol S-10.	98
4.12	Mean particle size of (a) palmitoleate-palmitoleic acid liposome and (b) oleate-oleic acid liposome with their mixture for a period of 30 days at 30 °C. ■ pure fatty acid, ▣ FA+Lecinol S-10, ◇ FA + DPPE-PEG2000, △ FA + DPPE-PEG2000 + Lecinol S-10, ○ FA + DPPE-PEG5000, ☆ FA+ DPPE-PEG5000 + Lecinol S-10. Error bars indicate the 95% confidence interval.	102
4.13	Mean particle size of (a) linoleate-linoleic acid liposome and (b) linolenate-linolenic acid liposome with their mixture for a period of 30 days at 30 °C. ■ pure fatty acid, ▣ FA+Lecinol S-10, ◇ FA + DPPE-PEG2000, △ FA + DPPE-PEG2000 + Lecinol S-10, ○ FA + DPPE-PEG5000, ☆ FA+ DPPE-PEG5000 + Lecinol S-10. Error bars indicate the 95% confidence interval.	103
4.14	Optical polarizing micrograph of 2 mM palmitoleate-palmitoleic acid-DPPE-PEG5000-Lecinol S-10 liposome at pH 8.5 after 30 days of storage.	106
4.15	Mean zeta potential of (a) palmitoleate-palmitoleic acid liposome and (b) oleate-oleic acid liposome with their mixture for a period of 30 days at 30 °C. ■ pure fatty acid, ▣ FA+Lecinol S-10, ◇ FA + DPPE-PEG2000, △ FA + DPPE-PEG2000 + Lecinol S-10, ○ FA + DPPE-PEG5000, ☆ FA+ DPPE-PEG5000 + Lecinol S-10. Error bars indicate the 95% confidence interval.	108
4.16	Mean zeta potential of (a) linoleate-linoleic acid liposome and (b) linolenate-linolenic acid with their mixture for a period of 30 days at 30 °C. ■ pure fatty acid, ▣ FA+Lecinol S-10, ◇ FA + DPPE-PEG2000, △ FA + DPPE-PEG2000 + Lecinol S-10, ○ FA + DPPE-PEG5000, ☆ FA+ DPPE-PEG5000 + Lecinol S-10. Error bars indicate the 95% confidence interval.	109
4.17	Relationship of electron phase density contrast in the final image of TEM with the distance of electron beam travelling through liposome.	112
4.18	TEM micrographs of (a) palmitoleate-palmitoleic acid liposome, (b*) oleate-oleic acid-DPPE-PEG2000 liposome, (c*) palmitoleate-palmitoleic acid-DPPE-PEG2000 liposome, (d*) oleate-oleic acid-DPPE-PEG5000 liposome, (e) palmitoleate-palmitoleic acid-Lecinol S-10-DPPE-PEG2000 liposome and (f*) oleate-oleic acid-Lecinol S-10 liposome. Arrows indicate the liposome, * = EFTEM micrograph.	113

Figure	Title	Page
4.19	TEM micrographs of (a) linoleate-linoleic acid liposome, (b) oleate-oleic acid-Lecinol S-10-DPPE-PEG2000 liposome, (c) linoleate-linoleic acid-DPPE-PEG2000 liposome, (d) linolenate-linolenic acid liposome, (e) linoleate-linoleic acid-DPPE-PEG5000 liposome and (f*) linolenate-linolenic acid-DPPE-PEG2000 liposome. Arrows indicate the liposome.	114
4.20	Separation of (a) calcein and (b) VE loaded in oleate-oleic acid-DPPE-PEG2000 liposome from the respective free molecules by size exclusion chromatography.	116
4.21	Loaded amount of substance in liposome with respect to the total amount of fatty acid. Solid line indicates experimental result while dotted line indicates the expected result as a function of added substance.	117
4.22	Effect of calcein amount on loading efficiency of fatty acid liposomes.	119
4.23	Amount of calcein loaded in (a) palmitoleate-palmitoleic acid liposome and (b) oleate-oleic acid liposome with respect to the total amount of fatty acid. ■ indicates only acid liposome, ● represents mixture of DPPE-PEG2000-fatty acid liposomes, ▲ represents mixture of DPPE-PEG5000-fatty acid liposomes.	121
4.24	Amount of calcein loaded in (a) linoleate-linoleic acid liposome and (b) linolenate-linolenic acid liposome with respect to the total amount of fatty acid. ■ indicates only fatty acid liposome, ● represents mixture of DPPE-PEG2000-fatty acid liposomes, ▲ represents mixture of DPPE-PEG5000-fatty acid liposomes.	122
4.25	Loading efficiency of (a) $n_{Cal}/n_{FA} = 0.12$ and (b) $n_{VE}/n_{FA} = 0.16$ in fatty acid liposome and their mixture at pH 8.5. ■ pure fatty acid, ▣ FA+Lecinol S-10, ◇ FA + DPPE-PEG2000, △ FA + DPPE-PEG2000 + Lecinol S-10, ○ FA + DPPE-PEG5000, ☆ FA+ DPPE-PEG5000 + Lecinol S-10.	123
4.26	Amount of VE loaded in PEGylated and pure (a) palmitoleate-palmitoleic acid liposome and (b) oleic-oleate acid liposome with respect to the total amount of fatty acid. ■ indicates pure fatty acid liposome, ● represents mixture of DPPE-PEG2000-fatty acid liposomes, ▲ represents mixture of DPPE-PEG5000-fatty acid liposomes.	128
4.27	Amount of VE loaded in PEGylated and pure (a) linoleate- linoleic acid liposome and (b) linolenic-linolenate acid liposome with respect to the total amount of fatty acid. ■ = pure fatty acid liposome, ● = mixture of DPPE-PEG2000-fatty acid liposomes, ▲ = mixture of DPPE-PEG5000- fatty acid liposomes.	129

Figure	Title	Page
4.28	Π - A isotherm of DPPE-PEG2000 and DPPE-PEG5000 at 25 °C on 50 mM phosphate buffer subphase. The inset shows compression modulus (C_s^{-1}) for the monolayer as a function of surface pressure. Solid line indicates DPPE-PEG2000 while dashed line for DPPE-PEG5000.	132
4.29	Conformation of short and long PEGylated lipid at surface pressure (a) lower than 5 mN m ⁻¹ and (b) higher than 5 mN m ⁻¹ .	133
4.30	Surface pressure–area (Π - A) isotherms of (a) palmitoleic acid, (b) oleic acid, (c) linoleic acid and (d) linolenic acid mixed with DPPE-PEG2000 at the air-aqueous interface at 25 °C.	135
4.31	Surface pressure–area (Π - A) isotherms of (a) palmitoleic acid, (b) oleic acid, (c) linoleic acid and (d) linolenic acid mixed with DPPE-PEG5000 at the air-aqueous interface at 25 °C.	136
4.32	Π - A isotherm of linolenic acid monolayer at 25 °C on a 50 mM phosphate buffer pH 7 subphase.	137
4.33	Compression modulus (C_s^{-1}) of (a) palmitoleic acid, (b) oleic acid, (c) linoleic acid and (d) linolenic acid mixed monolayer with DPPE-PEG2000 at 25 °C.	140
4.34	Compression modulus (C_s^{-1}) of (a) palmitoleic acid, (b) oleic acid, (c) linoleic acid and (d) linolenic acid mixed monolayer with DPPE-PEG5000 at 25 °C.	141
4.35	Area per molecule as a function of composition for mixed monolayer of (a) palmitoleic acid, (b) oleic acid, (c) linoleic acid and (d) linolenic acid with DPPE-PEG2000 at surface pressure ■ = 5 mN m ⁻¹ , □ = 10 mN m ⁻¹ , ▲ = 15 mN m ⁻¹ , △ = 20 mN m ⁻¹ , ★ = 25 mN m ⁻¹ , ☆ = 30 mN m ⁻¹ .	143
4.36	Area per molecule as a function of composition for mixed monolayer of (a) palmitoleic acid, (b) oleic acid, (c) linoleic acid and (d) linolenic acid with DPPE-PEG5000 at surface pressure ■ = 5 mN m ⁻¹ , □ = 10 mN m ⁻¹ , ▲ = 15 mN m ⁻¹ , △ = 20 mN m ⁻¹ , ★ = 25 mN m ⁻¹ , ☆ = 30 mN m ⁻¹ .	144
4.37	A_{exc}/A_{id} for mixed monolayer of (a) palmitoleic acid, (b) oleic acid, (c) linoleic acid and (d) linolenic acid as a function of $X_{DPPE-PEG2000}$ at 25 °C at surface pressure ■ = 5 mN m ⁻¹ , □ = 10 mN m ⁻¹ , ▲ = 15 mN m ⁻¹ , △ = 20 mN m ⁻¹ , ★ = 25 mN m ⁻¹ , ☆ = 30 mN m ⁻¹ .	147

Figure	Title	Page
4.38	$A_{\text{exc}}/A_{\text{id}}$ for mixed monolayer of (a) palmitoleic acid, (b) oleic acid, (c) linoleic acid and (d) linolenic acid as a function of $X_{\text{DPPE-PEG5000}}$ at 25 °C at surface pressure ■ = 5 mN m ⁻¹ , □ = 10 mN m ⁻¹ , ▲ = 15 mN m ⁻¹ , △ = 20 mN m ⁻¹ , ★ = 25 mN m ⁻¹ , ☆ = 30 mN m ⁻¹ .	148
4.39	Compression modulus (C_s^{-1}) for mixed monolayer of (a) palmitoleic acid, (b) oleic acid, (c) linoleic acid and (d) linolenic acid as a function of $X_{\text{DPPE-PEG2000}}$ at 25 °C and surface pressure ■ = 5 mN m ⁻¹ , □ = 10 mN m ⁻¹ , ▲ = 15 mN m ⁻¹ , △ = 20 mN m ⁻¹ , ★ = 25 mN m ⁻¹ , ☆ = 30 mN m ⁻¹ .	151
4.40	Compression modulus (C_s^{-1}) for mixed monolayer of (a) palmitoleic acid, (b) oleic acid, (c) linoleic acid and (d) linolenic acid as a function of $X_{\text{DPPE-PEG5000}}$ at 25 °C and surface pressure ■ = 5 mN m ⁻¹ , □ = 10 mN m ⁻¹ , ▲ = 15 mN m ⁻¹ , △ = 20 mN m ⁻¹ , ★ = 25 mN m ⁻¹ , ☆ = 30 mN m ⁻¹ .	152
4.41	The general trend of C_s^{-1} as a function of mole fraction PEGylated lipid.	154
4.42	Excess Gibbs free energy (ΔG_{exc}) for mixed monolayer of (a) palmitoleic acid, (b) oleic acid, (c) linoleic acid and (d) linolenic acid as a function of $X_{\text{DPPE-PEG2000}}$ at 25 °C and surface pressure ■ = 5 mN m ⁻¹ , □ = 10 mN m ⁻¹ , ▲ = 15 mN m ⁻¹ , △ = 20 mN m ⁻¹ , ★ = 25 mN m ⁻¹ , ☆ = 30 mN m ⁻¹ .	160
4.43	Excess Gibbs free energy (ΔG_{exc}) for mixed monolayer of (a) palmitoleic acid, (b) oleic acid, (c) linoleic acid and (d) linolenic acid as a function of $X_{\text{DPPE-PEG5000}}$ at 25 °C and surface pressure ■ = 5 mN m ⁻¹ , □ = 10 mN m ⁻¹ , ▲ = 15 mN m ⁻¹ , △ = 20 mN m ⁻¹ , ★ = 25 mN m ⁻¹ , ☆ = 30 mN m ⁻¹ .	161
4.44	Surface pressure–area (Π – A) isotherm of VE monolayer on a 50 mM phosphate buffer pH 7 at 25 °C. The inset showed the C_s^{-1} as a function of surface pressure for VE.	162
4.45	Surface pressure–area (Π – A) isotherms for mixed monolayer of VE with (a) palmitoleic acid, (b) oleic acid, (c) linoleic acid and (d) linolenic acid at air-aqueous interface at 25 °C.	164
4.46	Surface pressure–area (Π – A) isotherms for mixed monolayer of VE/2 % DPPE-PEG2000 with (a) palmitoleic acid, (b) oleic acid, (c) linoleic acid and (d) linolenic acid at the air-aqueous interface at 25 °C.	165

Figure	Title	Page
4.47	Surface pressure–area (Π – A) isotherms for mixed monolayer of VE/2 % DPPE-PEG5000 with (a) palmitoleic acid, (b) oleic acid, (c) linoleic acid and (d) linolenic acid at the air-aqueous interface at 25 °C.	166
4.48	Compression modulus (C_s^{-1}) for mixed monolayer of VE with (a) palmitoleic acid, (b) oleic acid, (c) linoleic acid and (d) linolenic acid at air-aqueous interface at 25 °C.	168
4.49	Compression modulus (C_s^{-1}) for mixed monolayer of VE/2 % DPPE-PEG2000 with (a) palmitoleic acid, (b) oleic acid, (c) linoleic acid and (d) linolenic acid at the air-aqueous interface at 25 °C.	169
4.50	Compression modulus (C_s^{-1}) for mixed monolayer of VE/2 % DPPE-PEG5000 with (a) palmitoleic acid, (b) oleic acid, (c) linoleic acid and (d) linolenic acid at the air-aqueous interface at 25 °C.	170
4.51	Area per molecule as a function of mole fraction X_{VE} in monolayer of (a) palmitoleic acid, (b) oleic acid, (c) linoleic acid and (d) linolenic acid at the air-aqueous interface at 25 °C and surface pressure ■ = 5 mN m ⁻¹ , □ = 10 mN m ⁻¹ , ▲ = 15 mN m ⁻¹ .	172
4.52	Area per molecule as a function of mole fraction X_{VE} in monolayer of 2 % DPPE-PEG2000 with (a) palmitoleic acid, (b) oleic acid, (c) linoleic acid and (d) linolenic acid at the air-aqueous interface at 25 °C and surface pressure ■ = 5 mN m ⁻¹ , □ = 10 mN m ⁻¹ , ▲ = 15 mN m ⁻¹ .	173
4.53	Area per molecule as a function of mole fraction X_{VE} in monolayer of 2 % DPPE-PEG5000 with (a) palmitoleic acid, (b) oleic acid, (c) linoleic acid and (d) linolenic acid at the air-aqueous interface at 25 °C and surface pressure ■ = 5 mN m ⁻¹ , □ = 10 mN m ⁻¹ , ▲ = 15 mN m ⁻¹ .	174
4.54	A_{exc}/A_{id} as a function of mole fraction X_{VE} in monolayer of (a) palmitoleic acid, (b) oleic acid, (c) linoleic acid and (d) linolenic acid at the air-aqueous interface at 25 °C and surface pressure ■ = 5 mN m ⁻¹ , □ = 10 mN m ⁻¹ , ▲ = 15 mN m ⁻¹ .	180
4.55	A_{exc}/A_{id} as a function of mole fraction X_{VE} in monolayer of 2 % DPPE-PEG2000 with (a) palmitoleic acid, (b) oleic acid, (c) linoleic acid and (d) linolenic acid at the air-aqueous interface at 25 °C and surface pressure ■ = 5 mN m ⁻¹ , □ = 10 mN m ⁻¹ , ▲ = 15 mN m ⁻¹ .	181
4.56	A_{exc}/A_{id} as a function of mole fraction X_{VE} in monolayer of 2 % DPPE-PEG5000 with (a) palmitoleic acid, (b) oleic acid, (c) linoleic acid and (d) linolenic acid at the air-aqueous interface at 25 °C and surface pressure ■ = 5 mN m ⁻¹ , □ = 10 mN m ⁻¹ , ▲ = 15 mN m ⁻¹ .	182

Figure	Title	Page
4.57	Compression modulus (C_s^{-1}) as a function of mole fraction VE (X_{VE}) in (a) palmitoleic acid, (b) oleic acid, (c) linoleic acid and (d) linolenic acid monolayer at the air-aqueous interface at 25 °C and surface pressure ■ = 5 mN m ⁻¹ , □ = 10 mN m ⁻¹ , ▲ = 15 mN m ⁻¹ .	186
4.58	Compression modulus (C_s^{-1}) as a function of mole fraction VE (X_{VE}) in monolayer of 2 % DPPE-PEG2000 with (a) palmitoleic acid, (b) oleic acid, (c) linoleic acid and (d) linolenic acid at the air-aqueous interface at 25 °C and surface pressure ■ = 5 mN m ⁻¹ , □ = 10 mN m ⁻¹ , ▲ = 15 mN m ⁻¹ .	187
4.59	Compression modulus (C_s^{-1}) as a function of mole fraction VE (X_{VE}) in monolayer of 2 % DPPE-PEG5000 with (a) palmitoleic acid, (b) oleic acid, (c) linoleic acid and (d) linolenic acid at the air-aqueous interface at 25 °C and surface pressure ■ = 5 mN m ⁻¹ , □ = 10 mN m ⁻¹ , ▲ = 15 mN m ⁻¹ .	188
4.60	Surface excess energy (ΔG_{exc}) as a function of mole fraction VE (X_{VE}) in (a) palmitoleic acid, (b) oleic acid, (c) linoleic acid and (d) linolenic acid monolayer at the air-aqueous interface at 25 °C and surface pressure ■ = 5 mN m ⁻¹ , □ = 10 mN m ⁻¹ , ▲ = 15 mN m ⁻¹ .	193
4.61	Surface excess energy (ΔG_{exc}) as a function of mole fraction VE (X_{VE}) in monolayer of 2 % DPPE-PEG2000 with (a) palmitoleic acid, (b) oleic acid, (c) linoleic acid and (d) linolenic acid at the air-aqueous interface at 25 °C and surface pressure ■ = 5 mN m ⁻¹ , □ = 10 mN m ⁻¹ , ▲ = 15 mN m ⁻¹ .	194
4.62	Surface excess energy (ΔG_{exc}) as a function of mole fraction VE (X_{VE}) in monolayer of 2 % DPPE-PEG5000 with (a) palmitoleic acid, (b) oleic acid, (c) linoleic acid and (d) linolenic acid at the air-aqueous interface at 25 °C and surface pressure ■ = 5 mN m ⁻¹ , □ = 10 mN m ⁻¹ , ▲ = 15 mN m ⁻¹ .	195

LIST OF TABLES

Table	Title	Page
1.1	The type of hydrophilic head group commonly found in surfactant.	3
2.1	Bilayer thickness of fatty acid.	27
4.1	The pka for fatty acid and their mixture with PEGylated lipid and Lecinol S-10.	83
4.2	CVC for palmitoleic acid and their mixtures at 30 °C.	97
4.3	Comparison on separation methods for 200 µL of 25 mM oleate-oleic acid-DPPE-PEG2000 liposome containing calcein and VE.	118
4.4	Loading efficiency for $n_{\text{Cal}}/n_{\text{FA}} = 0.12$ and $n_{\text{VE}}/n_{\text{FA}} = 0.16$ in palmitoleate-palmitoleic acid liposome and their mixtures at pH 8.5.	124
5.1	The optimum composition of mixed fatty acid and PEGylated lipid.	203
5.2	The optimum composition of fatty acid and mixed fatty acid/PEGylated lipid with VE.	204

LIST OF SYMBOLS AND ABBREVIATIONS

Γ	relaxation time
Π	surface pressure
ε	dielectric constant
ε'	extinction coefficient
γ	surface tension of subphase
η_{solution}	viscosity of the solution
η	solvent viscosity
κ^{-1}	Debye length
λ	wavelength of incident monochromatic and coherent light
θ_{173°	scattering angle, 173° in this study
θ_c	contact angle between the subphase and Wilhelmy plate
ρ_p	density of the subphase
ρ_l	density of the material of Wilhelmy plate
A	mean molecular area
Ac	baseline of the correlation function
A_{id}	ideal area per molecule that calculated according to additivity rule
A_{mixture}	area per molecule obtained experimentally from $\Pi - A$ mixed monolayer isotherm
A_{pure}	area per molecule for pure fatty acid
a_o	effective cross sectional area occupied by the hydrophilic head group
a_{eff}	effective area per molecule
B	intercept of the correlation function
Cal	calcein
C_s^{-1}	compression modulus
$C(t')$	correlation function
CVC	critical vesiculation concentration
D	mean distance between PEG chains
D_t	translational diffusion constant
d	mean particle size
DPPC	1,2-dipalmitoyl- <i>sn</i> -glycero-3-phosphocholine
DPPE-PEG2000	1,2-dipalmitoyl- <i>sn</i> -glycerol-3-phosphoethanolamine-N-[methoxy(polyethyleneglycol)-2000]
DPPE-PEG5000	1,2-dipalmitoyl- <i>sn</i> -glycerol-3-phosphoethanolamine-N-[methoxy(polyethyleneglycol)-5000]
DSPC	L- α -distearoyl phosphatidylcholine
DSPE-PEG2000	distearoylphosphatidyl-ethanolamine-poly(ethylene glycol)2000
Eq.	equation
FA	fatty acid
$f(ka)$	Henry's function
g	gravitational constant
h_1	depth of the Wilhelmy plate in the subphase
I_o	intensity of incident light
$I_{(t)}$	intensity of scattered light at time t
k	Boltzmann constant
l_p	length of Wilhelmy plate
l_b	thickness of the bilayer
l_c	chain length of the hydrocarbon group

l_{\max}	the length of fully extended saturated hydrocarbon chain
PA	phosphatidic acid
M	alkali metal
$M_{\text{fatty acid}}$	molarity of fatty acid
N	Number of measurement
N_A	avogadro number
n'	refractive index of the solution
n_o	refractive index of solvent
n_1	refractive index of particle
n_c	number of methylene carbon atoms
n^e	amount of substance loaded in liposome
$n^{e*}_x/n^{*}_{\text{FA}}$	optimum loaded ratio
n_r	n_1/n_o relative refractive index
n_x	amount of substance used in the preparation of liposome
N_{liposome}	amount of liposome
N_{tot}	total monomer in the formation of liposome
P	packing parameter
PC	phosphatidylcholine
PE	phosphatidylethanolamine
PEG	polyethylene glycol
PI	phosphatidylinositol
q	scattering vector
R	alkyl chain
R_g	radius of gyration of the polymer
R_h	hydrodynamic radius of particle
R_p	radius for particle
S_o	total surface area
S.D.	standard deviation
T	absolute temperature
TEM	transmission electron microscope
t'	time delay between two intensities measurements
t_p	thickness of Wilhelmy plate
U_E	electrophoretic mobility
V_c	volume of the hydrocarbon group
VE	α -tocopherol acetate
w_p	width of Wilhelmy plate
X	Mole fraction
X_h	halogen group
X_{opt}	mole fraction for optimum ΔG_{exc}
x	type of substance
z	zeta potential

List of publications:

1. Teo, Y.Y., Misran, M., Low, K.H. and Zain, M.S. (2011). *Bull. Korean Chem. Soc.* **32**(1), 1.
2. Teo, Y.Y., Misran, M. and Low, K.H. (2012). *E-Journal of Chemistry* **9**(2), 729-738.

List of article submitted for publication

1. Teo, Y.Y., Misran, M. and Low, K.H. "Studies of lateral interactions between C18 unsaturated fatty acid with polyethoxylated phospholipid mixed Langmuir monolayer at air-aqueous interface" *Journal of Chemistry*, Manuscript number 373174.

1.1 Background of liposome

In the year of 1961, British haematologists by the name of Dr. Alec D. Bangham and R.W. Horne discovered the formation of spherical structures via testing of a new electron microscope by hydrating the dried phospholipid film with negative staining agent. Their publication in 1964 has brought to the development of liposome studies [Bangham *et. al.*, 1964]. The spherical structure was then named as liposome or artificial vesicle. The word liposome is a combination of Greek words from “lipos” and “soma” with the meaning of “fat” for the former and “body” for the latter. However, there is some confusion in literature over the distinction between vesicles and liposomes. Some authors use the name ‘vesicle’ to include both single and multiple closed bilayer particle. They make dissimilarity between ‘liposome’ as it is made from phospholipids either formed naturally or synthetically, and ‘surfactant vesicle’ is formed from synthetic surfactants other than phospholipids. Other authors use ‘vesicle’ to describe single bilayer particles and remain ‘liposome’ as the name for multibilayer closed structures. In this study, we do not differentiate the argument on ‘liposome’ and ‘vesicle’. However, the term ‘liposome’ is applied throughout this thesis.

The formation of phospholipid liposomes was attributed to the molecular structure of phospholipid with amphiphilic nature of a surfactant. Surfactant is commonly found in our daily life. It is an organic molecule with adsorbing ability on the surface or interface. This is due to surfactant molecules are amphiphiles that possess both lyophobic and lyophilic group. Lyophobic group has the least affinity to solvent while lyophilic group has strong attraction with solvent system. If an aqueous solution is the solvent system, lyophilic group is known as hydrophilic head group whereas lyophobic group is named as the hydrophobic tail. In addition to the above mentioned criteria, another important characteristic of a surfactant molecule is their ability to self assemble and forms aggregate such as micelles, vesicles and liquid crystalline phases.

Surfactants are categorized according to the nature of hydrophobic tail and hydrophilic head groups. The hydrophobic tail may be composed of more than one linear or branched hydrocarbon as well as halogenated hydrocarbon chain or aromatic group. Similarly, the hydrophilic head group may be charge or neutral, large in size or may contain polymeric chain.

The solubility of surfactants in an aqueous solution may be determined by the interaction between hydrophilic head group and water molecules through hydrogen bonding. Therefore, it is common to classify surfactant based on the type of head group into cationic, anionic, zwitterionic and non-ionic as shown in table 1.1. In an aqueous solution, cationic surfactants dissociate into positively charge molecules whereas anionic surfactants dissociate into negatively charge molecules. Meanwhile, zwitterionic surfactants possess both positive and negative charges at the head group whereas non-ionic surfactant is neutral in charge when dissolves in an aqueous solution.

At low surfactant concentration, the amphiphiles are known as monomers because they are not interacting with each other. As soon as the surfactant concentration increases to the value higher than the critical aggregation concentration, monomers in the solution aggregate and form macromolecular structures such as micelles, reversed micelles, liposomes or liquid crystalline phase in the solution. This microphase separation phenomenon can be explained by the hydrophobic effect [Israelachvili and Mitchell, 1976; Tanford, 1980]. Addition of amphiphiles in an aqueous solution results in the ordered arrangement of water molecules surrounding the hydrocarbon chain. This leads to disturbance of the hydrogen bonding network and hence reduces the overall entropy of the system while increases the free energy of the system. In order to increase entropy of the system and minimize the interface interaction, hydrocarbon chains of the amphiphiles arrange themselves away from contact with water molecules either pointing towards the air at the surface or self assemble into aggregates in the solution. The

balance between attractive force of the hydrocarbon chain and repulsive force at the head group arises from steric hindrance, hydration and electrostatic forces that encourage the formation of aggregates.

Table 1.1 The type of hydrophilic head group commonly found in surfactant.

Class of surfactant	General structure
<u>Anionic</u>	
Carboxylate	$\text{R-COO}^- \text{M}^+$
Sulphonate	$\text{R-SO}_3^- \text{M}^+$
Sulphate	$\text{R-OSO}_3^- \text{M}^+$
Phosphate	$\text{R-OPO}_3^- \text{M}^+$
<u>Cationic</u>	
Ammonium	$\text{R}_x\text{H}_y\text{N}^+\text{X}_h^-$ ($x=1-4$; $y=4-x$)
<u>Zwitterionic</u>	
Betaines	$\text{RN}^+(\text{CH}_3)_2\text{CH}_2\text{COO}^-$
Sulphobetaines	$\text{RN}^+(\text{CH}_3)_2\text{CH}_2\text{CH}_2\text{SO}_3^-$
<u>Nonionic</u>	
Polyoxyethylene	$\text{R-OCH}_2\text{CH}_2(\text{OCH}_2\text{CH}_2)_n\text{OH}$
Polyols	Ethylene glycol, sucrose, glycerol

R= alkyl chain; X_h = halogen group; M= alkali metal

1.2 Structure and shape of aggregates

Solubilization of amphiphiles in an aqueous solution will result in formation of aggregates with various structures. As a consequence of physical but not chemical association of the amphiphilic molecules, small changes in the matrix environment can modify the size or shape of their microstructure. This is due to the hydrophilic head group or the hydrophobic tail of the amphiphiles may interact with the matrix and change the forces of the system. Hence, the type and size of aggregate formed is highly

dependent on the molecular structure of the amphiphiles, concentration of the amphiphiles, preparation pathway, and matrix effect such as temperature, pH as well as salt concentration [Zhang *et. al.*, 2003].

Geometric packing parameter (P) has been introduced by Israelachvili in 1976 to classify the type and structure of the aggregate formed. $P = \frac{V_c}{a_o l_c}$, where V_c and l_c are the volume and chain length of the hydrocarbon group, the effective cross sectional area occupied by the hydrophilic head group is denoted as a_o . Packing parameter relates the properties of molecule to the preferred curvature in the aggregates. Small value of P implies highly curved aggregates. The smallest aggregates with highly curved interfaces namely spherical micelles with diameter of a few nanometer are formed at $P < \frac{1}{3}$. Normally, spherical micelles are formed from single tail surfactants with head group of large surface area in an aqueous medium. However, the effective head group area may be reduced by addition of salt into the medium. As a result, the packing parameter might be greater than $\frac{1}{3}$ but less than $\frac{1}{2}$ and leading to the formation of cylindrical micelles.

The packing parameter increases to the value in between $\frac{1}{2}$ and 1 as the head group area becomes smaller while the volume of hydrocarbon chain become larger by increase of the hydrocarbon chain length or via formation of pseudo-double-chain surfactant. A pseudo-double-chain surfactant is achievable either through ionic interaction between anionic and cationic single tail surfactant or through hydrogen bonding association between two molecules. Packing parameter with value of $\frac{1}{2}$ to 1 may lead to the formation of lamellar or disc like micelles with the geometry of the external layer as slightly convex. The flexibility of lamellar promotes it to curve and close into a spherical liposome. As the packing parameter is greater than 1, reversed micelles tend to be formed in non-polar medium. The estimation of the packing parameter is also influenced by matrix condition, in other words, addition of ions, organic solvent or molecules into the system may modify their packing parameter as a

consequence of interaction between the hydrophobic tails or hydrophilic head groups [Israelachvili, 1992].

1.3 Morphology and liposome size

Liposomes are recognized as dynamic soft matters because they possess the properties of membrane fluidity and more likely to change in the shape and size which is caused by curvature transition. Liposomes can be generally categorized according to their size, shape and number of concentric bilayer into small unilamellar, large unilamellar or multilamellar that is shown in figure 1.1. Liposomes are grouped into small unilamellar if they have only one concentric bilayer with size range from 20 – 50 nm or else they are known as large unilamellar liposomes. On the other hand, multilamellar liposomes with the diameter range between 100 – 10 000 nm are separated by aqueous phase with a few number of bilayer. Liposome larger than 10 μm in diameter is known as giant liposome. Oligo liposome is another type of liposome whereby smaller size and non-concentric liposomes are entrapped in a larger size liposome. Although spherical is the common shape of liposomes, other shapes such as tubular, stomatocyte, discocyte and starfish may also possible [Kralj-Iglic *et. al.*, 2001; Bozic *et. al.*, 2002; Bozic and Svetina, 2004].

Liposomes with hydrodynamic diameter slightly below 100 nm are known as nanoliposomes. These types of liposomes are desirable due to their longer blood circulation time in a body system [Senior, 1987]. As a result, delivery of active ingredients by nanoliposomes is found more effective than the larger size liposomes. Another benefit of nanosize liposome is that they could penetrate deep into the skin rather than trapped in the stratum corneum of the outermost layer of epidermis.

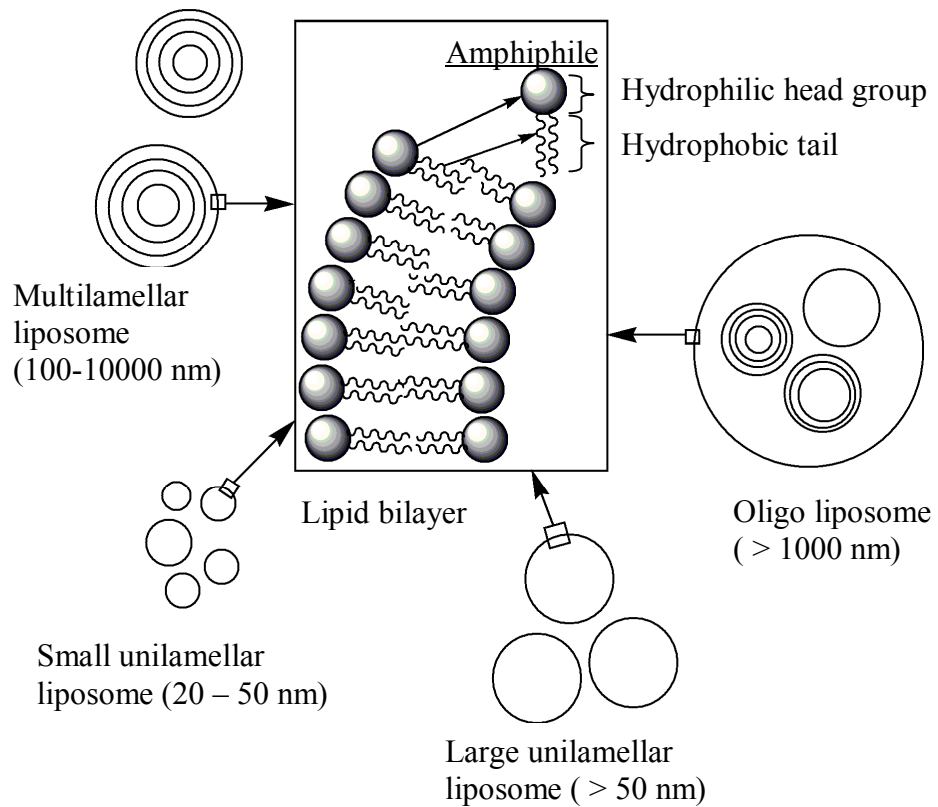


Figure 1.1. A schematic illustration of different types of liposomes. The lines represent the bilayers of the liposomes which are not drawn to scale.

1.4 Similarities between fatty acid liposomes and phospholipid liposomes

Both phospholipid and long chain fatty acid consist of hydrophilic head group and hydrophobic tail. Hence the general principles for the formation of liposome are also similar. They form liposome through the bending mechanism of bilayer into a sphere with an enclosed aqueous core. This process is enthalpically favorable to avoid exposure of the hydrophobic edges from contact with water. In addition, closed bilayer is also entropically favourable as they are smaller entities than as an infinite planar bilayer. The other physical properties of fatty acid liposomes such as hydrodynamic diameter, thermal stability, tensile strength and the potential of solute to permeate through the membrane bilayer were not significantly different from the phospholipid liposomes. [Hargreaves and Deamer, 1978; Mansy and Szostak, 2008; Chen *et. al.*, 2005; Sacerdote and Szostak, 2005]

1.5 Differences between fatty acid liposomes and phospholipid liposomes

Fatty acid liposomes display various distinct behaviors and properties that are different from phospholipid liposomes. Despite of the supramolecular structure of fatty acid liposomes, rapid dynamic equilibrium between fatty acid molecules in the bilayer and the surrounding solution were reported [Lange,1986; Kamp and Hamilton, 1992; Kamp *et. al.*, 1995; Zhang *et. al.*, 1996; Kleinfeld *et. al.*, 1997; Hamilton, 1998]. Fatty acid molecule composes of only one hydrocarbon chain whereas phospholipid molecule is a double tail amphiphile. Thus, the overall hydrophobicity strength in fatty acid molecule undoubtedly is weaker than phospholipid molecule. Due to this reason, the energy barrier to retain fatty acid molecule in the bilayer and equilibrate thermodynamically with bulk solution is considerably higher. Therefore the migration frequency of fatty acid molecules from bulk solution to bilayer is higher and vice versa. In other words, the resident time of fatty acid molecule in the bilayer is shorter and hence stability of the membrane bilayer is reduced as compared to phospholipid membrane. Hence, fatty acid molecules are easily disaggregated especially in the condition with low concentration of fatty acid.

In addition to the variation of hydrophobicity, formation of fatty acid liposome is pH dependence while phospholipid liposome can be formed in a solution of any pH. This is due to the formation of fatty acid liposome is relied on the concentration ratio of non ionized to ionized fatty acid. At the pH solution approximately equals to pKa of fatty acid, about half of the amount of fatty acid are ionized. The coexistence of carboxylate ions and carboxylic acid promotes the formation of dimer through hydrogen bonding between the carboxylate-carboxylic acid head group. This dimer of fatty acid molecules hence led to the formation of lamellar structure aggregates. However, formation of liposome is only possible if the concentration of fatty acid is higher than

the critical vesiculation concentration (CVC) whereupon CVC is the lowest fatty acid concentration required to initiate self assemble of monomers.

The chain length of the hydrophobic tail is an important factor in determining the membrane stability as restricted by the packing parameter. The minimum chain length required for single chain amphiphiles such as fatty acid, alkyl phosphate and alkyl sulphates to form membrane bilayer is at least eight carbon atoms [Monnard and Deamer, 2003; Hargreaves and Deamer, 1978; Deamer, 1997]. On the other hand, phosphatidylcholine with twelve carbon atoms at the hydrophobic tails aggregates into stable lipid bilayer membranes, whereas only micelles were formed by phosphatidylcholine with eight carbon atoms attached at the hydrophobic chains [Roberts, 1992].

1.6 Preparation of fatty acid liposome

Several methods have been introduced to prepare fatty acid liposomes. The variation of these methods results in liposomes with different range of particle size, stability and encapsulation efficiency. The most common preparation pathway is through dry lipid hydration. According to this method, fatty acid is dissolved in organic solvent prior to being evaporated to dryness and forms a film layer. Rehydration of the dry lipid film with appropriate buffer solution at temperature higher than the transition temperature of the fatty acid, causing hydration and swollen of outer hydrophilic head group. This process leads to the formation of lamellar followed by the peeling off of the lamellar. Subsequent input of mechanical energy induces the bilayers to convolute into large multilamellar liposome.

Injection method is also applicable for the formation of fatty acid liposome. In this method, fatty acid with concentration above CVC is dissolved in a small amount of aqueous miscible organic solvent such as ethanol or a mixture of ether and methanol

followed by injection into a buffer solution at pH range of liposome formation. The force of injection and stirring ensures attainment of a well mixed fatty acid monomer solution. Slow evaporation of ethanol leads to closing up of the lamellar or disc to liposome.

Despite of that, the above mentioned methods require the involvement of organic solvent in the preparation process. There are also limited alternative methods that do not involve external energy and organic solvent in the preparation of fatty acid liposomes. It has been reported that vesiculation process does occur either by directly mixing fatty acid with buffer solution accompanied with stirring or dissolving fatty acid in alkaline pH followed by pH adjustment to the desired pH whereby formation of liposome is attained [Hauser and Gains, 1982; Hauser, 1989; Hauser, 1990]. It should be noted that the conditions of liposome formation depend on the type of fatty acid and the liposomes produced are only stable at certain condition.

In order to obtain a more homogeneous liposome suspension, an additional technique such as sonication, extrusion or freeze-thawing is applied on the liposome solution. Small unilamellar liposome can be obtained by sonication method, whereby the multilamellar liposomes suspension is either subjected indirectly to a bath sonicator or directly to a tip sonicator at temperature higher than the transition temperature of fatty acid for 5 to 10 minutes. In addition to sonication, freezing of the large multilamellar liposomes at -196 °C by using liquid nitrogen encourage aggregation of liposomes to small unilamellar liposomes during the thawing process at 50 °C [Pick, 1981; Ohsawa *et. al.*, 1985; Liu and Yonethani, 1994]. This is due to the property of multilamellar has been disrupted by formation of ice during the process of freezing. The presence of ice breaks up the well arrangement of bilayer. During the thawing process, the hydrophobic part of the fatty acid in the bilayer will rearrange and form liposome of smaller size and less number of lamellar. On the other hand, the process of extrusion

involves forcing the liposome suspension through a double stacked polycarbonate membrane filter. This process occurred at a pressure as high as 250 psi which is generated by an inert gas such as nitrogen. Under the condition of high pressure, according to Hunter and co-workers, the liposomes have to reduce their volume either via breakdown of the liposomes or diffuse the water from liposome to the membrane [Hunter and Frisken, 1998] in order to pass through the membrane of smaller pore size. Another extrusion mechanism was mentioned whereby the liposome are forced to deform to cylindrical shape when passing through the membrane and reform a smaller spherical liposome once coming out from the membrane [Clerc and Thompson, 1994]. In order to effectively reduce the liposome size to about the pore size of membrane, repetition of extrusion is required.

1.7 Stability of fatty acid liposomes

Liposomes, just like any other suspended colloidal particles inherit similar characteristics of thermodynamic instability in suspension. Stability of liposome can be categorized into physical, chemical as well as biological. Physical stability is related to the ability of liposomes not to aggregate into clusters at a significant rate throughout the period of observation. Whereas, resistance of unsaturated acyl chains in fatty acid to oxidation is referred as chemical stability. Biological stability can be explained as the successfulness of fatty acid liposome in delivery of active ingredient *in vivo* to the target site without prior leakage or permeation.

In this study, physical stability of fatty acid liposome is highlighted. It is well known that liposome is thermodynamically not stable but kinetically stable. Therefore input of energy either through sonication or vigorous stirring is required for the preparation of liposome especially small unilamellar liposomes. It is believed that liposomes of smaller size are more stable than the larger size liposomes. Besides,

polydispersity of liposome suspension may cause either aggregation of liposome to a larger particle or in contrarily to a smaller particles through “budding” of larger liposome [Berndl *et. al.*, 1990; Döbereiner *et. al.*, 1993].

The appropriate pH range suitable for the formation of fatty acid liposomes is generally narrow as a consequence in fulfilling the requirement that the solution has to simultaneously consist of both ionized and non ionized carboxylic acid at the ratio equals to one. Any changes of the pH either to a more acidic or basic condition will cause the disruption of liposome either to become micelles or oil droplet. Similarly, the presence of divalent metal ions for instance Ca^{2+} or Mg^{2+} in the matrix of liposome suspension may accelerate the process of aggregation.

Physical stability of liposomes is attributed from the net forces of attraction and repulsion between the liposomes. The attractive forces included van der Waals force and hydrophobic force, while electrostatic forces such as steric force and hydration force are the repulsive forces presence in liposomes. As the liposomes approach each other, the electrical double layer surrounding their surface may act as a barrier. Close interaction or overlapping of the double layer is prevented thus maintaining the individuality of the liposome.

In addition, force balance between the hydrophobic tail and hydrophilic head group of the amphiphiles may also affect the stability of membrane bilayer and hence the liposomes. Therefore, different approaches have been attempted to enhance the stability of liposomes such as by modifying the packing parameter, surface charge density, temperature, pH of the liposome suspension solution and through steric stabilization.

Modification of packing parameter by using different type of material in the formation of liposome may enhance the stability of liposome. A reduced value in packing parameter of the liposomes is recommended in order to increase the curvature

of the system. It is believed that a smaller size liposome is more stable than a large liposome since a smaller radius contributes to less van der Waals interaction. In fact, by varying the head group area or hydrophobicity at the hydrocarbon tail it may control the intra molecular force in bilayer. Instead of single type surfactant, mixed surfactant can be used especially in the formation of pH sensitive liposomes to increase their stability in a wider pH range. Moreover, charge density on the surface of liposomes can be altered by using cationic, anionic, zwitterionic or nonionic surfactants to ensure the presence of inter particle electrostatic repulsion force. Nevertheless, sterically stabilized liposome is obtained through physically or chemically attached macromolecules such as glycoprotein (glycophorin A) [Jones, 1995], glycolipid (mono galactocyl diglycerides) [Sekiguchi, 1994], polysaccharides such as amylopectin [Kohno *et. al.*, 1988] and chitosan [Mertins and Dimova, 2011], proteins (cytochrome c) [Pinheiro and Watts, 1994; Abuchowski *et. al.*, 1977; Klibanov *et. al.*, 1991] and synthetic polymers [Lasic, 1994; Allen, 1994; Maruyama *et. al.*, 1995] into the liposomes.

1.7.1 Sterically stabilized liposomes

Liposomes containing an additional hydrophilic material that is phospholipid grafted with polymer on their surfaces is known as sterically stabilized liposomes. The development of attached hydrophilic material on the surface of liposome began in 1987 by Allen and Chonn. They found that incorporation of glycolipid ganglioside G_{M1} in the formation of liposome had substantially prolong the residence time of liposome in the blood stream and reduced their uptake by various component of the immune system [Allen and Chonn, 1987]. This could be due to the presence of hydrophilic sugar residues which creates a steric barrier and hence prevents the adsorption of various components from the immune system on the surface of liposome. Unfortunately, glycolipid ganglioside G_{M1} is not an ideal material for clinical application as it is

obtained from bovine brain and it is very costly. Therefore, research has instead concentrated on preparation of liposome with addition of synthetic lipid grafted with polymer and eventually found that they could efficiently improve the blood circulation time and provide steric stabilization to the liposomal suspensions [Lasic and Martin, 1995]. In addition, phospholipid grafted polymer is also able to control the surface activities of liposome by inhibit close interactions between the surfaces of liposomes.

Several hydrophilic polymers such as polyacrylamide, polyvinylpyrrolidone and polyethylene glycol (PEG) grafted to lipid are used to impart steric stabilization in liposomes [Torchilin *et. al.*, 1994]. Besides, the type of lipid anchors such as cholesterol, monostearate and phosphatidylethanolamine (PE) is also studied in order to obtain a stable liposome suspension. Cholesterol-PEG and monostearate-PEG are reported less effective in prolonging the lifetime of liposomes *in vivo* as a result of they exchanged readily with the lipid bilayer [Allen *et. al.*, 1991]. Nevertheless, a great success in the field of liposomes studies has been achieved with the invention of PEGylated lipid that is chemically conjugate PEG to the PE headgroup through succinate, carbamate, amide and direct linkage. The obtained molecule is negatively charged at the phosphate group. It is commonly added in the preparation of phospholipid liposome and formed sterically stabilized liposomes or also known as ‘stealth’ liposomes. This type of liposomes have been extensively studied and plenty of literatures are reported regarding this substance [Allen, 1994; Lasic, 1994; Lasic and Martin, 1995; Lasic and Needham, 1995; Maruyama *et. al.*, 1995; Lasic, 1997; Lasic, 1998; Winterhalter *et. al.*, 1997; Allen, 1998]. Strong concern is paid on phospholipid grafted PEG in the formation of liposomes because of PEG inertness, high solubility in aqueous solution, high flexibility of the polymer chain and their biocompatibility to medical application materials (Dumitriu, 2002).

Numerous studies have been carried out regarding the arrangement of PEGylated lipid in liposomes and their interaction as well as conformation on the surface of liposomes [Woodle and Lasic, 1992]. The hydrocarbon fragments of PEGylated lipid remains embedded at the hydrophobic region of the bilayer while the long hydrophilic PEG chain is located at the aqueous medium. As a result of the PEG group is significantly bulkier than the hydrocarbon moieties, this leads to coating of the liposomes' surface and generates steric force as the liposomes approach closer to each other. The magnitude of the steric force is related to the density and conformation of the polymer chains. The statistical conformation and thermodynamics of grafted PEG on the liposome surface can be predicted by applying a model proposed by De Gennes [DeGennes, 1976] and modified by Alexander [Alexander, 1977a, Alexander, 1977b]. In order to provide successful shielding on the surface of liposome from interacting with other substances, the grafted polymers must be able to provide sufficient thickness and surface coverage. The conformation of the grafted polymer chains and thickness of the surface coverage layer are dependent on the polymer size that is the radius of gyration of the polymer (R_g), the mean distance between PEG chains (D) [Fleer *et. al.*, 1993; DeGennes, 1976; DeGennes 1980; DeGennes 1987; Claesson *et. al.*, 1996] and the quality of the solvent. At low concentration and shorter chain of grafted PEG to a surface, the PEG may form a 'mushroom' like structure with $D \gg R_g$. The individual PEG chain is separated far away from each other and hence low in surface coverage. A transition named 'mushroom to brush' is approached as the polymer size is comparable to the distance between grafting sites ($D \sim R_g$) whereby the PEG chains begin to interact and overlap with each other in this system. Consequently, at high grafted PEG concentration and with longer PEG chains, the PEG chains take up extended conformations to form a 'brush' like conformation with $D < R_g$. This is due to the polymer size being larger than the distance between grafting sites. The PEG chains will

interact strongly with each other. In order to minimize the interaction, PEG chains must change their conformation to a stretching manner, resulting in a 'brush' like conformation. This 'brush' like conformation provides an adequate coverage and thickness on the surface of liposomes that is required in steric stabilization of liposomes [Szleifer, 1997].

1.7.2 Langmuir monolayer

Langmuir monolayer is an insoluble film deposited on the surface of an aqueous solution also known as subphase with the thickness equivalent to one molecular length. In the formation of Langmuir monolayer, the hydrophilic head group of amphiphiles remain anchored in the aqueous medium, while the hydrophobic tails pointed to the air. Purely hydrophobic material such as semifluorinated alkanes have also been reported to form Langmuir monolayer at the air-water interface successfully [Gaines, 1991; El-Abed *et. al.*, 2002].

This two dimensional plane of Langmuir monolayer at an air-aqueous interface can exist in various physical states analogous to the gas, liquid and solid state of matter in bulk. Hence, it is useful in the study of surface thermodynamic. The changes of phases depend on the nature of molecules and the matrix condition such as pH, temperature and ion concentration [Gaines, 1996]. Phase transition is caused by the molecular rearrangement upon compression of the monolayer. The variation of phase changes is revealed in the surface pressure-mean molecular area (Π - A) isotherm. The surface pressure is defined as the lateral pressure that must be applied to prevent the monolayer from spreading. However, area per molecule is defined as the availability of area for each molecule,

The stability of liposomes depends very much on the physical properties of bilayer. The differences in molecular structure may influence the intermolecular

interaction that dominate in organization of bilayer. The bilayer can be viewed as two parallel weakly interacting monolayer. Hence, Langmuir monolayer at the air-aqueous interface can be used as a model of bilayer. In this study, liposomes consisting mixtures of fatty acid and PEGylated lipid were prepared. Their intermolecular interaction and compatibility were studied by comparing the Π - A isotherms of single and mixed component monolayers. Similarly, the interaction of α -tocopherol acetate (VE) as a substance loaded in liposome with fatty acid as well as mixture of fatty acid/PEGylated lipid will also be studied in this work.

1.8 Effect of fatty acid on human health

Sufficient amount of fatty acids in human body is important to maintain the functionality of certain system such as nervous system, cardiovascular system and immune system. Nevertheless, excess of this chemical in human body may give rise to certain negative effects. The main factor that affects the application of fatty acid in human is their degree of unsaturation at the hydrocarbon chain. Unsaturated fatty acid with *trans* configuration of double bond and fully saturated fatty acid are reported bad for human health. The major health risk caused by high level consumption of the above mention fatty acid is heart diseases due to clogging of the capillaries by cholesterol. The level of cholesterol in human body is affected by the type of saturated fatty acid. Myristic acid is found more effective in increasing the cholesterol level than palmitic acid and lauric acid, whereas, stearic acid is reported in reducing the cholesterol level.

Long chain unsaturated fatty acid such as oleic acid, linoleic acid and linolenic acid are unable to be synthesized in human body, they are known as essential fatty acid. The presence of these substances in human body is through dietary. In addition to prevent from heart diseases, long chain unsaturated fatty acid is also important to

maintain the growing of brain. Deficiency of essential fatty acid may cause depression, allergy as well as growing of malignant tumor.

1.9 Applications of liposomes

Numerous valuable properties displayed by liposomes such as structure, particle size, surface characteristic and chemical composition may render them to be useful in various fields of applications. Moreover, liposomes prepared from natural substances are nontoxic, biodegradable and non immunogenic. A wide range of water soluble and water insoluble substances are solubilized in liposomes due to the presence of both hydrophilic and hydrophobic phases in membrane bilayer. Application of liposomes in the medicinal field can be categorized into therapeutic and diagnostic. The concept of using liposomes as a carrier in drug delivery system was introduced by Gregoriadis [Gregoriadis *et. al.*, 1971; Gregoriadis, 1974]. In the therapeutic field, liposomes are used to carry drugs [Sponton *et. al.*, 1985; Lasic, 1998; Ramaldes *et. al.*, 1996], biologically active compounds [Weingarten *et. al.*, 1981; Laham *et. al.*, 1988] and vaccines [Allison and Gregoriadis, 1974; Alving and Richards, 1990], whereas signal enhancers are entrapped in liposomes for diagnostic purposes.

In the early of 1980, a new approach was developed in order to avoid elimination of liposomes by immune system [Papahadjopoulos *et. al.*, 1990]. This lead to the development of surface modified liposomes with antibodies, peptides and other ligands to facilitate the drug deliver to the target sites [Singhal and Gupta, 1988; Agrawal *et. al.*, 1987; Agrawal and Gupta, 2000]. Drug loaded in liposomes provides various benefits for *in vivo* applications due to their ability to encapsulate hydrophilic and hydrophobic drugs, prevention of drug instability as well as degradation. Normally, drugs that are very potent, toxic and short in life times in the blood circulation will be encapsulated in liposome. Most of the chemotherapeutic drugs are restricted to toxic

effect even though at low dosage. This drawback has been accounted by directing the liposomes encapsulated drug to the infection site. This leads to lower uptake dosage, minimization of the toxic effects and reduction of cost for the therapy while enhancing the bioavailability of medication, especially in the case of poor lipid soluble drugs. In addition, liposomes delay the process of drug elimination when the drug is released to the target site at a sustainable manner. It is found that efficiency of drug penetration into tissues from liposome is improved for topical and transdermal delivery. This is due to liposomes are passively targeted to the immune system, especially to the cells of the mononuclear phagocytic system (MPS). The distribution of drug in the body is controlled by liposomes and disposable of liposomes does not occur in heart, kidneys, brain, and nervous system and this reduces the risk of toxicity. Another application of liposome in the field of genetic engineering is to deliver DNA fragment to the microorganisms or cells in order to modify their genetic code and produce certain protein or polypeptides [Nicolau and Cudd, 1989].

Liposomes are used in the field of cosmetic for delivery of active ingredients, such as vitamin, hyaluronic acid, thymus extract, tanning agent and others. It is believed that liposomes act as a penetration enhancer for cosmetic substances. In fact, liposome itself is a source of lipid to reduce dryness of skin that causes ageing.

Liposomes can also be used in agro-food processing industry such as fermentation processes due to high solubility of the substances, prevention of the substances from potentially destructive environment and release of the substances in a predictable and continuous manner. In fermentation process, enzymes are encapsulated in liposomes; slow release of the enzyme protects them from chemical degradation and hence shortens the period of fermentation and improves the products quality [Lawand King, 1991; Alkhalaf *et. al.*, 1988; Kirby, 1990]. On the other hand, biocides have been encapsulated in liposomes and shown less threatening to the nature although they

presence in a prolong period [Tahibi *et. al.*, 1991]. In addition, the surface of liposome can be made sticky in order for them to be remained on the leaves for longer times and prevent it from being washed into the ground.

Application of liposomes in the field of textile is related to wool chlorination. At $\text{pH} < 7$, liposomes encapsulated oxidizing agents are able to inhibit cystic acid formation in the wool fibre [Maza *et. al.*, 1991]. Other applications of liposomes include cleaning of radioactive metal and toxin from solution through liposomes consisting of chelators on the surface of membrane.

1.10 Objectives of research

- a) To study the effect of PEGylated lipid namely 1,2-dipalmitoyl-*sn*-glycero-3-phosphoethanolamine-N-[methoxy-(polyethylene glycol)-2000] (DPPE-PEG2000) and 1,2-dipalmitoyl-*sn*-glycero-3-phosphoethanolamine-N-[methoxy(polyethylene glycol)-5000] (DPPE-PEG5000) on fatty acid liposomes.
- b) To study the effect of Lecinol S-10 as a mixture of phospholipid in the formation of liposomes.
- c) To load calcein and VE in fatty acid liposomes.
- d) To determine the intermolecular interactions between PEGylated lipid and fatty acids.
- e) To study the compatibility of VE with fatty acid and mixed fatty acid/PEGylated lipid

1.11 References

1. Abuchowski, A., Van, T.E., Palczuk, N.C. and Davis, F.F. (1977). *J. Biol. Chem.* **252**, 3578.
2. Agrawal, A.K. and Gupta, C.M. (2000) *Adv. Drug Deliv. Rev.* **41**, 135.
3. Agrawal, A.K., Singhal, A. and Gupta, C.M. (1987). *Biochem. Biophys. Res. Commun.* **148**, 357.
4. Alexander, S. (1977a). *Le Journal de Physique* **38**, 977.
5. Alexander, S. (1977b). *Le Journal de Physique* **38**, 983.
6. Alkhalaf, W., Piard, J.C., Soda, E.M., Gripon, J.C., Desmezeaud, M. and Vassal, L. (1988). *J. Food Sci.* **53**, 1674.
7. Allen, T.M. (1994).. *Trends Pharma Sci.* **15**, 215.
8. Allen, T.M. (1998). *Drugs* **56**, 747.
9. Allen, T.M. and Chonn, A. (1987). *FEBS Lett.* **223**, 42.
10. Allen, T.M., Hansen, C., Martin, F., Redemann, C. and Young, A.Y. (1991). *Biochim. Biophys. Acta* **1066**(1), 29.
11. Allison, A.C. and Gregoriadis, G. (1974). *Nature* **252**.
12. Alving, C.R. and Richards, R.L. (1990). *Immunol. Lett.* **25** 275.
13. Bangham, A.D. and Horne, R.W. (1964). *J. Mol. Biol.* **8**,660.
14. Berndl, K., KSs, J., Lipowsky, R., Sackmann, E. and Seifert, U. (1990). *Europhys. Lett.* **13**, 659.
15. Bozic, B. and Svetina, S. (2004). *Eur Biophys J Biophys Lett.* **33**, 565.
16. Bozic, B., Gomiscek, G., Kralj-Iglic, V., Svetina, S. and Zeks, B. (2002). *Eur Biophys J.Biophys Lett.* **31**, 487.
17. Chen, I.A., Salehi-Ashtiani, K. and Szostak, J.W. (2005). *J. Am.Chem. Soc.* **127**, 13213.

18. Claesson, P., Blomberg, E., Paulson, O. and Malmsten, M. (1996). *Colloid Surf. A* **112**, 131.
19. Clerc, S.G. and Thompson, T.E. (1994). *Biophysical Journal* **67**(1), 475.
20. Deamer, D.W. (1997). *Microbiol. Mol. Biol. Rev.* **61**, 239.
21. DeGennes, P.G. (1976). *J. Physique* **37** 1445.
22. DeGennes, P.G. (1980). *Macromolecules* **13**, 1069.
23. DeGennes, P.G. (1987) *Adv Colloid Interface Sci.* **27**, 189.
24. Döbereiner, H.G., Käs, J., Noppl, D, Sprenger, I. and Sackmann, E. (1993). *Biophys. J*, **65**, 1396.
25. Dumitriu, S. editor. (2002). *Polymeric Biomaterials*. Marcel Dekker, New York.
26. El-Abed, A., Fauré, M.C., Pouzet, E. and Abillon, O. (2002). *Phys. Rev.* **E65**, 051603.
27. Fleer, G.J., Cohen, S.M.A., Scheutjens, J.M.H.M., Cosgrove, T. and Vincent, B. (1993). *Polymers at Interfaces*, Chapman and Hall, London.
28. Gaines, Jr.G.L. (1991). *Langmuir* **7**, 3054.
29. Gaines, Jr.G.L. (1996). *Insoluble monolayers at liquid-gas interfaces* Wiley-interscience, New York.
30. Gregoriadis, G. (1974). *Biochem. Soc. Trans.* **2**, 117.
31. Gregoriadis, G., Leathwood, P.D. and Ryman, B.E. (1971). *FEBS Lett.* **14**, 95.
32. Hamilton, J.A. (1998). *J. Lipid Res.* **39**, 467.
33. Hargreaves, W.R. and Deamer, D.W. (1978). *Biochemistry* **17**, 3759.
34. Hauser, H. (1989). *Proc. Natl. Acad. Sci. USA.* **86**, 5351.
35. Hauser, H. and Gains, N. (1982). *Proc. Natl. Acad. Sci. USA.* **79**, 1683.
36. Hauser, H., Mantsch, H.H. and Casal, H.L. (1990). *Biochemistry* **29**, 2321.

37. Hunter, D.G. and Frisken, B.J. (1998). *Biophysical Journal* **74**(6), 2996.
38. Israelachvili, J.N. (1992). *Intermolecular and Surface Forces* 2nd ed., Academic Press, San Diego, Chapter 17, 366.
39. Israelachvili, J.N. and Mitchell, D.J. (1976). *Journal of the Chemical Society-Faraday Transactions II* **72**, 1525.
40. Jones, M.N. (1995). *Adv. Colloid Interlace Sci.* **54**, 93.
41. Kamp, F, and Hamilton, J.A. (1992). *Proc. Natl.Acad. Sci. USA.* **89**, 11367.
42. Kamp, F., Zakim, D., Zhang, F., Noy, N. and Hamilton, J.A. (1995). *Biochemistry* **34**, 11928.
43. Kirby, C. (1990). *Chem. Br.* 847.
44. Kleinfeld, A.M., Chu, P. and Romero, C. (1997). *Biochemistry* **36**, 14146.
45. Klibanov, L., Khaw, B.A., Nossiff, N., O'Donnel, S.M., Huang, L., Slinkin, M.A. and Torchilin, V.P. (1991). *Am. J. Physiol.* 261.
46. Kohno, S., Miyazaki, T., Yamaguchi, K., Tanaka, H., Hayaski, T., Hirota, M., Saito, A., Hara, K., Sato, T. and Sunamoto, J. (1988). *J. Bioact. Compat. Polym.* **3**, 137.
47. Kralj-Iglic, V., Gomiscek, G., Majhenc, J., Arrigler, V. and Svetina, S. (2001). *Colloids Surf. A.* **181**, 315.
48. Laham, A., Claperon, N., Durussel, J.J., Fattal, E., Delattre, J., Puisieux, F., Couvreur, P. and Rossignol, P. (1988). *Pharmacol. Res. Commun.* **20**, 699.
49. Lange, Y. (1986). *The Physical Chemistry of Lipids: from Alkanes to Phospholipids*. D. M. Small, editor. Plenum Press, New York. 523.
50. Lasic, D.D. (1994). *Angew Chem Int Ed Eng.* **33**, 1685.
51. Lasic, D.D. (1997). *J. Control. Release* **48**, 203.
52. Lasic, D.D. (1998). *Trends Biotechnol.* **16**, 307.
53. Lasic, D.D. (1998). *Trends Biotechnol.* **16**, 307.
54. Lasic, D.D. and Martin, F. (1995). *Stealth Liposomes*. CRC Press, Boca Raton, FL.

55. Lasic, D.D. and Needham, D. (1995). *Chem. Rev.* **95**, 2601.
56. Law, B.A. and King, J.S. (1991). *J. Diary Res.* **52**, 183.
57. Liu, L. and Yonetani, T. (1994). *J. Microencapsulation* **11**, 409.
58. Mansy, S.S. and Szostak, J.W. (2008). *Proc. Natl. Acad. Sci. USA.* **105**, 13351.
59. Maruyama, K., Takizawa, T., Yuda, T., Kennel, S.J., Huang, L. and Iwatsuru, M. (1995). *Biophys. Acta* **1234**, 74.
60. Maza, D.A., Pana, J.L. and Bosch, P. (1991). *Text. Res. J.* **61**, 35.
61. Mertins, O and Dimova, R. (2011). *Langmuir*, **27**(9), 5506.
62. Monnard, P.A and Deamer, D.W. (2003). *Meth Enzymol.* **372**, 133.
63. Nicolau, C. and Cudd, A. (1989). *Crit. Rev. Therap. Drug Carr. Systems* **6**, 239.
64. Ohsawa T., Miura, H. and Harada, K. (1985). *Chem. Pharm. Bull.* **33**, 3945.
65. Papahadjopoulos, D. and Gabizon, A. (1990). *Prog. Clin. Biol. Res.* **343**, 85.
66. Pick, U. (1981). *Arch. Biochem. Biophys.*, **212**, 186.
67. Pinheiro, T.J.T. and Watts, A. (1994). *Biochemistry* **33**, 2459.
68. Ramaldes, G.A., Deverre, J.R., Grognet, J.M., Puisieux, F. and Fattal, E. (1996). *Int. J. Pharm.* **143**, 1.
69. Roberts, M. (1992). Short-chain phospholipids: useful aggregates in understanding phospholipase activity, 273–289. In Gaber, B.P. and Eswaren, K.R.K. (ed.), Biomembrane structure and function: the state of the art. *Adenine Press*, Schenectady, N.Y.
70. Sacerdote, M.G. and Szostak, J.W. (2005). *Proc. Natl. Acad. Sci. USA.* **102**, 6004.
71. Sekiguchi, A., Yamauchi, H., Manosroi, A., Manosroi, J. and Abe, M. (1994). *Colloid Surface B* **4**, 287.
72. Senior, J.H. (1987). *Crit. Rev. Ther. Drug Carrier Syst.* **3**, 123.
73. Singhal, A. and Gupta, C.M. (1986). *FEBS Lett.* **201**, 321.

74. Sponton, E., Drouin, D. and Delattre, J. (1985). *Int. J.Pharm.* **23**, 299.
75. Szleifer, I. (1997). *Curr.Opin. Solid State Mat. Sci.* **2**, 337.
76. Tahibi, A., Sakurai, J.D., Mathur, R. and Wallach, D.F.H. (1991). *Proc. Symp. Contr. Rel. Bioact. Mat.* **18**, 231.
77. Tanford, C. (1980). *The Hydrophobic Effect: Formation of Micelles and Biological Membranes*. John Wiley & Sons, New York.
78. Torchilin, V.P., Shtilman, M.I., Trubetskoy, V.S., Whiteman, K. and Milstein, A.M. (1994). *Biochim Biophys Acta* **1195**, 181.
79. Weingarten, C., Moufti, A. and Desjeux, J.F. (1981). *Life Sci.* **28**, 2747.
80. Winterhalter, M., Frederik, P.M., Vallner, J.J. and Lasic, D.D. (1997). *Adv. Drug. Deliv. Rev.* **24**, 165.
81. Woodle, M.C. and Lasic, D.D. (1992). *Biochim. Biophys. Acta* **1113**, 171.
82. Zhang, F., Kamp, F. and Hamilton, J.A. (1996). *Biochemistry* **35**, 16055.
83. Zhang, J.Z., Wang, Z.L., Liu, J., Chen, S.W. and Liu, G.Y. (2003). *Self-Assembled Nanostructures* Kluwer Academic Plenum Publishers, New York, Chapter 2, 19.

2.1 Fatty acid liposomes

Phospholipids were found to tend to aggregate into the structure of liposome due to the presence of double hydrocarbon tails in their molecular structure. However, under an appropriate condition, surfactants with single hydrocarbon chain have also been reported to form liposomes [Gebicki and Hicks, 1973; Hargreaves and Deamer., 1978; Kaler *et. al.*, 1989]. In fact, long chain fatty acids are commonly used in the preparation of liposomes [Gebicki *et. al.*, 1973; Hargreaves *et. al.*, 1978]. The formation of fatty acid liposomes is not affected by the degree of unsaturation of the long alkyl chain. Saturated fatty acid with alkyl chain length from eight to twelve carbon have been reported to successfully form liposomes [Hargreaves *et. al.*, 1978; Cistola *et. al.*, 1988; Morigaki *et. al.*, 2003; Namani and Walde., 2005; Morigaki, 1998]. Similarly, long chain unsaturated fatty acid, namely myristoleic acid (*cis*-9-tetradecenoic acid) [Fujikawa, 2005], oleic acid (*cis*-9-octadecenoic acid) [Hargreaves *et. al.*, 1978; Cistola *et. al.*, 1988; Haines, 1983; Walde *et. al.*, 1994a; Fukuda *et. al.*, 2001] and linoleic acid (*cis,cis*-9,12-octadecadienoic acid) [Gebicki and Hicks., 1976; Rogerson *et. al.*, 2006] were found suitable to prepare liposomes. These types of liposome were called “ufasomes” which means unsaturated fatty acid liposomes [Gebicki *et. al.*, 1973]. Highly polyunsaturated fatty acid namely *cis*-4,7,10,13,16,19-docosahexaenoic acid [Namani *et. al.*, 2007] and fatty acid with odd number in hydrocarbon chain such as 10-undecenoic acid have also been reported to form liposome successfully [Lee *et. al.*, 2009].

The discovery of unsaturated fatty acid liposomes was earlier than the saturated fatty acid. However, their physical properties such as stability, zeta potential and encapsulation efficiency have yet to be investigated. Hence, study on the physical properties of unsaturated fatty acid liposomes has attracted us to this research.

Fatty acid liposomes have been widely investigated as an alternative to phospholipid liposomes due to some advantages of fatty acid over phospholipid. One of the most concerning factor is the cost of raw material. Fatty acid is less expensive compared to the pure or synthetic phospholipid. In addition, the preparation route for fatty acid liposome is considerably simple. The formation of liposomes may only involve changes in pH of the solution. Similar to phospholipid liposomes, fatty acid liposomes are also capable in encapsulating water soluble as well as water insoluble substances. Moreover, toxicity of fatty acid is low because they are substances occurring naturally in the body system.

2.2 Aggregation number of fatty acid liposomes

The average amount of fatty acid monomer aggregated into liposome corresponds to aggregation number. It is just a guide line to estimate the amount of liposome in a suspension especially for their application in the delivery of active ingredient. This value is calculated according to the particle size of liposome, thickness of the bilayer and the area per head group of fatty acid. Therefore, a few assumptions such as spherical shape of liposome, lamellarity of liposome, mean diameter of liposome, area per head group and asymmetry of the bilayer have to be taken into consideration for estimation of the aggregation number.

If we consider a unilamellar liposome that is spherical in shape with mean particle size (d), effective area per head group (a_o), thickness of the bilayer (l_b) and N_{tot} is the total monomer in the formation of liposome, therefore the total surface area (S_o) for both of the monolayer in a unilamellar liposome is given in equation 1.

$$S_o = N_{tot} a_o = \left[4\pi \left(\frac{d}{2} \right)^2 + 4\pi \left(\frac{d}{2} - l_b \right)^2 \right] \quad (\text{Eq. 1})$$

The half of the bilayer thickness for saturated fatty acid can be calculated by applying Tanford equation, $l_{\max} \approx (0.154 + 0.127 n_c)$ nm [Tanford, 1980]. In this equation, the number of methylene carbon atoms (n_c) is used to determine the length of fully extended saturated hydrocarbon chain (l_{\max}). It has been reported that l_{\max} for decanoic acid is similar to the value for half of the bilayer thickness for decanoate-decanoic acid liposome as determined from cryo-TEM images [Namani *et. al.*, 2007]. On the other hand, bilayer thickness for unsaturated fatty acid was found rather within a similar range regardless the chain length and the degree of unsaturation. This is possibly due to low melting temperature of unsaturated fatty acid that render the occurring of conformational disorder within the bilayer. The bilayer thickness is found in the range of 2.1 – 3.2 nm as shown in table 2.1.

Table 2.1 Bilayer thickness of fatty acid.

Fatty acid	Bilayer thickness, nm	References
Decanoic acid (in 0.2 M BICINE buffer, pH 7.0)	2.6 ± 0.5	Namani and Walde, 2005
Decanoic acid (in 0.1 M sodium phosphate buffer, pH 7.0)	2.2 ± 0.5	Namani and Walde, 2005
Oleic acid (in 0.2 M BICINE buffer, pH 8.5)	3.6 ± 0.8	Namani and Walde, 2005
Oleic acid	2.08	Ewijk <i>et. al.</i> , 2002 Wiedenmann, 2002
<i>cis</i> -4,7,10,13,16,19-docosahexaenoic acid (in 0.2 M BICINE buffer, pH 8.5)	3.2 ± 0.7	Namani <i>et. al.</i> , 2007
<i>cis</i> -4,7,10,13,16,19-docosahexaenoic acid (in 0.2 M BICINE buffer, pH 9.0)	2.3 ± 0.5	Namani <i>et. al.</i> , 2007

The a_o is a quantity that depends on the electrolyte concentration. The increase in ionic strength may reduce the effective head group area of charge molecule due to

screening effect that lowered the repulsive energy between the head groups. The reported value of effective head group area for *cis*-4,7,10,13,16,19-docosahexanoic acid is 37 Å [Binder and Gawrisch, 2001].

By applying equation 1, the number of fatty acid molecules aggregating to form liposome can be estimated and is displayed in figure 2.1. We assumed that the bilayer thickness is 3.5 nm and the effective head group area varied from 20 – 40 Å² in view of the fact that this value is affected by the matrix condition. As revealed in the calculation, formation of a liposome with particle size of 100 nm with effective head group area 35 Å² and bilayer thickness of 3.5 nm may require 170000 fatty acid molecules. This calculated value is comparable with phospholipid liposome of similar particle size which only requires 95000 phospholipid molecules whereupon the thickness of bilayer is assumed to be 5 nm and the effective head group area is 60 Å² [Maurer *et. al.*, 2001].

As can be seen from figure 2.1, N_{tot} increases drastically as the particle size of liposome becomes larger. Assuming that 170,000 fatty acid molecules aggregate and form one unilamellar liposome of 100 nm. The amount of liposome, $N_{liposome}$, present in 1 mL of liposome solution with fatty acid concentration, $M_{fatty\ acid} = 1\ \mu M$ is estimated to be 3.5 billion as calculated by using equation 2, whereby N_A is Avogadro's number. At similar fatty acid concentration, only 0.4 billion of liposomes with particle size 300 nm are prepared as each liposome requires 1,600,000 fatty acid molecules.

$$N_{liposome} = \frac{M_{fattyacid} \times N_A}{N_{tot} \times 1000} \quad (\text{Eq. 2})$$

Therefore, the number of smaller size liposome present in one solution is comparably higher than the other that forms a larger size liposome although the fatty acid concentrations in both solutions are similar. This implicates that preparation of liposome smaller in particle size is more cost effective for their application. However, N_{tot} for liposome with similar particle size is found to decrease as the effective area per head group increases. This can be explained by the packing constraint in liposome. Although

molecule with larger effective head group area is preferable for the preparation of smaller size liposome, this factor is restricted to packing parameter of the aggregate. Hence consideration of the volume for hydrocarbon tail is needed whenever the head group area is increased in order to maintain the formation of bilayer that is within the packing parameter in between 0.5 and 1.

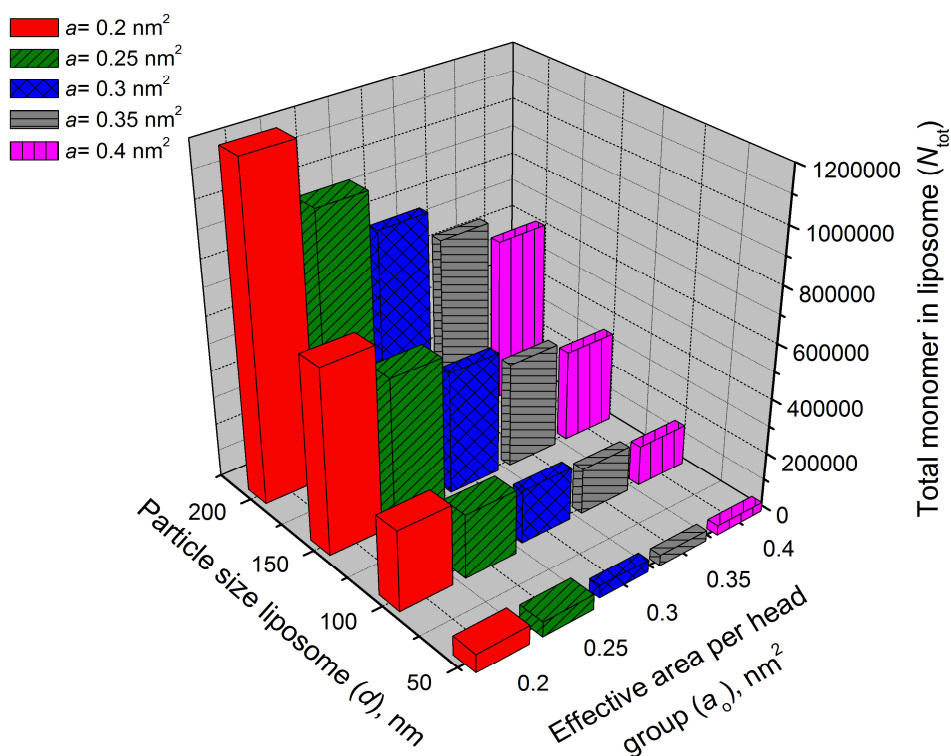


Figure 2.1. A 3-D bar chart of total fatty acid monomer in a liposome with respect to their particle size and effective area per head group with $l_b = 3.5 \text{ nm}$.

2.3 Characterization fatty acid liposomes

2.3.1 pH equilibrium plot

Formation of fatty acid liposomes is only achievable when the concentration of fatty acid is higher than CVC and the ratio of ionized to non-ionized fatty acid molecules is approximately equal to one [Cistola *et.al.*, 1988; Fontell and Mandell., 1993]. This ratio is important in maintaining the stability of fatty acid liposomes. In other words, as pH of bulk solution is close to the pKa of fatty acid, the coexisting of ionized and non-ionized carboxylic head groups is associated through hydrogen bonding to form dimer. The formation of dimers has been discovered by x-ray analysis [Tandon *et. al.*, 2001]. On the other hand, hydrophobic force at hydrocarbon chain stabilized the electrostatic repulsion force among the head groups. The dimer formed is analogous to diacyl chain phospholipid molecules which arranged themselves into bilayer manner [Apel *et al.*, 2001].

An overall negatively surface charge is carried by the dimer. This charge is contributed by the oxygen atoms from carboxylate head group. The anionic surface property for bilayer and micelle has been widely recognized by lipid pH indicators [Fernandez and Fromherz, 1977]. The information obtained for anionic surface charge density and ionic strength allows direct calculation of the pH at the surface [McLaughlin *et al.*, 1971]. It has been reported that the pH at surface is as much as 3.0 units lower than the bulk pH. Therefore, the pH suitable for the formation of fatty acid liposomes is in the range from 7.5 – 9.5. The plausible reason is due to protons sequestering on the surface of high negatively charge density, resulting in a decrease of proton activity in the bulk solution and thus the apparent bulk pH decreases. This implies pKa of the dimer is apparently varied from the monomer and therefore the stability of dimer is enhanced over a wider pH range [Haines, 1983].

An interesting observation has been reported that fatty acid molecules undergo autocatalytic process whereby they spontaneously self assemble into liposomes once an alkaline micellar solution is diluted in a buffer solution [Walde *et al.*, 1994b]. Fatty acid forms various type of phase behavior with respect to the pH of solution. The formation of aggregate has been constructed for fatty acids such as octanoic acid, decanoic acid and oleic acid [Cistola *et. al.*, 1988; Apel *et. al.*, 2001; Morigaki *et. al.*, 2003]. In addition, an equilibrium titration curve of alkaline fatty acid solution mixed with appropriate amount of hydrochloric acid has been described by Rosano and others when they were studying the influence of surface charge on lipid-water interface [Rosano *et. al.*, 1969]. In view of the fact that formation of fatty acid liposomes is pH dependence, this titration method has been applied to determine the effect of pH and the appropriate pH range suitable for the formation of fatty acid liposomes. This is because in a dilute fatty acid solution, transitions of non-ionized fatty acid molecules to ionized fatty acid can easily be induced by varying the pH of the solution. The suitable pH range for the formation of liposomes is very much relying on the chemical structure of fatty acids. It has been reported that fatty acid with a long aliphatic hydrocarbon chain is prone to form liposomes at a higher pH as a result of the molecules can be packed more tightly in the bilayer [Morigaki and Walde, 2007].

Basically, the equilibrium titration curve can be divided into three regions according to the pH of the solution during titration of alkaline fatty acids. At the high pH region, a transparent solution is obtained corresponding to micellar region in the phase diagram with the presence of monomers that fully ionized at the head group. As the pH is lowered by addition of acid, a turbid solution is observed attributed to the formation of liposomes. The solution becomes milky as the pH is further reduced as that indicates the oil droplets are dominant and followed by phase separation. Hence it is obvious that the formation of fatty acid liposomes is limited to a narrow pH range.

2.2.2 Determination of critical vesiculation concentration (CVC)

Fatty acid molecules in very low concentration are present as soluble monomers, even if at a defined condition of pH that promotes the formation of liposomes. However, a transition of the physical properties with respect to fatty acid solution will occur as the concentration of monomers exceeding a certain level. This implies that monomers are assembled into a bilayer structure to form liposomes. The concentration corresponding to the occurrence of this physical property transition is known as critical vesiculation concentration (CVC). Thus, it is important to have a better understanding on CVC so as not only to reduce the cost of experiment but also to avoid preparation of liposome solution with too high concentration for the physicochemical studies. This is supported by the fact that the rate of flocculation is slower in the solution with low vesicular concentration [Ninham *et. al.*, 1983]. In addition, the value of CVC also provides an implication on the bilayer stability whereby the smaller the CVC, the more stable is the bilayer formed and vice versa.

Since CVC is associated with physical properties transition of the fatty acid solution, the determination of CVC values can be achieved through physical property measurements on a series of fatty acid solutions with various concentrations. CVC can be estimated at the inflection point from the plot of physical property as a function of fatty acid concentrations. Physical properties such as surface tension, turbidity, molar conductivity and osmotic pressure are suitable for the estimation of CVC. Moreover, colorimetric analysis has also been widely used, which involved evaluating the changes in absorbance of fatty acid solution containing chromophore or dye.

The values of CVC are mainly affected by the alkyl chain length at the tail group of fatty acid molecules. The longer the hydrocarbon tail, the stronger the hydrophobic force and hence the lower the concentration of fatty acid required in the formation of liposomes. It has been reported in literature that CVC for octanoic acid at pH 6.9 is 130

mM, nonanoic acid at pH 7.0 is 85 mM [Apel *et. al.*, 2002a], sodium caprate at pH 7.4 is 32 mM [Morigaki *et. al.*, 2003; Namani *et. al.*, 2005], whereas the CVC values for long chain fatty acids are relatively lower with only 0.4 mM for sodium oleate at pH 8.5 [Walde *et. al.*, 1994]. An accurate CVC value for sodium linoleate is not known but the value is estimated less than 1.7 mM [Gebicki and Allen, 1969]. Nevertheless, temperature and type of medium may also influence the value of CVC. At 50 mM borate buffer pH 9, oleate-oleic acid is reported to form liposomes in the concentration range from 0.08 – 0.2 mM [Misran, 1999]. In contrary, CVC for oleate-oleic acid liposomes formed in the medium of glycerol is 27.1 mM that is very much higher than in the aqueous solution [Delample, 2011].

2.2.3 Transmission electron micrograph

Transmission electron microscopy is relatively a simple and rapid method to determine the shape and structure of liposome. However, liposomes display little contrast with respect to their surrounding in producing the image. Therefore, the surrounding of liposome is stained with heavy metal in order to diffract the electrons from the electron beam. The area with staining agent will appear as light grey to black in the image depending on the proportion of electrons diffracted. On the other hand, area without staining agent will appear white in the image as the electrons are transmitted and hit the phosphor screen and produce fluorescence. Yet, the process of staining and drying may introduce a certain level of artifacts such as liposomes fusion and flattening of the spherical liposomes [Forte and Nordhausen, 1986]. This is due to the high sensitivity of liposomes to the changes in environment for instance concentration and composition. Besides, there are other drawbacks and limitations of using TEM. In view of the analysis being carried out at a pressure of 10^{-6} mbar, this has caused structural collapse especially on the specimen of emulsion and liposome.

However, TEM technique will be a very useful tool if there is no structural damage on the particles. Therefore, the liposome produced must be very stable and strongly elastic in nature before it can be subjected to a very low pressure environment. Since this is the best method available for us, it has been applied in this study to ensure the presence of liposome.

Cryo-transmission electron microscopy is applied to characterize the liposomes structure and phase behavior of mixture without using staining agent. In this method, molecular motion in the bilayer is frozen by rapidly cooled the copper grid with liposome dispersion to -160 °C in liquid ethane. This is the preferable method for direct observation of undisturbed liposomes but the images obtained are low in contrast [Kulkarni *et. al.*, 1995].

The next technique to visualize liposomes is through freeze-fracture transmission electron microscope [Sternberg and Gregoriadis, 1992]. In this method, liposomes suspension are rapidly frozen and fractured into two symmetry portions followed by deposition of platinum and carbon on the exposed faces prior to examination under transmission electron microscope. This method is useful for dispersions in high concentration and the interior morphology of the liposomes is also revealed.

2.2.4 Stability of fatty acid liposomes

Stability of fatty acid liposome in aqueous suspension is prominent in extending their application. In general, fatty acid liposomes are thermodynamically not stable as a result of their formation requiring input of energy from sonication, vigorous stirring, vortexing or change of pH. Destabilization of fatty acid liposomes is mainly caused by the type of composition in the membrane bilayer, ionic strength, pH and temperature of the medium and surface properties of fatty acid liposomes. Modification in some of these parameters

will alter the packing efficiency of alkyl chain in the lamellar phase that causes imbalance of attractive-repulsive force among the amphiphilic molecules. The forces involve in determining the stability of liposome include electrostatic repulsion between the head groups on the surface of bilayer, the hydration force on the interface of water and bilayer as well as van der Waals force that arising from hydrophobic interactions among the hydrocarbon chains inside the bilayer. Imbalance of these forces may result in instability of lamellar phase and hence fatty acid liposome. As a consequence, liposomes in an aqueous suspension tend to aggregate that leads to transformation of their size and shape followed by flocculation and precipitation over a period of storage time [Kacperska, 2002].

There are several approaches recommended in enhancing the stability of fatty acid liposomes such as by using mixed surfactant, identify the appropriate temperature, pH and ionic strength for the preparation and storage of liposomes suspension solution. It is important to maintain the temperature whereby liposome suspension is stable upon the period of storage and during preparation of liposomes. Variation in the temperature may affect the stiffness of hydrocarbon chain and hence solubility of fatty acid molecules. Thus an inappropriate temperature may lead to dissolution of fatty acid molecules in the liposomes and resulting in the formation of micelles.

It is well known that pH plays a significant role in the determination of the stability of fatty acid liposome suspension. Modification in pH may induce changes in the ratio of ionized to non-ionized fatty acid molecules, which is the determining factor in the formation of fatty acid liposomes. It has been reported that mixed long chain alcohol and fatty acid formed stable liposomes at higher pH than in the pure fatty acid system. This is due to insufficient ionized fatty acid molecules at $\text{pH} \sim \text{pK}_a$ to form hydrogen bond with hydroxyl groups from fatty alcohol. Thus an elevated pH is necessary in order to attained more ionized fatty acid molecules [Apel *et. al.*, 2002b].

Besides, formation of fatty acid liposome at lower pH is also possible by the introduction of a substance with pKa lower than the fatty acid. Therefore, at pH of solution equal to pKa of fatty acid, the added substance will be completely ionized. The amount of non-ionized fatty acid required to form liposome is increased, resulting in a reduction of pH that is suitable for the formation of liposome. Sodium dodecylbenzenesulfonate mixed with decanoic acid [Namani and Walde, 2005] as well as sodium dodecylethercarboxylate, $\text{Na}^+\text{C}_{12}(\text{EO})_{4.5}\text{OCH}_2\text{COO}^-$ mixed with sodium laureate were found to efficiently enhance the stability of liposomes at lower pH [Vlachy *et al.*, 2008]. Another method is to introduce an additional carboxylic group to the fatty acid as done by the group of DeGroot in the preparation of 2-(4-butyloctyl) malonic acid liposome [DeGroot *et al.*, 1995]

Ionic strength is another important factor in determining the stability of charge liposome such as fatty acid liposomes. The effect of ionic strength on the properties of liposomes has been extensively studied [Cevc *et al.*, 1988; Kodama and Miyata, 1996; Sapia and Sportelli, 1993]. Fatty acid liposomes with anionic surface charge are separated at a certain distance from each other by the energy barrier arising from van der Waals attraction and electrostatic repulsion force. Addition of salt to the liposome suspension causes an electrostatic interaction between the salt and liposome surface hence disrupting the energy barrier and encourage liposomes fusion [Ohki *et al.*, 1982].

Steric stabilization is an alternative method that is commonly used in phospholipid type liposomes. In this method, stabilization of liposome is induced by coating of liposome's surface with bulky polymer chain. However, the conformational flexibility of the polymer may be an important factor in determining their role as a stabilizer in liposome. It has been reported that liposomes incorporated with rigid grafted polymer such as dextran did not show significant stabilization effect on liposome [Torchilin *et al.*, 1994]. On the other hand, PEG is a commonly used polymer

for this purpose. PEG grafted to phospholipids also known as PEGylated lipid has been widely incorporated into liposome membrane because it possesses the characteristic of surface activity as well as water soluble properties. Participation of PEGylated lipid in liposome involves both the phospholipid moiety that can be anchored on the surface of membrane and the hydrophilic PEG moiety which is soluble in aqueous solution. In addition to solubility, properties such as hydrophilicity, biocompatibility, low in toxicity, high in chain mobility and flexibility and also easy to handle have allowed its application in various field.

The presence of PEGylated lipid in liposome formation can effectively increase the density and thickness of the repulsive barrier that manage to overcome the attractive van der Waals force [Needham *et. al.*, 1992]. Hence a close approach between liposome is inhibited and stabilization of the liposome suspension is achieved. Yet, the behavior of PEG on stabilization of liposomes depends on the amount and molecular weight of PEGylated lipid. Incorporation of an excess amount PEGylated lipid and too bulky of the PEG group may induce the formation of micelles instead of stabilizing the liposomes [Hristova *et. al.*, 1995; Marsh *et. al.*, 2003]. Although this method has been widely used, their effectiveness on the fatty acid liposomes has yet to be explored.

2.3 Characterization of stability in fatty acid liposomes

In general, physical stability of liposome suspension refers to no change in their particle size and zeta potential throughout the storage period. However, destabilization process occurs in liposome suspension just like in other colloidal system. As a consequence of destabilization, a macroscopic change such as phase separation or increase in turbidity owing to aggregation and fusion can be observed. Hence, several methods have been applied to evaluate the changes of these physical properties even at the initial stage of destabilization. The parameter commonly used includes hydrodynamic size, zeta

potential and turbidity that render the detection of instability occurring in the liposome suspension.

Fatty acid liposome suspension solutions are heterogeneous with regards to their hydrodynamic diameter. Their hydrodynamic size is found in the range of micrometer with remarkable polydispersity. However, their size distribution can be effectively narrowed down through a mechanism known as matrix effect [Lonchin *et. al.*, 1999; Berclaz *et. al.*, 2001]. In this method, preformed liposomes with defined size are added into the same type of fatty acid micelle solution. The hydrodynamic size of liposomes formed via this mechanism is reported close to the size of preformed liposomes.

The particle size of liposomes may determine their effectiveness as a drug carrier for *in vivo* application. This is due to liposome with size greater than 5 μm may cause clogging of the blood vessels during intravenous injection. In addition, liposomes with large size are rapidly engulfed and digested by macrophage to some extent as compared to the small size liposomes [Harashima *et. al.*, 1994]. As a result, the number of small liposomes accumulated at the target site is higher.

Another useful parameter to evaluate the stability of liposome in addition to particle size is zeta potential. The changes in zeta potential over a period of time for liposome suspension may be assumed as the fluctuation of net charge on the surface of liposome. However, zeta potential is only an estimation of surface charge at an imaginary plane that is known as shear plane because a direct measurement at the particle surface cannot easily be achieved. The plane of shear forms by the associated counter ions is as a result of net charge on the surface of liposome. This phenomenon has led to accumulation of counter ions from the aqueous solution on the interface of liposome. They form an electrical double layer composing of a stern layer and a shear plane. Counter ions at the stern layer are strongly associated to the liposome surface

while ions at the shear plane are loosely bound. However, ions within the electrical double layers will travel along with the particle.

The larger the magnitude of zeta potential generally indicates the formation of a more stable liposome suspension. Hence, it is expected that liposome with an ionic head group is more stable than liposome neutral in charge. This is due to the repulsive force on the charged surface of liposomes prevent them from approaching each other and reducing the collision frequency that proceed to fusion of liposomes [Feng and Huang, 2001]. Nevertheless, this assumption is not always applicable especially for sterically stabilized liposome suspension. This is because their surface charge is shielded by the large group of stabilizers and hence accumulation of counter ion surrounding the liposomes is reduced and results in a decrease in magnitude of zeta potential.

Limited study is available in literature for the stability evaluation of fatty acid liposomes. There is only one literature reported on stability of extruded liposome suspension formed from *cis*-4,7,10,13,16,19-docosahexaenoic acid at pH 8.8 with an average diameter of ~80 nm and remained stable for at least 6 days [Namani *et. al.*, 2007].

Assessment on the turbidity change of a liposome solution may be another method to study the stability of liposome suspension against storage time. In this method, the intensity of light that travels through the liposome suspension is scattered and quantified. Most of the destabilization process is accompanied with aggregation of liposomes to a larger size. Hence, cloudiness of the liposome suspension increases and results in higher intensity of light being scattered. However, this method is only limited to liposome suspension with hydrodynamic size larger than 100 nm that has a visible turbidity.

The stability of liposome involves inter-particle interaction and also the intermolecular interaction in a bilayer. The inter-particle interaction may be studied

through their physical changes such as particle size, meanwhile intermolecular interaction in a bilayer may be analogous to the intermolecular interaction in a monolayer. The effect of changes in mole ratio for a substance in a mixture may be revealed in the thermodynamic properties of a monolayer. Langmuir monolayer is applied to study the stability of bilayer in liposome.

Langmuir monolayer analysis represents half of bilayer demonstrated a convenient method to evaluate the stability of two dimensional membrane bilayer structure at air-aqueous interface [Feng, 1999]. This method provides additional information about the structural characteristic, compatibility, packing of the molecules as well as intermolecular interaction of mixed substances in a monolayer. The effects of material type, pH and temperature of the subphase in the formation of monolayer and thus bilayer in liposomes are also revealed. Moreover, the most favorable composition for the formation of metastable monolayer that indirectly represents the appropriate composition for the formation of bilayer is also attained by using this method.

It has been reported that the degree of unsaturation in fatty acid may affect the intermolecular interaction with phospholipids in the monolayer. A miscible and metastable monolayer is formed only at certain mole ratio of fatty acid and phospholipid mixture. Unsaturated fatty acid interacts more strongly with phospholipid than saturated fatty acid due to the larger cross sectional area of unsaturated fatty acids that effectively separates the phospholipid molecules and reduces the electrostatic repulsion between the pure phospholipid molecules. However, a ternary mixture consisting two types of phospholipid and one type of fatty acid induces destabilization to the monolayer regardless the amount of fatty acid. This is due to steric effect that disrupts the van der Waals force between hydrophobic parts of the molecules [Wydro *et. al.*, 2009].

Study on the interaction between unsaturated fatty acid and cholesterol at the air-water interface has also been carried out by Seoane *et. al.*. Their results revealed that

saturated fatty acid was not miscible with cholesterol whereas unsaturated fatty acid formed a stable monolayer with cholesterol [Seoane *et. al.*, 2001]. In fact, the behavior of the mixed monolayer was found dependent on the degree of unsaturation. Furthermore, the influence of linoleic acid on mixed cholesterol and 1,2-dipalmitoyl-*sn*-glycero-3-phosphocholine (DPPC) has been revealed in the work of Makyla and Paluch. They reported that only higher content of linoleic acid and at surface pressure below 27 mN m⁻¹ was found miscible with mixture of cholesterol and DPPC [Makyla and Paluch, 2009].

PEGylated lipids have been extensively applied in steric stabilization of phospholipid liposomes. Their properties in a monolayer are greatly affected by the degree of polymerization in PEG that is attached to the phospholipid moiety. The effect of an increase in polymerization degree of PEG will give a remarkable shift in the area per molecule [Siegel and Naumann, 2010]. In addition, it is suggested that PEG chain with higher degree of polymerization will form an elongated and coiled conformation above the low transition surface pressure. Nevertheless, a rodlike or fibrillar conformation is proposed for PEG chain with lower degree of polymerization [Coffman and Naumann, 2002]. The presence of 'extended' conformation at PEG chain may effectively prohibit the close approach of liposomes due to excluded volume interaction and hence increase the stability of liposomes from fusion and forming aggregates [DeGennes, 1987; Hristova and Needham, 1994; Hristova *et. al.*, 1995; Vermette and Meagner, 2003]. In addition to 'brush' conformation, another type of conformation known as 'mushroom' has also been identified present at the PEG chain. Transition of these conformations is very much dependent on their concentration as well as degree of polymerization in PEG. It has been reported that 'mushroom' to 'brush' transition is observed not only at high concentration of PEGylated lipid but also at high degree of polymerization at the PEG chain.

Observation of the conformational transition and the behavior of pure PEGylated lipid monolayer at the air-water interface has been widely investigated after the first studied by Baekmark *et. al.* [Baekmark *et. al.*, 1995; Richards, *et. al.*, 1997; Majewski *et. al.*, 1997; Barentin *et. al.*, 1998; Rex, 1998; Naumann *et. al.*, 1999; Naumann *et. al.*, 2001; Chou and Chu, 2002; Vermette and Meagner, 2003; Foreman *et. al.*, 2003; Ohe *et. al.*, 2006; Jebrail *et. al.*, 2006; Jebrail, 2007]. In their study, isotherm with surface pressure as a function of area per molecule was generated. Pseudo-plateau is observed in the isotherm at surface pressure around 8 to 10 mN m⁻¹ and it is clearly seen in the plot of compression modulus as a function of surface pressure or area per molecule. The appearance of this pseudo-plateau is suggested to correspond to the conformational transition in the PEG chain from 'mushroom' to 'brush' [Rex, 1998; Faure' *et. al.*, 1999]. Jebrail *et. al.* suggested that there is another transition occurring at higher surface pressure upon compression of the monolayer. In their studies, an additional transition was found at surface pressure around 26 mN m⁻¹ and 19 mN m⁻¹ for monolayer composing of pure 1,2-Dipalmitoyl-*sn*-Glycero-3-Phosphatidylethanolamine-*N*-[(polyethylene glycol)₂₀₀₀] and 1,2-Distearoyl-*sn*-Glycero-3-Phosphatidylethanolamine-*N*-[poly(ethylene glycol)₂₀₀₀], respectively. They found that this high pressure transition could be attributed from the formation of collapse nuclei such as micelles. Occurrence of this transformation from 'brush' conformation at the monolayer to collapse nuclei in the solution is essential to reduce the steric repulsion force from the intermolecular interaction between PEG chains with brush conformations [Jebrail *et. al.*, 2008].

The intermolecular interaction between L- α -distearoyl phosphatidylcholine (DSPC) and distearoylphosphatidylethanolamine poly(ethylene glycol)₂₀₀₀ (DSPE-PEG2000) in a mixed monolayer has been investigated [Chou and Chu, 2002]. They found that the mixed monolayers formed are miscible and energetically stable if the mole fraction of DSPE-PEG2000 is greater than 0.05. Studies on mixed monolayer of

PEGylated lipid and phospholipid may provide valuable information on the concentration limit of PEGylated lipid suitable for the formation of vesicle with phospholipid. This is due to an excess amount of PEGylated lipid molecules in a monolayer causes a stronger steric repulsive force at the head group than the cohesive force at the hydrocarbon tails. This discrepancy may lead to solubilization of the PEGylated lipid in the solution or also known as collapse of 'brush' conformation and results in the formation of aggregates such as micelles. Micelles formation is preferable due to their cone-shape molecular nature that is shown by PEGylated lipid with bulky PEG head group than phospholipid [Hristova, K. and Needham, 1994; Hristova *et. al.*, 1995; Israelachvili, 1991; DeGennes, 1991].

In view of the fact that unsaturated fatty acid is compatible with phospholipid and phospholipid is found compatible with PEGylated lipid, hence, we can deduce that unsaturated fatty acid may also exhibit a certain level of compatibility with PEGylated lipid. Therefore, we will carry out the investigation in this study.

2.4 Encapsulation of hydrophilic and hydrophobic materials in fatty acid liposomes

Similar to phospholipid liposomes as a carrier in drug delivery, fatty acid liposomes also possess the potential to encapsulate hydrophilic, hydrophobic and amphiphilic materials [Khosravi *et. al.*, 2007; Mozafari *et. al.*, 2008a]. This is due to the presence of a bilayer structure with both lipid and aqueous phases being available in a fatty acid liposome. The ability of liposome in encapsulation has prevented various materials from changes with respect to the environment and chemical reaction such as pH, temperature, enzymatic and chemical effect [Mozafari *et. al.*, 2008a; Mozafari *et. al.*, 2008b]. In addition, liposomes have greatly enhanced the stability of water soluble material even though in a high water content medium [Desai and Park, 2005].

Encapsulation of water insoluble materials such as ibuprofen (Dua *et. al.*, 2006) is found located at the hydrophobic region in the membrane bilayer while water soluble materials such as L-ascorbate or known as vitamin C are either entrapped in the central core of the liposomes or attached at the hydrophilic surface of the liposomes [Liu and Park, 2010]. Nevertheless, amphiphilic materials are likely to be entrapped at the interface between the hydrophobic region and the aqueous compartment.

The development of liposome as a drug carrier was first started in 1995. During that time, application of sterically stabilized liposomes known as Doxil® in the clinical area was began after their availability in the market with approval from US Food and Drug Administration. Doxil® is used in the treatment of cancer with their encapsulated anticancer drug namely doxorubicin.

There are several techniques available for encapsulation of water soluble and water insoluble substances into fatty acid liposomes. Lipid hydration method is commonly applied in encapsulation of drug in liposomes. Depending on the solubility of substances, the sequence for incorporation of substances to be encapsulated in liposome is varied. Water soluble substances to be encapsulated are added in the aqueous buffer whereas water insoluble substances are dissolved in organic solvent and mixed with fatty acid prior to evaporation. In lipid hydration technique, the entrapment process begins with dissolving fatty acid in organic solvent. Then, the solvent is evaporated under reduced pressure to form a viscous gel. The hydration process is carried out at temperature above gel-liquid crystalline transition temperature of fatty acid or above the highest melting temperature of the component in a mixture. During this process, swelling of the lamellar occurred due to the formation of repetitive water layer in between the lamellar. This has induced a larger distance between bilayer for capturing of the drug. After the swollen lamellar experiencing agitation, they will finally convolute and seal up into the form of liposomes [Laughlin, 1997]. A schematic

representation the formation of liposome by lipid hydration method is shown in figure 2.2. A more homogeneous liposome suspension can be obtained through extrusion, sonication or freeze-thaw treatment. The disadvantages of this method include formation of liposomes with low encapsulation efficiency, low in internal volume and highly polydisperse in size [Bangham *et. al.*, 1965; Bangham *et. al.*, 1974].

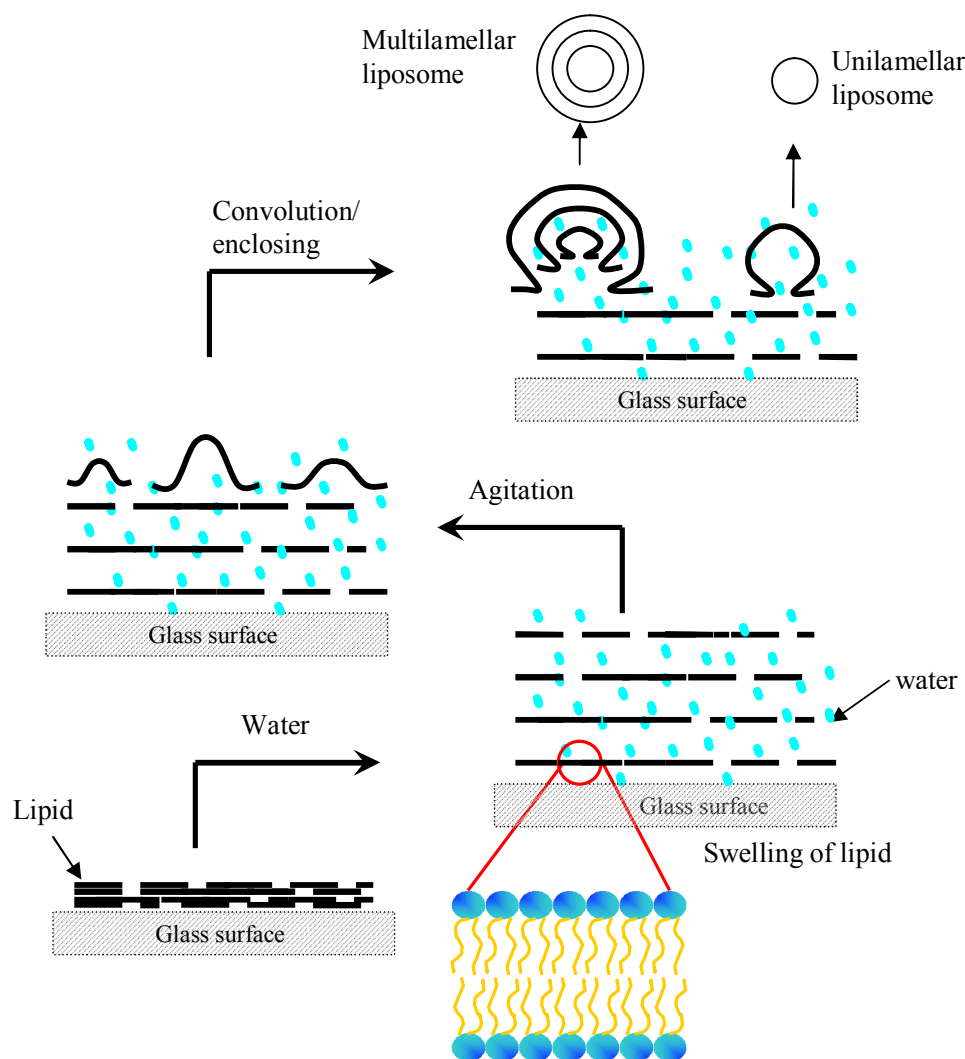


Figure 2.2. A proposed pathway of liposome formation by hydration method.

Reverse phase evaporation technique is also recommended for encapsulation of drug in liposome. In this method, water in oil emulsion is formed by rapid injection of aqueous solution with drug into an organic solvent such as chloroform and diethyl ether containing the lipid. The mixture is subjected to sonication followed by removal of the

organic solvent by rotary evaporator, resulting in the formation of semi solid gel. Large unilamellar liposomes are formed as mechanical agitation is induced to the semi solid gel. During this process, some of the water droplets remained entrapped in the aqueous core whereas some of them collapse to form the external phase [Szoka and Papahadjopoulos, 1978]. The drawback of this method is the possibility of drugs degradation during mechanical agitation.

Another method suggested by Batzri and Korn was injection method. This method is used due to its simplicity and excluded from chemical and physical treatments. Ethanol, diethyl ether or their mixture are usually used in this method to dissolve the lipid. The resulting solution is injected into an aqueous solution containing the substances to be encapsulated through a syringe needle. Successive removal of organic solvent under vacuum promotes the formation of liposomes. Normally, small unilamellar liposomes are obtained. However, factors such as amphiphile concentration and the injection rate may affect the size of liposome. On the other hand, the limitations of this method are low percentage of encapsulation, the liposomes are heterogeneous in size distribution and total removal of ethanol from the solution is difficult as it forms an azeotrope with water [Batzri and Korn, 1973].

2.5 Separation of encapsulated substance in liposomes from non-encapsulated substance

The method to separate the substance loaded in liposomes from those non-loaded should meet certain criteria. In consideration of the amount of samples, the method applied must be able to separate immediately the non-loaded substances from those loaded in liposome. In other words, it has to be a fast and simple method. In addition, sample dilution should be avoided whereas fraction collection should be allowed for further analysis. Besides, it should give a high recovery efficiency of each fraction that has been collected.

Centrifugation is a widely use technique to separate the substance loaded in liposome from those non-loaded. In this method, liposome solution is subjected to a high centrifugal force ($100\,000 - 150\,000 \times g$) for about half an hour. The supernatant containing non-loaded substance is discarded while the solid flake is collected and then re-suspended in an aqueous solution [Xuan *et. al.*, 2009]. Besides, dialysis method and size exclusion chromatography have also been applied for the same purpose.

In size exclusion chromatography technique, the separation concept is related to the size of molecules and the pore size of the solid phase. Various gel matrixes are available to be applied as solid phase in a column. They consist of tiny spherical beads with defined pore size on their surface. Hence, during the separation process, non-loaded substance with smaller size compared to the substance encapsulated in liposomes is likely to be trapped in the pores [Shimanouchia, *et. al.*, 2009]. On the other hand, liposomes with loaded substance are larger in size that leads them to bypass the pore and first eluted from the column. However, this method is time consuming and cause dilution in the liposome suspension.

Another rapid separation method has been introduced by Fry *et. al.* is known as minicolumn centrifugation method [Fry *et. al.*, 1978]. In this method centrifugation and modified size exclusion chromatography are combined in order to separate the non-loaded substance from those encapsulated in liposomes. In contrary to the ordinary size exclusion chromatography, this method uses a plastic syringe of 1 mL or 5 mL as the column instead of the glass column with length about 30 cm. Moreover, after introduction of sample into the mini column, centrifugation is applied to the mini column in order to increase the rate of separation [Jithan and Swathi, 2010; New RRC, 1990; Mishra *et. al.*, 2006]. The non-encapsualted substance can be simply recovered by introduction of a small volume of buffer into the mini column. The advantage of this

method is that plenty of samples can be processed concurrently within minutes with about 100 % recovery [Fry *et. al.*, 1978].

References

1. Apel, C.L., Deamer, D.W. and Mautner, M.N. (2001) *Biochim. Biophys. Acta.* **1559**, 1.
2. Apel, C.L., Deamer, D.W. and Mautner, M.N. (2002a). *Biochim. Biophys. Acta*, **1559**.
3. Apel, C.L., Deamer, D.W. and Mautner, M.N. (2002b). *Biochim. et Biophys. Acta* **1559**, 1.
4. Baekmark, T.R., Elender, G., Lasic, D.D. and Sackmann, E. (1995). *Langmuir* **11**, 3975–3987. (correction) (1996). *Langmuir* **12**: 4980.
5. Bangham, A.D., Hill, M.W. and Miller, N.G.A. (1974). In: *Methods in Membrane Biology* (Korn N.D., ed.) Plenum. N.Y., Vol.1, 1.
6. Bangham, A.D., Standish, M.M. and Watlins, J.C. (1965). *J. Mol. Biol.* **13**: 238.
7. Barentin, C., Muller, P. and Joanny, J.F. (1998). *Macromolecules* **31**, 2198.
8. Batzri, S. and Korn, E.D. (1973). *Biochimica et Biophysica Acta* **298**(4), 1015.
9. Berclaz, N., Blochliger, E., Muller, M. and Luisi, P.L. (2001). *J. Phys. Chem. B.* **105**, 1065.
10. Binder, H. and Gawrisch, K. (2001). *J. Phys. Chem. B* **105**(49), 12378.
11. Cevc, G., Seddon, J.M., Hartung, R. and Eggert, W. (1988). *Biochimica Et Biophysica Acta.* **940**(2), 219.
12. Chou, T. and Chu, I. (2002). *Colloids Surf. A* **211**, 267.
13. Cistola, D.P, Hamilton, J.A., Jackson, D. and Small, D.M. (1988). *Biochemistry* **27**, 1881.
14. Coffman, J.P and Naumann, C.A. (2002). *Macromolecules* **35**, 1835.
15. DeGennes, P.G. (1987). *Adv. Colloid Interface Sci.* **27**, 189.

16. DeGennes, P.G. (1991). *C.R. Acad. Sci.* **313**(11), 1117.
17. DeGroot, R.W., Wagenaar, A., Sein, A. and Engberts, J.B.F.N. (1995). *Recl. TraV.Chim. Pays-Bas* **114**, 371.
18. Delample, M., Jérôme, F., Barrault, J. and Douliez, J.P. (2011). *Green Chem.* **13**, 64.
19. Desai, K.G.H. and Park, H.J. (2005). *Drying technology* **23**, 1361.
20. Dua, L.W. Liu, X.H., Huang, W.M. and Wang, E.K. (2006). *Electrochimica Acta* **51**, 5754.
21. Ewijk, v.G.A., Vroege, G.J. and Philipse, A.P. (2002). *J. Phys., Condens. Matter* **14** 4915.
22. Faure', M.C., Bassereau, P., Lee, L.T., Menelle, A. and Lheveder, C. (1999). *Macromolecules* **32**, 8538.
23. Feng, S. and Huang, G. (2001). *J. Control. Rel.* **71**, 53.
24. Feng, S.S (1999). *Langmuir* **15**, 998.
25. Fernandez, M.S. and Fromherz, P. (1977). *J. Phys. Chem.* **73**, 601.
26. Fontell, K. and Mandell, L. (1993). *Colloid Polym. Sci.* **271**, 974.
27. Foreman, M.B., Coffman, J.P., Murcia, M.J., Cesana, S., Jordan, R., Smith, G.S. and Naumann, C.A. (2003). *Langmuir* **19**, 326.
28. Forte, T.M. and Nordhausen, R.W. (1986). *Methods Enzymol.* **128**, 442.
29. Fry, D.W., Whit, J.C. and Goldman, I.D. (1978). *J Anal Biochem.* **90**, 809.
30. Fujikawa, S.M., Chen, I.A. and Szostak, J.W. (2005). *Langmuir* **21**(26), 12124.
31. Fukuda, H., Goto, A., Yoshioka, H., Goto, R., Morigaki, K. and Walde, P. (2001). *Langmuir* **17**, 4223.
32. Gebicki, J.M. and Allen, A.O. (1969). *J. Phys. Chem.* **73** 2443.
33. Gebicki, J.M. and Hicks, M. (1973). Ufasomes are stable particles surrounded by unsaturated fatty acid membranes. *Nature* **243**, 232.

34. Gebicki, J.M. and Hicks, M. (1976). *Chem. Phys. Lipids* **16**, 142.
35. Haines, T.H. (1983). *Proc. Nat.l Acad. Sci. USA*. **80**, 160.
36. Haines, T.H. (1983). *Proc. Natl. Acad. Sci. U.S.A.* **80**, 160.
37. Harashima, H., Sakata, K., Funato, K. and Kiwada, H. (1994). *Pharm. Res.* **11**,402.
38. Hargreaves, W.R. and Deamer, D.W. (1978). *Biochemistry* **17**, 3759.
39. Hristova, K. and Needham, D. (1994). *J. Colloid Interface Sci.* **168**, 302.
40. Hristova, K., Kenworthy, A. and McIntosh, T. (1995). *J. Macromol.* **28**, 7693.
41. Hristova, K., Kenworthy, A. and McIntosh, T.J. (1995). *Macromolecules* **28**, 7693.
42. Israelachvili, J. (1991). *Intermolecular and Surface Forces*, Elsevier, New York.
43. Jebrail, M. (2007) Effect of aliphatic chain length on the stability of poly(ethyleneglycol)-grafted phospholipid monolayers at the air/water interface. *MSc Thesis*, York University, Toronto.
44. Jebrail, M., Schmidt, R., DeWolf, C. and Tsoukanova, V. (2006). *Proceedings of Surface Canada Conference*, Kingston, 2006.
45. Jebrail,M., Schmidt, R., DeWolf, C.E. and Tsoukanova, V. (2008). *Colloids and Surfaces A: Physicochem. Eng. Aspects* **321**, 168.
46. Jithan, A.V. and Swathi, M. (2010). *International Journal of Pharmaceutical Sciences and Nanotechnology* **3**(2), 986.
47. Kacperska, A. (2002). *J. Mol. Liq.* **95**, 305.
48. Kaler, E.W., Murthy, A.K., Rodriguez, B.E. and Zasadzinski, J.A.N. (1989). *Science*, **245**, 1371.
49. Khosravi, D.K., Pardakhty, A., Honarpisheh, H., Rao, V.S.N.M., and Mozafari, M.R. (2007). *Micron* **38**, 804.
50. Kodama, M. and Miyata, T. (1996). *Colloids and Surfaces A-Physicochemical and Engineering Aspects* **109**, 283.
51. Kulkarni, V.S., Anderson, W.H. and Brown, R.E. (1995). *Eur. Microscopy Anal.* **17**.

52. Langmuir Monolayers *Adv Polym Sci.* **223**, 43.
53. Laughlin, R.G. (1997). *Colloids and Surfaces Physicochemical and Engineering Aspects* **128** (1-3), 27.
54. Lee, J.H., Danino, D. and Raghavan, R.S. (2009). *Langmuir* **25**(3), 1567.
55. Liu, N. and Park, H.J. (2010). *Colloids and Surfaces B: Biointerfaces* **76**, 16.
56. Lonchin, S., Luisi, P.L., Walde, P. and Robinson, B.H. (1999). *J. Phys. Chem.B.* **103**, 10910.
57. Majewski, J., Kuhl, T.L., Gerstenberg, M.C., Israelachvili, J.N. and Smith, G.S. (1997). *J. Phys.Chem. B* **101**, 3122.
58. Makyla, K. and Paluch, M. (2009). *Colloids and Surfaces B: Biointerfaces* **71**, 59.
59. Marsh, D., Bartucci, R. and Sportelli, L. (2003). *Biochim. Biophys. Acta* **1615**, 35.
60. Maurer, N., Fenske, B.D. and Cullis, R.P. (2001). *Expert Opin. Biol. Ther.* **1**(6), 1.
61. McLaughlin, S.G.A., Szabo, G. and Eisenman, G. (1971). *J. Gen.Physiol.* **58**, 667.
62. Mishra, N., Gupta, P.N., Mahor, S., Khatri, K., Goyal, A.K. and Vyas, S.P. (2006). *Indian Journal of Experimental Biology* **45**, 237.
63. Misran, M. (1999). Thermodynamics and kinetics of spontaneous vesicle formation and breakdown of surfactants in aqueous media-sodium 6-phenyltridecane sulphonate and fatty acid. *PhD. Thesis* University of East Anglia, England.
64. Morigaki, K. (1998). Chiral Fatty Acid Vesicles and Peptide/Vesicle Complexes, A dissertation submitted to Swiss Federal Institute of Technology (ETH) Zurich for the degree of Doctor of Natural Sciences
65. Morigaki, K. and Walde, P. (2007). Fatty acid vesicles. *Current Opinion in Colloid & Interface Science* **12**, 75.
66. Morigaki, K., Walde, P., Misran, M. and Robinson, B.H. (2003). *Colloids Surf. A: Physicochem. Eng. Aspects* **213**, 37.
67. Mozafari, M.R., Khosravi, D.K., Borazan, G.G., Cui, J., Pardakhty, A. and Yurdugul, S. (2008a). *International Journal of Food Properties*, **11**, 833.

68. Mozafari, M.R., Johnson, C., Hatziantoniou, S. and Demetzos, C. (2008b). Nanoliposomes and their applications in food nanotechnology. *Journal of Liposome Research* **18**, 309.
69. Namani, T. and Walde, P. (2005). *Langmuir* **21**, 6210.
70. Namani, T., Ishikawa, T., Morigaki, K. and Walde, P. (2007). *Colloids and Surfaces B: Biointerfaces* **54**, 118.
71. Naumann, C.A., Brooks C.F., Fuller, G.G. Knoll, W. and Frank, C.W. (1999). *Langmuir* **15**, 7752.
72. Naumann, C.A., Brooks, C.F., Fuller, G.G., Knoll, W., Frank, C.W. (2001). *Macromolecules* **34**, 3024.
73. Needham, D., McIntosh, T.J. and Lasic, D.D. (1992). *Biochim. Biophys. Acta* **1108**, 40.
74. New R.R.C. (1990). Preparation of liposomes in liposomes: a practical approach, New RRC, ods; Oxford university press: oxford, U.K. 33.
75. Ninham, B.W., Evan, D.F. and Wei, G.J. (1983). *J. Phys. Chem.* **87** 5020.
76. Ohe, C., Goto Y., Noi, M., Arai, M., Kamijo, H. and Itoh, K. (2006). *J. Phys. Chem. B* **111**, 1693.
77. Ohki, S., Duzgunes, N. and Leonards, K. (1982). *Biochemistry* **21**(9), 2127.
78. Rex, S., Zuckerman, M.J., Lafleur, M. and Silviu, J.R. (1998). *Biophys. J.* **75**, 2900.
79. Richards, R.W., Rochford, B.R. and Webster, J.R.P. (1997). *Polymer* **38**, 1169.
80. Rogerson, M.L., Robinson, B.H., Bucak, S. and Walde, P (2006). *Colloids Surf. B: Biointerfaces* **48**, 24.
81. Rosano, H.L., Christodoulou, A.P. and Feinstein, M.E. (1969). *J. Colloid Interface Sci.* **29**, 335.
82. Sapia, P. and Sportelli, L. (1993).. *Colloids and Surfaces a-Physicochemical and Engineering Aspects* **72**, 257.
83. Seoane, R., Dynarowicz, T.P., Minones, J.J. and Rey, G.S.I. (2001). *Colloid Polym. Sci.* **279**, 562.

84. Shimanouchia, T., Ishii, H., Yoshimotob, N., Umakoshia, H. and Kuboia, R. (2009). *Colloids and Surfaces B: Biointerfaces* **73**, 156.
85. Siegel, A.P. and Naumann, C.A. (2010). *Adv Polym Sci.* **223**, 43
86. Sternberg, B. and Gregoriadis, G. (Ed.) (1992). In *Liposome Technology*; CRC Press: Boca Raton, **1**, 363.
87. Szoka, F. and Papahadjopoulos, D. (1978). *Proceeding to the National Academy of Sciences* **75**, 4194.
88. Tandon, P., Raudenkolb, S., Neubert, H.H.R., Rettig, W. and Wartewig, S. (2001). *Chemistry and Physics of Lipids* **109**(1), 37.
89. Tanford C. (1980). *The Hydrophobic Effect* JohnWiley&Sons, New York.
90. Torchilin V.P., Omelyanenko, V.G and Papisov, M.I. (1994). *Biochim. Biophys. Acta* **1195**, 110.
91. Tsukanova, V. and Salesse, C. (2003). *Macromolecules* **36**, 7227.
92. Vermette, P. and Meagner, L. (2003). *Colloids Surf. B* **28**, 153.
93. Vlachy, N., Merle, C., Touraud, D., Schmidt, J., Talmon, Y., Heilmann, J. and Kunz, W. (2008). *Langmuir* **24**(18), 9983.
94. Walde, P., Wick, R., Fresta, M., Mangone, A. and Luisi, P.L. (1994a). *J. Am. Chem. Soc.* **116**, 1649.
95. Walde, P., Wick, R., Fresta, M., Mangone, A. and Luisi, P.L. (1994b). *J. Am. Chem. Soc.* **116**, 11649.
96. Walde, P., Wick, R., Fresta, M., Mangone, A. and Luisi, P.L. (1994). *J. Am. Chem.Soc.* **116**, 11649.
97. Wiedenmann, A (2002). in *Lecture notes on Physics*; Odenbach S, Ed. Springer Verlag; 33.
98. Wydro, K.H., Jedrzejek, K. and Latka, P.D. (2009). *Colloids and Surfaces B: Biointerfaces* **72**, 101.
99. Xuan, H., Yong, Z.D, Hong, Y. and Fu, Q.H. (2009). *Carbohydrate Polymers* **76**, 368. York University, Toronto.

3.1 Materials

3.1.1 Introduction

The surfactants, chemicals and solvents used in this study are listed in this chapter. The purities and sources of these substances will be provided for reference. All of the surfactants and chemicals were used as received without further purification. Some of the solvents were used without further treatment but some were distilled prior to use as specified. In addition, all of the methods used in this study will be clarified. The instrumentations and calculations involved in this work will be briefly explained.

3.1.2 Surfactants

Palmitoleic acid (*cis*-9-hexadecenoic acid, ≥ 98.5 %), oleic acid (*cis*-9-octadecenoic acid, ≥ 99.0 %) and linoleic acid (*cis, cis*-9,12-octadecadienoic acid, ≥ 99.0 %) were purchased from Fluka (Buchs, Switzerland). Alpha-linolenic acid (*cis, cis, cis*-9,12,15-octadecatrienoic acid) were from Sigma (St. Louis, USA) with purity ≥ 99.0 %. Lecinol S-10 was a gift from NIKKO Co. Ltd.. It was added in the formation of liposome to study their effect on fatty acid liposomes and to reduce the cost of production. Lecinol S-10 is a type of commercially available hydrogenated phospholipid. The lecithin substances are extracted from soy bean hence it is low in toxicity and available for plenty of application especially in the cosmetic field as a moisturizer. It is composed of 39 % phosphatidylcholine (PC), 38 % phosphatidylethanolamine (PE), 17 % phosphatidylinositol (PI), and 6 % phosphatidic acid (PA). The fatty acid compositions at the hydrocarbon chain in the phospholipid were reported consisting of 20.1 % palmitic acid, 69.9 % stearic acid and 10.0 % oleic

acid [Bae *et. al.*, 2009]. 1,2-dipalmitoyl-*sn*-glycero-3-phosphoethanolamine- N-[methoxy-(polyethylene glycol)-2000] (DPPE-PEG2000) and 1,2-dipalmitoyl-*sn*-glycero-3-phosphoethanolamine-N-[methoxy(polyethylene glycol)-5000] (DPPE-PEG 5000) were from Avanti Polar Lipids Inc.(Alabama, USA). Their molecular structures are shown in figure 3.1.

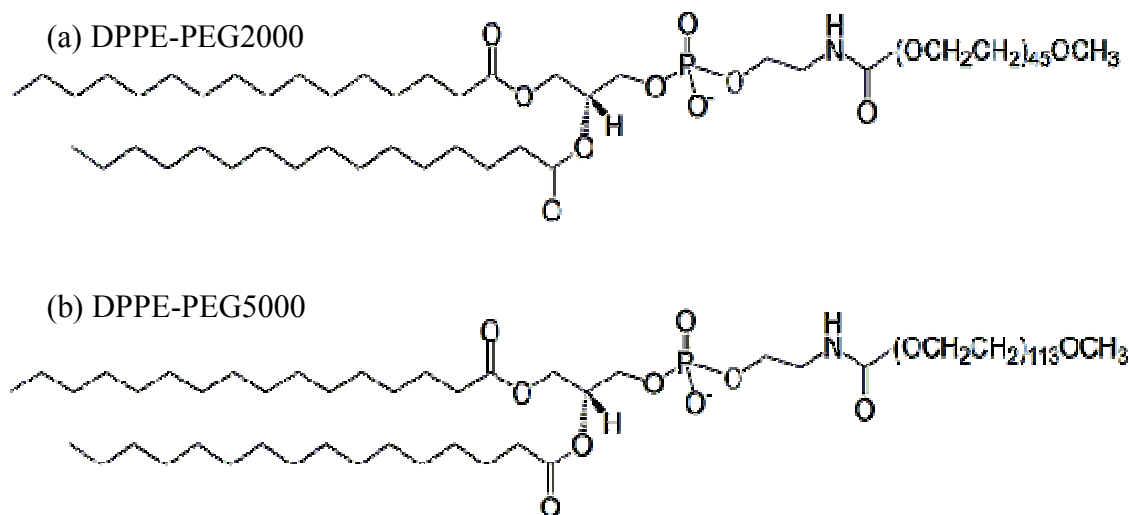


Figure 3.1. Molecular structure of (a) DPPE-PEG2000 and (b) DPPE-PEG5000.

3.1.3 Chemicals

Hydrochloric acid and sodium hydroxide 98 % were purchased from HmBG Chemicals. Boric acid (H_3BO_3) and sodium tetraborate decahydrate ($\text{Na}_2[\text{B}_4\text{O}_5(\text{OH})_4] \cdot 10\text{H}_2\text{O}$) with minimum purity 99.5 % for both were purchased from Fluka (Buchs, Switzerland). Monosodium dihydrogen phosphate dihydrate ($\text{NaH}_2\text{PO}_4 \cdot 2\text{H}_2\text{O}$) 95 % and disodium hydrogen phosphate dihydrate ($\text{Na}_2\text{HPO}_4 \cdot 2\text{H}_2\text{O}$) 99.5 % were supplied by System. Calcein (Bis[N,N-bis(carboxymethyl)aminomethyl]fluorescein) was purchased from Merck. DL- α -tocopherol acetate (3,4-Dihydro-2,5,7,8-tetramethyl-2-(4,8,12-trimethyltridecyl)-2H-benzopyran-6-yl acetate) of purity 96 % was obtained from Sigma (St. Louis, USA).

3.1.4 Solvents

Deionized water with conductivity 18.2 $\mu\text{S cm}^{-1}$ was obtained from Barnstead NANO pure[®] Diamond[™] ultrapure water system throughout the course of work. Deionized water was further distilled and deaerated under nitrogen gas prior to use. HPLC grade methanol, ethanol and acetonitrile were from Merck. Chloroform of analytical grade was obtained from HmBG Chemicals and distilled prior to use.

3.2 Instrumentation

3.2.1 Particle size

3.2.1.1 Dynamic light scattering

Dynamic light scattering or also known as photon correlation spectroscopy is a method to determine the sub micron hydrodynamic size of particle that is suspended in a solution. The rate of intensity fluctuations of scattered light due to Brownian motion of the aggregates is measured. Rayleigh equation as shown in equation 3 is applied to quantify the scattered light by small size particle.

$$\frac{I_{173^\circ}}{I_o} = \frac{16\pi^4 R_p^6}{r_p^2 \lambda^4} \left[\frac{(n_r^2 - 1)}{(n_r^2 + 2)} \right]^2 \quad \text{where} \quad \text{(Eq. 3)}$$

λ wavelength of incident monochromatic and coherent light
 I_o intensity of incident light
 n_o refractive index of solvent
 n_1 refractive index of particle
 R_p radius for particle
 n_r n_1/n_o relative refractive index

From equation 3, we observed that intensity of scattered light ratio is dependent on the number, size and shape of the particles as well as the detection angle. Nevertheless, the particle size is the major contributor to the ratio of scattered intensity as a result of R^6 .

The measurement begins with irradiation of a monochromatic and coherent light source for instance laser to a solution with suspended particles. In this case, laser is preferable due to its precise frequency that is suitable for highly dynamic particles. The incident light will be scattered in all directions. A fluctuation on the intensity of scattered light with respect to time will be observed. This fluctuation originates from the movement of particles in the suspension. Particles move as a consequence of collision with solvent molecules during diffusion. The speed of particles moving is defined as translational diffusion coefficient. A large particle will result in low intensity fluctuation in the scattered light with time or in other words high correlation of the signal intensity with time. This is due to movement of larger particles is slower. On the other hand, small particles are moving rapidly in the solution. Therefore, the intensity fluctuation on scattered light is likely to be higher. This correlation between speed and size of a particle due to Brownian motion is defined in Stokes-Einstein equation as shown in equation 4.

$$D_t = \frac{kT}{6\pi\eta R_h} \quad \text{Where} \quad (\text{Eq. 4})$$

D_t translational diffusion constant
 k Boltzmann constant
 T absolute temperature
 η solvent viscosity
 R_h hydrodynamic radius of particle

A correlation function $C(t')$ as shown in equation 5 is applied by the correlator in the instrument to illustrate the intensity fluctuation of the scattered light from the sampling.

$$C(t') = \langle I_t \cdot I_{(t+t')} \rangle \quad \text{where} \quad (\text{Eq. 5})$$

$I_{(t)}$ intensity of scattered light at time t
 t' time delay between two intensities measurements

In a monodisperse solution, the correlation function can be written as mono exponential decay function as shown in equation 6.

$$C(t') = A_c [1 + B \exp(-2\Gamma t')] \quad \text{where} \quad (\text{Eq. 6})$$

A_c baseline of the correlation function
 B intercept of the correlation function
 Γ relaxation time $= 2Dq^2$
 q scattering vector
 $q = \frac{4\pi n'}{\lambda} \sin\left(\frac{\theta_{173^\circ}}{2}\right)$
 n' refractive index of the solution
 θ_{173° scattering angle, 173° in this study

Alternatively, the correlation function will offer information of scattering for every population in a polydispersed solution. In other words, an integral that includes all of the possible Γ values will be taken into calculation. Thus, a variety of diffusion coefficients are involved.

The slope of the relaxation rate as a function of square scattering results in a linear plot and pass through origin. This suggests the apparent diffusion coefficient is due to Brownian motion of the particles. The average hydrodynamic radius is thus determined from the diffusion coefficient that is related in Stokes-Einstein equation (Eq. 4). The scattered light intensity particle size distribution could be measured. The width of the size distribution compared to the median value is known as polydispersity. The larger value of polydispersity may indicate the particle size in a sample is not uniformly distributed. In liposome system, the median of liposome size may affect directly the polydispersity. The distribution of liposome size may become more polydisperse as the median liposome size increase.

3.2.1.2 Operation of DLS for size measurement

Hydrodynamic particle size of liposomes was measured using Malvern Nano ZS particle size analyzer from Malvern Instruments Ltd. UK. First of all, an incident monochromatic Argon ion laser with wavelength 633 nm is illuminated on the sample within a cell chamber that has been thermostated at 30 °C. Prior to the incident laser reaching the cell, it has to travel through an attenuator to control the intensity of the scattering. Then, the scattered light is detected by a detector that positioned at 173° from the light passing through the sample. The detected signal is transferred to a correlator. The correlator will evaluate the intensity of each scattered light and relate it to time. Finally, the information obtained from the correlator is then delivered to the computer for data analysis.

3.2.2 Zeta potential

Zeta potential measurement is a convenient way to assess the stability of particles suspended in a solution. This parameter provides the information on the magnitude of repulsive interaction between colloidal particles. Particles with high magnitude of zeta potential tend to repel each other and prevent the formation of aggregate. The magnitude of zeta potential is influenced by the surface charge density that depends on the nature of substances in a particle as well as the environment of the suspension.

The development of surface charge on a particle leads to the formation of electrical double layer whereupon a higher concentration of ions with opposite charge is accumulated on the surface of particle as compared to the bulk solution. The first layer with the ions that interacts strongly on the surface of particle is named as Stern layer. In

addition, another layer of ions is interacting weakly and known as the diffuse layer. During the process of measurement, electric field pulls the particle in one direction, at the same time, it will also pulling the counterions in the opposite direction. Some of the counterions will move with the particle so the measured charge will be a nett charge and taking that effect into account. The junction between the strongly bound ions and the diffuse layer is marked by the broken line in figure 3.2. The electrostatic potential at that surface is called zeta potential and it is that potential which is being measured, when one measures the velocities of the particles in d.c. electric field.

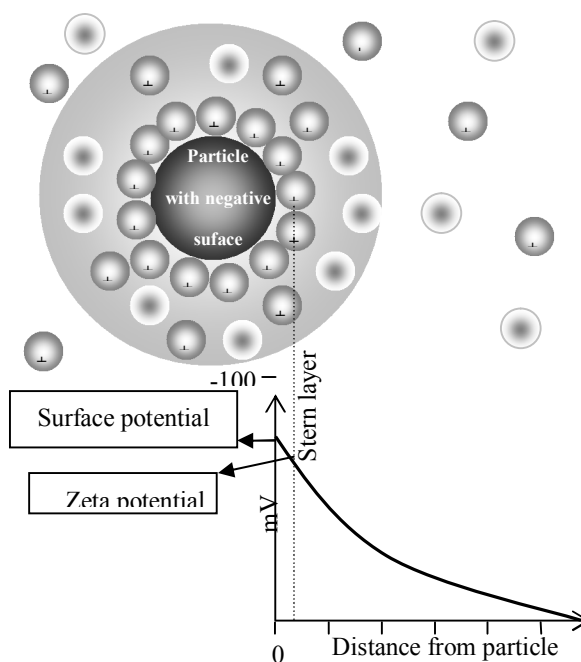


Figure 3.2. Schematic representation of zeta potential

3.2.2.1 Electrophoretic mobility

In view of the presence of surface charge and hence the electrical double layer on a particle, application of an electric field across the solution will move the particles to the electrode with an opposite charge. However, the movement of particle is against the viscous force from the solution and therefore this reduces the travel speed of the particle.

Nevertheless, a constant velocity is achieved when an equilibrium is obtained between these two forces. This effect is defined as electrophoresis. The strength of electrical field, zeta potential of the particle, viscosity and dielectric constant are influencing the velocity of the particle towards the electrode.

Electrophoretic mobility is expressed as velocity of a particle in a unit of applied electric field. The value of zeta potential is derived from the Henry equation (Eq. 7) that relates to electrophoretic mobility.

$$U_E = \frac{2\varepsilon z f(\kappa a)}{3\eta_{\text{solution}}} \quad \text{where} \quad \text{(Eq. 7)}$$

U_E	electrophoretic mobility
z	zeta potential
ε	dielectric constant
η_{solution}	viscosity of the solution
$f(\kappa a)$	Henry's function

Henry function is related to Debye length (κ) and reciprocal of Debye length (κ^{-1}) provides the information of electric double layer thickness for a particle. Hence κa is deduced as ratio of the particle radius to the thickness of electric double layer ($a/(1/\kappa)$). Smoluchowski approximation is applied for particle present in a polar solvent with $F(\kappa a) = 1.5$ whereas Hückel approximation with $F(\kappa a) = 1.0$ is used in the calculation for a non polar solvent.

3.2.2.2 Operation of zetasizer for zeta potential measurement

In this studies, measurement of electrophoretic mobility of liposome was carried out by using Malvern Zetasizer Nano ZS. A combination technique of laser Doppler electrophoresis and M 3 – PALS is used in this instrument to determine the velocity of a particle in condition of electrophoresis. The purpose of this instrument is to measure the

frequency of fluctuation in the intensity of scattered light that can be correlated to the particle speed.

A schematic diagram in figure 3.3 shows the operation route for zetasizer in measuring zeta potential. The operation of this instrument starts from splitting of the laser light source into a reference and an incident beam. The reference beam is directed to the combining optics unit without passing through the sample. On the other hand, incident beam is directed into an attenuator in order to limit the intensity of scattered light prior irradiation to the centre of a cell. Folded capillary cell is used for electrophoretic mobility measurement. It appears as a 'U' shape with an electrical field applied across a pair of electrodes at either end of the cell. Application of an electrical field has driven the charge particles from the centre to the electrode that is opposite in charge with their surface and at the same time they scattered the incident beam. Movement of the charged particles results in intensity fluctuation for the scattered light which is proportional to the velocity of the particle. The scattered light at an angle of 17° from the non scattered beam that passes through the cell is collected and combined with the reference beam in a combining optics followed by directing them to the detector. However, the scattered light has to pass through a compensation optic unit in order to correct for the deviation of cell wall thickness and dispersant refraction prior to directing to the combining optics. Information from the detector will be processed by digital signal processor in order to obtain the frequency of fluctuation in the scattered light. Finally, the computer software will generate the frequency spectrum from electrophoretic mobility and hence calculation of zeta potential by applying Henry equation.

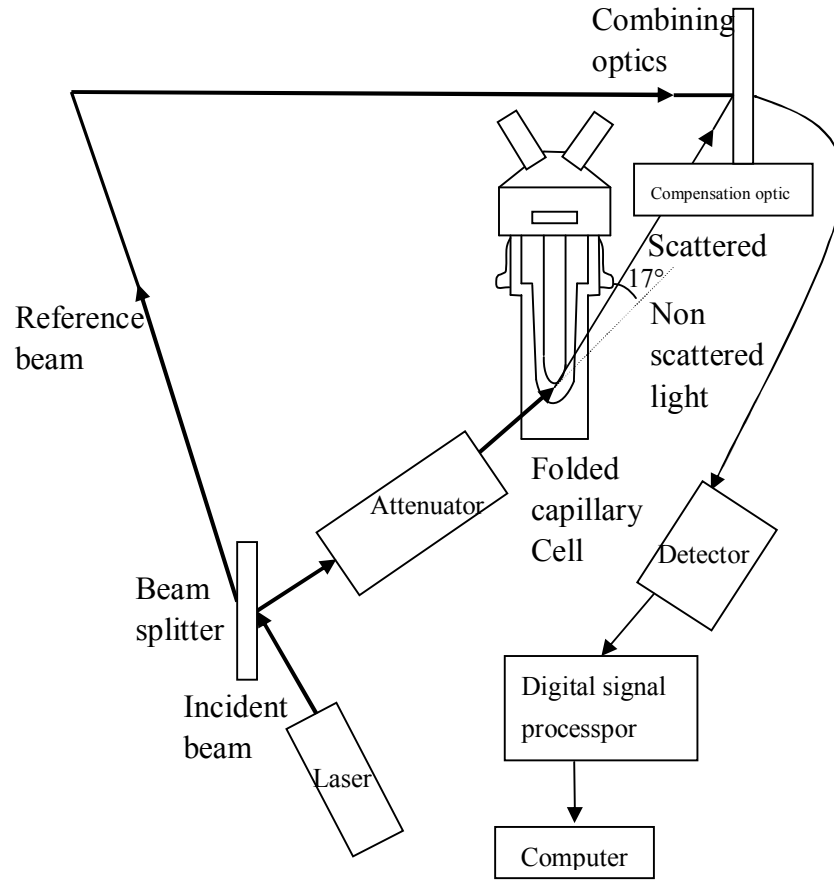


Figure 3.3. Schematic of zeta potential measurement route.

3.2.3 Langmuir monolayer

Measurement of surface pressure is carried out by Wilhelmy plate method [Popiel, 1978] at a constant temperature. Throughout the measurement, Wilhelmy plate is partially immersed in the subphase as shown in figure 3.4. Forces acting on the Wilhelmy plate are measured by the microbalance. The forces are contributed by surface tension of the monolayer and gravity that pulls the Wilhelmy plate downward. Nevertheless an opposite force is also experienced by the Wilhelmy plate that is known as buoyancy. The net force is shown in equation 8.

$$F = \rho_p g l_p w_p t_p + 2\gamma(t_p w_p)(\cos \theta_c) - \rho_l g t_l w_l h_l \quad (\text{Eq. 8})$$

The dimension of Wilhelmy plate is denoted as l_p for length, w_p for width and t_p is the thickness. ρ_p and ρ_l representing the density of the subphase and the material of Wilhelmy plate. The depth of the Wilhelmy plate in the subphase is denoted as h_l , θ_c is the contact angle between the subphase and Wilhelmy plate, g is the gravitational constant and γ is the surface tension of subphase. Surface pressure of the monolayer is determined from the difference between the force that act on the Wilhelmy plate in a subphase without sample introduction and a subphase after sample introduction. For a completely wetted Wilhelmy plate, $\theta_c = 0$, $\cos \theta_c = 1$. Thus the surface pressure of the monolayer can be simplified as in equation 9.

$$\Pi = -\Delta\gamma = -\left[\frac{\Delta F}{2(t_p + w_p)}\right] = -\frac{\Delta F}{2w_p} \quad \text{if } w_p \gg t_p \quad (\text{Eq. 9})$$

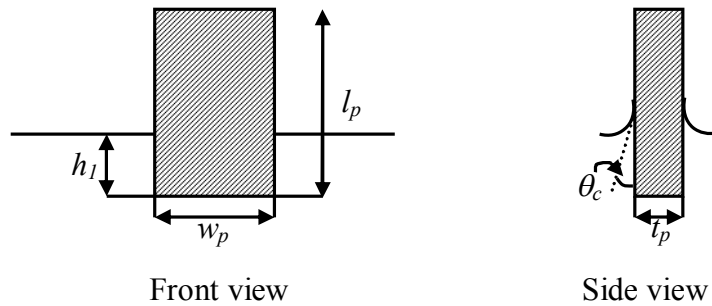


Figure 3.4. A schematic representing partially Wilhelmy plate immersed in subphase.

3.2.3.1 Π - A isotherm

Langmuir-Blodgett KSV 5000 integrated with a computer was used in this study. Prior to each measurement, parameter and condition such as length and width of the trough, temperature and pH of the subphase, concentration of additive in the subphase, the

concentration, molecular weight, density, and volume of the sample solution were entered into the “Experimental Setup” page. The software will record the data for instance temperature, barrier position, barrier speed, area (cm^2), mean molecular area ($\text{\AA}^2 \text{ molecule}^{-1}$) and surface pressure (mN m^{-1}) throughout the measurement. In fact, measurement for the isotherms are not obtained at the state of equilibrium. Thus, the measured mean molecular area depends on the conditions such as compression rate. However, all of the measurements in this study were obtained at an identical temperature and compression protocol. Thus, the phase behavior of the monolayers are comparable.

A schematic Π – A isotherm as generated by the software is as shown in figure 3.5. Langmuir monolayer is formed by spreading of an organic solution containing surfactant on an aqueous solution namely subphase. The organic solvent is allowed to evaporate and leave behind one layer of surfactant molecules on the subphase. At this stage, interactions between the surfactant molecules are weak, hence they are freely moving in a disordered orientation similar to a two dimensional gas. This stage is known as the gas phase in the Π – A isotherm. Compression of this monolayer by moving the barriers symmetrically will limit the distance between the molecules and lead to gas-liquid expanded transition phase. In this phase, the surface pressure is constant. This is due to slow liquefaction of the gaseous phase. As the compression continues, it may cause further reduction of the distance between the surfactant molecules and hence they interact with each other in the liquid expanded state. On further compression, the surfactant molecules in the monolayer rearrange themselves to a more ordered manner resulting in a liquid-expanded to liquid condensed transition and followed by liquid

condensed stage. In this stage, the head groups of the molecules are arranged in a compact manner while the tails are tilted from the interface. Hence the compressibility of the monolayer is lower than in the previous stage. A slightly decrease of area per molecule is associated with a steep rise in surface pressure. As the compression is further applied on the monolayer, the liquid film will finally ‘solidify’ where by the surfactant molecules are all arrange in an ordered form with the head groups pack closely and the tail groups are arrange vertically to the surface of subphase as represented in figure 3.6. Further closing of the barriers will lead to collapse of the monolayer into a three dimensional structure. At this point, the surface pressure will either remain constant for liquid type surfactant or plummet for solid like surfactant.

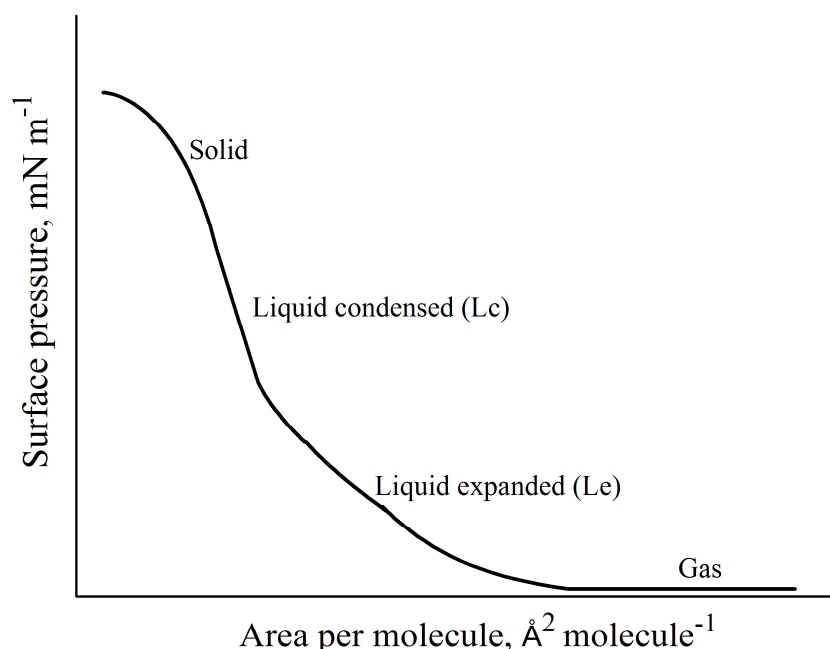


Figure 3.5. A schematic representing Π - A isotherm.

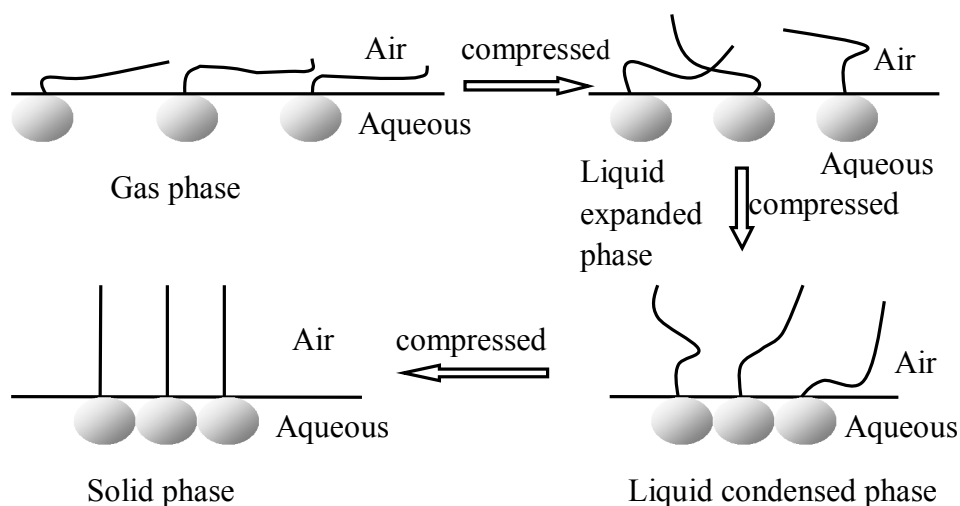


Figure 3.6. Transformation of molecular orientation upon compression of Langmuir monolayer.

3.3 Methods

3.3.1 Preparation of 0.25 M borate buffer pH 8.5

Borate buffer 0.25 M of pH 8.5 was prepared by dissolving 3.18 g boric acid and 6.05 g sodium tetraborate decahydrate in deionized water with stirring. pH of the buffer was adjusted to 8.5 by 0.2 M NaOH solution and 0.2 M HCl solution before top up to the marked level of 250 mL in a volumetric flask. pH of the final solution was also checked.

3.3.2 Preparation of 0.50 M phosphate buffer pH 7.0

Monosodium dihydrogen phosphate dihydrate weighed at 5.77 g was mixed with 10.47 g disodium hydrogen phosphate dihydrate and dissolved in deionized water into a 2 L volumetric flask. The obtained solution is in the pH range of 7.01 – 7.05.

3.3.3 Preparation of stock solution

An alkaline fatty acid stock solution containing (12.50 ± 0.05) mM fatty acid and (27.50 ± 0.05) mM NaOH was prepared by stirring the solution for approximately 20 minutes until a transparent solution was obtained. On the other hand, preparation of binary mixture of fatty acid and PEGylated lipids (DPPE-PEG2000 and DPPE-PEG5000) or Lecinol S-10 as well as ternary mixture composing of fatty acid, PEGylated lipid and Lecinol S-10 had been carried out. In the binary mixture, fatty acid was firstly mixed with either PEGylated lipid at the mole ratio of fatty acid to PEGylated lipid at 50 to 1 or Lecinol S-10 in the weight ratio of fatty acid to Lecinol S-10 at 10 to 3 in a small amount of chloroform. Secondly, the mixed solution was sonicated in order to dissolve all of the substances. It was followed by removal of the chloroform under reduced pressure using a rotary evaporator. Gel-like mixture was obtained and rehydration with warm deionized water (50 °C) and NaOH solution results in a colourless solution. The procedure for preparation of ternary mixed fatty acid, PEGylated lipid and Lecinol S-10 was similar to the above mentioned method.

3.3.4 Titration of the stock solution with HCl

A series of samples with fixed amount of fatty acid at various pH were prepared by mixing 1.50 mL of stock solution with an appropriate amount of 0.1 M HCl and deionized water. The mixture was left to vortex for a minute by using Uzusio VTX 3000L vortex mixer before pH measurement was carried out by a Mettler Toledo pH meter which had been pre-calibrated at the titration temperature with buffer pH 4.01, 7.00 and 9.21. An average of 3 measurements was recorded for each sample.

3.3.5 Transmission electron microscopy

Liposome images were obtained by using Hitachi H-7100 transmission electron microscope (TEM) and Libra 120-Carl Zeiss energy filtered transmission electron microscope (EFTEM) through negative-staining method. Preparation of specimen was carried out by immersing the formvar-coated copper grid into a drop of the liposome suspension solution. Thereafter, it was allowed to stand for 10 minutes. The excess of liposome solution was blotted with filter paper before doing the staining process by using 3% (w/v) phosphotungstic acid. It was ready to be viewed under TEM after the grid was allowed to stand for another 10 minutes for air-drying purpose. The specimens were viewed and photographed with a TEM operating at accelerating voltage of 100 kV and EFTEM operating at accelerating voltage of 120 kV.

3.3.6 Determinations of critical vesiculation concentration (CVC)

A series of solutions with different concentration of fatty acid at pH 8.5 in 50 mM borate buffer were prepared. The solutions were filtered through a 25 mm diameter and 0.2 μm pore size Minisart[®] NY nylon filter (Germany) prior to measurements. The CVC determinations were carried out at a range of temperature from $(20.0 \pm 0.5) ^\circ\text{C}$ to $(40.0 \pm 0.5) ^\circ\text{C}$ by tensiometer balance from KRUSS with K12 tensiometer processor via du Nouy ring method. Calibration of this machine was carried out by deionized water at $(25.0 \pm 0.5) ^\circ\text{C}$ prior to measurements. Surface tension for deionized water was found to be $(71.50 \pm 0.03) \text{ mN m}^{-1}$.

3.3.7 Particle size measurement

Liposome solutions at concentration of 2 mM and pH 8.5 were first filtered through 0.2 μm nylon membrane filter prior to extrusion. The filtered solutions were extruded through a 100 nm pore diameters of Whatman polycarbonate membranes filter using Lipex Biomembrane extruder followed by hydrodynamic size measurement. The z-average diameter (the mean hydrodynamic diameter based upon the intensity of the scattered light) of the liposome was estimated by Malvern Nano ZS particle size analyzer from Malvern Instruments Ltd. UK at 30 °C. An average particle size was obtained from triplicate measurements of each liposome suspension solution whereby each measurement consisting of 5 runs on the sample. All of the solutions were kept at room temperature (28 °C) in order to study their stability. Measurement of the z-average diameter was performed throughout a period of 30 days.

3.3.8 Zeta potential measurement

Electrophoretic mobility of liposome was measured at 30 °C and the value of zeta potential for the liposome solutions were calculated by applying Henry equation. Determinations of zeta potential for all of the liposome suspensions were using the same instrument and condition as in the measurement of particle size. Stability of liposome suspensions were also evaluated by analysis of the changes of zeta potential with time throughout a period of 30 days.

3.3.9 Langmuir monolayer analysis

KSV 5000 Langmuir Blodgett balance (KSV Instrument Ltd., Helsinki, Finland) was used to record the surface pressure–area (Π – A) isotherm. The TEFLON trough with dimension of 150 mm \times 512 mm was placed on an anti-vibration bench and kept in a clear perspex chamber in order to isolate the trough from the surrounding environment. The trough was connected with a temperature controller by means of water circulator and two mechanically coupled Delrin[®] barriers for symmetric compression. Platinum Wilhelmy plate suspended from a microbalance was used to continuously monitor the surface pressure. The trough preparation and Π – A measurements procedures were described elsewhere [Silva *et. al.*, 1996]. The instrument was calibrated by using a monolayer of stearic acid on deionised water subphase prior to the samples measurements. The Langmuir isotherm for stearic acid is shown in figure 3.7. The typical characteristic was observed that is the deviation from zero surface pressure is at area per molecule around 25 Å² molecule⁻¹. In addition, at surface pressure about 25 mN m⁻¹, a significant change of the slope was observed. The slope rose steeply beginning at this surface pressure. The extrapolated area per molecule is found at in the range of (20 \pm 1) Å² molecule⁻¹.

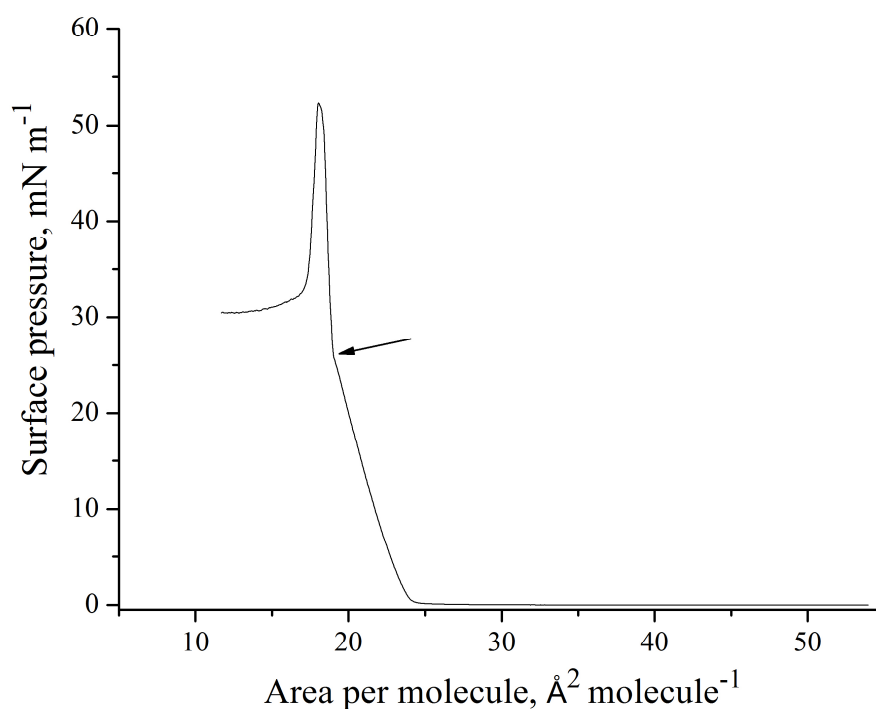


Figure 3.7. Langmuir monolayer isotherm of stearic acid on deionized water as the subphase at 25.0 °C.

Surface purity of the subphase was confirmed prior to the measurement by expanding and compressing the barriers, whereby π readings did not differ by more than $\pm 0.2 \text{ mN m}^{-1}$. Phosphate buffer pH 7 (50 mM) as a subphase was thermo equilibrated at $(25.0 \pm 0.5) ^\circ\text{C}$. A series of stock solution for pure fatty acid (FA), pure VE and pure PEGylated lipids were dissolved in chloroform/ethanol (4:1 v/v) for Langmuir monolayer studies. Moreover, binary mixtures including FA/PEGylated lipid, FA/VE and ternary mixture of FA/PEGylated lipid/VE with various mole fractions, X were also prepared by appropriate dilution of stock solutions using chloroform/ethanol (4:1 v/v). A proper amount of sample was deposited drop by drop on the subphase by using a Hamilton microsyringe. The solvent was allowed to evaporate for about 10 minutes at the same time to achieve thermal equilibration. The experiment was then started at a

constant compression rate of 10 mm min^{-1} . The experiment was repeated at least twice to obtain a reproducible Π – A isotherm

3.3.9.1 Analysis of Langmuir monolayer isotherm

Isotherm of surface pressure as a function of area per molecule generated from the Langmuir monolayer measurement provides invaluable information about the intermolecular interaction. The behavior of a mixture in the monolayer and hence can be related to the bilayer is attainable from this study. There are a few parameters such as collapse pressure, extrapolated area per molecule, excess area, compressibility or compression modulus and excess free energy of the intermolecular interaction that can be extracted from the isotherm. Evaluation of these parameters provides a better understanding about the interaction among the molecules and hence the compatibility of the mixture.

The presence of interaction between the components in a mixed monolayer is reflected as dependency of the curve position and shape to the composition of mixture. According to surface phase rule [Crisp, 1958], components in a mixed monolayer at condensed and collapse state is considered miscible if their collapse pressure is different from the collapse pressures of their pure components monolayer.

Another indirect way to determine the compatibility and ideality of mixed monolayer at the air-aqueous interface is through evaluation of excess area per molecule, A_{exc} for the mixture at constant surface pressures. Equation 10 was used to calculate the A_{exc} values for binary mixture of FA/PEGylated lipid and equation 11 for

FA/VE. A_{exc} for ternary mixture of fatty acid/PEGylated lipid/VE is written in equation 12.

$$\begin{aligned} A_{\text{exc}} &= A_{\text{FA/PEGylated lipid}} - A_{\text{id}} \\ &= A_{\text{FA/PEGylated lipid}} - (A_{\text{FA}} X_{\text{FA}} + A_{\text{PEGylated lipid}} X_{\text{PEGylated lipid}}) \end{aligned} \quad (\text{Eq. 10})$$

$$\begin{aligned} A_{\text{exc}} &= A_{\text{FA/VE}} - A_{\text{id}} \\ &= A_{\text{FA/VE}} - (A_{\text{FA}} X_{\text{FA}} + A_{\text{VE}} X_{\text{VE}}) \end{aligned} \quad (\text{Eq. 11})$$

$$\begin{aligned} A_{\text{exc}} &= A_{\text{FA/PEGylated lipid/VE}} - A_{\text{id}} \\ &= A_{\text{FA/PEGylated lipid/VE}} - (A_{\text{FA/PEGylated lipid}} X_{\text{FA/PEGylated lipid}} + A_{\text{VE}} X_{\text{VE}}) \end{aligned} \quad (\text{Eq. 12})$$

where A_{mixture} or also known as $A_{\text{FA/PEGylated lipid}}$, $A_{\text{FA/VE}}$ and $A_{\text{FA/PEGylated lipid/VE}}$ are the area per molecule obtained experimentally from Π - A mixed monolayer isotherm. A_{id} is defined as ideal area per molecule calculated according to additivity rule at specific mole fraction of the pure component. A_{FA} , $A_{\text{PEGylated lipid}}$ and A_{VE} individually are the area per molecule for pure fatty acid, pure PEGylated lipid and pure VE at the same surface pressure, respectively. Mole fraction of pure fatty acid, pure PEGylated lipid and pure VE are represented by X_{FA} , $X_{\text{PEGylated lipid}}$ and X_{VE} , respectively. If an ideal mixed monolayer is formed at a given surface pressure, molecules in the system do not interact with each other, hence the value of excess area, A_{exc} will be zero and a linear plot of A_{mixture} as a function of mole fraction will be obtained. However, there are always deviations from linearity as a result of intermolecular forces either attraction or repulsion among the molecules that is present in the mixed monolayer.

The influence of DPPE-PEG2000, DPPE-PEG5000 and VE on fatty acid monolayer can be further analyzed in a more precise manner on the basis of compression modulus (C_s^{-1}). A reciprocal of C_s^{-1} is known as compressibility of the

monolayer. These values were obtained by numerical calculation of the first derivative from the isotherm data points according to equation 13.

$$C_s^{-1} = -A \left(\frac{\partial \Pi}{\partial A} \right)_T \quad (\text{Eq. 13})$$

C_s^{-1} is useful for evaluation of the conformation change in acyl chain and head group upon compression of the monolayer. The larger the C_s^{-1} value, more energy is required to compress the monolayer due to compactness arrangement of the molecules at the air-aqueous interface. The compact arrangement may lead to less flexibility of the monolayer at the air-aqueous interface.

Excess Gibbs free energy of a mixture at air-aqueous interface, ΔG_{exc} is applied to study the strength of interaction among molecules in a mixed monolayer with reference to the interaction between molecules in a pure monolayer. Equation 14 is applied in order to obtain this value for binary mixture whereas equation 15 is for ternary mixture. A negative value of ΔG_{exc} is associated with stronger interaction between the mixed molecules and vice versa.

$$\begin{aligned} \Delta G_{\text{exc}} &= N_A \int_0^\Pi A_{\text{exc}} d\Pi \\ &= N_A \int_0^\Pi [A_{\text{FA/PEGylated lipid}} - (X_{\text{FA}} A_{\text{FA}} + X_{\text{PEGylated lipid}} A_{\text{PEGylated lipid}})] d\Pi \end{aligned} \quad (\text{Eq. 14})$$

$$= N_A \int_0^\Pi [A_{\text{FA/PEGylated lipid/VE}} - (X_{\text{FA/PEGylated lipid}} A_{\text{FA/PEGylated lipid}} + X_{\text{VE}} A_{\text{VE}})] d\Pi \quad (\text{Eq. 15})$$

The symbols in equation 14 and 15 are similar to those in the calculation of excess area.

R is gas constant, T is the absolute temperature and N_A is Avogadro's number.

3.3.10 Loading efficiency of liposome

3.3.10.1 Encapsulation of calcein

Calcein at different mole ratio as dissolved in 50 mM borate buffer pH 8.5 then added into 25 mM fatty acid. The mixture solution was kept stirring until all of the fatty acid dissolved. The resulting mixture was then adjusted to pH 8.5 by 0.5 M NaOH and 0.5 M HCl solution. The encapsulation method for fatty acid containing PEGylated lipid and/or Lecinol S-10 was almost similar to the encapsulation of calcein in pure fatty acid liposome. The only difference being that the fatty acid with PEGylated lipid and/or Lecinol S-10 was firstly dissolved in chloroform followed by removal of chloroform using rotary evaporator. This resulted in the formation of a viscous mixture. Then, buffer solution at ~ 50 °C containing calcein was added into the viscous mixture and stirred. The subsequent process in encapsulation of calcein was similar to those mentioned above for pure fatty acid. A reference solution with only calcein present was prepared and treated in similar manner to the above mentioned method.

3.3.10.2 Encapsulation of DL- α -tocopherol acetate (VE)

Liposome suspensions comprising of 25 mM fatty acid with various mole ratio of VE were prepared. Fatty acid and VE in an appropriate mole ratio was firstly dissolved in chloroform and subsequently dried under rotor evaporator to remove the chloroform. This mixture was then blown with stream of N₂ gas to ensure total removal the trace amount of CHCl₃ followed by rehydration with 50 mM borate buffer at pH 8.5. The pH of the solution was adjusted by 0.5 M sodium hydroxide and 0.5 M hydrochloric acid until pH 8.5 is achieved. Encapsulation of VE in fatty acid liposomes containing

PEGylated lipid in the mole ratio 50 to 1 and/or Lecinol S-10 at the weight ratio of fatty acid to Lecinol S-10 at 10 to 3 were prepared in a similar manner as previously described in the encapsulation of VE in pure fatty acid liposomes. The only difference is that PEGylated lipid and/or Lecinol S-10 was added during the process of dissolving fatty acid and VE.

3.3.10.3 Separation method

Prior to loading efficiency determination of the liposome, the loaded substance must first be separated from the free substance in a liposome suspension. Size exclusion chromatography and ultrafiltration technique or also known as minicolumn method was applied in this study to separate the loaded and the free calcein as well as VE in a liposome suspension. A schematic diagram is shown in figure 3.8 representing the separation of calcein by applying both of the above mentioned method. The principle behind the separation is based on the size of a particle. Larger size particle will first be eluted out followed by smaller size particle as shown in figure 3.8.

(a) Size exclusion chromatography

In size exclusion chromatography, a glass column with length 30 cm and diameter 1 cm was firstly packed with Sepharose 4B as the solid phase whereas liposome suspension solution with concentration just above the CVC was prepared as the eluent. Prior to packing of the column, pretreatment of sepharose 4B was carried out by first washing in deionized water for at least three times followed by washing with eluent for another three times. Then presaturation of sepharose 4B was done by soaking it in the eluent for

half an hour. The pretreatment step is vital in order to avoid breakdown of liposomes due to excessive dilution.

This method was repeated twice for each sample. A sample of 200 μL was introduced dropwise onto the column. Subsequently every 2 mL of eluate was collected and each fraction was diluted with ethanol to a total volume of 5 mL and a clear solution was obtained. However, the total dilution volume depended on the amount of calcein present in the sample. Ethanol was applied instead of Triton-X to overcome the self-quenching effect especially for calcein as proposed by Ishii and Nagasaka [Ishii and Nagasaka, 2001]. In fact, addition of ethanol addresses disruption of the vesicles and consequently fully release those encapsulated species [Nii *et. al.*, 2002].

(b) Ultrafiltration method

In this method, the loaded and free substances were separated by using minicolumn coupled with centrifugation. This method has been widely used to determine the encapsulation efficiency of liposomes [Blume and Cerv, 1993; Mishra *et. al.*, 2006; Garg *et. al.*, 2007; Shimanouchi *et. al.*, 2009; Jithan and Swathi, 2010]. In this method, a plastic syringe of 5 mL was used in the preparation of minicolumn. A small piece of cotton was placed at the bottom of the barrel to avoid leakage prior packing with pretreated Sepharose 4B. Then the minicolumn was inserted into a centrifugal tube so that it would be securely supported at the top of the test tube by the finger grips of the syringe. Excess eluent in the minicolumn was removed by gravity force. A sample of 50 μL liposome suspension solution containing encapsulated and free substance was applied to the Sepharose bed followed by 3×0.5 mL of mobile phase. The minicolumns

were spun at knob 4 for 2 minutes in an MSE centrifuge with swinging buckets. The first fraction to be collected in the centrifugal tube was the substance loaded in liposome. It was diluted to 5 mL with ethanol. The free solutes were retained by the Sepharose 4B and recovered by washing the minicolumn with eluent followed by centrifugation at similar speed for three times. The accumulated eluate from the washing was diluted with ethanol, resulting in a clear solution. This method was repeated at least three times for each sample with a freshly packed syringe.

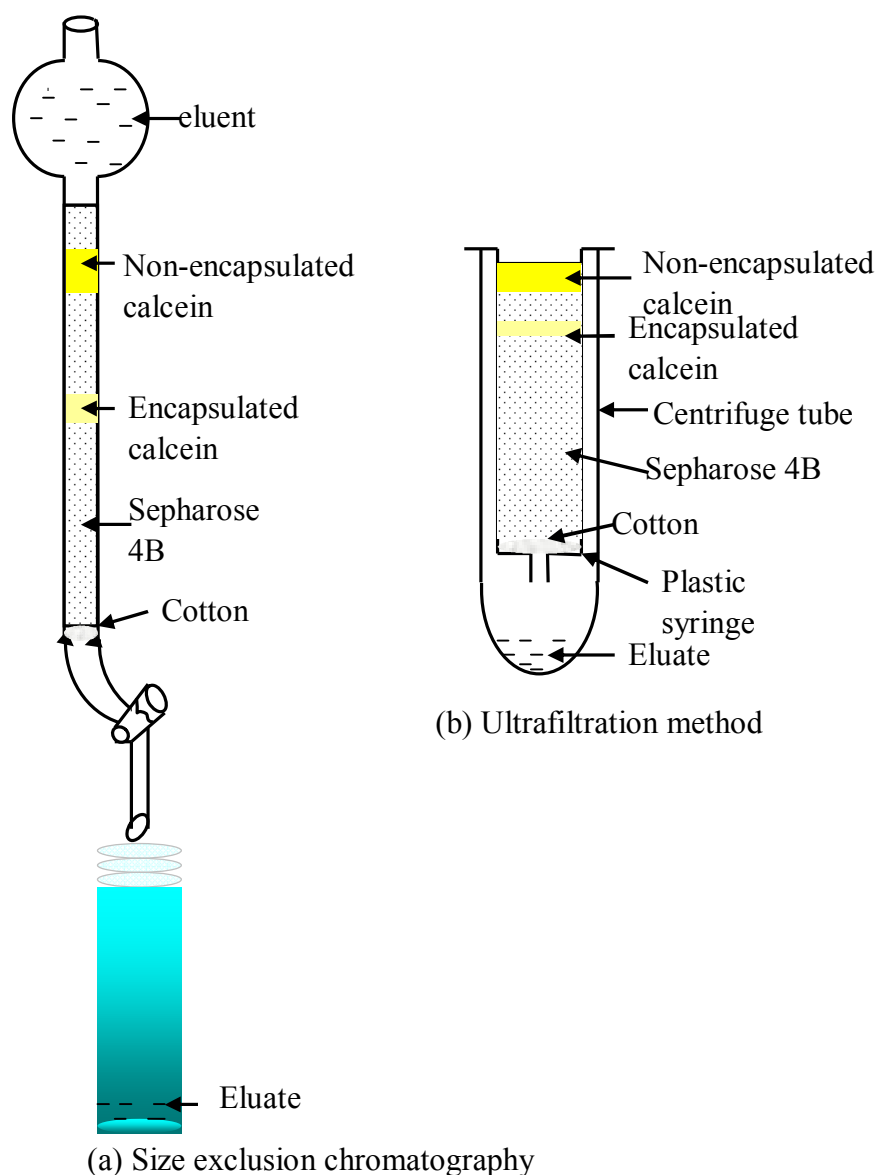


Figure 3.8. Separation of calcein by using (a) size exclusion chromatography and (b) ultrafiltration methods.

3.3.10.4 Determination of loading efficiency

The absorbance for both calcein loaded in liposomes and free calcein in the bulk medium were measured by Varian Cary 50 UV-Vis spectrophotometer at 496 nm which is the maximum absorbance for calcein [Namani *et. al.*, 2007]. The loading efficiency was calculated in the percentage value as written in equation 16.

On the other hand, the amount of VE was analyzed by Shimadzu LC-20AT High Performance Liquid Chromatography (HPLC) coupled with SPD-20A prominence UV/Vis detector. Isocratic mobile phase system composed of a mixture of all HPLC grade solvents; ethanol/methanol/acetonitrile (10 % acetonitrile, 45 % ethanol and 45 % methanol) was delivered to the column at a flow rate of 1 mL min⁻¹. A sample of 20 µL was injected into the C18 reverse phase Purospher[®] Star column with dimension 4.6 mm × 250 mm and the particle diameter of 5 µm. The eluate was monitored at 287 nm, and the detector temperature was set at 25 °C. The percentage of loading efficiency was calculated as stated in equation 16. It was calculated as the percentange value of area under peak at retention time 9.2 min for the loaded VE in liposomes over the total area under peak at the same retention time for both loaded and unloaded VE

$$\text{Loading efficiency (\%)} = \frac{\text{Absorbance or area of loaded substance}}{\text{Absorbance or area of total amount of subsatance}} \times 100\%$$

(Eq. 16)

3.4 References

1. Bae, D.H., Shin, J.S., Jin, F.L., Shin, G.S. and Park, S.J. (2009). *Bull. Korean Chem. Soc.* **30**(2), 339.
2. Blume, G. and Cevc, G. (1993). Molecular Mechanism of the Lipid Vesicle Longevity *In Vivo*. *Biochim. Biophys. Acta* **1146**, 157.
3. Crisp, D.I. in: Danielli, J.F., Pankhurst, K.G.A. and Riddeford A.C. (Eds.), (1958). *Surface Phenomena in Chemistry and Biology* Pergamon Press, London, 17.
4. Garg, M., Dutta, T. and Jain, K.N. (2007). *AAPS PharmSciTech.* **8**(2), 38.
5. Ishii, F. and Nagasaka, Y. (2001). *Journal of Dispersion Science and Technology* **22**, 97.
6. Jithan, A.V. and Swathi, M. (2010) *International Journal of Pharmaceutical Sciences and Nanotechnology* **3**(2), 986-993.
7. Mishra, N., Gupta, P.N., Mahor, S., Khatri, K., Goyal, A.K. and Vyas, S.P. (2006). *Indian Journal of Experimental Biology* **45**, 237.
8. Namani, T., shikawa, T., Morigaki, K. and Walde, P. (2007). *Coll. Surf. B: Biointerfaces.* **54**, 118-123.
9. Nii, T., Takamura, A., Mohri, K. and Ishii, F. (2002). *Colloids and Surfaces B: Biointerfaces* **27**, 323.
10. Popiel, W.J. (1978). *Introduction to colloid science (1st edition)* New York: Exposition 52.
11. Shimanouchia, T., Ishii, H., Yoshimotob, N., Umakoshia, H. and Kuboia, R. (2009). *Colloids and Surfaces B: Biointerfaces* **73**, 156.
12. Silva, da A.M.G., Guerreiro, J.C., Rodrigues, N.G. and Rodrigues, T.O. (1996). *Langmuir* **12**, 4442.

4.1 Titration curve

The appropriate pH range for the formation of liposomes for each fatty acid namely palmitoleic acid, oleic acid, linoleic acid, linolenic acid and their mixtures with DPPE-PEG2000, DPPE-PEG5000 and/or Lecinol S-10 were identified from the equilibrium titration curve as shown in figure 4.1 and 4.2. At pH greater than pH 9.5, all of the solutions were observed as clear, regardless the composition of solutions. This is an indication that all of the fatty acid molecules were in fully ionized form and soluble in the solution. At an increased concentration of hydrochloric acid with pH at around 9, the solutions appeared to be slightly turbid arising from scattering of larger particles in the aqueous suspension. At this region, only a small change of pH was observed with respect to the amount of hydrochloric acid added as shown in figure 4.1 and figure 4.2. This is due to the buffering effect of fatty acid owing to the presence of both ionized and non-ionized fatty acid molecules in solution. It has been reported that liposomes were observed at the pH regions that are close to the pK_a s of the fatty acids. The pK_a s for all of the solutions prepared in this study were estimated from the titration equilibrium plots and shown in table 4.1. The pK_a s for mixed solutions do not show a large variation as can be seen from table 4.1. At the pH range approximating to pK_a , about half of the amount of the corresponding acid are ionized and promote the formation of pseudo-double-chain amphiphile through hydrogen bonding. This pseudo-double-chain amphiphile is smaller in head group size compared to the apparent fatty acid monomer and brings to a more cylindrical molecular shape that favors the formation of bilayer and hence liposomes. Further addition of hydrochloric acid into the solution results in the formation of milky solution and oil droplet. This is due to the formation of emulsion and further to phase separation whereby all of carboxylate group were protonated to carboxylic acid in the presence of excess hydrochloric acid.

Table 4.1 The pKa for fatty acid and their mixture with PEGylated lipid and Lecinol S-10.

pKa	Pure FA	FA + Lecinol S-10	FA + DPPE- PEG2000	FA + DPPE- PEG2000 + Lecinol S-10	FA + DPPE- PEG5000	FA + DPPE- PEG5000 + Lecinol S-10
Palmitoleic acid	8.2	8.2	8.1	7.8	8.0	8.6
Oleic acid	8.2 (9.85)*	9.7	8.9	8.7	8.9	8.7
Linoleic acid	8.7 (9.24)*	8.5	8.5	8.4	8.3	8.7
Linolenic acid	8.5 (8.25)*	8.3	8.3	7.6	8.1	9.3

* Kanicky and Shah, 2002

The titration result revealed that the trend of titration curve is almost similar regardless the fatty acid type. Their buffering regions were extended to pH 7.5 compared to pH 8.0 as the degree of unsaturation at the hydrocarbon chain increased. Both figures 4.1 and 4.2 also showed that addition of DPPE-PEG2000, DPPE-PEG 5000 into fatty acid solutions did not significantly change the trend of equilibrium curve. The ratio of fatty acid to PEGylated lipid is fixed at 50 to 1. Further explanation on the selection of this ratio will be discussed in the sub section 4.6.1. However, addition of DPPE-PEG5000 into mixture of fatty acid with Lecinol S-10 solution caused a different feature on the equilibrium titration curve. We found that pH of this ternary mixture solution drop markedly during addition of hydrochloric acid, an obvious buffer region is not revealed.

On the other hand, the appropriate pH for the formation of liposomes is also estimated from the change of mean particle size and zeta potential with respect to pH of the mixture solution. As we have mentioned earlier, phase transitions have occurred during the titration of fatty acid solution from highly basic to acidic. Therefore the changes of particle size and zeta potential are also expected to vary. From figures 4.3 – 4.6, we found that the trend of change in mean particle size and zeta potential with pH is almost similar for all of the fatty acid solution as well as their mixtures. During the addition of hydrochloric acid into the alkaline fatty acid solution, the mean particle size dropped to a smaller size region from pH 9 to about pH 8. Further addition of hydrochloric acid would induce the formation of larger particle. This is deduced as the appropriate pH range for the formation of liposomes was from pH 8 to 9. The results obtained here are in agreement with those reported elsewhere for liposomes form from oleic acid and linoleic acid [Rogerson *et. al.*, 2006].

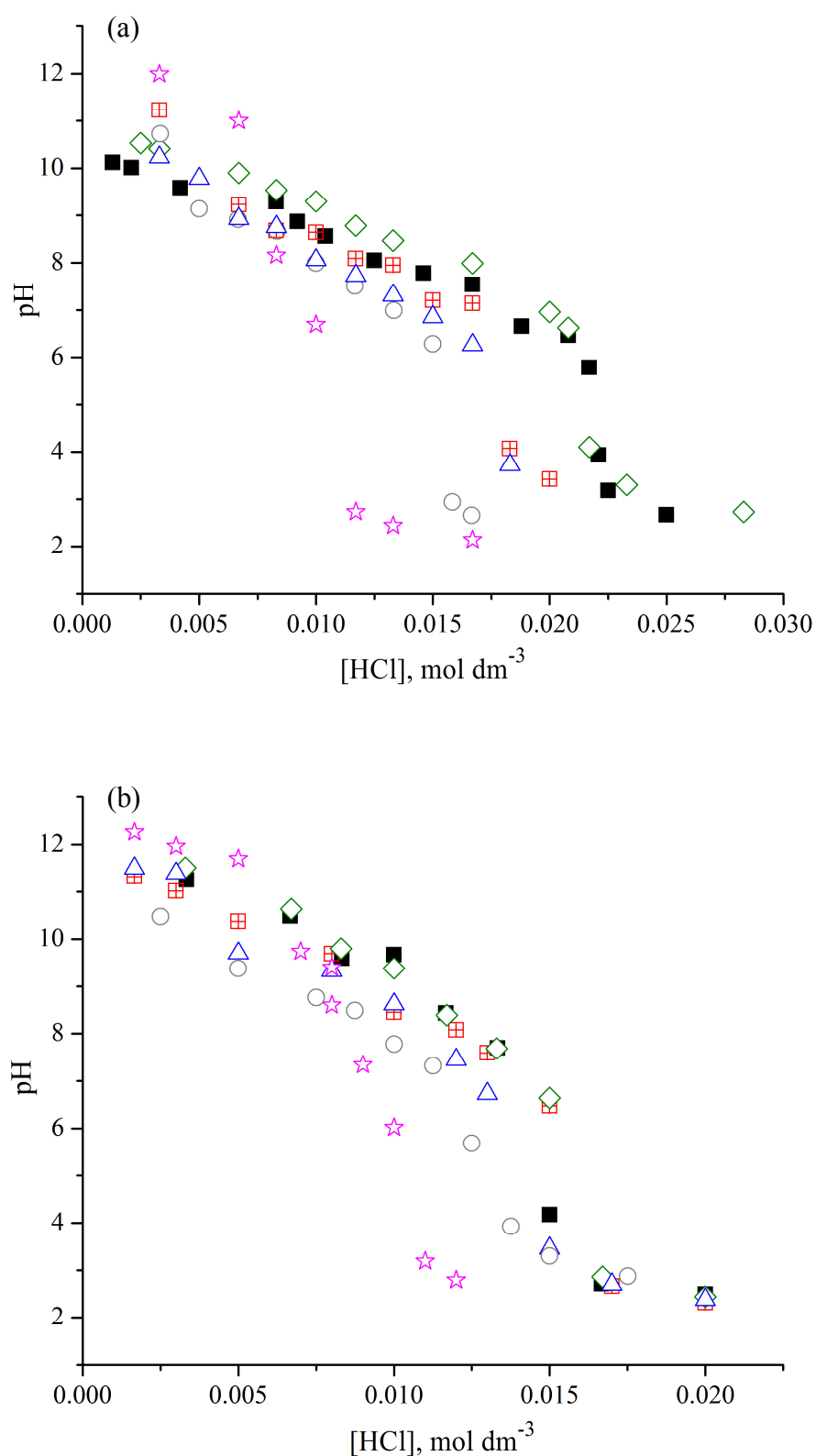


Figure 4.1. Equilibrium titration curve for (12.50 ± 0.05) mM (a) palmitoleic acid and (b) oleic acid with their mixture solutions at 28 °C. ■ pure fatty acid, ■ FA+Lecinol S-10, ◇ FA + DPPE-PEG2000, △ FA + DPPE-PEG2000 + Lecinol S-10, ○ FA + DPPE-PEG5000, ☆ FA+ DPPE-PEG5000 + Lecinol S-10.

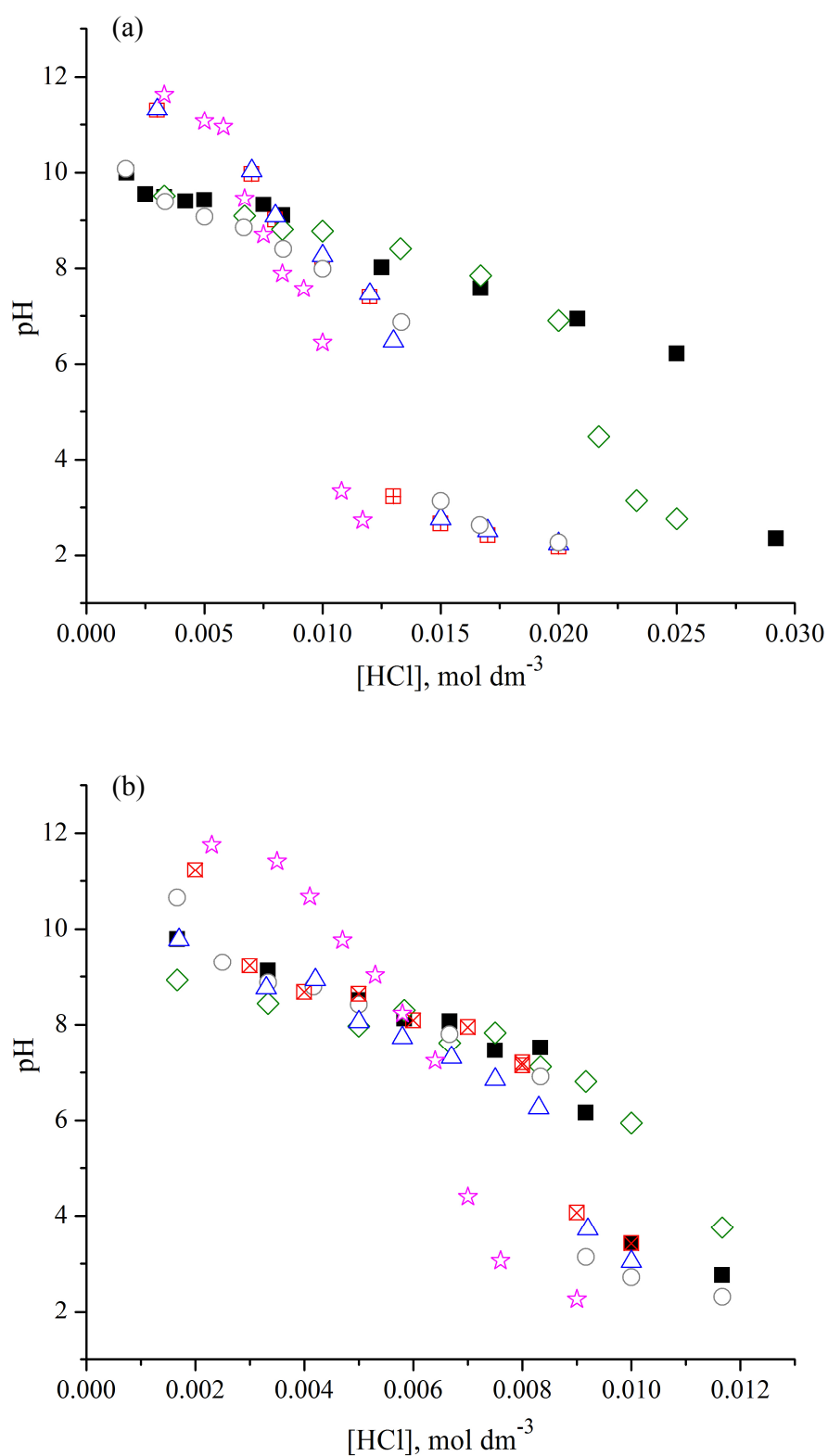


Figure 4.2. Equilibrium titration curve for (12.50 ± 0.05) mM (a) linoleic acid and (b) linolenic acid with their mixture solutions at 28 °C. ■ pure fatty acid, ■ FA+Lecinol S-10, ◇ FA + DPPE-PEG2000, △ FA + DPPE-PEG2000 + Lecinol S-10, ○ FA + DPPE-PEG5000, ☆ FA+ DPPE-PEG5000 + Lecinol S-10

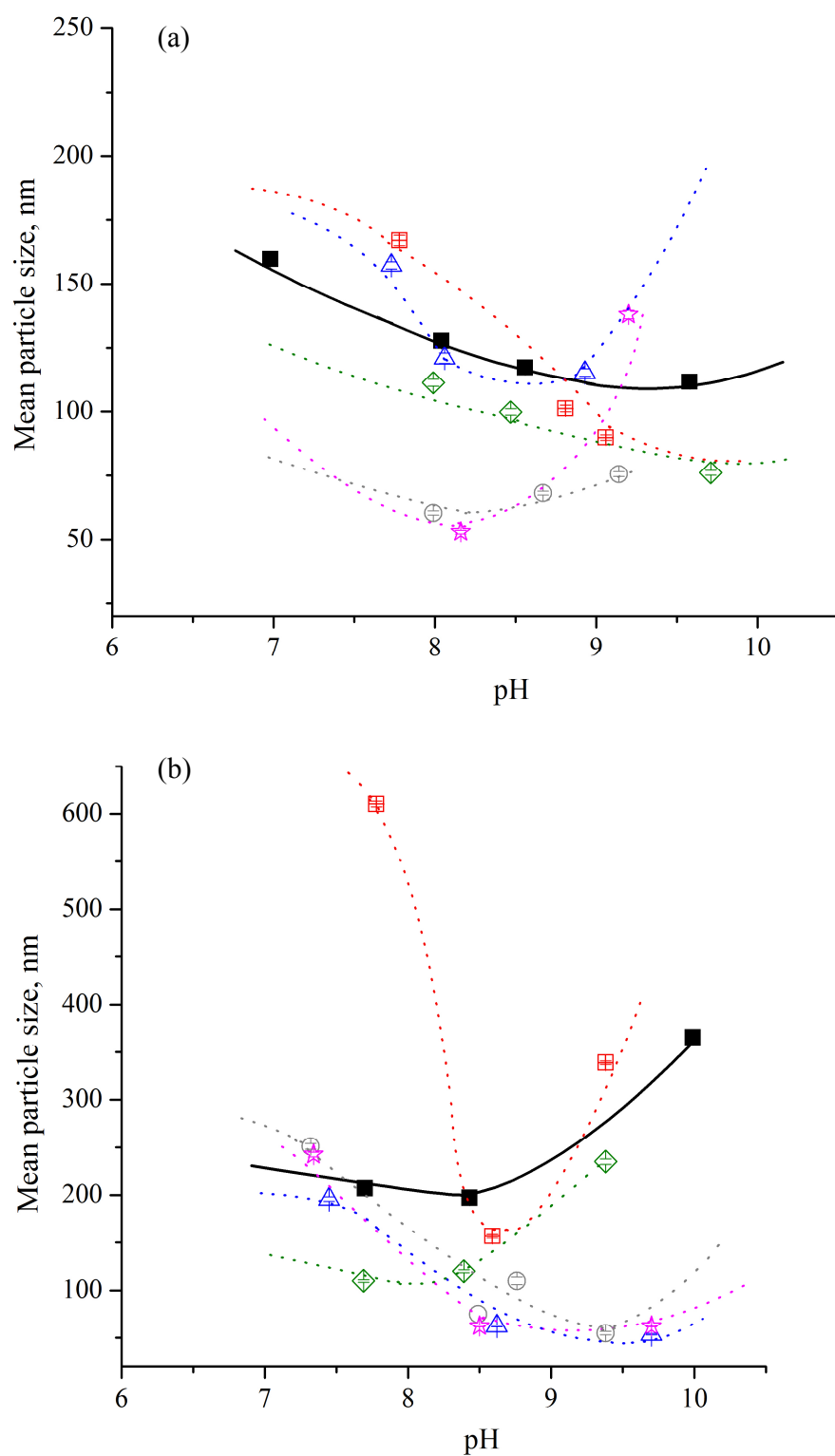


Figure 4.3. Changes of mean particle size with respect to pH for (a) palmitoleic acid and (b) oleic acid with their mixture solutions at 30 °C. ■ pure fatty acid, ■ FA+Lecinol S-10, ◇ FA + DPPE-PEG2000, △ FA + DPPE-PEG2000 + Lecinol S-10, ○ FA + DPPE-PEG5000, ☆ FA+DPPE-PEG5000 + Lecinol S-10.

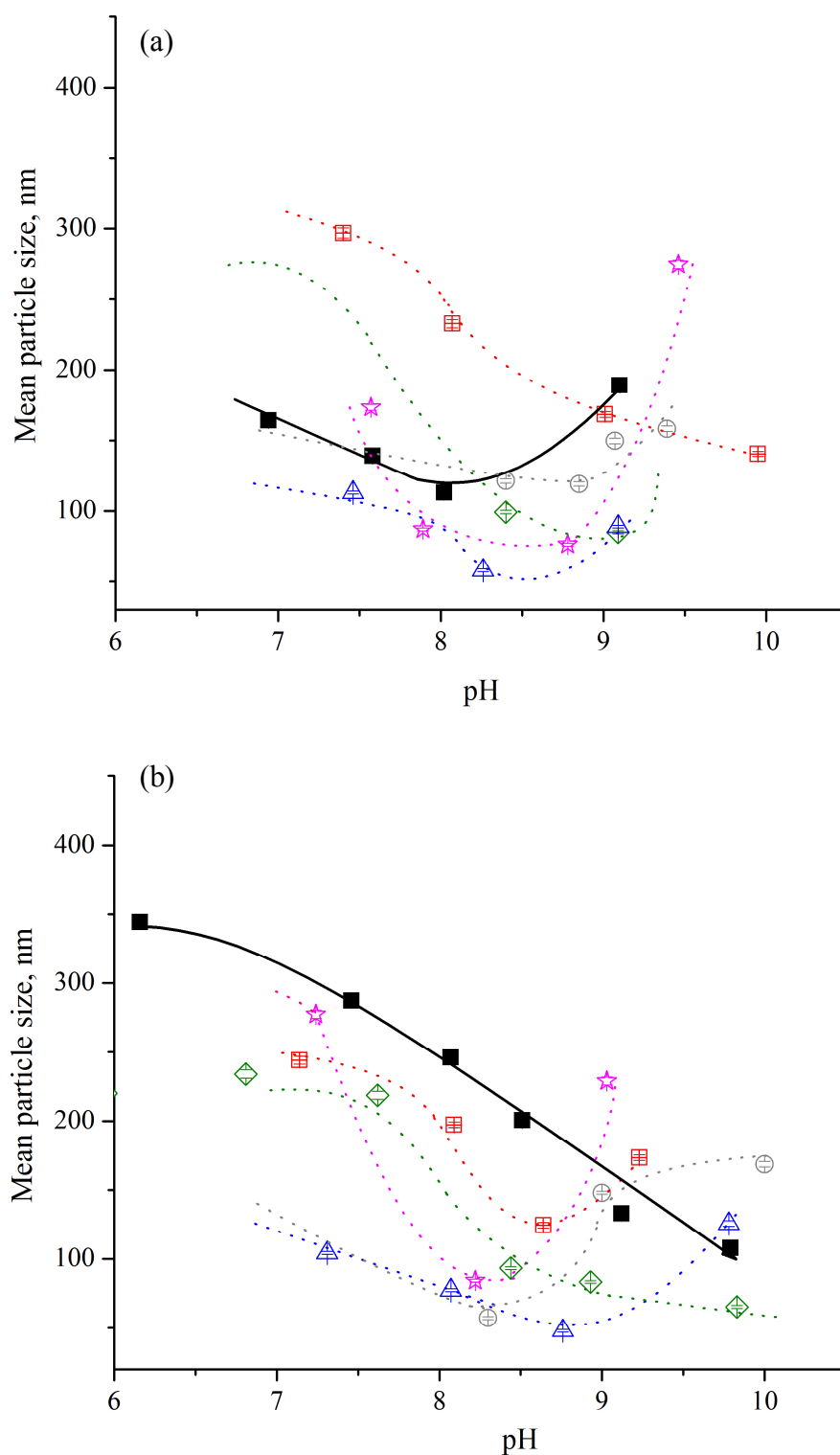


Figure 4.4. Changes of mean particle size with respect to pH for (a) linoleic acid and (b) linolenic acid with their mixture solutions at 30 °C. ■ pure fatty acid, ▣ FA+Lecinol S-10, ◇ FA + DPPE-PEG2000, △ FA + DPPE-PEG2000 + Lecinol S-10, ○ FA + DPPE-PEG5000, ☆ FA+ DPPE-PEG5000 + Lecinol S-10.

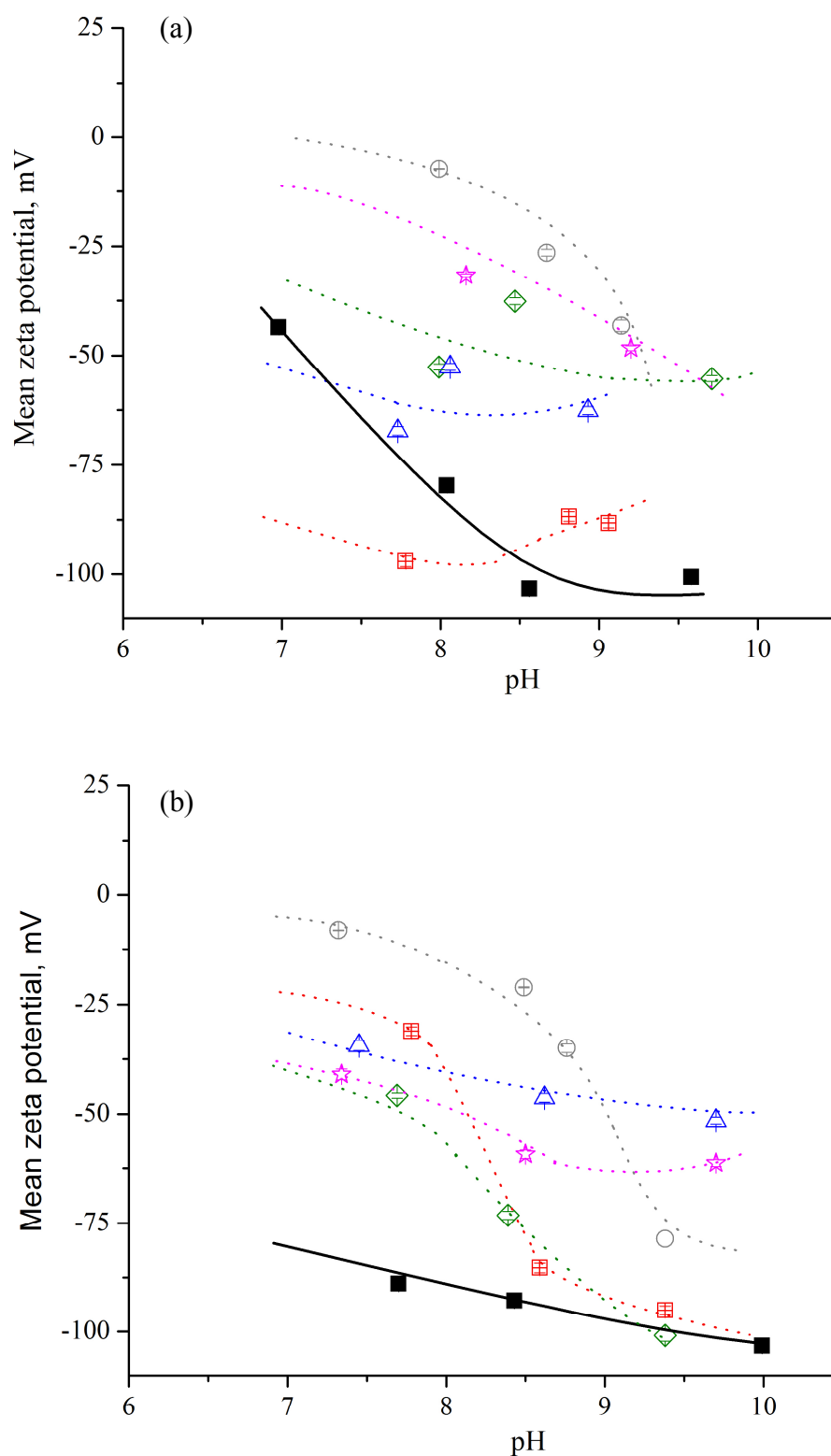


Figure 4.5 Changes of mean zeta potential for (a) palmitoleic acid and (b) oleic acid with their mixture solutions as a function of pH at 30 °C. ■ pure fatty acid, ▣ FA+Lecinol S-10, ◇ FA + DPPE-PEG2000, △ FA + DPPE-PEG2000 + Lecinol S-10, ○ FA + DPPE-PEG5000, ☆ FA+ DPPE-PEG5000 + Lecinol S-10.

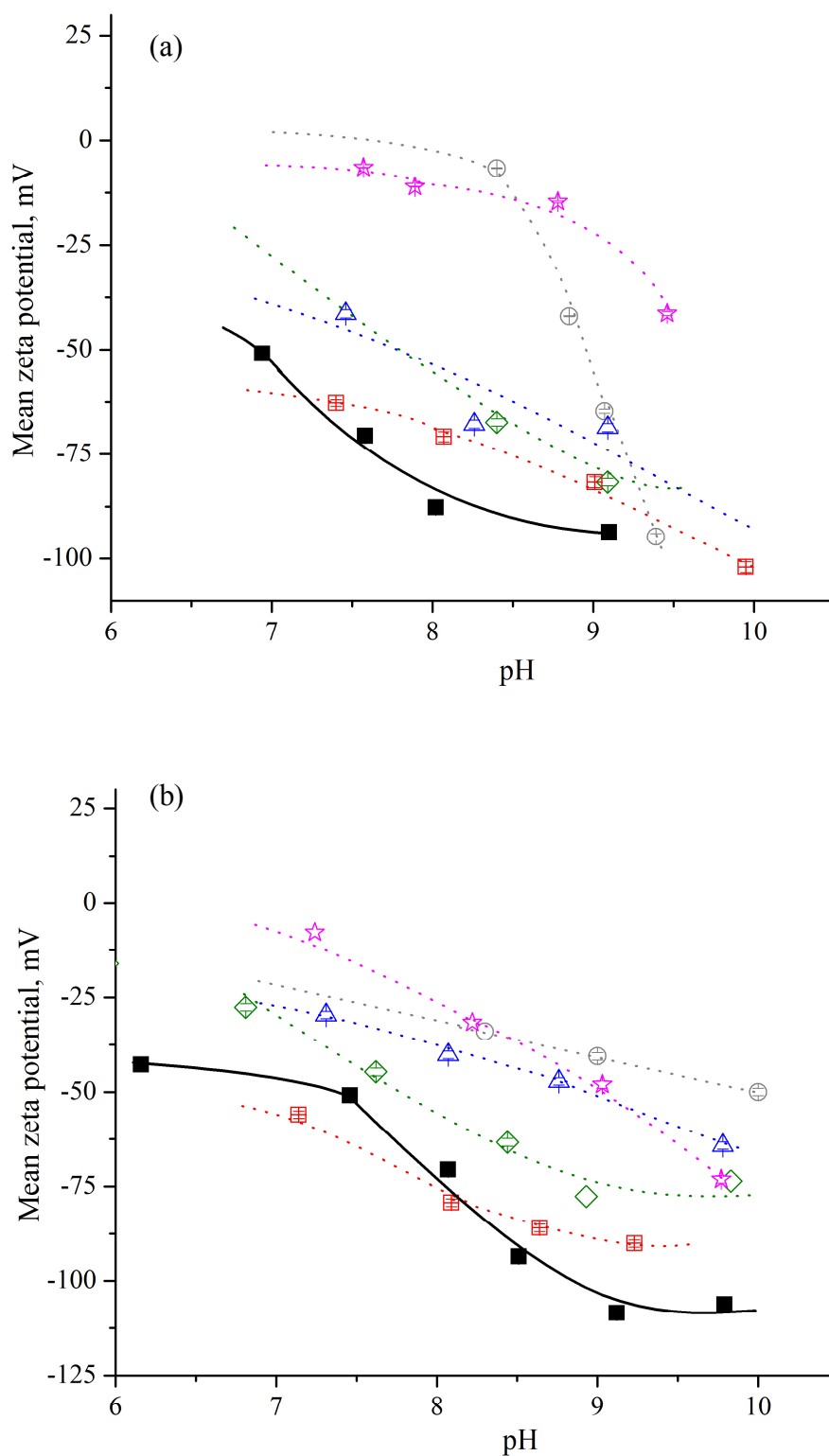


Figure 4.6. Changes of mean zeta potential for (a) linoleic acid and (b) linolenic acid with their mixture solution as a function of pH at 30 °C. ■ pure fatty acid, ▣ FA+Lecinol S-10, ◇ FA + DPPE-PEG2000, △ FA + DPPE-PEG2000 + Lecinol S-10, ○ FA + DPPE-PEG5000, ☆ FA+ DPPE-PEG5000 + Lecinol S-10.

4.2 Critical vesiculation concentration (CVC)

CVC is a quantitative parameter which is referred to as the minimum concentration to estimate the tendency of fatty acid and their mixture self assemble to form a bilayer structure of liposomes. This parameter mainly depends on the solubility of fatty acid and hydrophobicity of the acyl chain. The lower value of CVC suggests that the self assembly of fatty acid molecules into bilayer structure is more favorable. In this study, the effect of DPPE-PEG2000 and DPPE-PEG5000 on CVC of palmitoleic acid, oleic acid, linoleic acid and linolenic acid as well as the mixtures of fatty acid and Lecinol S-10 were investigated by using surface tension method. CVC is affected not only by the molecular structure of the molecules but also condition of the medium such as pH, temperature and salinity.

The influence of temperature on CVC was studied. All CVC values were determined at the inflection point of a plot of mean surface tension as a function of natural logarithm concentration of fatty acid as shown in figures 4.7 – 4.10 for palmitoleic acid, oleic acid, linoleic acid and linolenic acid. The CVC for all of the solution prepared did not change significantly with the temperature range in this study. As expected, surface tension for all of the solutions in this study was observed to decrease with an increase in temperature. This is due to weaker intermolecular interactions among the molecules, leading to lower surface energy and also surface tension [Drost, 1965; Hoke and Patton, 1992; Hoke and Chen, 2001].

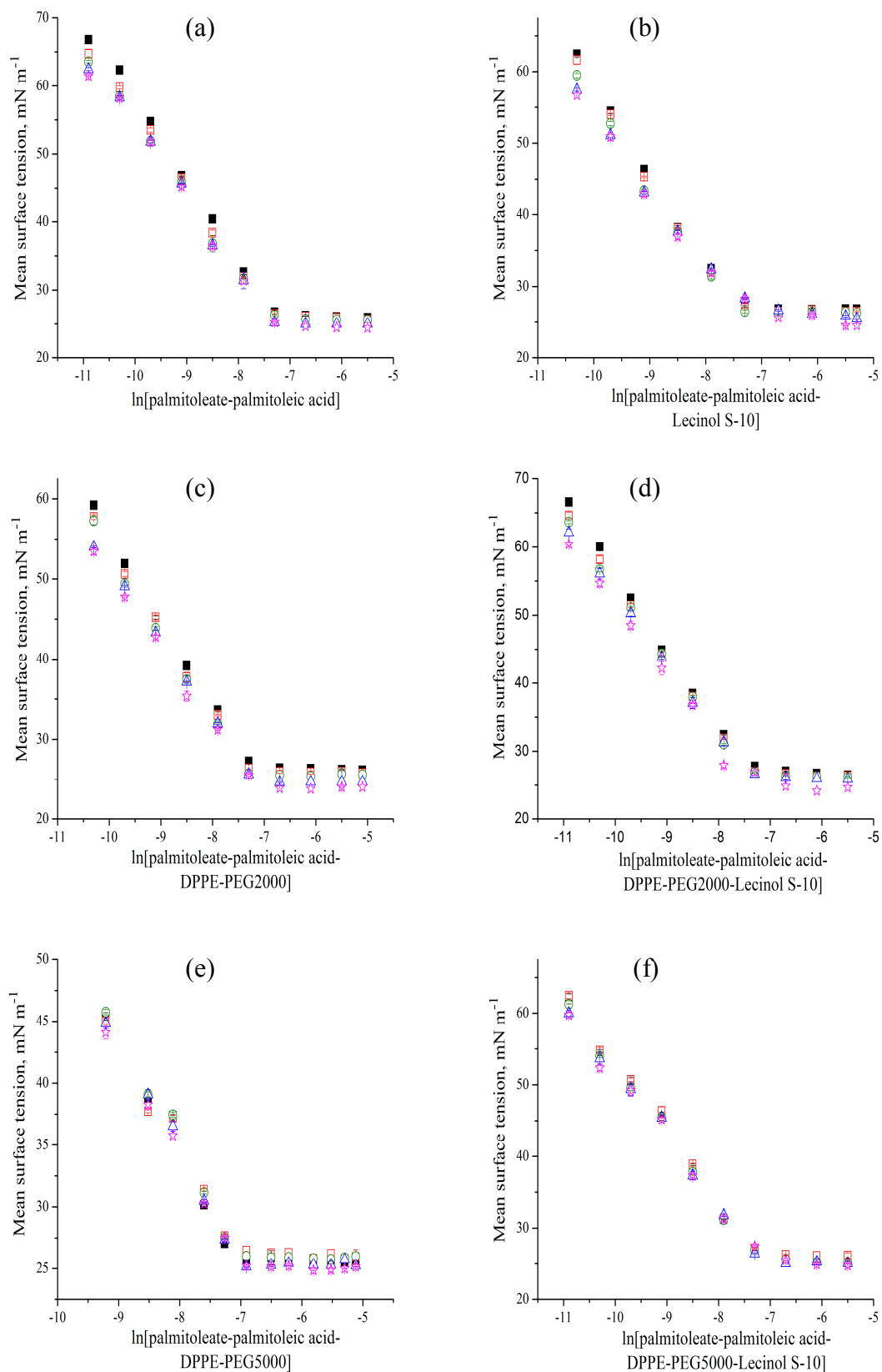


Figure 4.7. Variation in mean surface tension for different concentration of (a) palmitoleic acid solution and their mixtures with (b) Lecinol S-10, (c) DPPE-PEG2000, (d) DPPE-PEG2000-Lecinol S-10, (e) DPPE-PEG5000 and (f) DPPE-PEG5000-Lecinol S-10 at 20.0 °C to 40.0 °C. ■ = 20 °C, □ = 25 °C, ○ = 30 °C, △ = 35 °C and ☆ = 40 °C. Error bars indicate S.D. for $N = 5$.

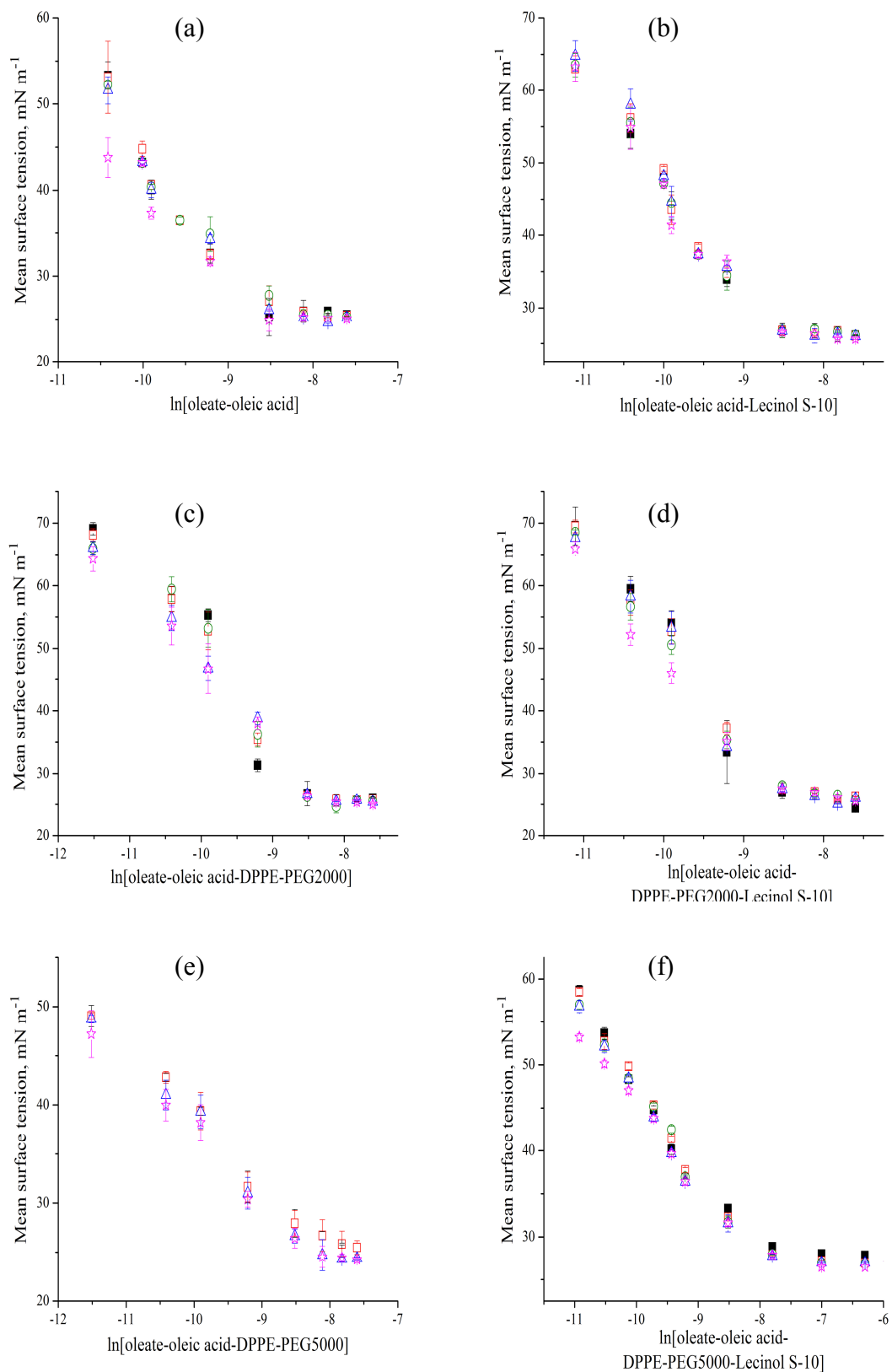


Figure 4.8. Variation in mean surface tension for different concentration of (a) oleic acid solution and their mixtures with (b) Lecinol S-10, (c) DPPE-PEG2000, (d) DPPE-PEG2000-Lecinol S-10, (e) DPPE-PEG5000 and (f) DPPE-PEG5000-Lecinol S-10 at 20.0 °C to 40.0 °C. ■ = 20 °C, □ = 25 °C, ○ = 30 °C, △ = 35 °C and ☆ = 40 °C. Error bars indicate S.D. for $N = 5$.

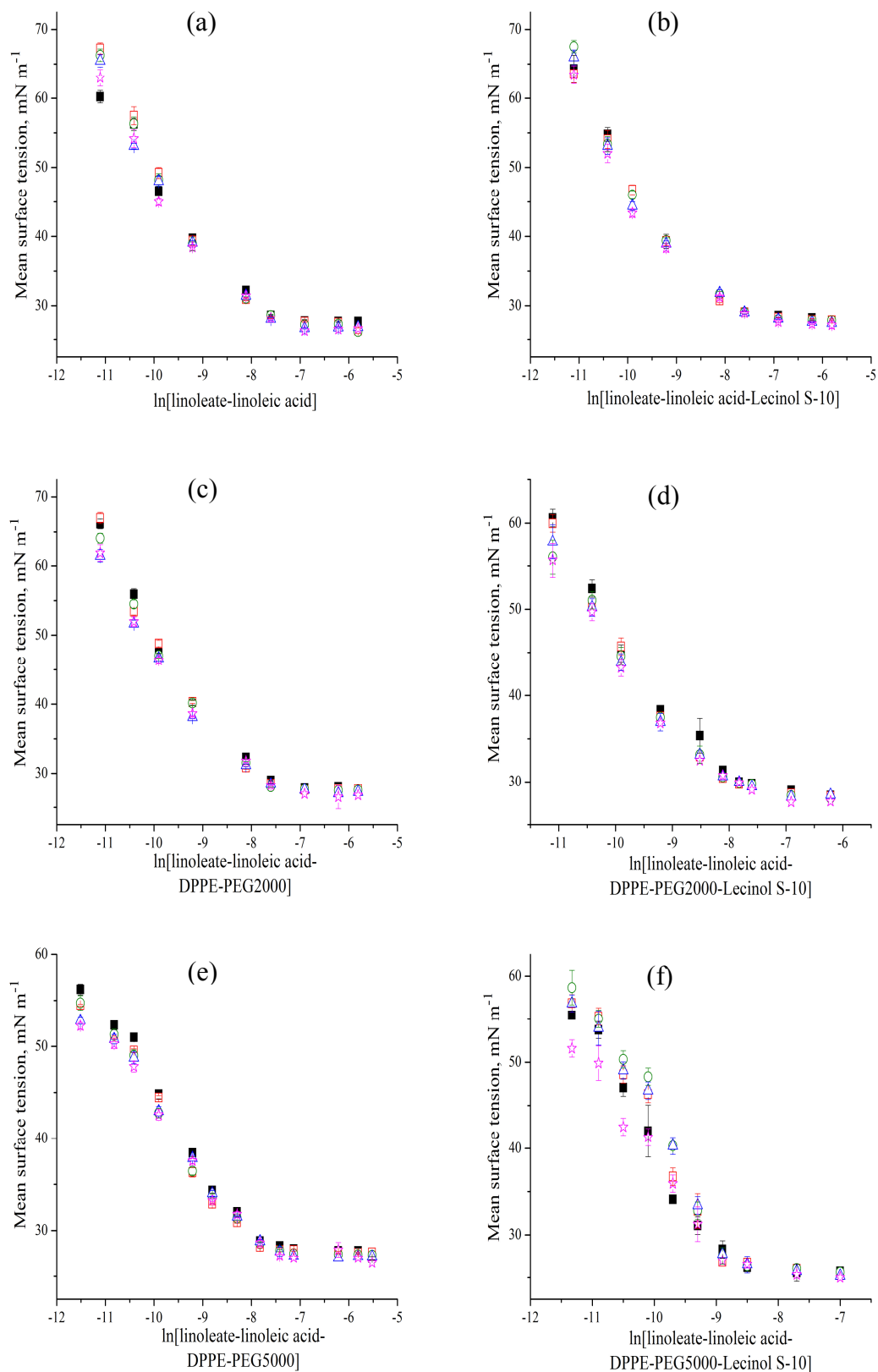


Figure 4.9. Variation in mean surface tension for different concentration of (a) linoleic acid solution and their mixtures with (b) Lecinol S-10, (c) DPPE-PEG2000, (d) DPPE-PEG2000-Lecinol S-10, (e) DPPE-PEG5000 and (f) DPPE-PEG5000-Lecinol S-10 at 20.0 °C to 40.0 °C. ■ = 20 °C, □ = 25 °C, ○ = 30 °C, △ = 35 °C and ☆ = 40 °C. Error bars indicate S.D. for $N = 5$.

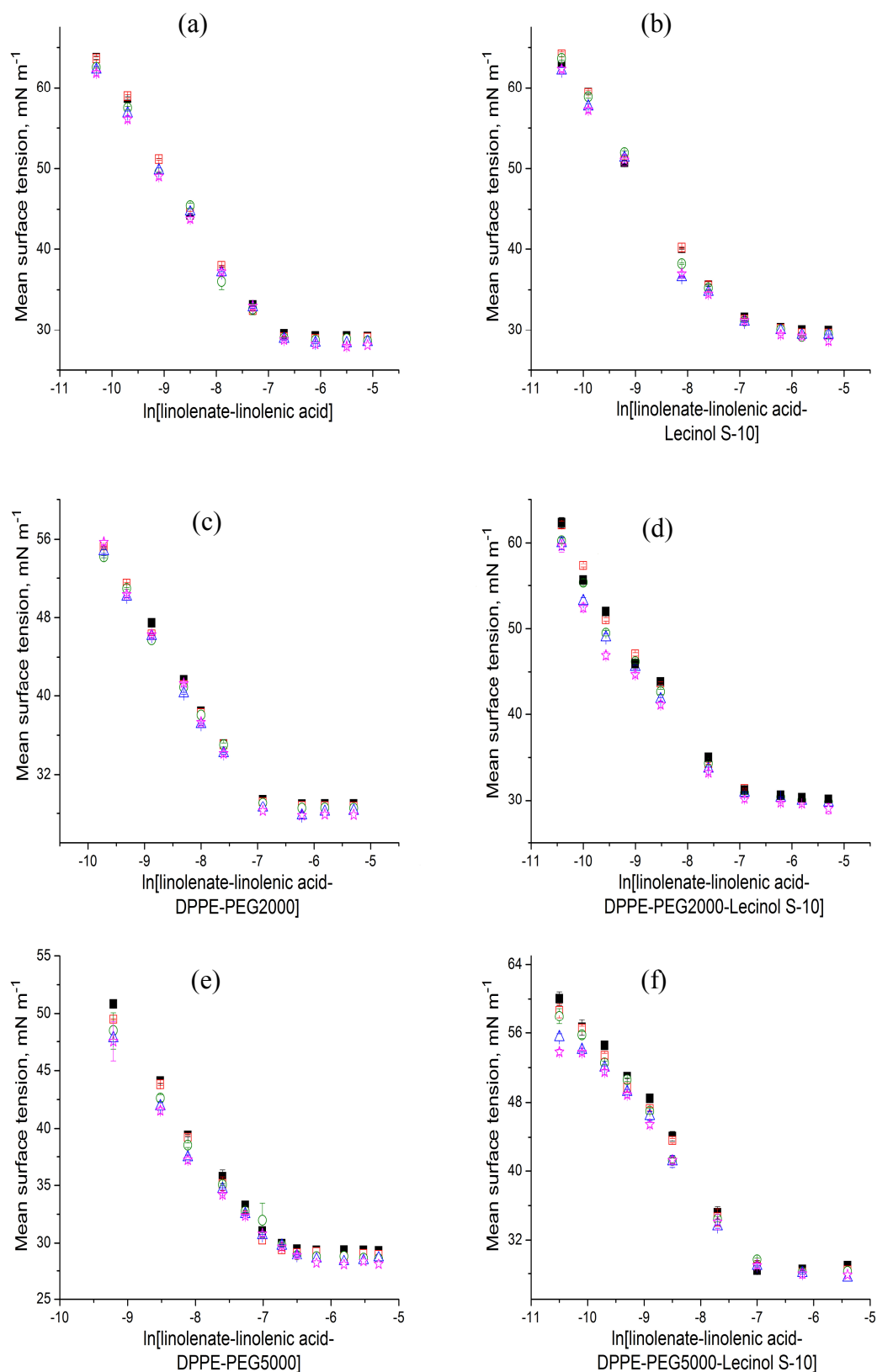


Figure 4.10. Variation in mean surface tension for different concentration of (a) linolenic acid solution and their mixtures with (b) Lecinol S-10, (c) DPPE-PEG2000, (d) DPPE-PEG2000-Lecinol S-10, (e) DPPE-PEG5000 and (f) DPPE-PEG5000-Lecinol S-10 at 20.0 °C to 40.0 °C. ■ = 20 °C, □ = 25 °C, ○ = 30 °C, △ = 35 °C and ☆ = 40 °C. Error bars indicate S.D. for N = 5.

In addition to the effect of temperature on CVC, we also study the effect of hydrocarbon chain length, degree of unsaturation at the acyl chain of fatty acid as well as the mix substances in the formation of fatty acid liposomes. Figure 4.11 shows the variation of CVC at 30 °C for C18 fatty acid and table 4.2 listed the CVC for palmitoleic acid at 30 °C with respect to the factors that have just been mentioned. Among the fatty acid used in this study, CVC for oleic acid is found to be the lowest whereas linolenic acid has the highest value of CVC. Nevertheless, CVC for palmitoleic acid is relatively higher than oleic acid. In general, the strength of hydrophobicity is weaker if the hydrocarbon chain length is shorter and the number of unsaturated double bond in the aliphatic chain is higher. Therefore, palmitoleic acid molecules with shorter chain length are less hydrophobic and more soluble in an aqueous solution than oleic acid molecules which leads to higher CVC. On the other hand, oleic acid possessing only one unsaturated double bond in the aliphatic chain has a stronger hydrophobicity property compared to linoleic acid and linolenic acid both having the same chain length but different in degree of unsaturation. Hence, oleic acid molecules are less soluble in an aqueous solution. This further explains why oleate-oleic acid solution indicated the lowest CVC value. Similarly, linolenate-linolenic acid solution that corresponds to three unsaturated double bonds has the highest CVC value owing to the fact that it has the weakest hydrophobicity property. The similar trend was observed for liposomes with incorporation of DPPE-PEG2000, DPPE-PEG5000 and Lecinol S-10. However, CVC values are higher with the presence of DPPE-PEG2000 and DPPE-PEG5000 compared to those without addition of PEGylated lipid. This is due to the presence of PEGylated lipid as anionic molecules in the solution that increases the ratio of ionized to non-ionized molecules that perturbs the formation of pseudo-double chain amphiphile. Thus, higher amounts of non-ionized fatty acid molecules are required to maintain the ratio of ionized to non-ionized molecule that is appropriate for the formation of liposome. It can

be achieved by increasing the concentration of fatty acid while maintaining the pH of the solution. Nevertheless, the increase in CVC is more pronounced for mixture of fatty acid and DPPE-PEG5000 compared to DPPE-PEG2000. The plausible reason is due to the presence of bulky polyethoxylate chain in DPPE-PEG5000 that increases the steric repulsion force and thereby inhibits self-assembly at low concentration of fatty acid [Mohanty and Dey, 2006].

CVC for liposomes prepared from mixture composing Lecinol S-10 were found comparably lower. This indicates that the cooperative participation of Lecinol-S10 in the formation of liposomes is more favorable as generally understood than phospholipids induce liposome formation. The reason could be due to an increase in the hydrophobicity in the system arising from the addition of lecithin in the solution and that later facilitates the assembly of fatty acids to form liposome even at low concentration of fatty acid.

Table 4.2 CVC for palmitoleic acid and their mixtures at 30 °C.

Substance	CVC, mM
Pure palmitoleic acid	0.67
Lecinol S-10	0.62
DPPE-PEG2000	0.75
DPPE-PEG2000 + Lecinol S-10	0.64
DPPE-PEG5000	0.91

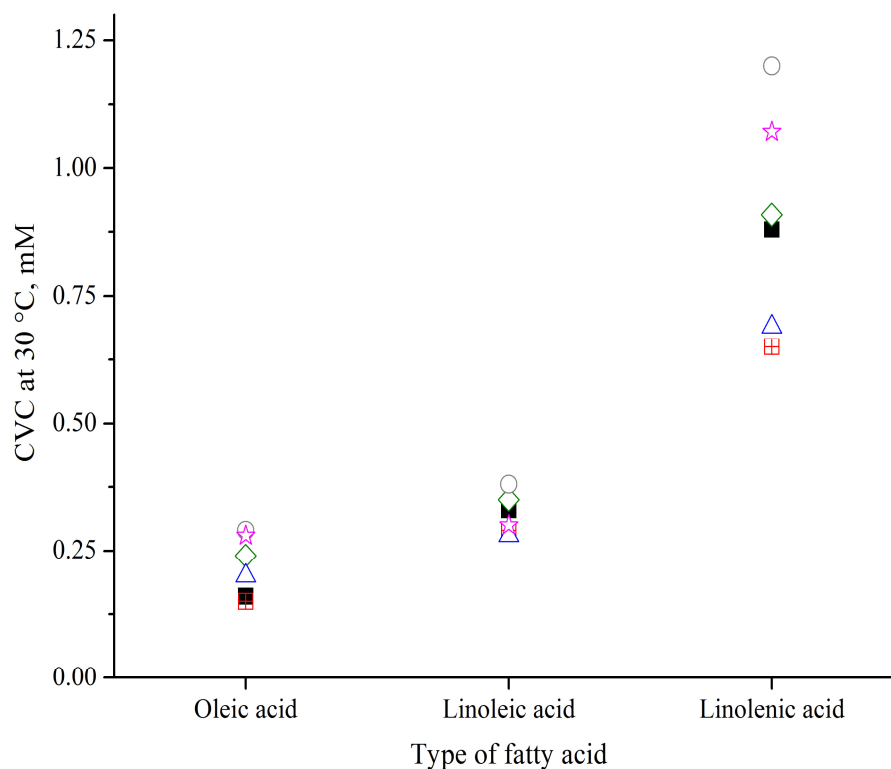


Figure 4.11. CVC at 30 °C as a function of C18 fatty acid mixtures. ■ pure fatty acid, ▣ FA+Lecinol S-10, ◇ FA + DPPE-PEG2000, △ FA + DPPE-PEG2000 + Lecinol S-10, ○ FA + DPPE-PEG5000, ☆ FA+ DPPE-PEG5000 + Lecinol S-10.

4.3 Stability of fatty acid liposomes

4.3.1 Particle size

Physical stability of liposome also referred as colloidal stability which means the liposomes do not aggregate into cluster at a significant rate. By monitoring the change in particle size over time, the stability of liposome suspension can be evaluated. All of the data for mean particle size of the liposome in this study are based on scattering intensity distribution. The factor that may influence the particle size of liposome includes the method for preparation of liposome, pH of the bulk solution, molecular structure and the composition of the substances in formation of liposome. The following discussion will be focused on the effect of molecular structure and composition of liposomes.

Fatty acid molecules with different acyl chain length and degree of unsaturation may result in variation of liposome size. It is expected that the presence of more saturated bonds in the hydrocarbon chain; the larger the size of the liposome that will be formed. The plausible explanation could be the nature of intermolecular interaction that caused more stacking in the membrane as the number of unsaturation bond is less, thus leading to the formation of a more rigid and “flatter” bilayer. On the other hand, unsaturated fatty acid with *cis* conformation whereby the hydrogen atoms that bonded to carbon atoms in the double bond are positioned on the same side and therefore they create a kink in the hydrocarbon chain. In addition, they also create free electron or slightly negatively charge surrounding the double bond and results in repelling between the molecules. Therefore, by increasing the degree of unsaturation in the lipid acyl chain may cause more bends and kinks in the molecule and result in a higher degree of freedom in rotational motion of the molecules. As a result, molecules in the bilayer are loosely packed and hence an increase in the bilayer fluidity. This resulting in a more flexible bilayer with higher curvature and tends to form a smaller size liposome [Stubbs *et. al.*, 1981; Keough *et. al.*, 1987; Cevc, 1991; Liu and Park, 2010].

The mean particle size and zeta potential of fatty acid liposome suspension solutions with their mixture such as DPPE-PEG2000, DPPE-PEG5000 and Lecinol S-10 were monitored for a period of 30 days at fatty acid concentration of 2 mM which is well above their CVC value. Figures 4.12, 4.13, 4.15 and 4.16 demonstrated the changes of these two parameters over a period of time. As we observed in figure 4.12 and 4.13, the particle size of liposomes that formed from only fatty acids were found larger than those with addition of PEGylated lipid and/or Lecinol S-10. Their mean particle size was about 140 nm – 200 nm and the distribution of size was expressed as polydispersity index 0.1 – 0.5 as a result of their polydispersity nature. Particle size for palmitoleate-palmitoleic acid liposome was found slightly larger than oleate-oleic acid liposome.

Although both of the fatty acids comprise of one unsaturated double bond, additional of two methylene group in the acyl chain of oleic acid promotes a higher flexibility in the molecule than in palmitoleic acid. Hence, thickness of the bilayer for oleate-oleic acid is expected to be less than the fully extended hydrocarbon chain length due to the more fluidic property of the lipid bilayer compared to bilayer of palmitoleate-palmitoleic acid with shorter acyl chain length. Hence the bending rigidity for bilayer of oleate-oleic acid is less and therefore encourages the formation of liposomes with a higher curvature.

On the other hand, particle size for liposomes formed from oleate-oleic acid molecules was found to be the largest whilst linolenate-linolenic acid liposomes were the smallest. By comparing the three types of fatty acids with the same hydrocarbon chain length but different in degree of unsaturation, bilayer formed from oleate-oleic acid with only one unsaturation is considered to be less flexible due to a lower degree of freedom in the motion of hydrocarbon chain which leads to a closer packing of the molecules forming a more rigid bilayer. Hence less curvature of bilayer was formed leading to the formation of larger liposomes. On the other hand, molecules with two or more unsaturations are likely to form a more flexible bilayer than the mono unsaturated fatty acid. Convolution of this dynamics and more fluidic bilayer may promote the formation of high curvature liposome and therefore smaller particle size. This explains the formation of smaller size linolenate-linolenic acid liposomes compared to the other type of fatty acids.

The presence of Lecinol S-10 in the formation of fatty acid liposomes causes suppression in the size of liposomes regardless the type of fatty acids. This suggests a cooperative participation of Lecinol S-10 in the formation of fatty acid bilayer. The reduction in particle size of liposome is directly related to the curvature principle of the bilayer. Lower bilayer curvature will form larger size liposomes whereas higher bilayer curvature will result in smaller size liposomes. The spontaneous curvature of a bilayer is

determined by the uneven distribution of composition in both the inner leaflet and outer leaflet of the bilayer. If both layers are symmetric either physically or chemically, the resulting spontaneous curvature is equal to zero. Therefore, bilayer with only one component can not result in a non-zero spontaneous curvature. However, spontaneous curvature may exist in the environment with asymmetry distribution of composition in a bilayer [Safran *et. al.*, 1990]. In our study, Lecinol S-10 with the major component composing of 39 % PC and 38 % PE that attached to two long saturated hydrocarbon fatty acid chains may distribute asymmetrically in the bilayer of fatty acid liposome. This is due to the properties of PE with an inverted cone shape may pack efficiently in the inner monolayer. Therefore, it has a higher preferential to occupy the inner leaflet of the bilayer. As a result, the curvature difference between the two monolayers is increased compared to the system composing of pure fatty acid thus favoring the formation of smaller size liposome [Risselada and Marrink, 2009].

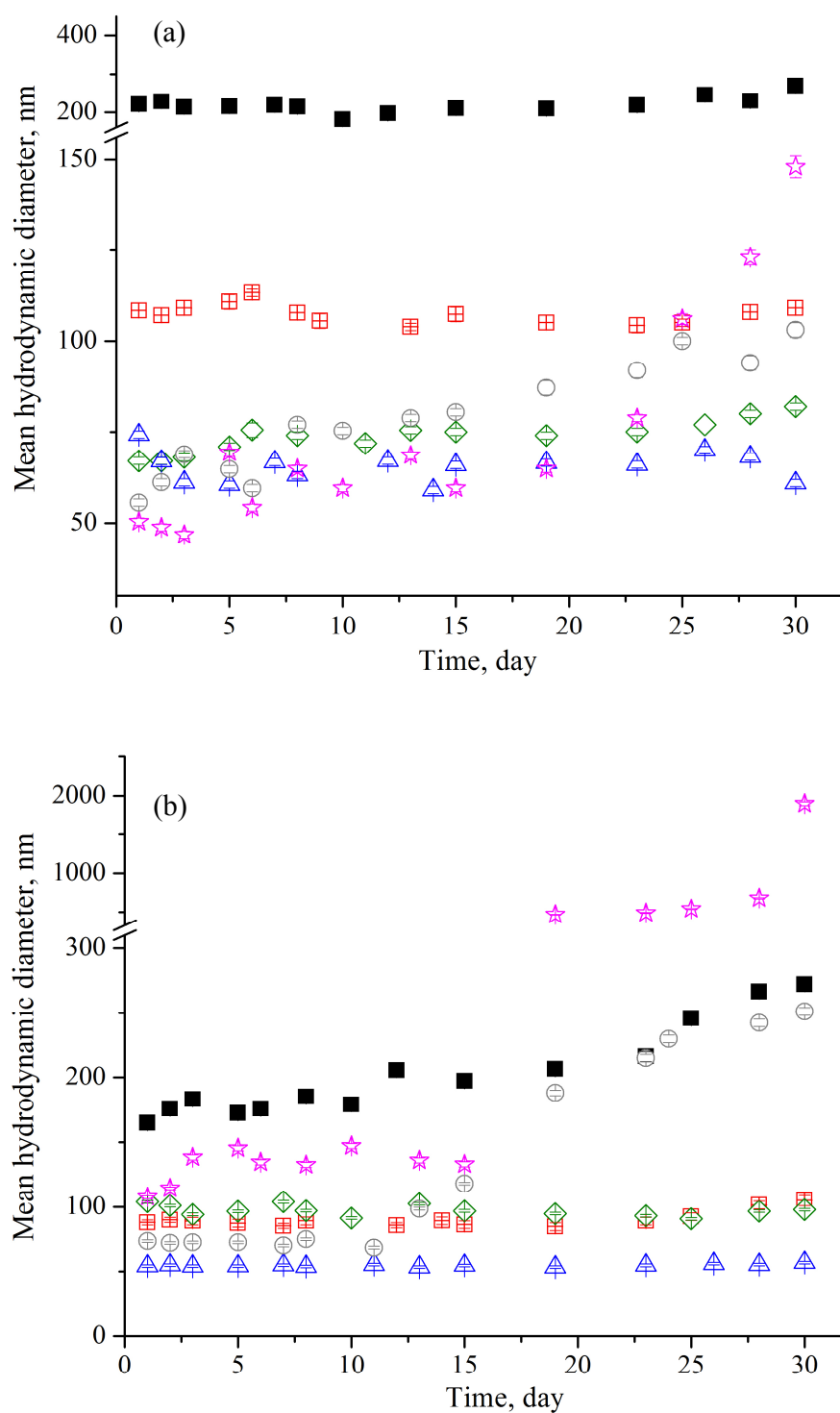


Figure 4.12. Mean particle size of (a) palmitoleate-palmitoleic acid liposome and (b) oleate-oleic acid liposome with their mixture for a period of 30 days at 30 °C. ■ pure fatty acid, ■ FA+Lecinol S-10, ◇ FA + DPPE-PEG2000, △ FA + DPPE-PEG2000 + Lecinol S-10, ○ FA + DPPE-PEG5000, ☆ FA+ DPPE-PEG5000 + Lecinol S-10. Error bars indicate the 95% confidence interval.

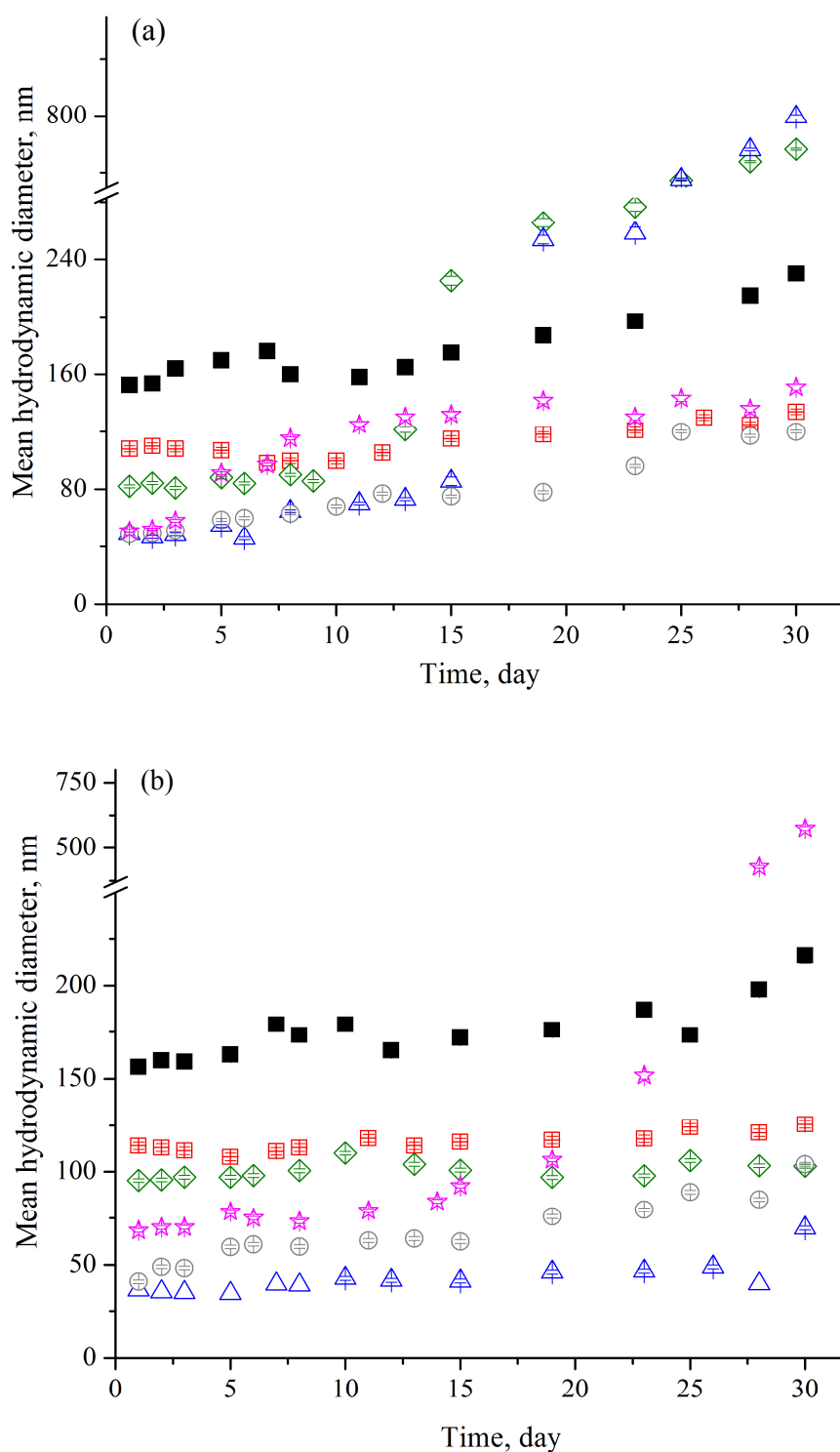


Figure 4.13. Mean particle size of (a) linoleate-linoleic acid liposome and (b) linolenate-linolenic acid with their mixture for a period of 30 days at 30 °C. ■ pure fatty acid, ▣ FA+Lecinol S-10, ◇ FA + DPPE-PEG2000, △ FA + DPPE-PEG2000 + Lecinol S-10, ○ FA + DPPE-PEG5000, ☆ FA+ DPPE-PEG5000 + Lecinol S-10. Error bars indicate the 95% confidence interval.

On the other hand, incorporation of PEGylated lipid in the preparation of fatty acid liposomes was found responsible for the formation of liposome with smaller particle size of about 100 nm. This observation supports the theory of successful insertion of PEGylated lipid into the bilayer of liposomes. The plausible reason for the formation of smaller size liposomes is due to the presence of long PEG chain that is more dynamic in an aqueous solution. As a result, the effective head group area is larger and results in a smaller packing parameter compared to the packing parameter for liposome formed from pure fatty acid molecules. However, the reduced value of packing parameter is expected to be within the value for formation of liposome that is greater than 0.5 but smaller than 1. Therefore, formation of liposome with high bilayer curvature is expected for packing parameter that is reduced to the value approximately 0.5. Besides, the formation of smaller size liposome with incorporation of PEGylated lipid is intentionally to decrease the steric repulsion force between the head groups. This is due to the presence of bulky polyethoxylate group at the surface of the bilayer that has induced an extensive hydration around the polar head group causing a steric repulsion among the polyethoxylate group. In order to reduce the degree of repulsion force, an area expansion was obtained by bending the bilayer into a higher degree of curvature [Sriwongsitanont and Ueno, 2004]. Therefore, in view of the above mentioned explanation, DPPE-PEG5000 with bulkier PEG tends to form smaller size liposomes compared to DPPE-PEG2000. Similar results were observed for ternary mixture of fatty acid, DPPE-PEG2000 and Lecinol S-10. In contrary, ternary mixture of C18 fatty acid, DPPE-PEG5000 and Lecinol S-10 demonstrated larger size of liposome compared to those in their binary mixed system. This might be due to the structural incompatibility between C18 fatty acid with the bulky DPPE-PEG5000 and Lecinol S-10.

The stability assessment on liposome suspension solutions demonstrated that the particle size of purely fatty acid liposomes were only stable for a period of one week.

Therefore, efforts on enhancing the stability of liposome were carried out by varying their compositions with addition of Lecinol S-10. It has been shown that all of the fatty acids, regardless their chain length and degree of unsaturation were acceptably stable. There was no apparent change in the particle size of liposome although their particle size was larger than 100 nm. In order to obtain a stable liposome suspension with particle size less than 100 nm throughout the storage time, another trial was done by the addition of PEGylated lipid with 45 unit monomer of polyethoxylated group and 131 unit polyethoxylated monomer in the preparation of liposomes. It has been observed that DPPE-PEG2000 has effectively promoted stabilization to a certain extent for all of the fatty acid liposomes. However, limited stability in linoleate-linoleic acid-DPPE-PEG2000 liposomes was observed as a drastic increase in the liposome size after five days of storage. On the other hand, DPPE-PEG2000 was added into the binary system of fatty acid and Lecinol S-10. The results were similar to those in binary mixture of fatty acid and Lecinol S-10 but with formation of smaller size liposomes. Thus, DPPE-PEG5000 with a more bulky hydrophilic group was added in the preparation of fatty acid liposome for the same purpose. Unfortunately, oleate-oleic acid-DPPE-PEG5000 liposomes and linoleate-linoleic acid-DPPE-PEG5000 liposomes were found only stable for the first eight and five days of storage, respectively. Similar result was also observed in the liposome system of palmitoleate-palmitoleic acid-DPPE-PEG5000. Surprisingly, changes in liposome size for mixed system of linoleate-linoleic acid-DPPE-PEG5000 was not as dramatic as those in linoleate-linoleic acid-DPPE-PEG2000. This implies a more stable liposome suspension was formed in mixture of linoleic acid and DPPE-PEG5000. Nevertheless, particle size for all of the fatty acid liposomes containing ternary mixtures of fatty acid/DPPE-PEG5000/Lecinol S-10 was found to increase gradually. This may be due to the formation of flocs in the solution as can be observed

through the polarizing microscope in figure 4.14. In addition, polydispersity indices for liposome prepared from ternary mixture regardless the type of fatty acid were found to increase from ~ 0.3 to ~ 0.6 throughout the storage time.

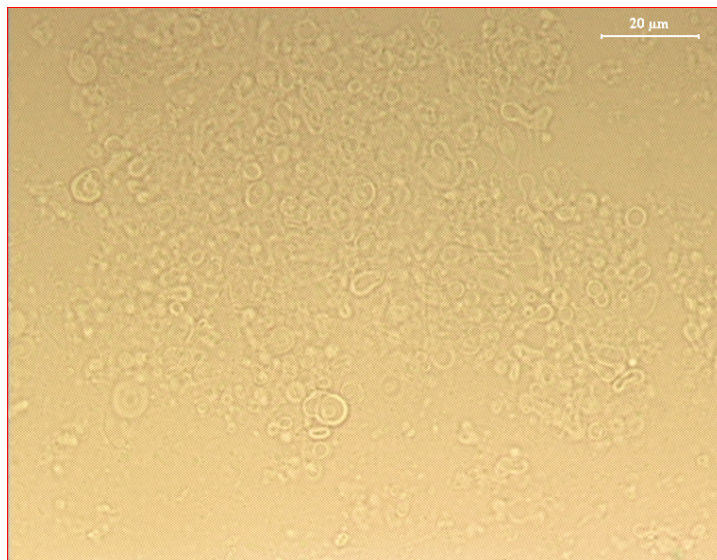


Figure 4.14. Optical polarizing micrograph of 2 mM palmitoleate-palmitoleic acid-DPPE-PEG5000-Lecinol S-10 liposome at pH 8.5 after 30 days of storage.

4.3.2 Zeta potential

The effective surface charge of liposome is quantified as zeta potential. It is a parameter that has commonly been used to determine the stability of a colloidal suspension solution. The larger the magnitude of zeta potential, the more stable is the liposome suspension. The value of zeta potential may be affected by the bilayer composition of the liposome. In this particular study, negative values of zeta potential were obtained arising from the carboxylate group in the ionized form of fatty acid molecules that contributes to the negatively charge surface of liposomes.

Figure 4.15 and 4.16 show the variation of zeta potential with respect to the storage time. A relatively lower magnitude of zeta potential is observed for fatty acid

liposomes in the presence of Lecinol S-10 compared to pure fatty acid liposome. Similar result is also found in the mixture of fatty acid liposome made up of PEGylated lipid and mixture of PEGylated lipid/Lecinol S-10. Although both Lecinol S-10 and PEGylated lipid do reduce the magnitude of zeta potentials, the reduction of zeta potential to a lesser negative value is much more pronounced for liposome containing PEGylated lipid. There are two possibilities that may explain this phenomenon. One of the reasons could probably due to a long and bulky polyethoxylate group that is coating around the liposomes surface. This in turn causes a slower liposome mobility and hence lower their zeta potential [Sakai *et. al.*, 2002; Heurtault *et. al.*, 2004; Centis and Vermette, 2008]. Another possible explanation is that the presence of bulky polyethoxylate group with different degree of polymerization, choline and inositol group from Lecinol S-10 have effectively shielded the negatively charge on the surface of liposome. Therefore, extension of these bulky groups from the surface of liposome has shifted the shear plane far apart from the surface of liposome that results in a lower magnitude in zeta potential [Woodle *et. al.*, 1992]. On the other hand, magnitudes of zeta potential for liposome prepared from ternary mixture were found higher than those from binary mixture. The plausible reason is the interaction between choline group, inositol group with polyethoxylate group could reduce the distance of shear plane from the liposome surface. As shown from our findings, we can deduce that Lecinol S-10 and PEGylated lipid have shown cooperative participation in the bilayer formation.

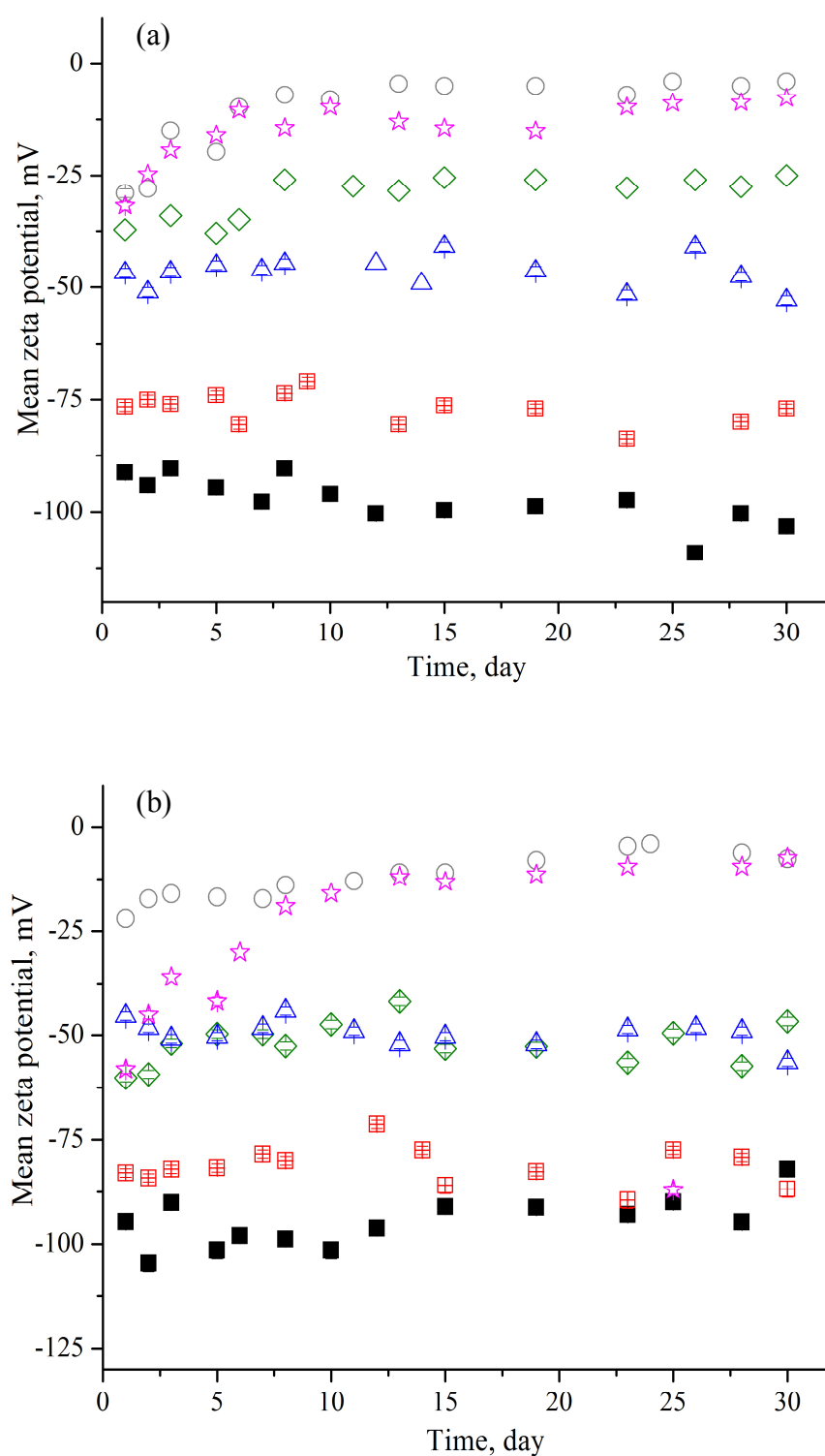


Figure 4.15. Mean zeta potential of (a) palmitoleate-palmitoleic acid liposome and (b) oleate-oleic acid liposome with their mixture for a period of 30 days at 30 °C. ■ pure fatty acid, ▣ FA+Lecinol S-10, ◇ FA + DPPE-PEG2000, △ FA + DPPE-PEG2000 + Lecinol S-10, ○ FA + DPPE-PEG5000, ☆ FA+ DPPE-PEG5000 + Lecinol S-10. Error bars indicate the 95% confidence interval.

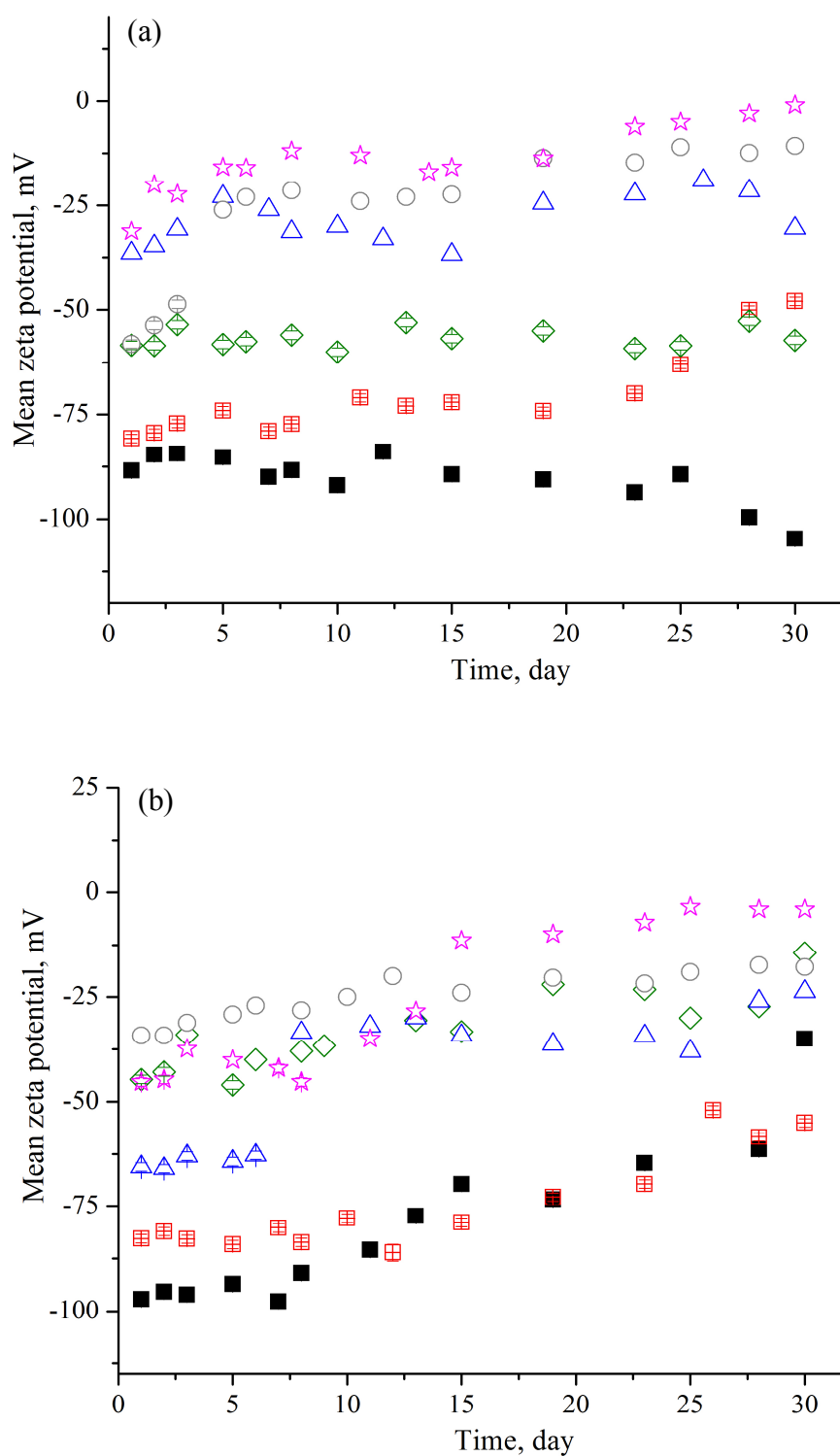


Figure 4.16. Mean zeta potential of (a) linoleate-linoleic acid liposome and (b) linolenate-linolenic acid liposome with their mixture for a period of 30 days at 30 °C. ■ pure fatty acid, ▣ FA+Lecinol S-10, ◇ FA + DPPE-PEG2000, △ FA + DPPE-PEG2000 + Lecinol S-10, ○ FA + DPPE-PEG5000, ☆ FA+ DPPE-PEG5000 + Lecinol S-10. Error bars indicate the 95% confidence interval.

Another method for assessing liposome stability is by monitoring the zeta potential over a period of time. The liposome system with longer chain length is more stable as shown in the plots in figure 4.15(a) and 4.15(b). This is shown by the more negative value of zeta potential for oleate-oleic acid liposomes than palmitoleate-palmitoleic acid liposomes. The overall trend in zeta potential were found consistent for both of the fatty acid liposome suspensions either in the pure system or binary mixture with Lecinol S-10, DPPE-PEG2000 or their ternary mixture. Similar result is also observed in the binary mixture of oleate-oleic acid-DPPE-PEG5000 liposome. However, a gradual decrease in the magnitude of zeta potential is shown in the liposome system containing palmitoleate-palmitoleic acid-DPPE-PEG-5000 as well as in the ternary mixture of fatty acid-DPPE-PEG5000-Lecinol S-10 regardless of the chain length in the fatty acids.

The effect of degree of unsaturation on zeta potential are shown in figure 4.15(a) and figure 4.16. The magnitude of zeta potential for linolenate-linolenic acid liposomes is the smallest while oleate-oleic acid liposomes is the largest. This shows the stability of the liposome is reduced as the double bond in the hydrocarbon chain of fatty acid increases. In all of the liposome systems that containing linoleic acid, the magnitude of zeta potential decreases gradually over the storage time. On the other hand, the zeta potential are shown to be about constant with the storage period for linolenate-linolenic acid liposome as well as their binary mixture with Lecinol S-10 or DPPE-PEG2000 and their ternary mixture liposomes. However, addition of DPPE-PEG5000 into the formation of linolenate-linolenic acid liposome result in a gradual decrease in the magnitude of zeta potential.

We can deduce from the result of zeta potential that addition of DPPE-PEG2000 or Lecinol S-10 into the formation of fatty acid liposome helps stabilize the liposome system. On the other hand, addition of DPPE-PEG5000 with larger polyethoxylate

chain into the liposome system may render destabilization of the liposome. The results obtained from zeta potential measurements are also in agreement with those found in the particle size measurements.

4.4 Transmission electron micrographs

Transmission electron microscopy technique has been the best available option to observe the presence of liposomes in the solution. This is due to most of the liposomes that have been produced in our method were well below 500 nm which could not be viewed using normal light or polarizing microscope. TEM micrograph of fatty acid liposomes at 40 mM are shown in figures 4.18 and 4.19. Most of the liposomes were present on a bright background as spherical rings accompany with some oval in shape and oil droplets. Deeper colour is observed at region inside the ring compared to the background. The image of liposomes that is observed on the fluorescence screen which is placed at position 180° from the electron source is produced from the projection of various electrons being scattered as they passed through the liposomes. As an electron beam travels through the liposome, they interact with the atoms in the membrane and travelling through different thicknesses of the membrane. The longer the distance the electrons travel, the more interaction may occur with the atoms in the membrane and hence the more electrons will be diffracted. Therefore the lower the electron phase density that reaches the fluorescence screen and the darker the final image will be observed compared to the background as shown in figure 4.17. This results in variation of electron phase density around liposome and generates the contrast between the sample and background. The highest transmitted electron phase density occur at the center of the bilayer. Hence the final image appeared to be grey at this position. The change in contrast may indicate the outer radius of liposome.

Observation of oil stain in the images of liposome is possibly related to the elasticity of the membrane bilayer in liposomes. As a particle is exposed to an environment of very low pressure, the shearing effect may occur. If the bilayer were high in elasticity, it remains unperturbed by the vacuum condition. Nonetheless, collapse of the bilayer could also be observed as oil droplet stains arising from collapse of liposomes with low bilayer elasticity.

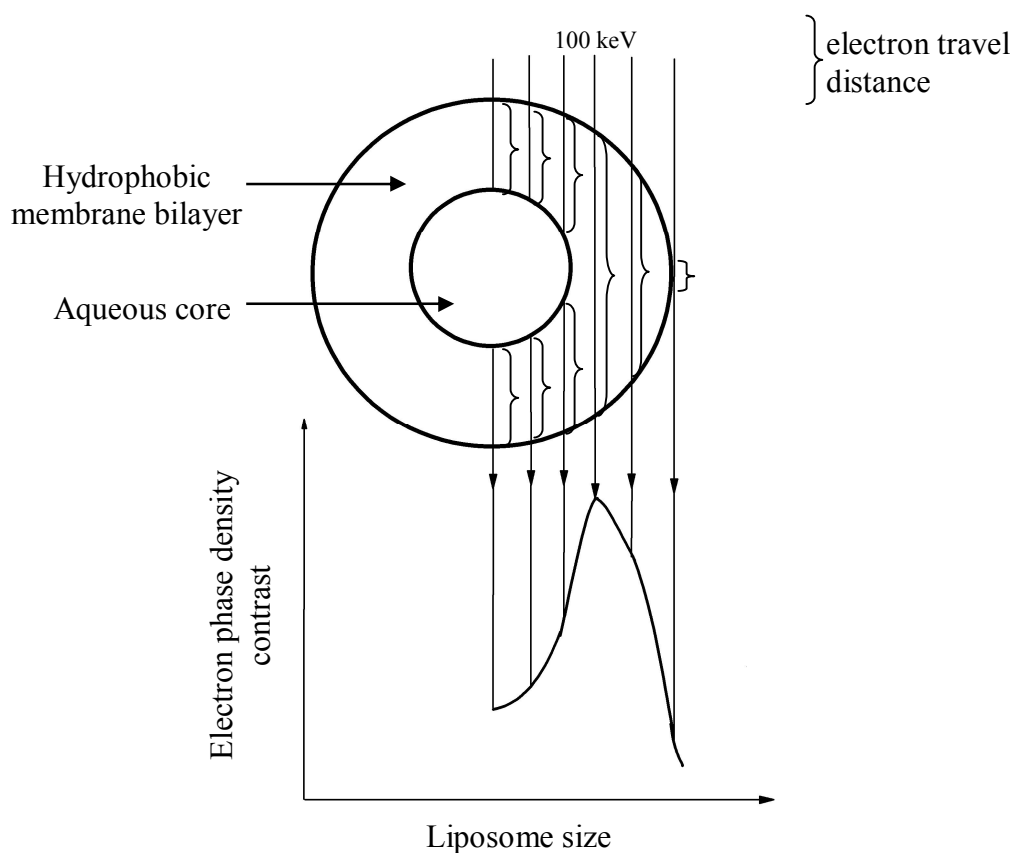


Figure 4.17. Relationship of electron phase density contrast in the final image of TEM with the distance of electron beam travelling through liposome.

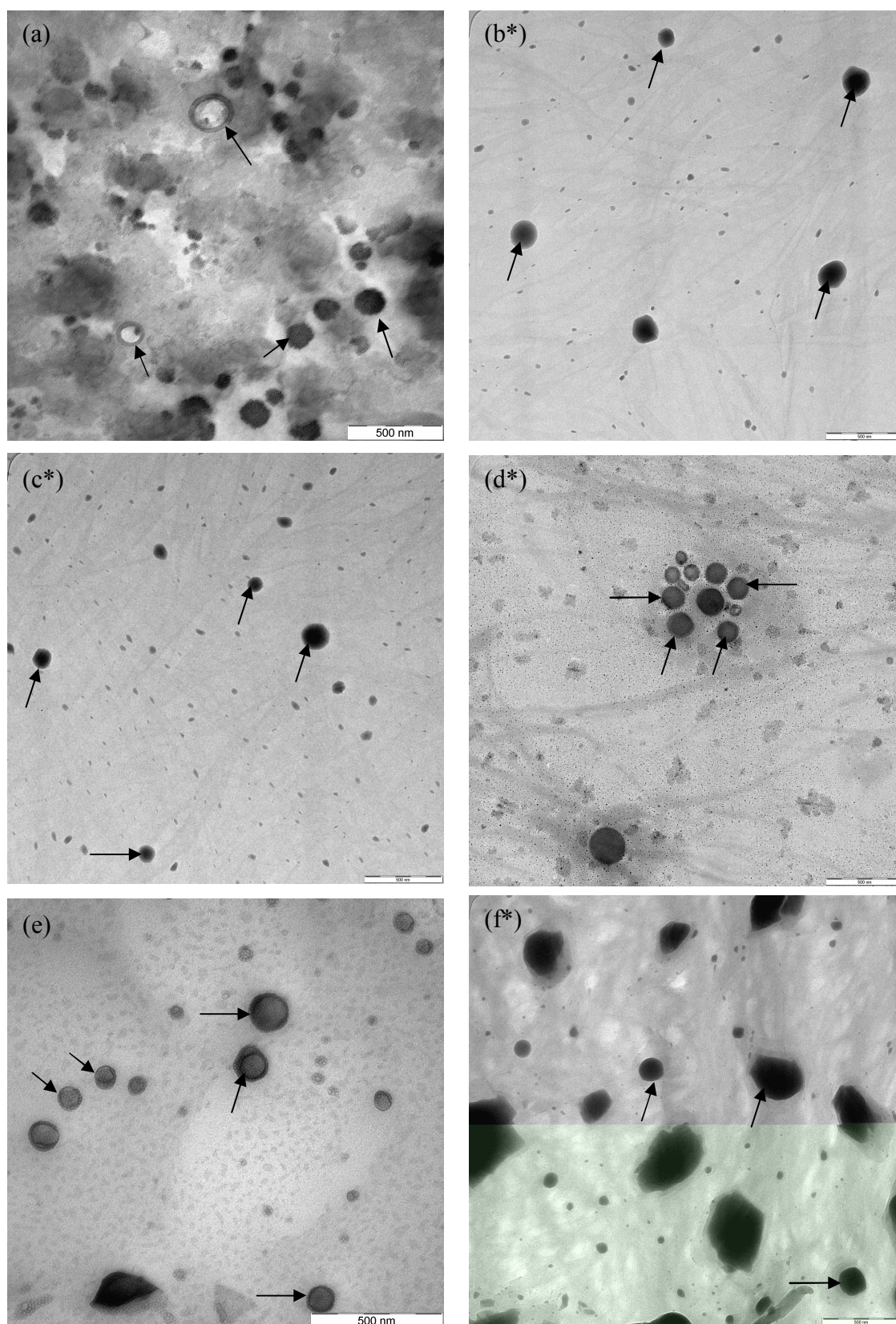


Figure 4.18. TEM micrographs of (a) palmitoleate-palmitoleic acid liposome, (b*) oleate-oleic acid-DPPE-PEG2000 liposome, (c*) palmitoleate-palmitoleic acid-DPPE-PEG2000 liposome, (d*) oleate-oleic acid-DPPE-PEG5000 liposome, (e) palmitoleate-palmitoleic acid-Lecinol S-10-DPPE-PEG2000 liposome and (f*) oleate-oleic acid-Lecinol S-10 liposome. Arrows indicate the liposome, * = EFTEM micrograph.

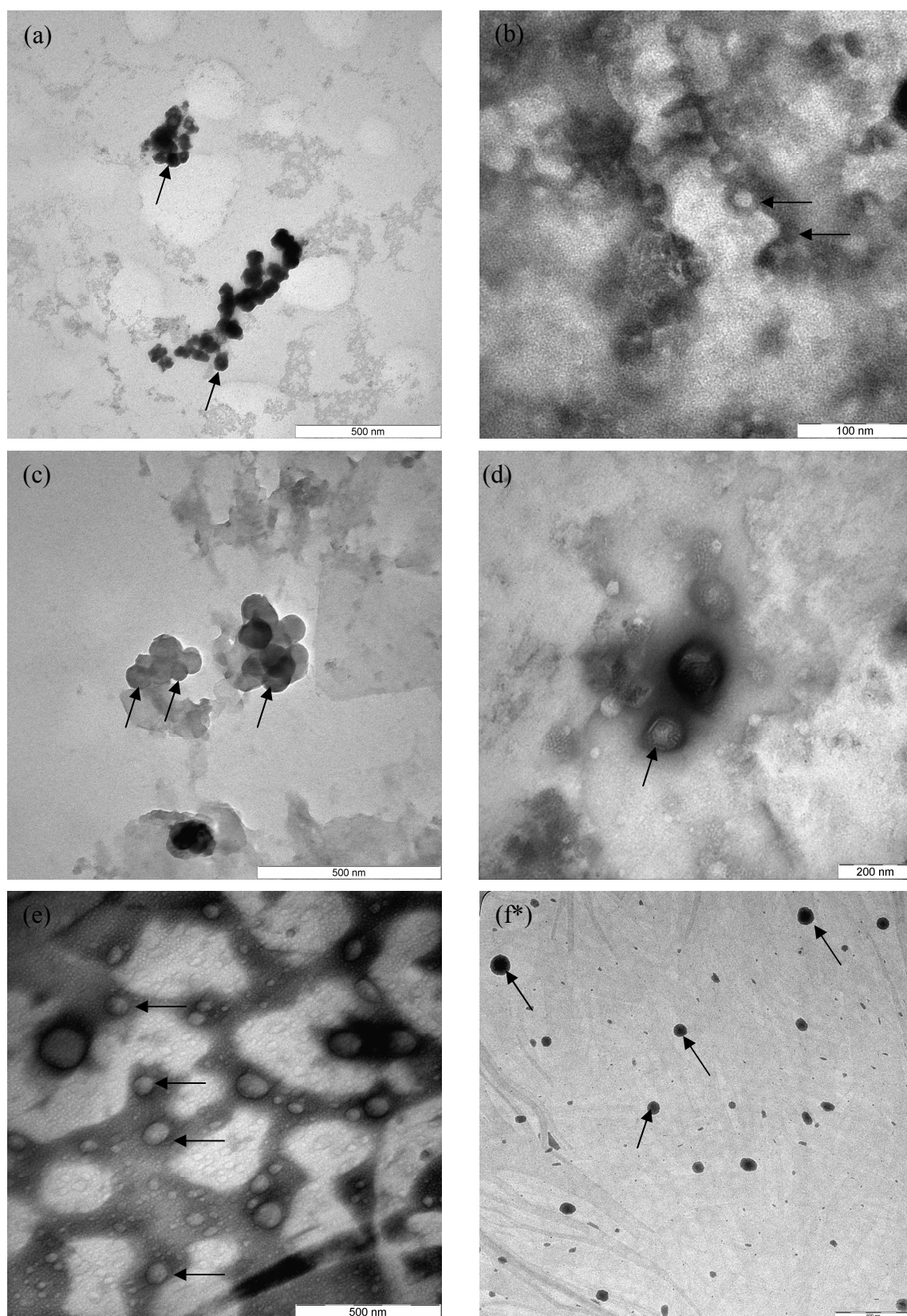


Figure 4.19. TEM micrographs of (a) linoleate-linoleic acid liposome, (b) oleate-oleic acid-Lecinol S-10-DPPE-PEG2000 liposome, (c) linoleate-linoleic acid-DPPE-PEG2000 liposome, (d) linolenate-linolenic acid liposome, (e) linoleate-linoleic acid-DPPE-PEG5000 liposome and (f*) linolenate-linolenic acid-DPPE-PEG2000 liposome. Arrows indicate the liposome. * = EFTEM micrograph

4.5 Encapsulation of calcein and DL- α -tocopherol acetate (VE)

As soon as the stability of the liposome has been identified, encapsulation of water soluble calcein and water insoluble VE were also studied. In view of the formulation for PEGylated liposomes at mole fraction of PEGylated lipid of 0.02 in 50 mM borate buffer pH 8.5 was found compatible for the formation of liposome, this combination was applied in the study of loading efficiency. The loading efficiencies and the amount of substance loaded in liposomes were then calculated. The effect of PEGylated lipid as well as the effect of degree of unsaturation in hydrocarbon chain of fatty acid on loading efficiencies of liposomes were explored.

4.5.1 Separation method by size exclusion chromatography vs ultrafiltration

In this study, there are two available methods to separate the loaded substances in liposomes from those free in the bulk medium, *t*-test was performed in order to statistically evaluate the effect of these two methods on the mean value of loading efficiencies. Hence, separations of free VE as well as calcein from those loaded in oleate-oleic acid-DPPE-PEG2000 liposome were carried out by using both of these methods. The loading efficiencies determined by both separation methods were calculated and shown in table 4.3. The result of *t*-test revealed no significant difference between the separation methods with $p > 0.05$. Hence, both separation methods were employed in this study.

Size exclusion chromatograms as shown in figure 4.20 were obtained from separation of loaded and free calcein as well as VE. The chromatograms for the reference solutions as a control in the experiment were also displayed in figure 4.20. By comparing the chromatogram for the reference and those liposome suspension solutions containing loaded and free substance, we deduced that the encapsulated substances in liposomes were first eluted out from the column followed by the free substances.

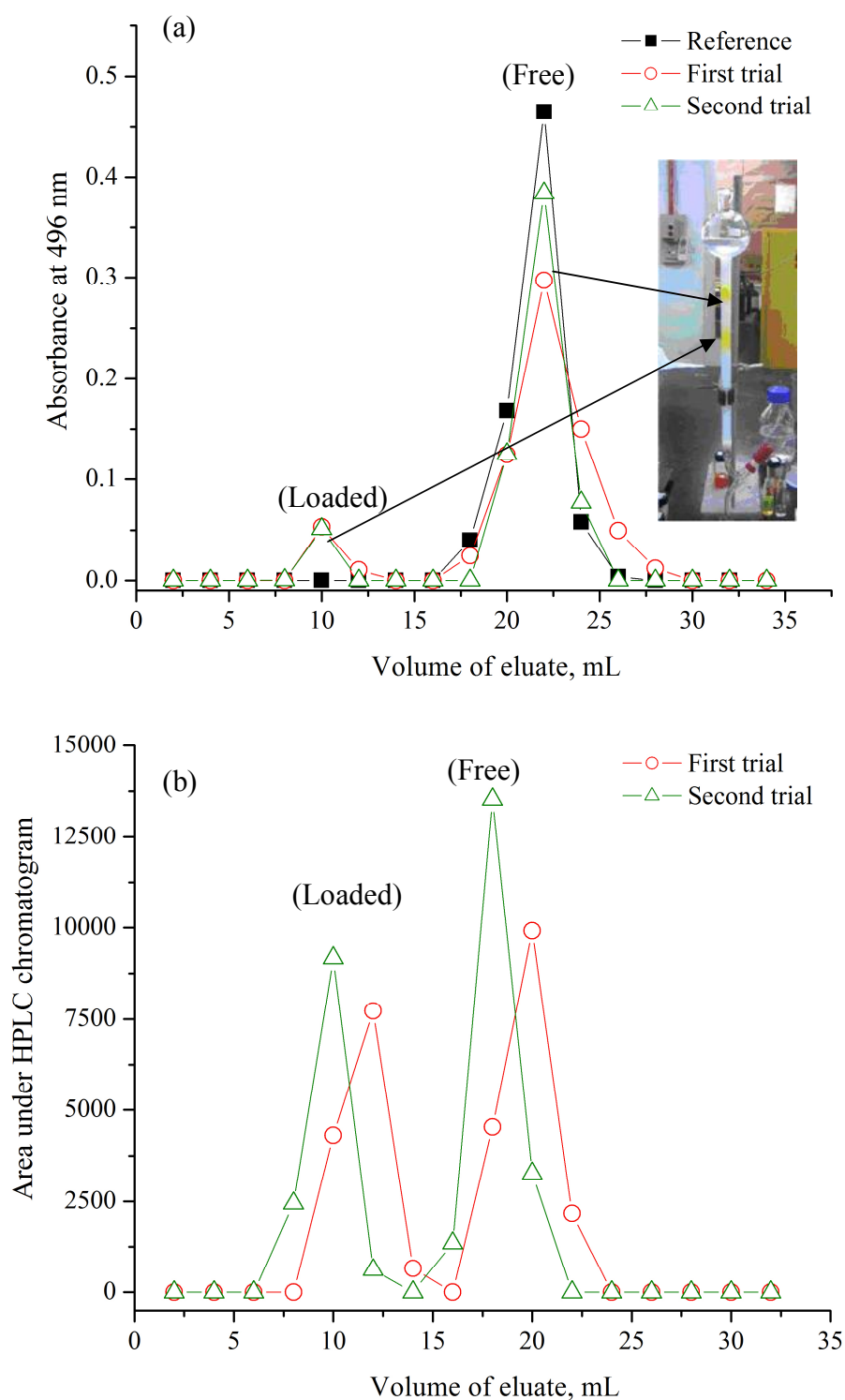


Figure 4.20. Separation of (a) calcein and (b) VE loaded in oleate-oleic acid-DPPE-PEG2000 liposome from the respective free molecules by size

Then, the loading efficiency is defined as percentage of the amount of substance loaded in liposome to the total amount of substance in the system, $(n_x^e/n_x)\%$, where x is denoted as the type of substance, n_x^e is the amount of substance loaded in liposome and n_x is the amount of substance used in the preparation of liposome. However, if we applied this calculation in the determination of loading efficiency, we have observed that, for a fixed amount of fatty acid used, there is an optimum loading efficiency as a result of varying the amount of substance in the system. Therefore we defined it as optimum loaded ratio, n_x^{e*}/n_{FA}^* as shown in figure 4.21.

The loading efficiencies determined by both separation methods were calculated and shown in table 4.3. Almost similar results of loading efficiencies were obtained by applying both separation methods.

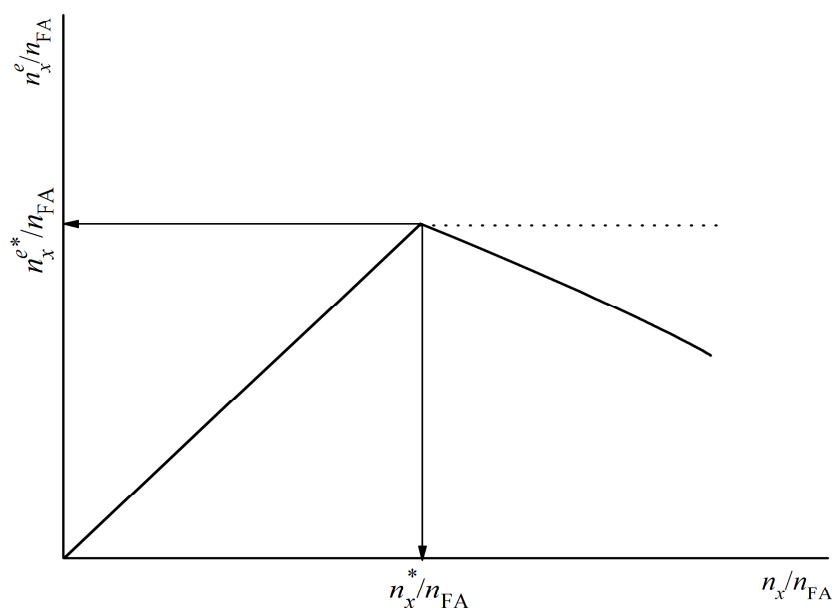


Figure 4.21. Loaded amount of substance in liposome with respect to the total amount of fatty acid. Solid line indicates experimental result while dotted line indicates the expected result as a function of added substance.

Table 4.3. Comparison on separation methods for 200 μL of 25 mM oleate-oleic acid-DPPE-PEG2000 liposome containing calcein and VE.

Method	Mean loading efficiency, %	
	0.5 mM calcein	3 mM VE
Size exclusion chromatography number of trial = 2	8.5 ± 0.5	42 ± 2
Ultrafiltration number of trial = 3	8.6 ± 0.6	42 ± 3
(Mean \pm S.D.)		

4.5.2 Encapsulation of calcein

In this study, the molar extinction coefficient (ϵ') for calcein is found to be $64153 \text{ M}^{-1} \text{ cm}^{-1}$ at 496 nm. Eluates with high concentration of calcein were further diluted in order to reach a measurable absorbance value.

All of the liposomes prepared in this study were shown to have different encapsulation efficiency towards the investigated compounds. The effect of mole of calcein used with respect to mole of fatty acid, $n_{\text{Cal}}/n_{\text{FA}}$ on the ratio of amount of calcein loaded in the fatty acid liposome with respect to mole of fatty acid, $n_{\text{Cal}}^e/n_{\text{FA}}$ was shown in figures 4.23 and 4.24. It can be observed from these figures that at very low $n_{\text{Cal}}/n_{\text{FA}}$, the amount of calcein loaded in the liposome is also low, while increase in $n_{\text{Cal}}/n_{\text{FA}}$ leads to higher loaded amount of calcein in fatty acid liposomes. The plausible reason that affects loading efficiency could be the high solubility of calcein in the bulk medium at pH 8.5. Therefore, at low concentration of calcein, the probability to entrap calcein in liposomes is lower. Nevertheless, as the concentration of calcein increases, the probability of calcein to be trapped in the core of liposome during bilayer convolution is expected to be higher. However, further increase of calcein concentration results in a reduction of loading efficiency. An increase in the amount of calcein may also be accompanied with the increase of Na^+ in the bulk medium. This is due to the presence

of calcein may reduce the pH of the bulk solution. Therefore, addition of sodium hydroxide solution is necessary to maintain the pH of the solution at 8.5. An increase in the amount of Na^+ is believed to increase the amount of associated counter ions on the surface of the negatively charge membrane, hence this results in further compression of diffused double layer. Therefore, as the amount of Na^+ increases, it may hinder the adsorption of calcein on the membrane surface. As a consequence, most of the calcein will be pushed away from the interface during convolution of the membrane as illustrated in figure 4.22. This could explain the reduction in the amount of calcein loaded in liposome as the amount of calcein present in the system is higher.

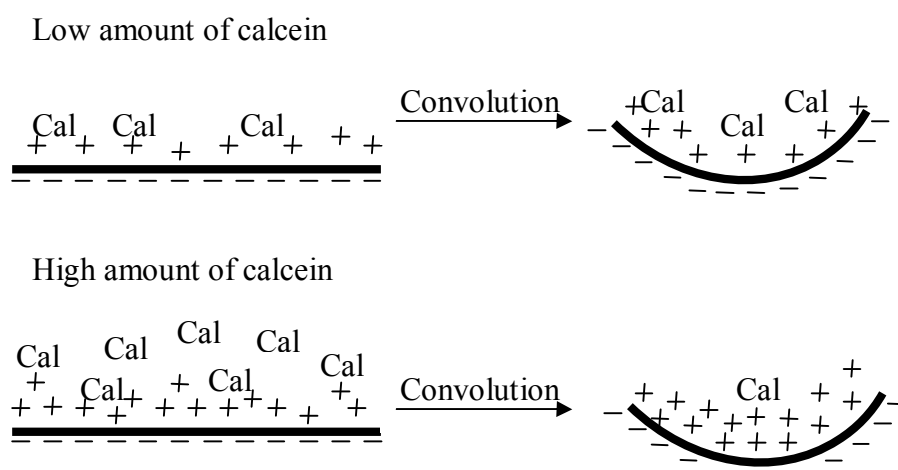


Figure 4.22. Effect of calcein amount on loading efficiency fatty acid liposomes.

The optimum loading efficiency of calcein in fatty acid liposome and their mixture with DPPE-PEG2000, DPPE-PEG5000 were observed in figure 4.23 and figure 4.24. We found that the optimum loading efficiency is not much affected by the presence of PEGylated fatty acid liposomes. The ratio of $n_{\text{Cal}}/n_{\text{FA}} = 0.12$ shows high value of loading efficiency for most of the fatty acid liposomes hence this ratio was selected to study the effect of the type fatty acid as well as PEGylated lipid on loaded amount of calcein as shown in figure 4.25(a) for C18 polyunsaturated fatty acid liposomes and

table 4.4 for palmitoleate-palmitoleic acid liposomes and their mixture. The result showed that palmitoleate-palmitoleic acid liposomes and oleate-oleic acid liposomes are capable in loaded with higher amount of calcein. However, the amount of calcein loaded in linoleate-linoleic acid liposomes and linolenate-linolenic acid liposomes are comparably lower. This is due to small trapping volume in linoleate-linoleic acid liposome and linolenate-linolenic acid liposome as a result of their smaller hydrodynamic size. This is because the size of liposome is significantly correlated with its loading efficiency [Nii *et. al.*, 2003]. Another possible reason is that palmitoleic acid and oleic acid have only one unsaturated double bond in the hydrocarbon tail leading to a close packing of the bilayer that results in fewer leakage of calcein. On the contrary, linoleic acid and linolenic acid consisting of two and three double bonds tend to form bilayer with higher fluidity that could facilitate the leakage of calcein into the bulk solution [Kulkarni *et al.*, 1995]. Thus the, inclusion of Lecinol S-10 in the formation of liposome may possibly affect the packing geometry in bilayer and cause a reduction in the loading efficiency compared to the pure fatty acid liposome. Furthermore, as shown in figure 4.25(a), inclusion of PEGylated lipid either in fatty acid liposomes or mixed fatty acid with Lecinol S-10 liposomes results in lower loading efficiency that could be due to the same reasons. Although different composition of liposome displays variation in calcein loading efficiency, an average of 10 % calcein was loaded in the prepared liposomes. The loading efficiencies of calcein in liposomes may vary from 0.1 % to 39.5 % [Memoli *et. al.*, 1994; Manosroi *et. al.*, 2003; Fan *et. al.*, 2007; Bahiaa *et. al.*, 2010; Liu and Park, 2010].

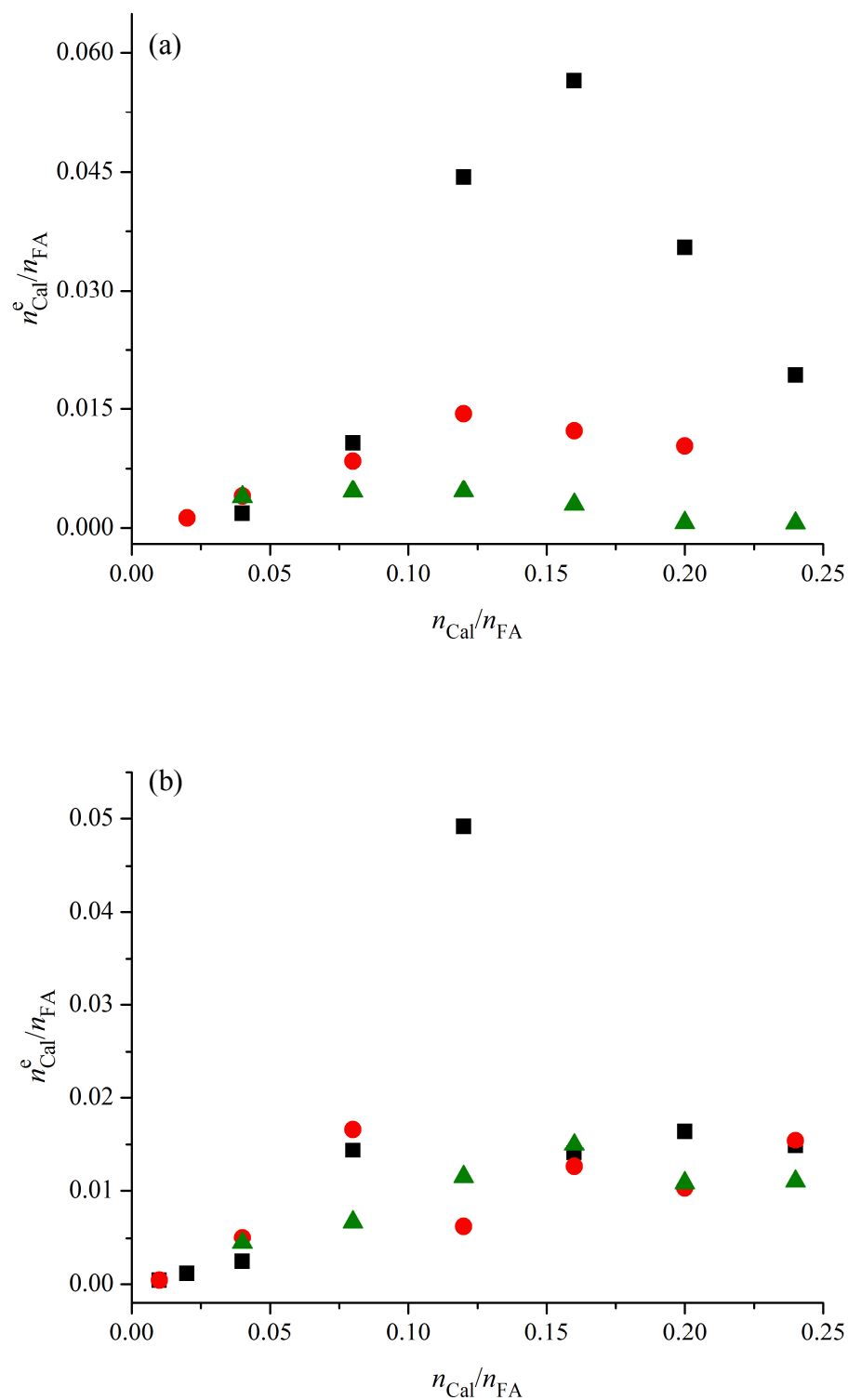


Figure 4.23. Amount of calcein loaded in (a) palmitoleate-palmitoleic acid liposome and (b) oleate-oleic acid liposome with respect to the total amount of fatty acid. ■ indicates only acid liposome, ● represents mixture of DPPE-PEG2000-fatty acid liposomes, ▲ represents mixture of DPPE-PEG5000-fatty acid liposomes.

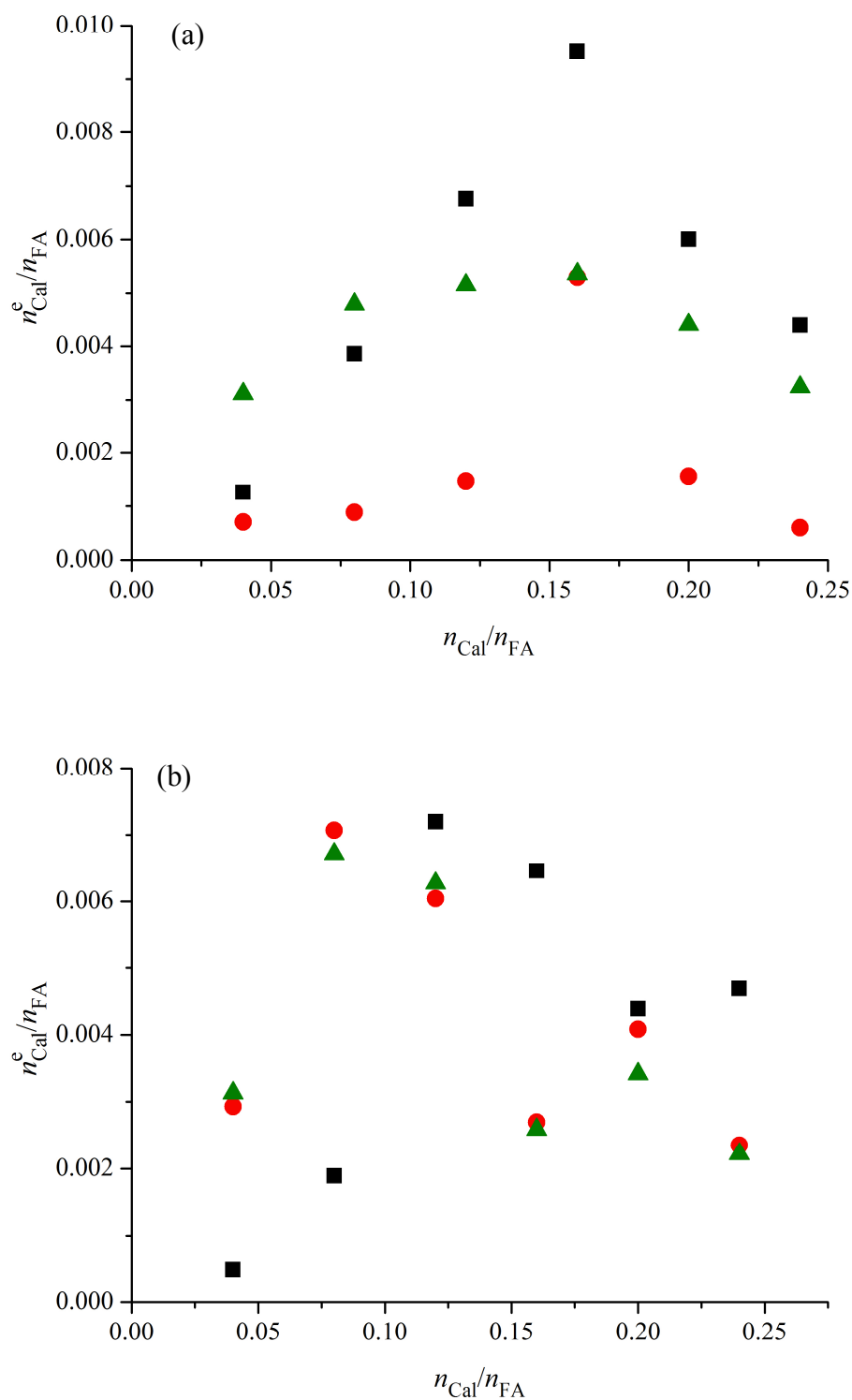


Figure 4.24. Amount of calcein loaded in (a) linoleate-linoleic acid liposome and (b) linolenate-linolenic acid liposome with respect to the total amount of fatty acid. ■ indicates only fatty acid liposome, ● represents mixture of DPPE-PEG2000-fatty acid liposomes, ▲ represents mixture of DPPE-PEG5000-fatty acid liposomes.

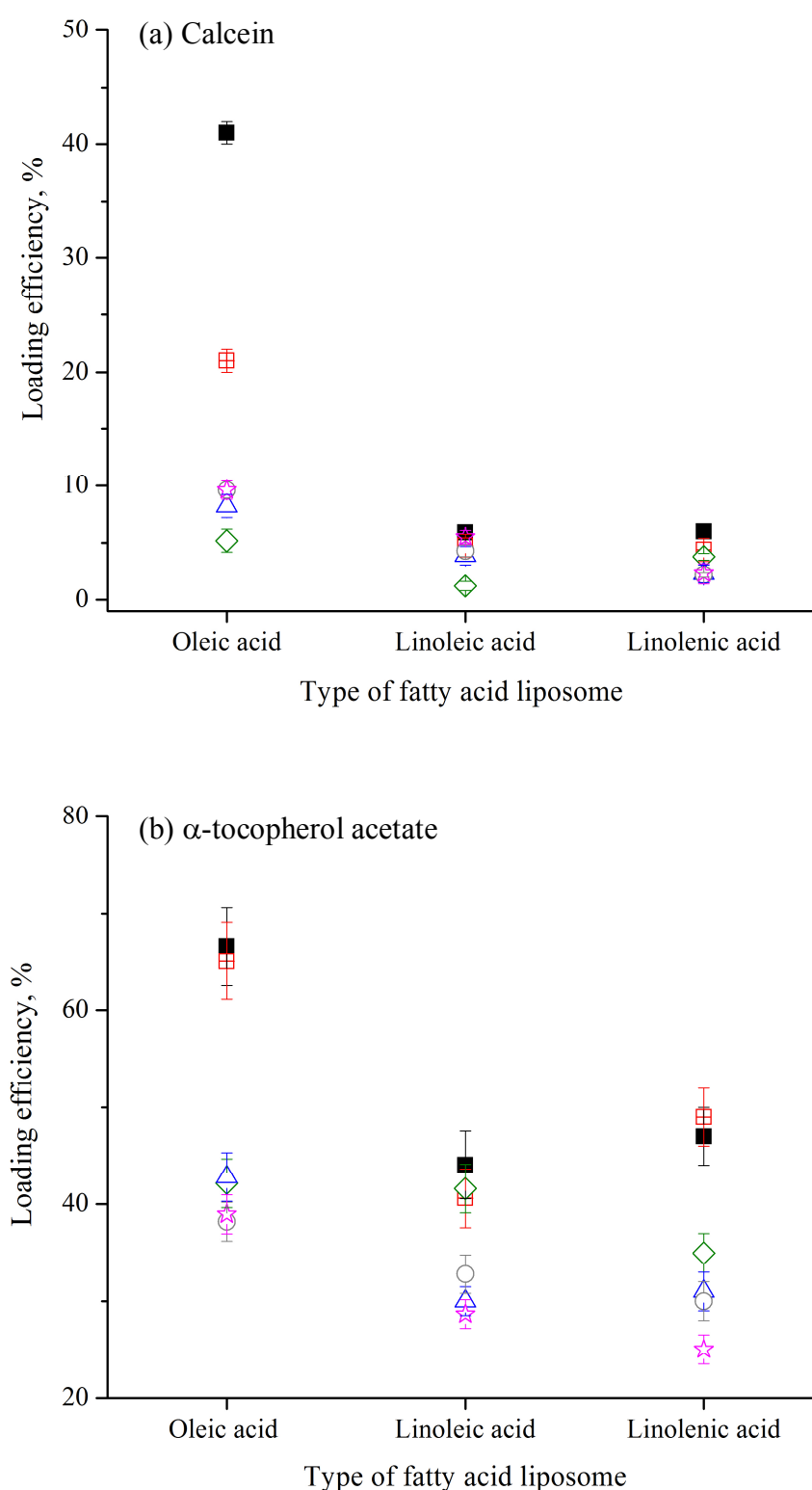


Figure 4.25. Loading efficiency of (a) $n_{\text{Cal}}/n_{\text{FA}} = 0.12$ and (b) $n_{\text{VE}}/n_{\text{FA}} = 0.16$ in fatty acid liposome and their mixture at pH 8.5. ■ pure fatty acid, ⊞ FA+Lecinol S-10, ◇ FA + DPPE-PEG2000, △ FA + DPPE-PEG2000 + Lecinol S-10, ○ FA + DPPE-PEG5000, ☆ FA+ DPPE-PEG5000 + Lecinol S-10.

Table 4.4. Loading efficiency for $n_{\text{Cal}}/n_{\text{FA}} = 0.12$ and $n_{\text{VE}}/n_{\text{FA}} = 0.16$ in palmitoleate-palmitoleic acid liposome and their mixtures at pH 8.5.

Composition of palmitoleate-palmitoleic acid liposome	Loading efficiency, %	
	Calcein	α -tocopherol acetate
Palmitoleic acid	36 ± 1	68 ± 2
Lecinol S-10	12 ± 1	53 ± 4
DPPE-PEG2000	12 ± 1	38 ± 5
Lecinol S-10 + DPPE- PEG2000	7 ± 1	38 ± 5
DPPE-PEG5000	4 ± 1	35 ± 3
Lecinol S-10 + DPPE- PEG5000	12 ± 1	31 ± 3

4.5.4 Encapsulation of VE

The ability of fatty acid liposomes to encapsulate lipophilic substance was studied by evaluating the loading efficiency of VE in liposome suspension solution. The amount of VE loaded in palmitoleic acid, oleic acid, linoleic acid and linolenic acid liposomes as well as their mixture with PEGylated lipid and Lecinol S-10 with respect to the total amount of fatty acid, $n_{\text{VE}}^e/n_{\text{FA}}$ as a function of the amount of VE with respect to the total fatty acid, $n_{\text{VE}}/n_{\text{FA}}$ were shown in figure 4.26 and 4.27. The amount of VE loaded in all of liposomes containing pure fatty acid or their mixture with PEGylated lipids were found to be increased with the amount of VE in the sample. Further increase in $n_{\text{VE}}/n_{\text{FA}}$ results in a sudden change of the trend and this was observed at around $n_{\text{VE}}/n_{\text{FA}} = 0.16$. The observed trend can be explained by the nature of hydrophobicity in VE whereupon they are preferably to be located in the hydrophobic region of membrane bilayer rather than in the bulk aqueous medium. As a result, encapsulation of VE in liposomes is slightly higher at lower amount of VE. As the amount of VE in the sample increased, $n_{\text{VE}}^e/n_{\text{FA}}$ of liposome was found to level off in order to maintain the partition equilibrium between the bilayer and aqueous bulk phase. Further increase of $n_{\text{VE}}/n_{\text{FA}}$ caused a decrease in $n_{\text{VE}}^e/n_{\text{FA}}$ loaded in liposome. This is

possibly due to the presence of excess VE in the bulk aqueous solution has perturbed the stability of the bilayer membrane hence disrupted the formation of liposome thereby reducing the number of liposomes present in the suspension solution. As a consequence, we observed a decrease in the encapsulation efficiency of VE in the fatty acid liposomes as VE is increased.

Loading efficiencies of VE in oleate-oleic acid liposomes and palmitoleate-palmitoleic acid liposomes were the highest. About 70% of VE at $n_{VE}^e / n_{FA} = 0.16$ was loaded in the liposomes. However, loading efficiencies for the other two types of C18 unsaturated fatty acid liposomes decrease with increase of the double bond in the hydrocarbon chain. This reduction could be due to less hydrophobicity of the membrane as the number of double bond within the hydrocarbon chain of fatty acid increases resulting in the formation of smaller size liposomes. Consequently, limited bilayer surface area is rendered to accommodate VE in liposomes formed from higher unsaturation degree of fatty acid.

There are various factors that may contribute to the efficiency of VE to be loaded in liposome. One of the factors is compatibility of VE with the bilayer. The degree of compatibility is obtainable from the analysis of Langmuir monolayer and will be discussed in the sub section 4.6.2. In addition, particle size of liposome may also affect the loading efficiency of VE in liposome. Obviously, larger particle size may accommodate higher amount of VE. Besides the mentioned factors, packing parameter of the liposome with inclusion of VE may also be considered. Encapsulation of VE is suggested to be located at the outer layer of the bilayer. The reason is that VE tends to induce curvature to liposome as a result of their bulky head group with two rings and a carboxylate group. As a consequence, packing parameter of the liposomes is disrupted and pushes VE to the outer layer of bilayer. In this situation, VE has a higher tendency to diffuse to the bulk solution and results in a lower loading efficiency.

On the other hand, the loading efficiencies of fatty acid liposome with the inclusion of PEGylated lipid were remarkably lower than those for pure fatty acid liposome. There were only about 30-45 % of n_{VE}/n_{FA} successfully loaded in fatty acid liposome with inclusion of PEGylated lipid as shown in figure 4.25(b). Nevertheless, loading efficiency for mixture of DPPE-PEG2000 and fatty acid liposomes were found slightly higher than those of DPPE-PEG5000. In view of smaller size liposomes were formed with inclusion of PEGylated lipid, hence the availability of surface area to embed VE into the bilayer may relatively become smaller and hence a lower loading efficiency. Another possible explanation is the number of lamellar is being reduced with incorporation of PEG as reported by Belsito *et. al.* [Belsito *et. al.*, 2001]. Therefore, the amount of VE that can be loaded into the bilayer is limited. Similar reason is also applied to fatty acid mixed with Lecinol S-10 and their mixture with PEGylated lipid as shown in figure 4.25(b).

In comparison to loading efficiency for water soluble substances, it is observed that VE has a higher loading efficiency under our working conditions compared to calcein. The plausible explanation for this observation is based on hydrophobicity nature of VE that shows higher preferences to be interdigitated in the bilayer. Moreover, the probability of leakage due to diffusion of VE into the bulk aqueous solution is relatively low, thus contributes to the high loading efficiency in liposomes. In contrary, solubility of calcein in an aqueous solution at pH 8.5 is enhanced due to the presence of tetra anionic hydrophiles with $pK_a < 5.5$. Therefore they have a higher tendency of escaping into the bulk solution during the process of bilayer convolution. As a result, the loaded calcein that contributes to the percent of loading efficiency may be either from the calcein entrapped at the hydrophilic layer of the membrane or those within the multilamellar structure. This explains the low percentage of calcein encapsulated by the liposomes.

The results obtained have shown the loading efficiency of fatty acid liposomes is dependent on several factors that arising from the properties of the liposomes as well as the substances to be encapsulated. In relation to the properties of liposomes, the type and composition of fatty acid in the formation of liposome may play an important role in the determination of the physicochemical properties such as entrapped volume, rigidity of the membrane and the surface area of the bilayer [Kulkarni *et al.*, 1995]. On the other hand, the properties of substances to be encapsulated such as solubility in an aqueous solution and their concentration may also affect the loading efficiency.

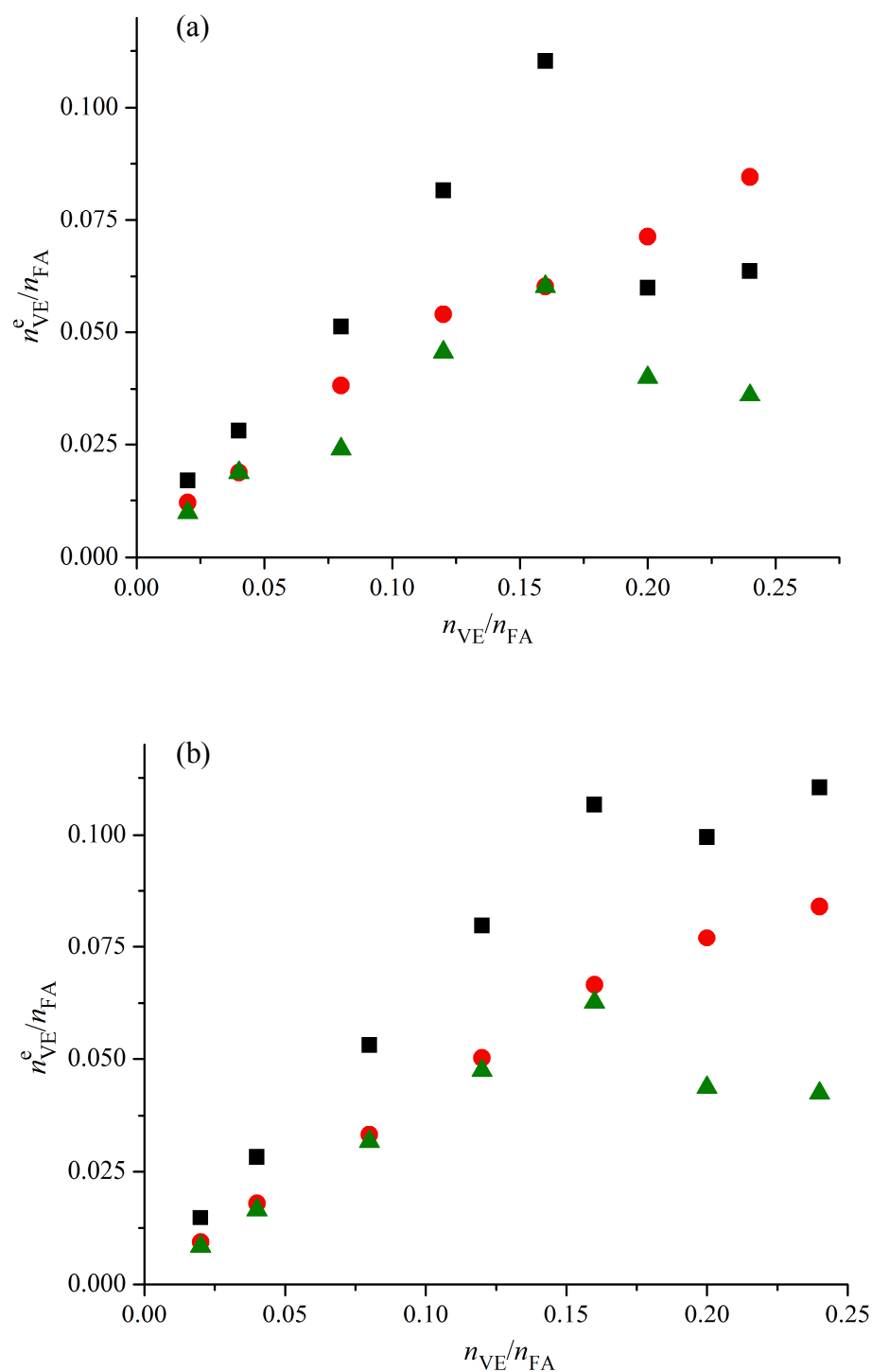


Figure 4.26. Amount of VE loaded in PEGylated and pure (a) palmitoleate-palmitoleic acid liposome and (b) oleic-oleate acid liposome with respect to the total amount of fatty acid. ■ indicates pure fatty acid liposome, ● represents mixture of DPPE-PEG2000-fatty acid liposomes and ▲ represents mixture of DPPE-PEG5000-fatty acid liposomes.

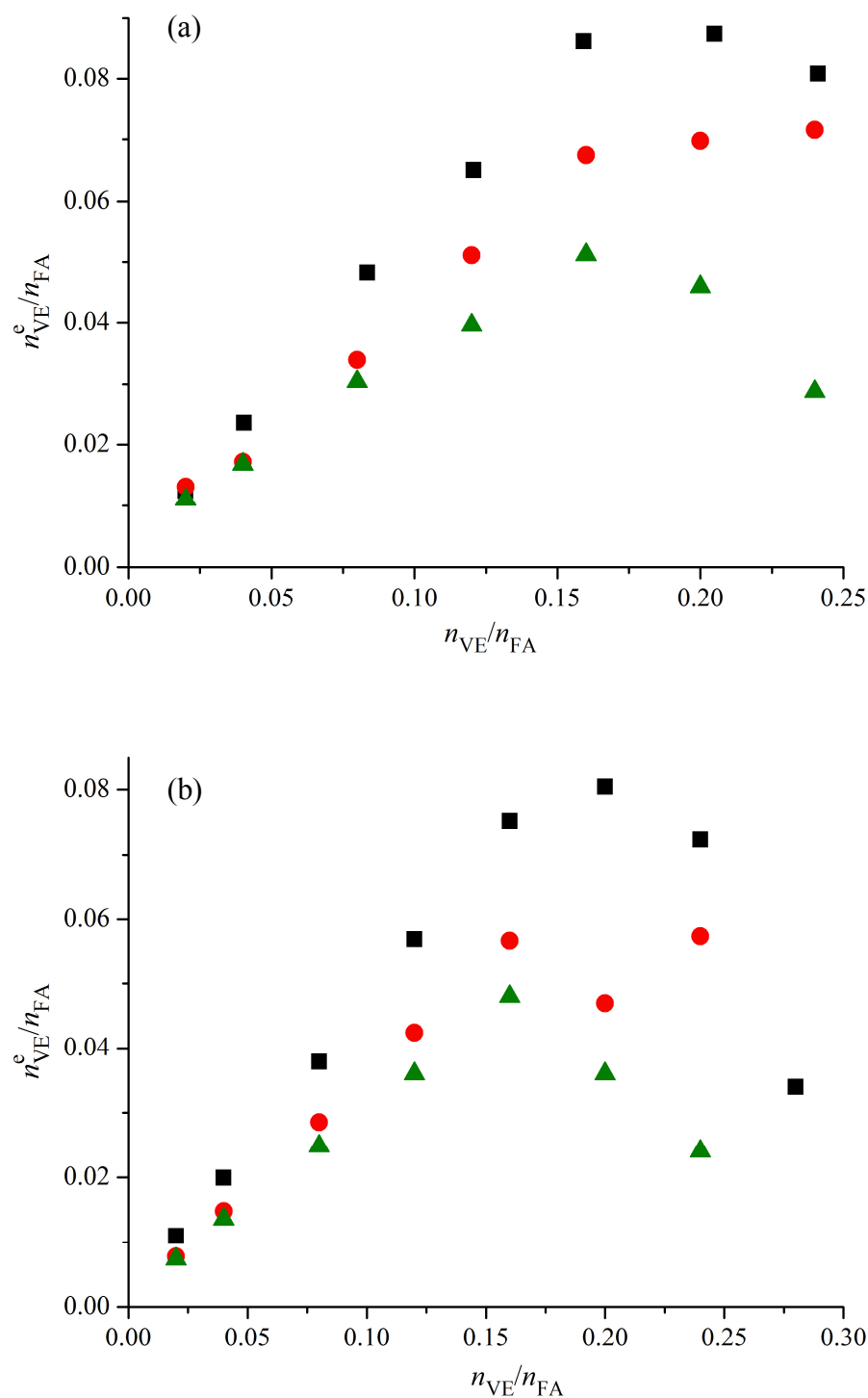


Figure 4.27. Amount of VE loaded in PEGylated and pure (a) linoleate-linoleic acid liposome and (b) linolenic-linolenate acid liposome with respect to the total amount of fatty acid. ■ indicates pure fatty acid liposome, ● represents mixture of DPPE-PEG2000-fatty acid liposome and ▲ represents mixture of DPPE-PEG5000-fatty acid liposomes.

4.6 Langmuir monolayer analysis

In this study, the Π - A isotherms were recorded during the compression of monolayer on 50 mM phosphate buffer pH 7 at 25 °C until a maximum value of surface pressure was obtained. The experiments were performed at pH 7.5 to enhance the possibility of pseudo-double chain surfactant formation between COOH and COO⁻ through hydrogen bonding that is similar to the molecular structure in bilayer membrane of liposome. The amount of fatty acid used was dominant while the amount of PEGylated lipids and α -tocopherol acetate (VE) were limited to a small amount in order to resemble the same environment as that of in liposome. In this study, the effect of PEGylated lipids on the cooperative intermolecular interaction with fatty acid and VE as well as their compatibility in governing the tendency of bilayer formation in liposome is highlighted. Information on the intermolecular forces was qualitatively analyzed from Langmuir monolayer isotherm that can be analogue to half a membrane bilayer [Feng 1999; Marsh, 1996; Nagle, 1986, Gong *et. al.*, 2002]. Hence, the compatibility of fatty acid with PEGylated lipid in a liposome was also evaluated through the value of surface excess area for the mixed monolayer. The excess free energy of the mixture in a monolayer that is related to the interaction force between two substances was analyzed by applying surface thermodynamic analysis. The most stable combination for each mixed fatty acid/PEGylated lipids in the formation of liposome was also suggested.

4.6.1 Langmuir monolayer for mixture of fatty acid and PEGylated lipids

The interactions between fatty acid and PEGylated lipid (DPPE-PEG2000 and DPPE-PEG5000) were investigated by compression of the mixed monolayer on a subphase of 50 mM phosphate buffer pH 7 at 25 °C. Both DPPE-PEG2000 and DPPE-PEG5000 have the same head group type and hydrocarbon chain length at the tail. However, the degree of polymerization for the ethoxylate group in DPPE-PEG5000 is

1.5 times higher than those in DPPE-PEG2000 as shown in figure 3.1. Since the PEG group is relatively larger than the phosphate group, therefore PEG plays a more dominant role in determining the intermolecular interaction in a monolayer. The Π - A isotherm of the pure DPPE-PEG2000 and pure DPPE-PEG5000 monolayer at an air-aqueous interface are shown in figure 4.28. The molecular area at the departure of surface pressure from zero for DPPE-PEG5000 is greater than DPPE-PEG2000 as expected. This would be due to stronger intermolecular electrostatic repulsive interaction between DPPE-PEG5000 molecules than DPPE-PEG2000 molecules at low surface pressure. The strong electrostatic interaction is inherently arisen from the negatively net force of long polyethoxylate chain. The negatively charge of the non-ionic polyethoxylate moiety is proposed to originate from the adsorbed hydroxyl ions that are released from the dissociation-association of water molecules. The hydroxyl ion is adsorbed specifically at the bulky PEGylated lipid molecular interface that is covered with polyethoxylate group via hydrogen bonding at the ether oxygen [Becher *et. al.*, 1987; Marinova *et. al.*, 1996]. Another reason could be due to the steric effect attributed from the mushroom-like conformation by the long polyethoxylate group. Hence, DPPE-PEG5000 in a monolayer tends to occupy larger area than DPPE-PEG2000. Nevertheless, both of the isotherms displayed conformation transition at the polyethoxylate chain as shown in the inset of figure 4.28. This observation might be caused by the extension of the long polyethoxylate chain from the air-aqueous interface. In this transition, it is suggested that polyethoxylate chain in mushroom conformation modify their structure to rod like or fibrillar structure for short polyethoxylate chains and to an elongated coiled conformation for long polyethoxylate chains as shown in figures 4.29(a) and 4.29(b) [Majewski *et. al.*, 1997]. At high surface pressure, both of the isothermal curves in this study do not converge. This result is similar to the monolayer composing L- α -distearoylphosphatidylcholine (DSPC) and distearoyl-

phosphatidylethanolamine poly(ethylene glycol)2000 (DSPE-PEG2000) [Chou and Chu, 2002]. However, it is contradictory to the study reported by Kuhl *et. al.* for mixed monolayer of distearoylphosphatidylethanolamine (DSPE)/DSPE-PEG2000 [Kuhl *et. al.*, 1995]. It is reported that at high surface pressure, the long polyethoxylate chain does not affect the molecular packing in a monolayer due to the extension of this long polyethoxylate chain into the aqueous subphase [Majewski, *et. al.*, 2000]. However, we found that the effective hydrocarbon tail end area, a_{eff} and bulkiness of the head group may play a significant role in determining the convergence of the isotherm at high surface pressure. The result indicates that changes of isotherm profile depend mainly on the polymerization degree of ethoxylate group, while the presence of phosphate head group is of secondary importance. Whereupon at higher degree of polymerization for DPPE-PEG5000, inefficiency of molecular close packing in the monolayer results in a larger effective area per molecule (a_{eff}) than DPPE-PEG2000 at high surface pressure as shown in figure 4.29(b).

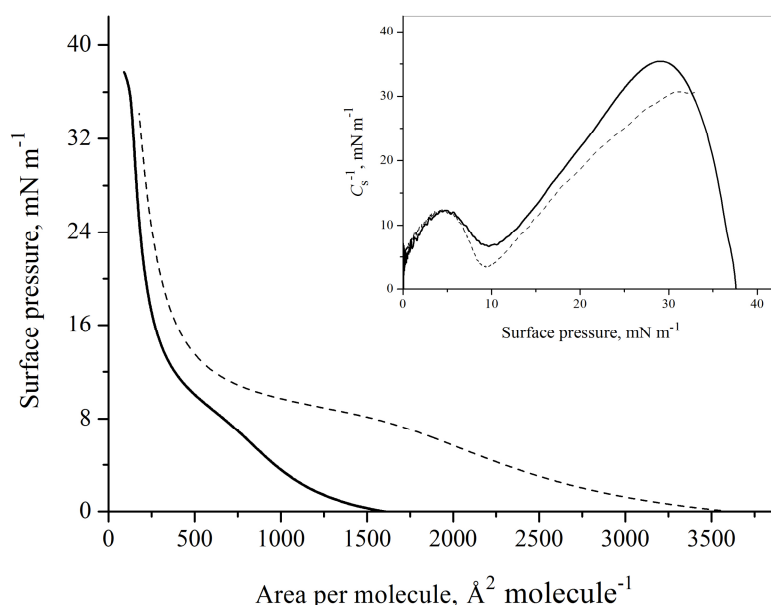


Figure 4.28 Π - A isotherm of DPPE-PEG2000 and DPPE-PEG5000 at 25 °C on 50 mM phosphate buffer subphase. The inset shows compression modulus (C_s^{-1}) for the monolayer as a function of surface pressure. Solid line indicates DPPE-PEG2000 while dashed line for DPPE-PEG5000.

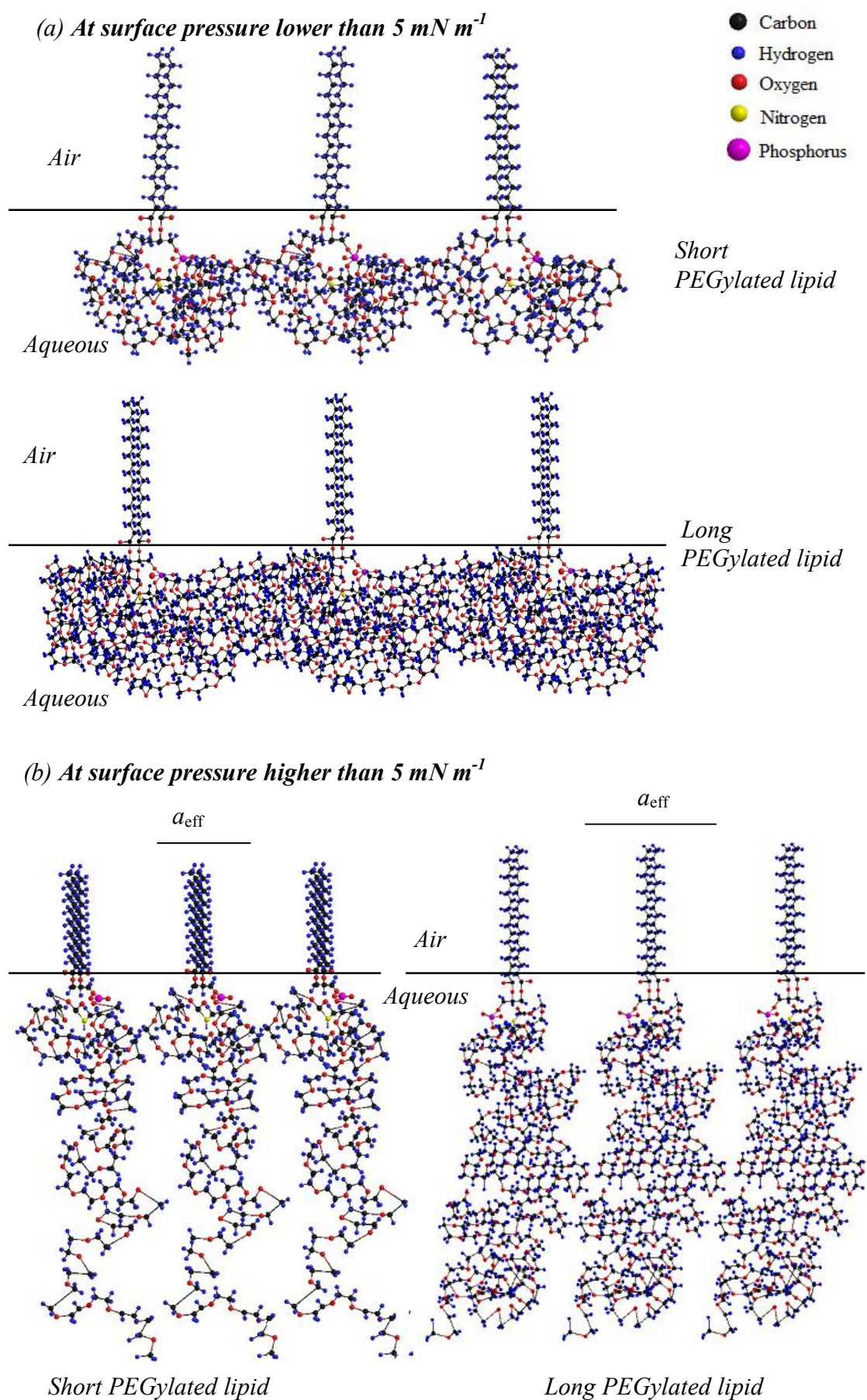


Figure 4.29. Conformation of short and long PEGylated lipid at surface pressure (a) lower than 5 mN m^{-1} and (b) higher than 5 mN m^{-1} .

The Π - A isotherm of the pure fatty acid monolayer and their mixture with DPPE-PEG2000 and DPPE-PEG5000 at various concentration are represented in figure 4.30 and figure 4.31, respectively. The Π - A isotherms of pure fatty acid is similar to typical “liquid” surfactant isotherm as indicated by the occurrence of liquid expanded state. The limiting molecular area for fatty acids are 21 Å² per molecule, 32 Å² per molecule, 42 Å² per molecule and 17 Å² per molecule for palmitoleic acid, oleic acid, linoleic acid and linolenic acid, respectively. The presence of *cis* double bond in a molecule may prevent close packing. This is due to the repulsion force arising from the π - π interaction. This can also be seen in figure 4.33 and figure 4.34 for the plot of C_s^{-1} as a function of surface pressure for the pure fatty acid monolayer whereupon the maximum value of C_s^{-1} is lower for a molecule with a higher number of double bond indicating a loose packing of the molecules in a monolayer. Therefore, limiting area per molecule for linoleic acid is larger than oleic acid although they are different by only one double bond. Similarly, palmitoleic acid with a shorter chain is less bulky and hence occupies a smaller area per molecule compared to oleic acid. However, limiting area per molecule for linolenic acid is smaller compared to the reported value whereupon the experiment was carried out on deionized water as subphase [Seoane *et. al.*, 2001]. This might be due to the slight dissolution of alkyl carboxylate into the buffer subphase at pH 7. Nevertheless, evaluation of the interaction between linolenic acid and PEGylated lipids is still valid as the results of the monolayers were reproducible as shown in figure 4.32.

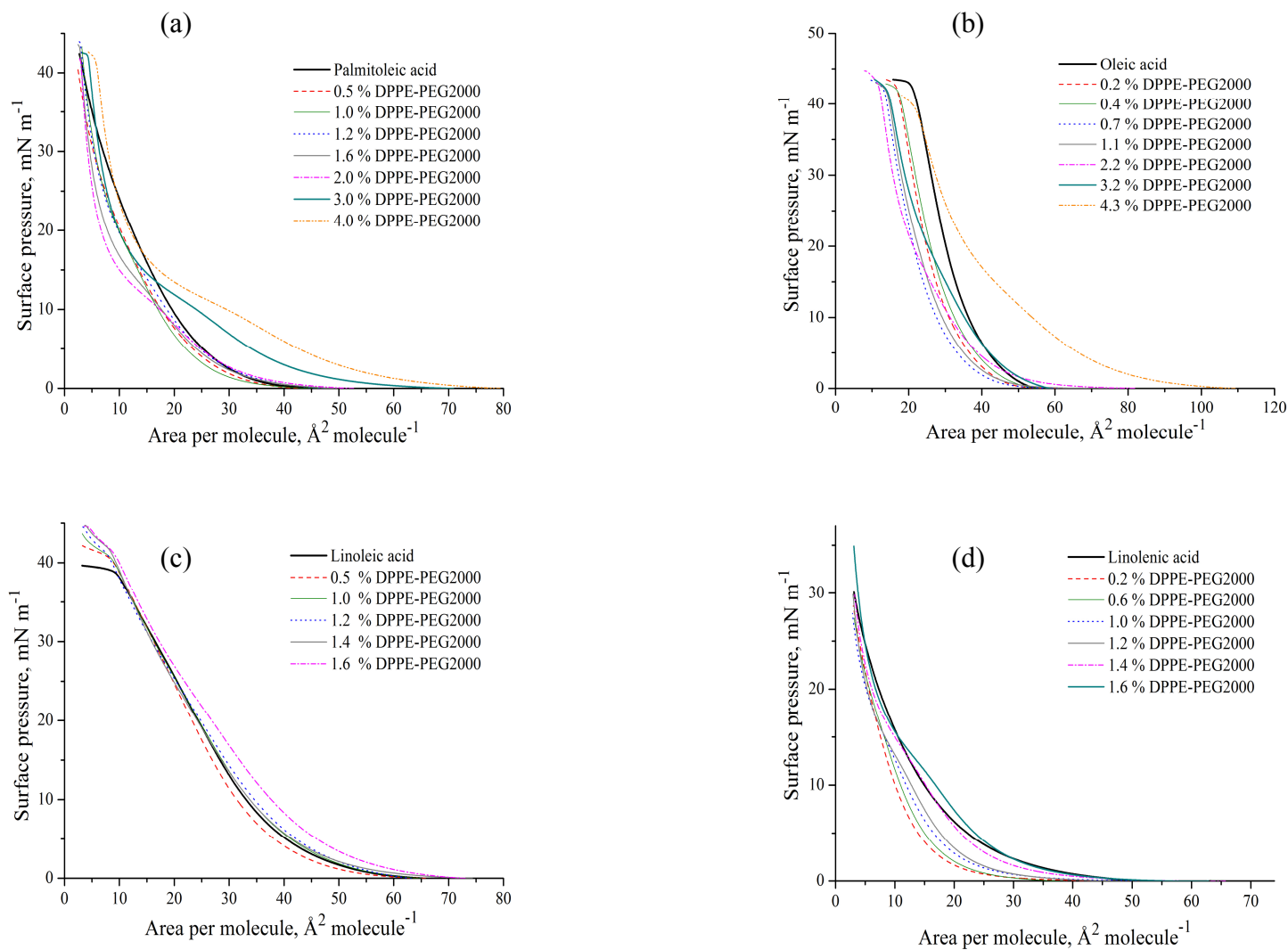


Figure 4.30. Surface pressure–area (Π – A) isotherms of (a) palmitoleic acid, (b) oleic acid, (c) linoleic acid and (d) linolenic acid mixed with DPPE-PEG2000 at the air–aqueous interface at 25 °C.

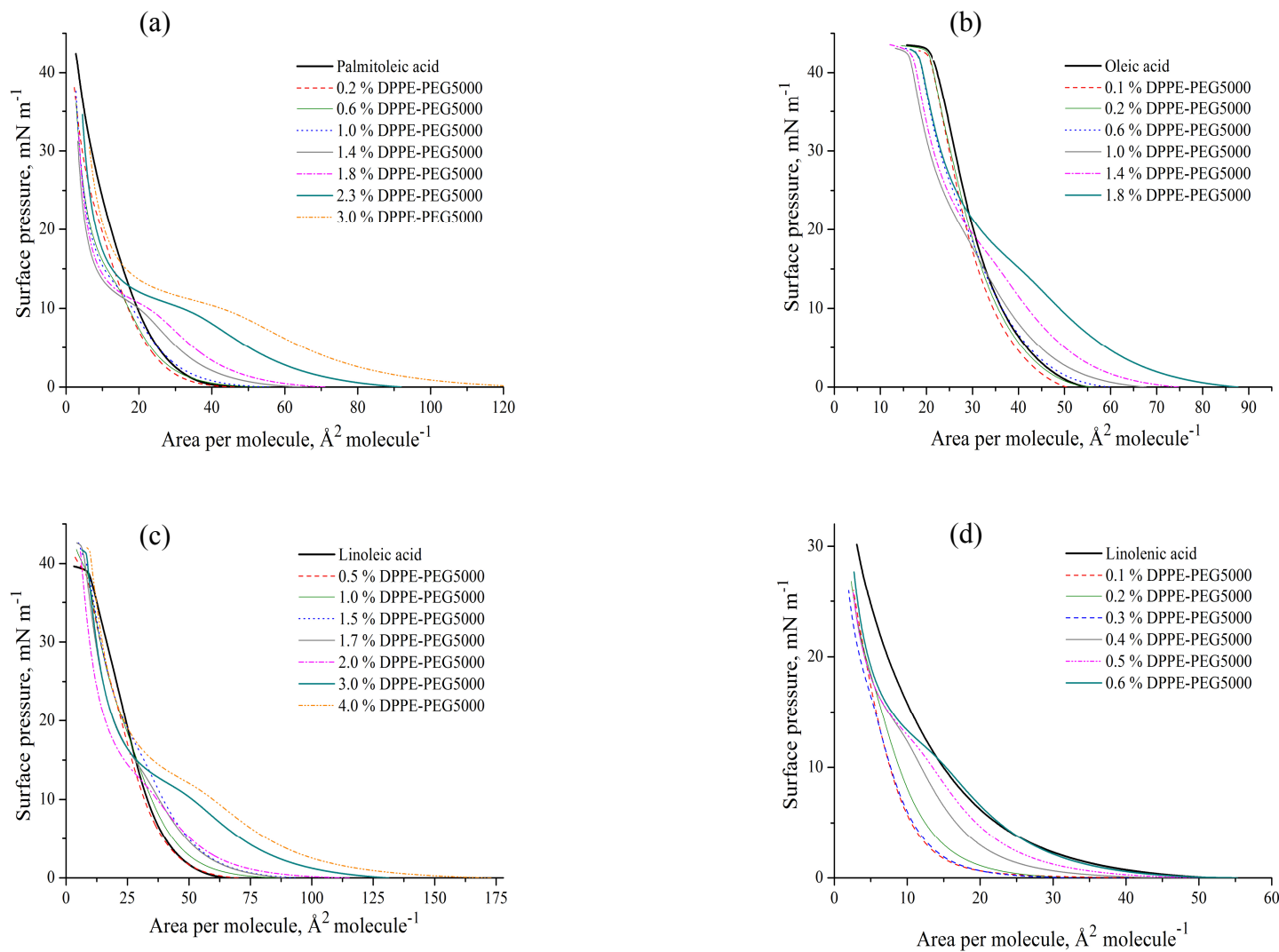


Figure 4.31. Surface pressure–area (Π – A) isotherms of (a) palmitoleic acid, (b) oleic acid, (c) linoleic acid and (d) linolenic acid mixed with DPPE-PEG5000 at the air–aqueous interface at 25 °C.

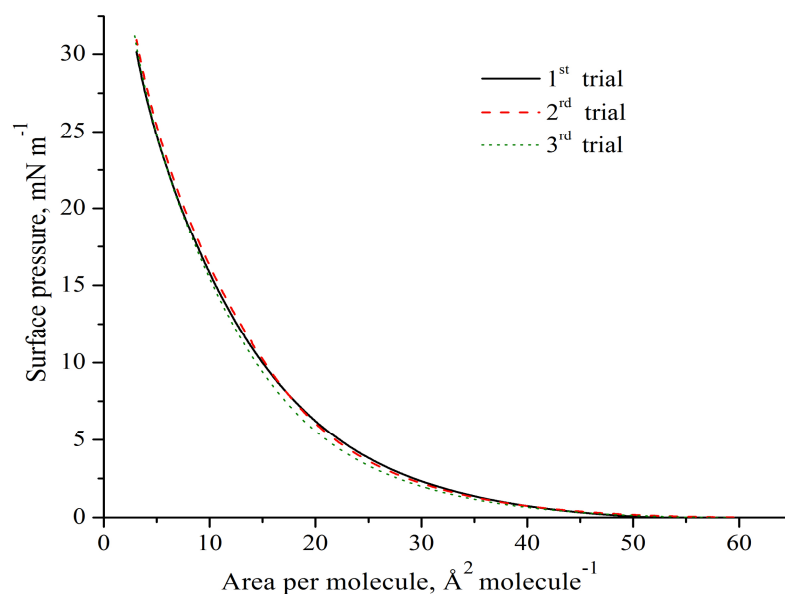


Figure 4.32. Π - A isotherm of linolenic acid at 25 °C on a 50 mM phosphate buffer pH 7 subphase.

The effect of DPPE-PEG2000 and DPPE-PEG5000 on fatty acid monolayers were shown in figure 4.30 and figure 4.31, respectively. We observed that incorporation of PEGylated lipids into fatty acid monolayer does not cause a remarkable change in the Π - A isotherm curves at low mole fraction of PEGylated lipids. However, a typical plateau transition of PEGylated lipid is observed in the Π - A isotherm as increase the mole fraction of PEGylated lipids is increased. A distinct feature is observed that the isotherms are shifted towards lower molecular area than the pure fatty acid at low mole fraction of PEGylated lipid. This suggests the out of plane protrusion of long PEG groups from the two dimensional monolayer. The plausible reason for the occurrence of protrusion is due to the solubility of the PEG group [Majewski *et. al.*, 2000].

It can be observed from the plot of compression modulus (C_s^{-1}) as a function of surface pressure as shown in figure 4.33 for mixture of fatty acid/DPPE-PEG2000 and figure 4.34 for mixture of fatty acid/DPPE-PEG5000. The appearance of two peaks become more pronounced as the amount of PEGylated lipid increases in a mixed monolayer. This effect can be seen in all of the fatty acid mixed monolayer with DPPE-

PEG2000 at $X_{\text{DPPE-PEG2000}}$ higher than 0.6 %. Nevertheless, the presence of two peaks can be observed at $X_{\text{DPPE-PEG5000}}$ as low as 0.1 % in the mixed monolayer of fatty acid and DPPE-PEG5000. This may be due to the molecules in the mixtures are separated into the form of micro phase. Therefore, the first peak at lower surface pressure may be dominantly resulting from the compression of the head group of PEGylated phospholipid as they are the largest in size hence more sensitive to the compression compared to fatty acid molecules or the hydrocarbon tails of the PEGylated lipid. In addition, C_s^{-1} for this peak is gradually decreasing as the amount of PEGylated lipid is increased. Nevertheless, the peak at higher surface pressure may be identified as arising from the effect of hydrocarbon tails at the PEGylated lipid and fatty acid molecules in the monolayer. This is because the changes in the second peak are more pronounced as we increase the amount of PEGylated lipid with double hydrocarbon tails. This is not observed in the pure fatty acid monolayer, whereby only one peak is observed.

The changes in C_s^{-1} for the first peak of the monolayer during compression may indicate the orientation of fatty acid molecules as it is progressively arranged into an organized manner and more closely packed. At the same time, the bulky PEG group is compressed to a state of closely packed as C_s^{-1} approaching maximum. However, further compression of the monolayer results in desorption of the bulky polyethoxylate group from the air-aqueous interface into the bulk aqueous phase, whereupon conformation transition occurred at the bulky polyethoxylate group from mushroom-like to extended shape conformation. Therefore, we may expect a reduction in C_s^{-1} as a result of the monolayer gradually becomes more compressible.

Further compression of the monolayer results in an increase of C_s^{-1} until the achievement of maximum C_s^{-1} . This indicates both of the hydrocarbon tails from PEGylated lipid are compressed to the state of closely packed. It can be clearly observed in the monolayer for mixture of linoleic acid and PEGylated lipid, whereby

the appearance of shoulder in second peak is more pronounced as the amount of PEGylated lipid increases. However, the value of C_s^{-1} at a fixed surface pressure with certain amount of PEGylated lipid is observed to be higher in the mixture of fatty acid with DPPE-PEG2000 than DPPE-PEG5000. This indicates that the polyethoxylate group still playing a role in the determination of the packing in monolayer although at a higher surface pressure of the monolayer. A similar trend is also seen in the monolayer of pure PEGylated lipid as shown in the inset of figure 4.28. If compression of the monolayer is continued, it is observed that the C_s^{-1} value is decreased. This may be caused by the molecules are slipping onto each other in the monolayer prior to the collapse of the monolayer regardless of the fatty acid molecules or PEGylated lipid involved.

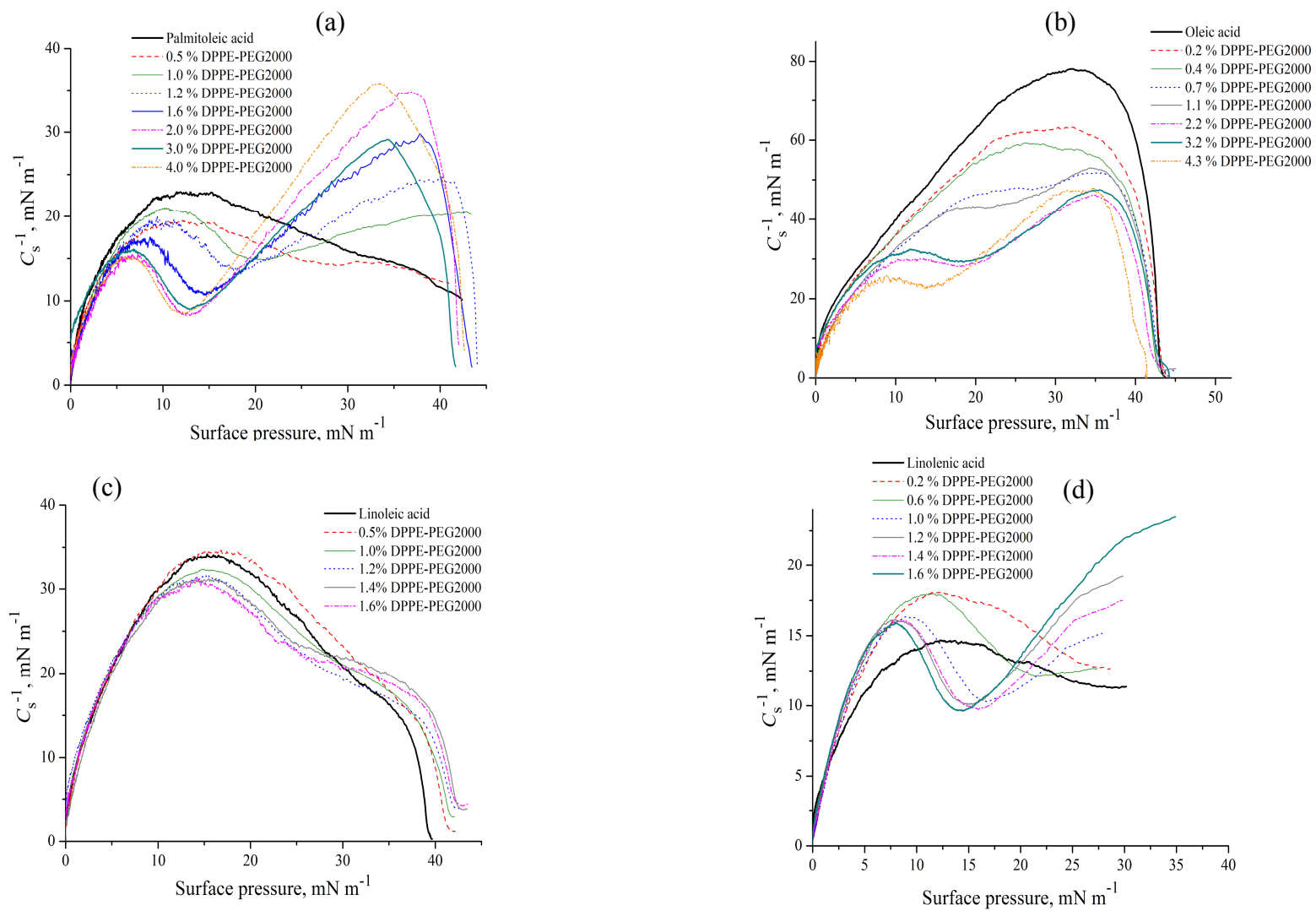


Figure 4.33. Compression modulus of (C_s^{-1}) (a) palmitoleic acid, (b) oleic acid, (c) linoleic acid and (d) linolenic acid mixed monolayer with DPPE-PEG2000 at 25 °C.

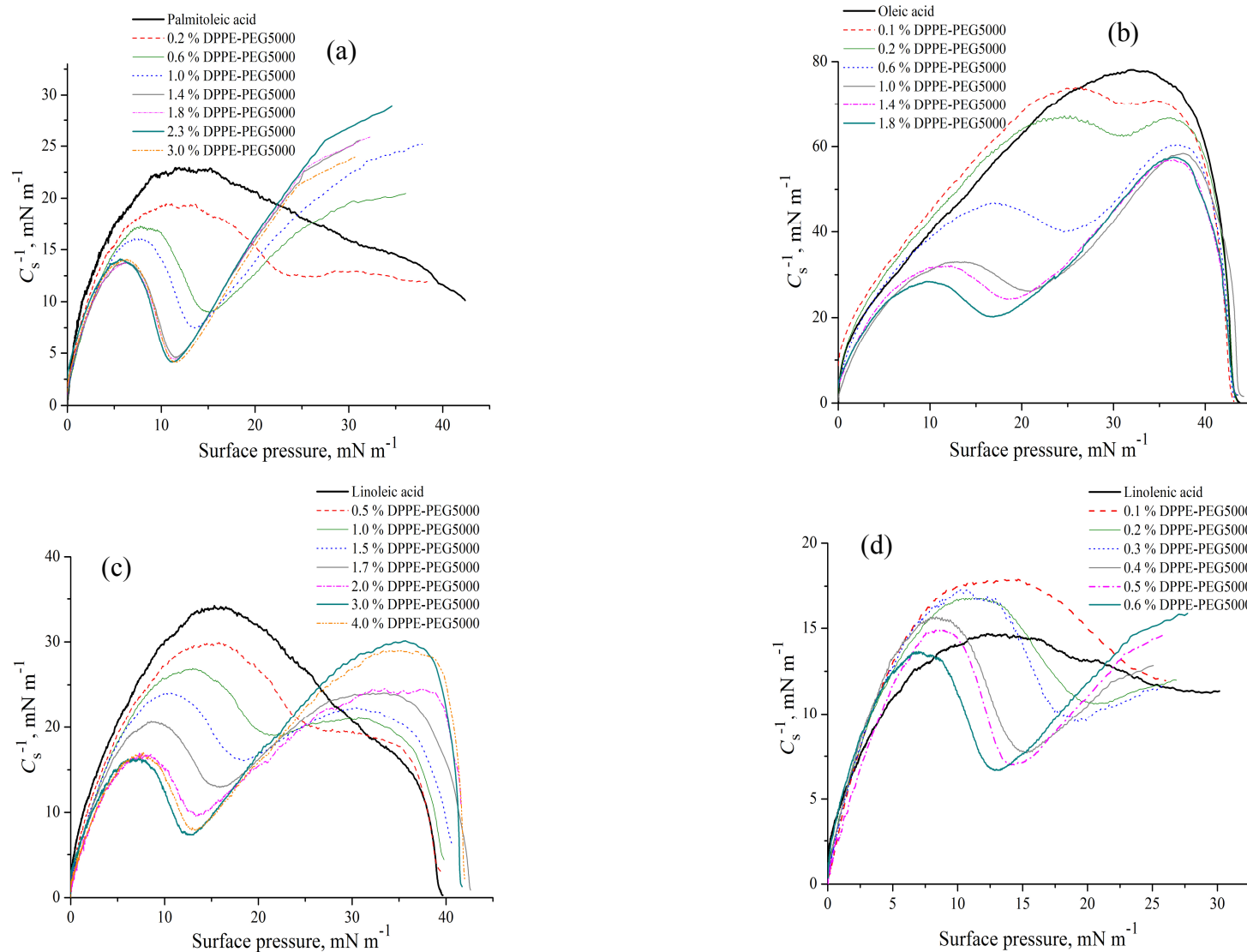


Figure 4.34. Compression modulus (C_s^{-1}) of (a) palmitoleic acid, (b) oleic acid, (c) linoleic acid and (d) linolenic acid mixed monolayer with DPPE-PEG5000 at 25 °C.

Meanwhile, as shown in figure 4.30 and figure 4.31, the collapse pressure for the mixed monolayer isotherms are dependent on the composition of PEGylated lipid. Thus, we can deduce that the mixtures are compatible as predicted by the phase rule. In addition, a non-ideal behaviour of fatty acid/PEGylated lipid mixed system is also confirmed by the non-linear course of the area per molecule as a function of mole fraction for DPPE-PEG2000 and DPPE-PEG5000 as shown in figure 4.35 and 4.36, respectively. The dotted lines correspond to area per molecule that is calculated on the basis of additivity rule. Deviations from ideality (dotted line) are observed for almost all fatty acid/PEGylated lipid mixed monolayer. These results further revealed the compatibility of the components in a monolayer with respect to the composition and surface pressures being studied.

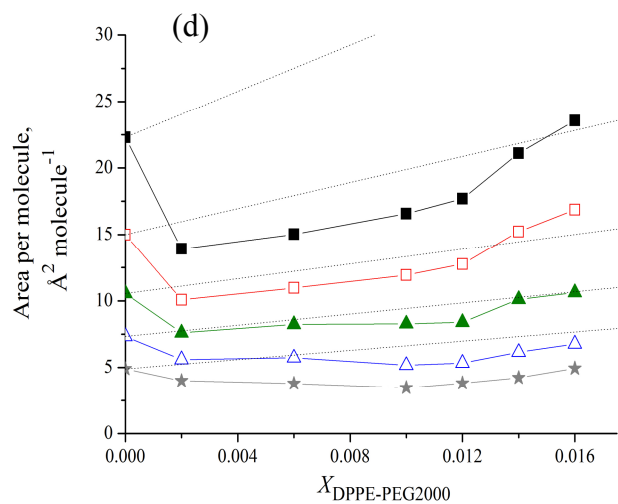
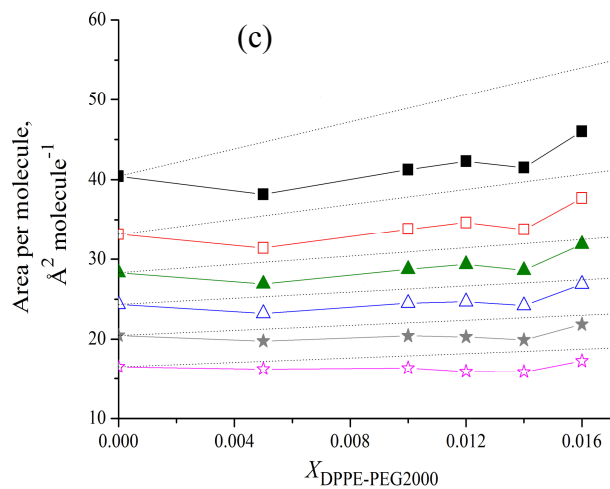
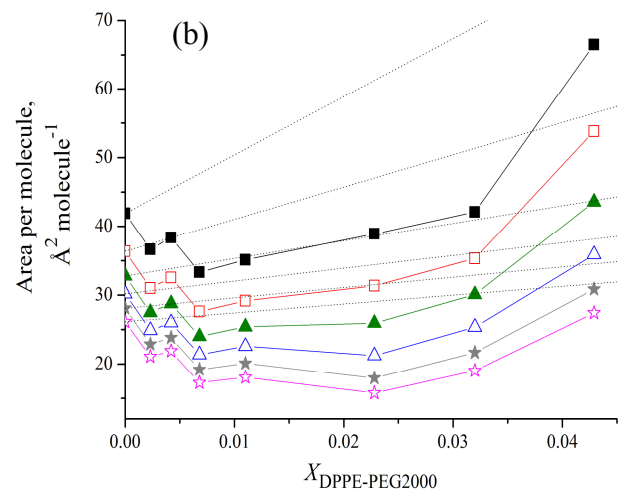
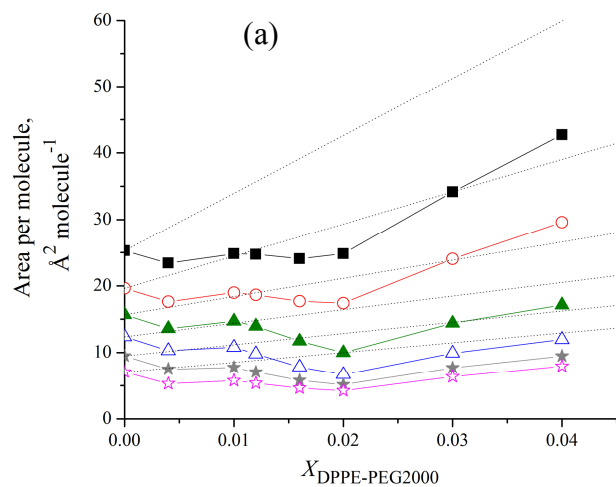


Figure 4.35. Area per molecule as a function of composition for mixed monolayer of (a) palmitoleic acid, (b) oleic acid, (c) linoleic acid and (d) linolenic acid with DPPE-PEG2000 at surface pressure ■ = 5 mN m⁻¹, □ = 10 mN m⁻¹, ▲ = 15 mN m⁻¹, △ = 20 mN m⁻¹, ★ = 25 mN m⁻¹, ☆ = 30 mN m⁻¹.

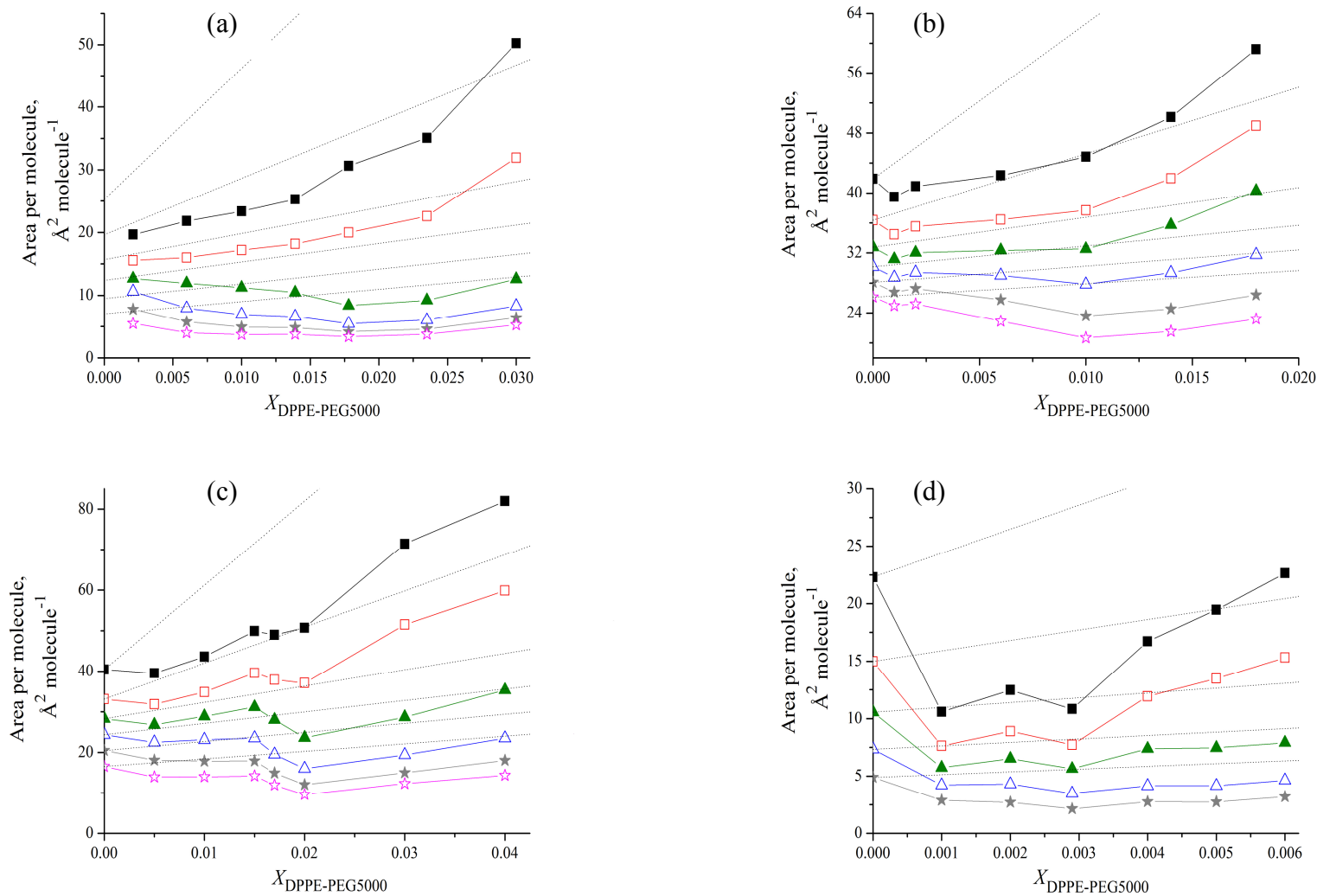


Figure 4.36. Area per molecule as a function of composition for mixed monolayer of (a) palmitoleic acid, (b) oleic acid, (c) linoleic acid and (d) linolenic acid with DPPE-PEG5000 at surface pressure $\blacksquare = 5 \text{ mN m}^{-1}$, $\square = 10 \text{ mN m}^{-1}$, $\blacktriangle = 15 \text{ mN m}^{-1}$, $\triangle = 20 \text{ mN m}^{-1}$, $\star = 25 \text{ mN m}^{-1}$, $\star = 30 \text{ mN m}^{-1}$.

In addition of the above study, analysis of surface excess area was applied to further evaluate the phenomena of non-ideal mixing. The plots of $A_{\text{exc}}/A_{\text{id}}$ at different surface pressure for mixed monolayer of palmitoleic acid, oleic acid, linoleic acid and linolenic acid with DPPE-PEG2000 and DPPE-PEG5000 are shown in figure 4.37 and figure 4.38, respectively. All the plots of fatty acid/PEGylated lipid mixed monolayer show a general trend with the presence of a minimum.

From both of the figures mentioned above, negative deviations are observed in all of the studied mole fraction range of DPPE-PEG2000 and DPPE-PEG5000 mixed with palmitoleic acid, linoleic acid and linolenic acid in this study. Similar result is also observed for most of the mixture consisting oleic acid/DPPE-PEG2000 and oleic acid/DPPE-PEG5000. This negative deviation is possibly due to geometric accommodation and intermolecular hydrophobic interaction that contribute to the condensing effect of DPPE-PEG2000 and DPPE-PEG5000 on fatty acid monolayers. Nevertheless, mixture of oleic acid/DPPE-PEG2000 at $X_{\text{DPPE-PEG2000}} = 4.3 \%$ regardless of surface pressure and oleic acid containing 1.8 % DPPE-PEG5000 at surface pressure $= 15 \text{ mN m}^{-1}$ displayed slightly different result. Apparently, a positive value of $A_{\text{exc}}/A_{\text{id}}$ is observed. This suggests that at this composition, the intermolecular interaction between oleic acid and PEGylated lipid is weaker than the interaction between their pure components. Both of the oleic acid and PEGylated lipid molecules cannot accommodate in a closely packed environment with each other that result in a larger area per molecule than in their pure monolayer.

Although the deviation trend of $A_{\text{exc}}/A_{\text{id}}$ is not affected by surface pressure in a monolayer, their values become less negative with surface pressure increases from 5 mN m^{-1} to 15 mN m^{-1} for mixture of oleic acid/DPPE-PEG5000 as well as DPPE-PEG2000 mixed with linoleic acid or linolenic acid. The magnitude of $A_{\text{exc}}/A_{\text{id}}$ decreases from surface pressure 5 mN m^{-1} to 10 mN m^{-1} is observed for monolayer

consisting mixture of oleic acid or palmitoleic acid with DPPE-PEG2000 and mixture of palmitoleic acid, linoleic acid and linolenic acid with DPPE-PEG5000. This observation suggests that increase in surface pressure from 5 mN m^{-1} to 10 mN m^{-1} results in a weaker interaction among the mixed molecules compared to the interaction between the pure molecules. Nevertheless, the condensing effect becomes more significant with further increase of the surface pressure in all of the monolayers. This indicates a stronger interaction among the mixed molecules than those between the pure molecules as the surface pressure is further increased. Thus, the arrangement of mixed molecules in a monolayer is believed to be in a more ordered manner than in its pure system.

The common feature that is observed from all of the plots is that PEGylated lipids produce a maximum area condensing effect on fatty acid monolayer, regardless of surface pressure. Palmitoleic acid is found compatible with both DPPE-PEG2000 and DPPE-PEG5000 with an almost same value of $A_{\text{exc}}/A_{\text{id}}$. Combination of oleic acid/DPPE-PEG2000 was found more compatible as revealed by the larger deviation of $A_{\text{exc}}/A_{\text{id}}$ to more negative value in comparison to mixture of oleic acid/DPPE-PEG5000. On the other hand, DPPE-PEG5000 participates better into the monolayer of linoleic acid or linolenic acid. Apparently, addition of PEGylated lipid to higher amount may disrupt the packing of fatty acid monolayer and result in a less deviation of $A_{\text{exc}}/A_{\text{id}}$.

Both of the deviation from additivity rule as observed in figure 4.35 and figure 4.36 as well as the variations of collapse pressure with composition as shown in figure 4.30 and figure 4.31 may imply the common compatibility of palmitoleic acid, oleic acid, linoleic acid and linolenic acid with DPPE-PEG2000 and DPPE-PEG5000 at the air-aqueous interface. It is also observed that the magnitude of interaction between the molecules at the interface depends on the surface pressure as can be seen in figure 4.37 and figure 4.38.

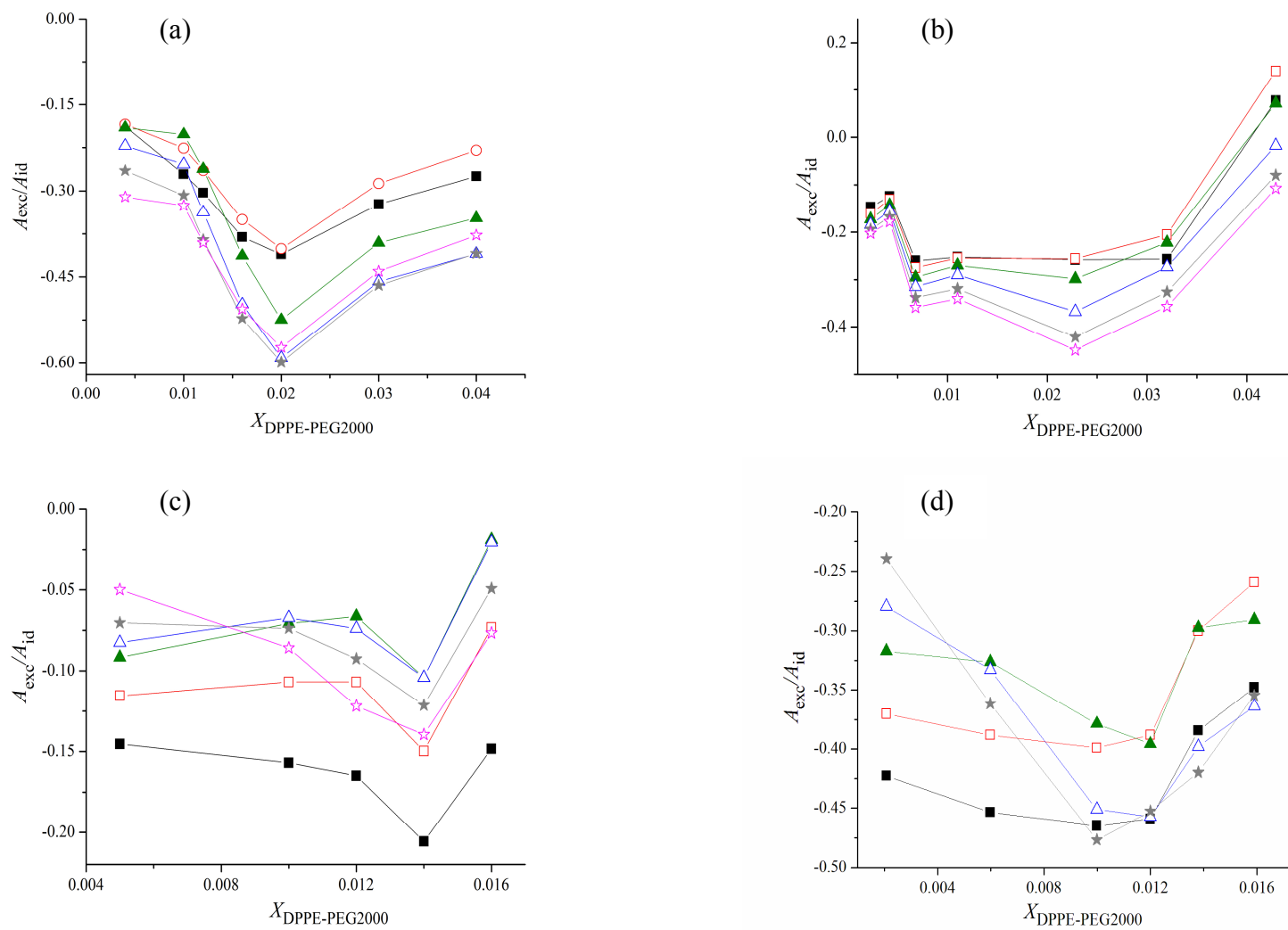


Figure 4.37 A_{exc}/A_{id} for mixed monolayer of (a) palmitoleic acid, (b) oleic acid, (c) linoleic acid and (d) linolenic acid as a function of $X_{DPPE-PEG2000}$ at 25 °C at surface \blacksquare = 5 mN m⁻¹, \square = 10 mN m⁻¹, \blacktriangle = 15 mN m⁻¹, \triangle = 20 mN m⁻¹, \star = 25 mN m⁻¹, \star = 30 mN m⁻¹.

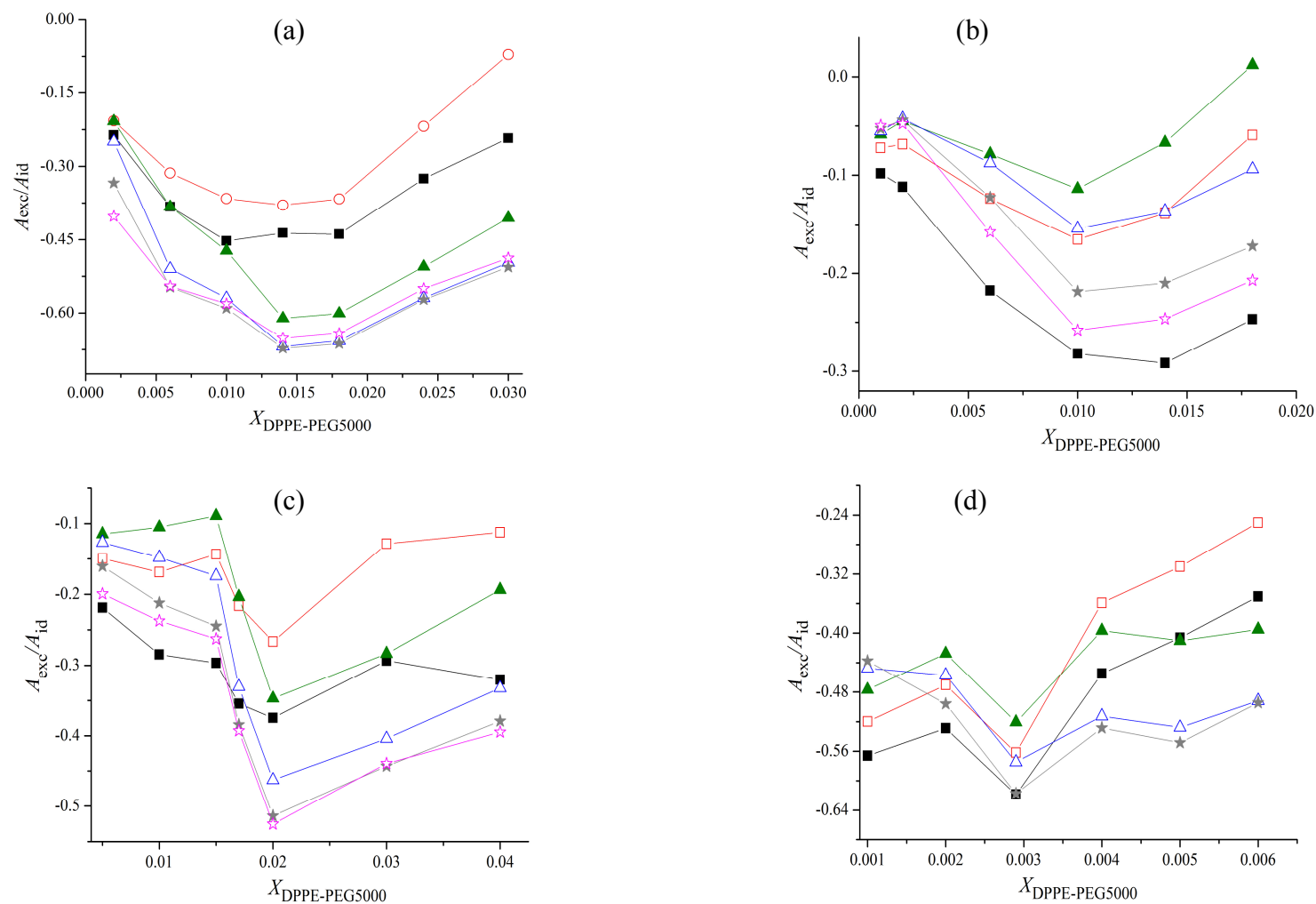


Figure 4.38. A_{exc}/A_{id} for mixed monolayer of (a) palmitoleic acid, (b) oleic acid, (c) linoleic acid and (d) linolenic acid as a function of $X_{DPPE-PEG5000}$ at 25 °C at surface pressure $\blacksquare = 5 \text{ mN m}^{-1}$, $\square = 10 \text{ mN m}^{-1}$, $\blacktriangle = 15 \text{ mN m}^{-1}$, $\triangle = 20 \text{ mN m}^{-1}$, $\star = 25 \text{ mN m}^{-1}$, $\star = 30 \text{ mN m}^{-1}$.

Figure 4.39 and figure 4.40 show the plots of C_s^{-1} as a function of mole fraction DPPE-PEG2000 and DPPE-PEG5000 at various constant surface pressures, respectively. C_s^{-1} values for pure fatty acid are indicated at zero PEGylated lipid content. As the number of double bond in the hydrocarbon chain of fatty acid increases, the value of C_s^{-1} is found to be smaller. The compressibility of the fatty acids is in the order of linolenic acid > linoleic acid > oleic acid. The presence of double bonds with kinks and bends in the molecules induces π - π repulsion interaction that hinders closed packing of the monolayer at the air-aqueous interface. This could be the reason for the low C_s^{-1} value especially in the case of linolenic acid. On the other hand, oleic acid and palmitoleic acid both with one unsaturated double bond but different by additional of two methylene group in oleic acid has displayed a slight variation on the C_s^{-1} value. Monolayer of palmitoleic acid is found more compressible than oleic acid monolayer. The plausible reason is the higher rigidity of the shorter hydrocarbon chain in palmitoleic acid relative to oleic acid that hinders close packing of the molecules. Hence, more space is rendered for compression in palmitoleic acid monolayer.

This parameter is drastically affected by the presence of impurities in the monolayer. Hence, C_s^{-1} values for the pure unsaturated fatty acids were included in both of the above mentioned figures for comparison purposes. The result shows that C_s^{-1} for pure oleic acid monolayer is increasing with surface pressure. This implies oleic acid monolayer is more resistance to compression at high surface pressure. However, C_s^{-1} for monolayer of palmitoleic acid, linoleic acid and linolenic acid display slightly different results, whereupon C_s^{-1} increases from surface pressure 5 mN m⁻¹ to 15 mN m⁻¹. This implies the molecules are approaching closer to each other especially the hydrocarbon tail with large surface area, whereby the head group is still far from each other. Further compression of the monolayer at surface pressure higher than 15 mN m⁻¹ results in a drop of C_s^{-1} that indicates the presence of more space in between the molecules. The

plausible explanation could be hydrocarbon tail of linoleic acid and linolenic acid with two and three double bonds, respectively, are interacting and hence slipped into the gap in between the hydrocarbon region. Similarly, palmitoleic acid with the more rigid hydrocarbon tail than oleic acid are forced to packed closely during the compression hence their C_s^{-1} is varied from oleic acid monolayer.

The C_s^{-1} for mixed palmitoleic acid/DPPE-PEG2000 and palmitoleic acid /DPPE-PEG5000 are shown in figure 4.39(a) and 4.40(a) respectively. C_s^{-1} for monolayer of palmitoleic acid mixed with DPPE-PEG2000 increase with surface pressures from 15 mN m^{-1} at $X_{\text{DPPE-PEG2000}} \geq 1.6 \%$ whereas at $X_{\text{DPPE-PEG5000}} \geq 0.6 \%$ for palmitoleic acid/DPPE-PEG5000 mixed monolayer. This is in agreement with the general expectation that high C_s^{-1} will be observed when the monolayers are more condensed. Moreover, C_s^{-1} reaches an almost consistent value at each surface pressure regardless the increased amount of PEGylated lipid.

As observed in figure 4.39(b) and 4.40(b), at low surface pressures ($\Pi = 5 \text{ mN m}^{-1}$), the C_s^{-1} values are small for mixture of oleic acid/DPPE-PEG2000 and oleic acid/DPPE-PEG5000. This implies the monolayers are in their expanded state at low surface pressures with higher interfacial elasticity and the monolayers are with more liquid-like property. In contrary, the monolayer becomes more condensed whereby mixed molecules are arranged into more ordered manner as the monolayers were being further compressed. Hence, C_s^{-1} values increase as the surface pressures increase regardless the content of PEGylated lipid. However, this observation is only limited to oleic acid/DPPE-PEG2000 mixed monolayer. At surface pressure 20 mN m^{-1} , the C_s^{-1} values for mixture of oleic acid/DPPE-PEG5000 are in fact lower than those at surface pressure of 10 mN m^{-1} and 15 mN m^{-1} for $X_{\text{DPPE-PEG5000}}$ greater than 0.8% . This may suggest that the monolayer physically can be further compressed.

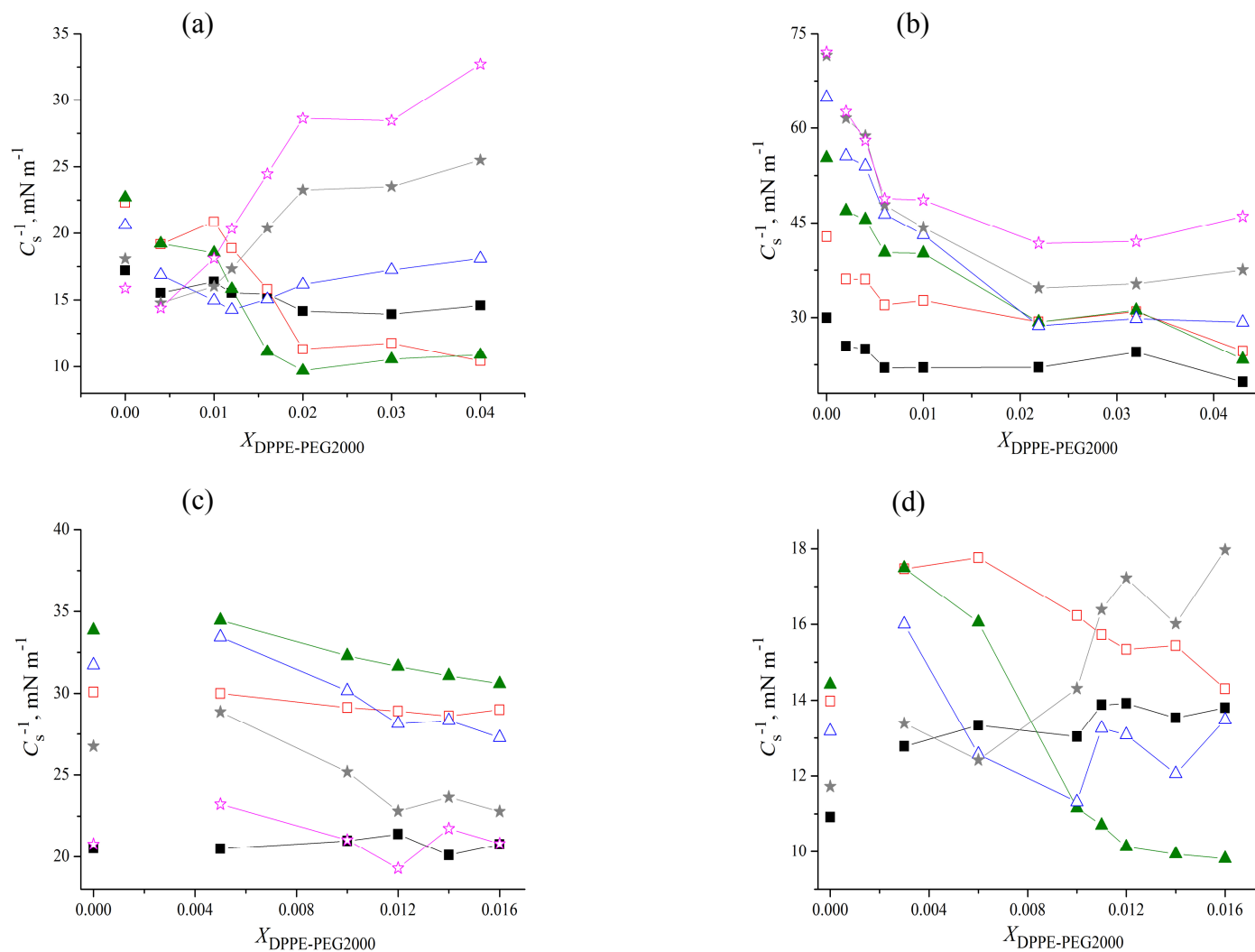


Figure 4.39. Compression modulus (C_s^{-1}) for mixed monolayer of (a) palmitoleic acid, (b) oleic acid, (c) linoleic acid and (d) linolenic acid as a function of $X_{\text{DPPE-PEG2000}}$ at 25 °C and surface pressure $\blacksquare = 5 \text{ mN m}^{-1}$, $\square = 10 \text{ mN m}^{-1}$, $\blacktriangle = 15 \text{ mN m}^{-1}$, $\triangle = 20 \text{ mN m}^{-1}$, $\star = 25 \text{ mN m}^{-1}$, $\star = 30 \text{ mN m}^{-1}$.

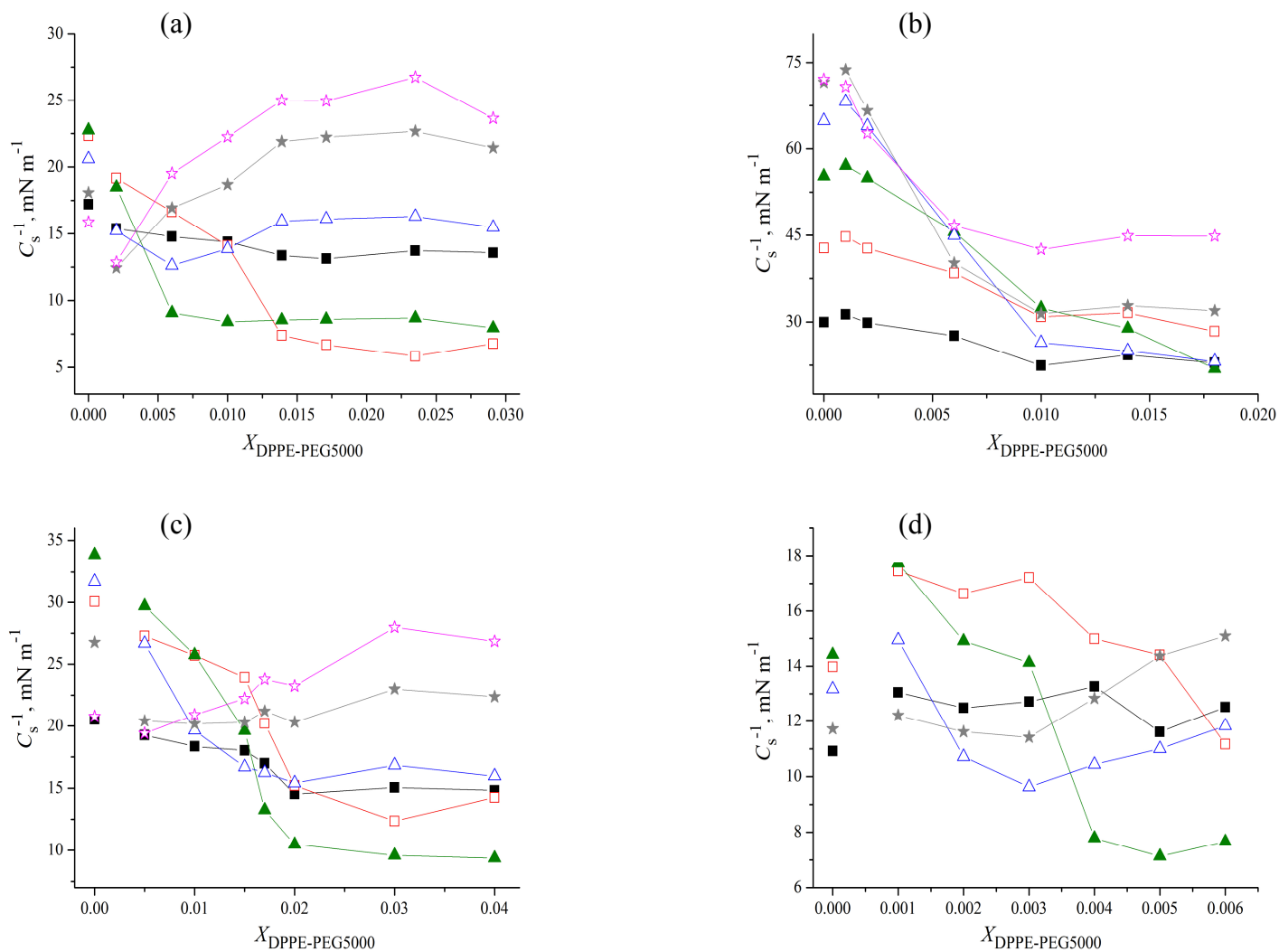


Figure 4.40. Compression modulus (C_s^{-1}) for mixed monolayer of (a) palmitoleic acid, (b) oleic acid, (c) linoleic acid and (d) linolenic acid as a function of $X_{\text{DPPE-PEG5000}}$ at 25 °C and surface pressure ■ = 5 mN m⁻¹, □ = 10 mN m⁻¹, ▲ = 15 mN m⁻¹, △ = 20 mN m⁻¹, ★ = 25 mN m⁻¹, ☆ = 30 mN m⁻¹.

Figure 4.39(c) illustrates the effect of DPPE-PEG2000 on C_s^{-1} of linoleic acid monolayer. C_s^{-1} increase gradually as the compression progressed from 5 mN m⁻¹ to 15 mN m⁻¹, regardless of the composition in monolayers. Nevertheless, C_s^{-1} values reduce as the surface pressure further rises from 20 mN m⁻¹ to 30 mN m⁻¹. It is possibly attributed to the more disordered arrangement in the hydrocarbon chain during the compression. A similar trend also observed for monolayer of pure palmitoleic acid, linoleic acid and linolenic acid. Therefore, this observation indicates that addition of DPPE-PEG2000 into linoleic acid monolayer did not significantly affect the value of compression modulus.

It can be obviously seen in figure 4.40(c) that C_s^{-1} for mixed monolayer of linoleic acid/DPPE-PEG5000 increases with surface pressure from 15 mN m⁻¹ at $X_{\text{DPPE-PEG5000}} \geq 1\%$. This is in agreement with the general expectation that high C_s^{-1} will be observed when the monolayers are more condensed. Moreover, at surface pressure 10 mN m⁻¹, 15 mN m⁻¹ and 20 mN m⁻¹, C_s^{-1} values underwent reduction and reached an almost consistent value as the amount of DPPE-PEG5000 increased. These in turns prove that molecular orientation was changed and caused the molecules to be arranged in a looser structure and formed a more fluid monolayer.

As depicted in figures 4.39(d) and 4.40(d), a similar trend to mixture linoleic acid/DPPE5000 at $\Pi = 15$ mN m⁻¹ is also exhibited by linolenic acid mixed with DPPE-PEG2000 and DPPE-PEG5000. From figure 4.39(d), considerable fluctuations of C_s^{-1} are obvious. On the contrary, addition of DPPE-PEG5000 of more than 0.3 % at surface pressure 20 mN m⁻¹ and 25 mN m⁻¹ induces systematic increase of C_s^{-1} .

The values of C_s^{-1} for the mixed monolayer are dependent on the molecular weight of PEGylated lipid and the degree of unsaturation of the fatty acid molecules. As the degree of polymerization increases, their effect on compressibility is more pronounced. In addition, the shorter as well as the higher the degree of unsaturation at

the hydrocarbon chain of fatty acid the less rigid is the monolayer formed. Hence, it is obvious that the addition of DPPE-PEG2000 and DPPE-PEG5000 into fatty acid monolayers have rendered variation on C_s^{-1} values with respect to surface pressure as shown in figure 4.39 and figure 4.40. Nevertheless, effect of DPPE-PEG5000 on the monolayer is more pronounced compared to DPPE-PEG2000. This might be due to DPPE-PEG5000 possesses longer polyethoxylated chain, hence larger surface coverage per molecule and less water soluble than DPPE-PEG2000 that causes a significant effect during the compression of mixed monolayers. At surface pressure as low as 5 mN m⁻¹ for all of the fatty acid mixed monolayers, C_s^{-1} was not significantly influenced by the amount of PEGylated lipid. This could be due to the hydrocarbon chain of the molecules is at the state of disorder and free to move. However, a general trend is observed for mixed monolayer of palmitoleic acid and linolenic acid containing PEGylated lipids as shown in figure 4.41. The same trend is also found in mixed

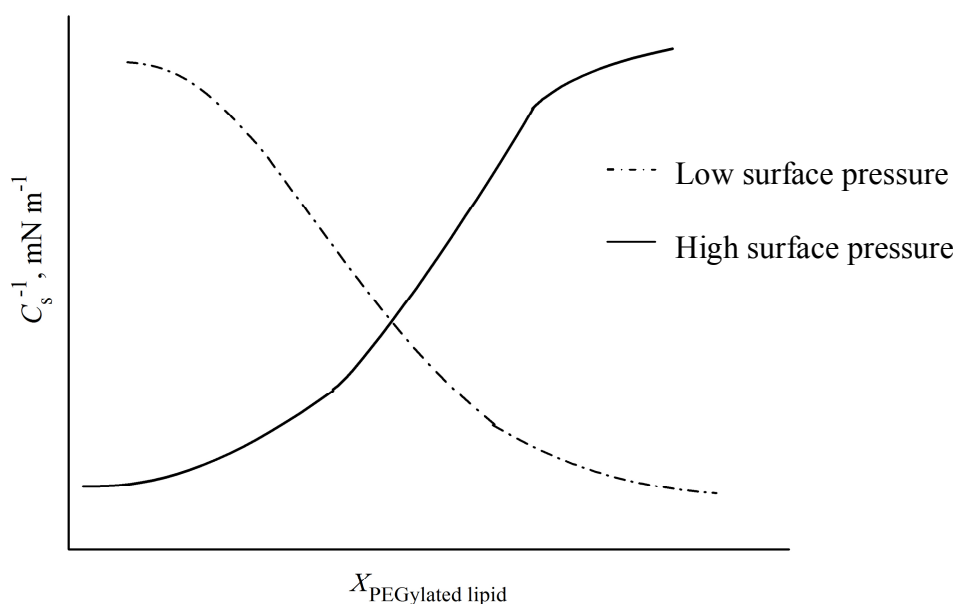


Figure 4.41. The general trend of C_s^{-1} as a function of mole fraction PEGylated lipid.

monolayer of linoleic acid/DPPE-PEG5000 as shown in figure 4.40(c). At low $X_{\text{DPPE-PEG5000}}$ and low surface pressure, higher values of C_s^{-1} are found compared to those with high $X_{\text{DPPE-PEG5000}}$ and low surface pressure. However, the value of C_s^{-1} is slightly lower than those in pure fatty acid monolayer that implies less rigid monolayers are formed with addition of DPPE-PEG5000. The plausible reason is that fatty acid molecules are more dominant compared to DPPE-PEG5000 and hence C_s^{-1} obtained is almost similar to the pure fatty acid. Similarly, at low $X_{\text{DPPE-PEG5000}}$ and high surface pressure, lower C_s^{-1} values are obtained. On the other hand, as higher $X_{\text{DPPE-PEG5000}}$ is present in the monolayer, compressibility of the monolayer is increasingly affected by the polyethoxylated chain. Whereupon, C_s^{-1} value is low at low surface pressure that implies the monolayers are in their expanded state due to the “mushroom-like” conformation of polyethoxylated group that resists the molecules from coming closer to each other. At high surface pressure and high amount of DPPE-PEG5000, it is observed that C_s^{-1} value is concomitantly higher. This indicates the formation of more rigid and less compressible monolayer as a result of the molecules being arranged in a more ordered manner. The plausible explanation is due to the closely packing of the double hydrocarbon chains as a result from the extension of polyethoxylated group into the subphase at high surface pressure. On the other hand, C_s^{-1} values show a significant decreasing trend at surface pressure of $5 \text{ mN m}^{-1} - 15 \text{ mN m}^{-1}$. This might be due to the monolayer is experiencing a phase transition. As the monolayer was further compressed, polyethoxylated chain may extend into the aqueous subphase to reduce the repulsion force arising from close approach of the polyethoxylated chain. As a result, it creates more spaces between the molecules and therefore decreases C_s^{-1} . It is obvious that monolayer of linoleic acid mixed with DPPE-PEG2000 and DPPE-PEG5000 display a different result at high surface pressure ($20 \text{ mN m}^{-1} - 30 \text{ mN m}^{-1}$) whereupon, C_s^{-1} values decrease as surface pressure increases for linoleic acid/DPPE-PEG2000 mixed

monolayer. This might be caused by slipping of molecules on each other due to extension of PEG into the bulk solution that encourages close packing of the hydrocarbon tails from PEGylated lipid.

The compression modulus of the mixed monolayers is much more dependent on the surface pressure than the composition of PEGylated lipids as can be realized from figures 4.39 and figure 4.40. Additions of PEGylated lipids into the fatty acid monolayer do not significantly change the trend of C_s^{-1} with respect to degree of unsaturation. In the investigated mole fraction range of PEGylated lipids, C_s^{-1} value of oleic acid with PEGylated lipid remains the highest in comparison to mixture of PEGylated lipid with linoleic acid or linolenic acid. Nevertheless, PEGylated lipids have imposed an effect on the conformation of hydrocarbon chain in fatty acid mixed monolayers.

Once compatibility of the mixed monolayer has been identified, the strength of interaction between molecules in a mixed monolayer relative to the interaction between molecules in a pure monolayer can be quantitatively evaluated from the excess Gibbs free energy of mixture at the interface, ΔG_{exc} . The ΔG_{exc} values were calculated at various compositions of PEGylated lipid and surface pressure as illustrated in figure 4.42 for FA/DPPE-PEG2000 and figure 4.43 for FA/DPPE-PEG5000.

It is obvious that ΔG_{exc} of fatty acid mixed monolayer is dependent on the composition of PEGylated lipid. In other words, addition of PEGylated lipids into fatty acid monolayer has affected some changes in the molecular packing. These changes may either result in a stronger interaction between the molecules or weaken the interaction between the molecules as can be deduced from the signs of ΔG_{exc} . In this study, most of the ΔG_{exc} values are negative. However, there is an exception that positive value of ΔG_{exc} is observed for mixture of oleic acid/ $X_{\text{DPPE-PEG2000}} = 4.3\%$ at surface pressure 5 mN m^{-1} to 15 mN m^{-1} as well as oleic acid/ $X_{\text{DPPE-PEG5000}} = 1.8\%$ at surface pressure 15 mN m^{-1} . This implies the interaction is weaker within this condition as compared to their pure substances at air-aqueous interface. In addition, the magnitude of ΔG_{exc} increases as the mixed monolayer of palmitoleic acid/DPPE-PEG2000, palmitoleic acid/DPPE-PEG5000 and oleic acid/DPPE-PEG2000 are compressed. This shows an increasing intermolecular attraction interaction and the molecules are therefore arranged in a more ordered manner. However, ΔG_{exc} for mixed monolayer of oleic acid/DPPE-PEG5000, linoleic acid/DPPE-PEG2000 and linoleic acid/DPPE-PEG5000 changed towards a less negative value as surface pressure increases to 10 mN m^{-1} . It is also observed that beyond 15 mN m^{-1} of surface pressure, ΔG_{exc} for the mixed monolayer became more negative. This could be due to the initial interaction between the mixed molecules becomes weaker followed by a stronger interaction as the monolayers are in a more compressed state.

Nevertheless, emergence of a minimum in all of the plots of ΔG_{exc} as a function of mole fraction indicates the most favorable mole fraction composition with the strongest interaction between the mixed molecules. The minimum ΔG_{exc} for mixtures of palmitoleic acid and oleic acid with DPPE-PEG2000 are observed at $X_{\text{DPPE-PEG2000}} = 0.02$ and 0.022 , respectively. These mixed components are with higher $X_{\text{DPPE-PEG2000}}$ than those for linoleic acid ($X_{\text{DPPE-PEG2000}} = 0.014$) and linolenic acid ($X_{\text{DPPE-PEG2000}} = 0.012$) with two and three *cis* unsaturated double bond, respectively. However, the amount of DPPE-PEG5000 required to achieve the minimum ΔG_{exc} in the mixture with linolenic acid was the lowest ($X_{\text{DPPE-PEG5000}} = 0.003$) followed by oleic acid ($X_{\text{DPPE-PEG5000}} = 0.01$) and palmitoleic acid ($X_{\text{DPPE-PEG5000}} = 0.017$). Linoleic acid still maintains its ability to accommodate the amount of DPPE-PEG5000 ($X_{\text{DPPE-PEG5000}} = 0.02$) in order to achieve the minimum ΔG_{exc} . Nevertheless, the results obtained from this studied are relatively lower than phospholipid/PEGylated lipid monolayer which recorded a minimum of ΔG_{exc} at 5 – 7 mol% of PEG-lipid [Chou and Chu, 2002; Tirosh *et. al.*, 1998]. This is due to the differences of molecular structure in fatty acid and phospholipid.

The values of excess free energy for monolayer of palmitoleic acid/DPPE-PEG2000 and oleic acid/DPPE-PEG2000 are more negative than their mixture with DPPE-PEG5000. This indicates that palmitoleic acid and oleic acid have a stronger interaction with DPPE-PEG2000 that suggests a higher compatibility with DPPE-PEG2000 and form a favorable monolayer than those in the respective pure fatty acid monolayer. A plausible reason for this observation could be due to the smaller size of hydrophilic head group in DPPE-PEG2000 compared to DPPE-PEG5000 that may fit the gaps between the head group of oleic acid and palmitoleic acid. On the contrary, the thermodynamic effect accompanying incorporation of DPPE-PEG5000 molecules into linoleic acid or linolenic acid monolayer is stronger than those in the case of palmitoleic

acid and oleic acid. ΔG_{exc} for mixed system of linoleic acid/DPPE-PEG5000 and linolenic acid/DPPE-PEG5000 are more negative than mixed linoleic acid/DPPE-PEG2000 and linolenic acid/DPPE-PEG2000. As mentioned earlier, packing of linoleic acid and linolenic acid monolayer at air-aqueous interface are less dense compared to oleic acid as a result of more unsaturated bonds are present in the molecules. Therefore, the gap between head group of linoleic acid and linolenic acid is bigger than oleic acid. In order to reduce the intermolecular distance and form a stronger van der Waals interaction, DPPE-PEG5000 with bulkier head group than DPPE-PEG2000 enables formation of closely packed monolayer. Similar scenario is also applied for less negative ΔG_{exc} values observed for DPPE-PEG2000 mixed with linoleic acid and linolenic acid compared to oleic acid. This effect is more pronounced as the monolayers were compressed to higher surface pressure as a consequence of reduced distance between the molecules during compression. As shown in this result, most of the mixture consisting of 2 mol % of PEGylated lipids with fatty acid may result in a favorable intermolecular interaction. Hence, this combination of mixture was applied in the preparation of PEGylated fatty acid liposome.

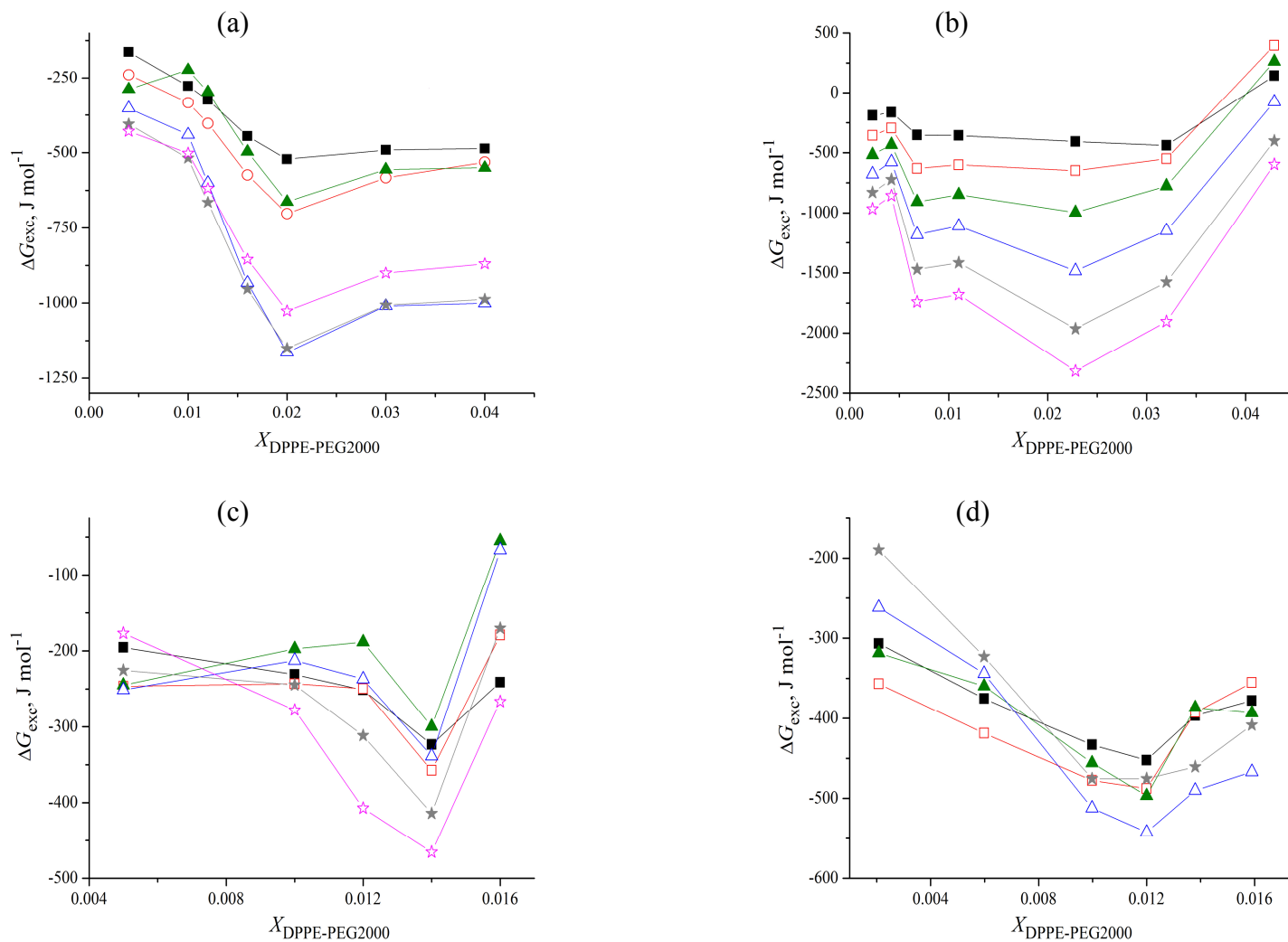


Figure 4.42. Excess Gibbs free energy (ΔG_{exc}) for mixed monolayer of (a) palmitoleic acid, (b) oleic acid, (c) linoleic acid and (d) linolenic acid as a function of $X_{\text{DPPE-PEG2000}}$ at 25 °C and surface pressure $\blacksquare = 5 \text{ mN m}^{-1}$, $\square = 10 \text{ mN m}^{-1}$, $\blacktriangle = 15 \text{ mN m}^{-1}$, $\triangle = 20 \text{ mN m}^{-1}$, $\star = 25 \text{ mN m}^{-1}$, $\star = 30 \text{ mN m}^{-1}$.

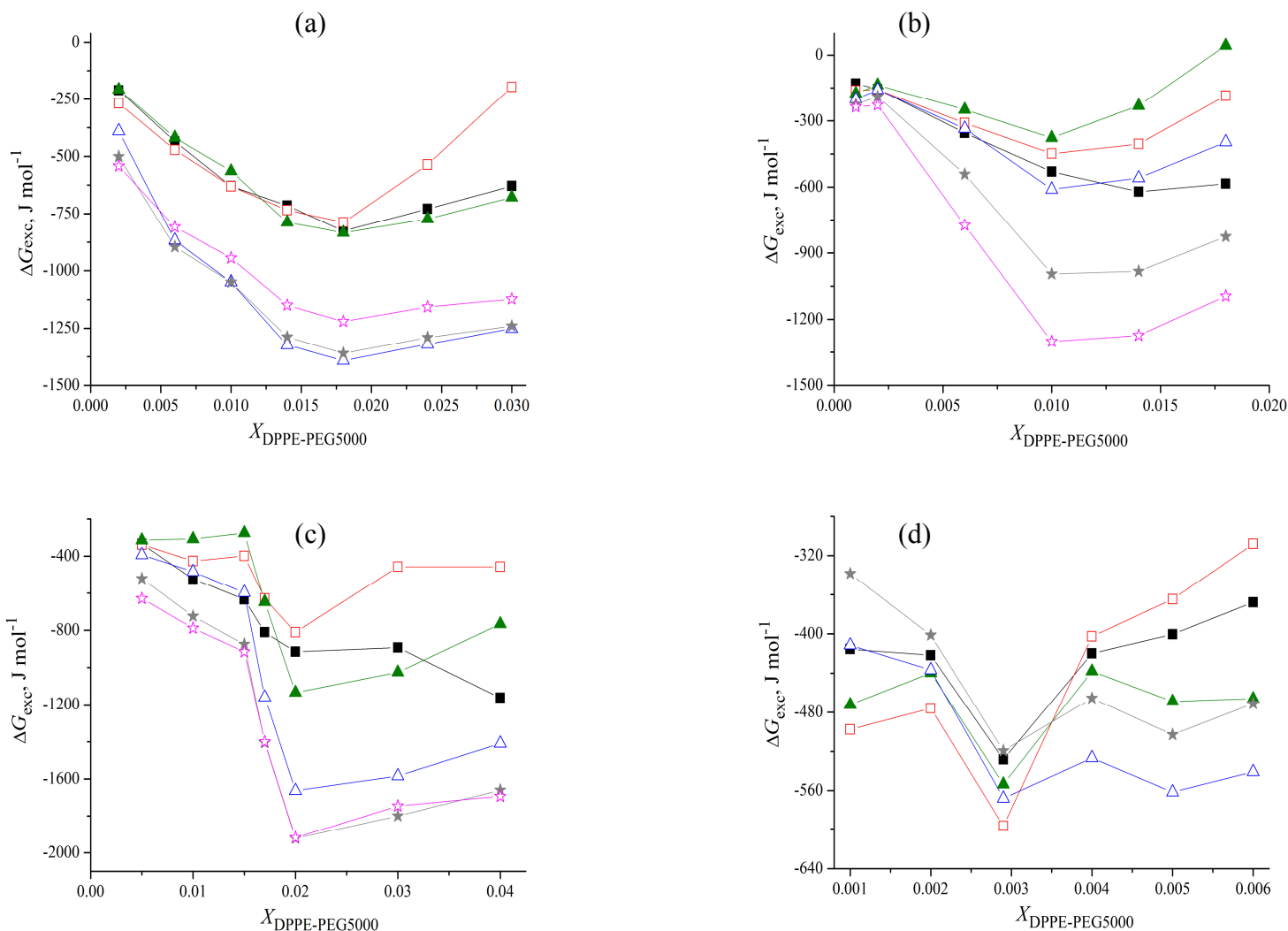


Figure 4.43. Excess Gibbs free energy (ΔG_{exc}) for mixed monolayer of (a) palmitoleic acid, (b) oleic acid, (c) linoleic acid and (d) linolenic acid as a function of $X_{\text{DPPE-PEG5000}}$ at 25 °C and surface pressure ■ = 5 mN m^{-1} , □ = 10 mN m^{-1} , ▲ = 15 mN m^{-1} , △ = 20 mN m^{-1} , ★ = 25 mN m^{-1} , ☆ = 30 mN m^{-1} .

4.6.2 Langmuir monolayer for mixture of fatty acid, PEGylated lipids and VE

The Π - A isotherm and compression modulus as a function of surface pressure for pure VE are shown in figure 4.44. The extrapolated area per molecule for pure VE is 67.5 \AA^2 and the monolayer collapses at 17.6 mN m^{-1} surface pressure. The area per molecule for VE is larger than the area per molecule for pure fatty acid. This might be attributed to the bulkiness of their head group that inhibits efficient molecular packing and thus reduces the cohesion and van der Waals attraction between the hydrocarbon chains. Although VE is categorized as water insoluble substance, the presences of chromanol ring with delocalization of π -electrons in the benzene ring may render them to be present at the air-aqueous interface. This is shown in the inset of figure 4.44 whereupon C_s^{-1} increase gradually during the compression of monolayer. It is suggested that monolayer of pure VE is moving towards a rather rigid monolayer with molecular rearrangement and conformation change upon compression of the monolayer.

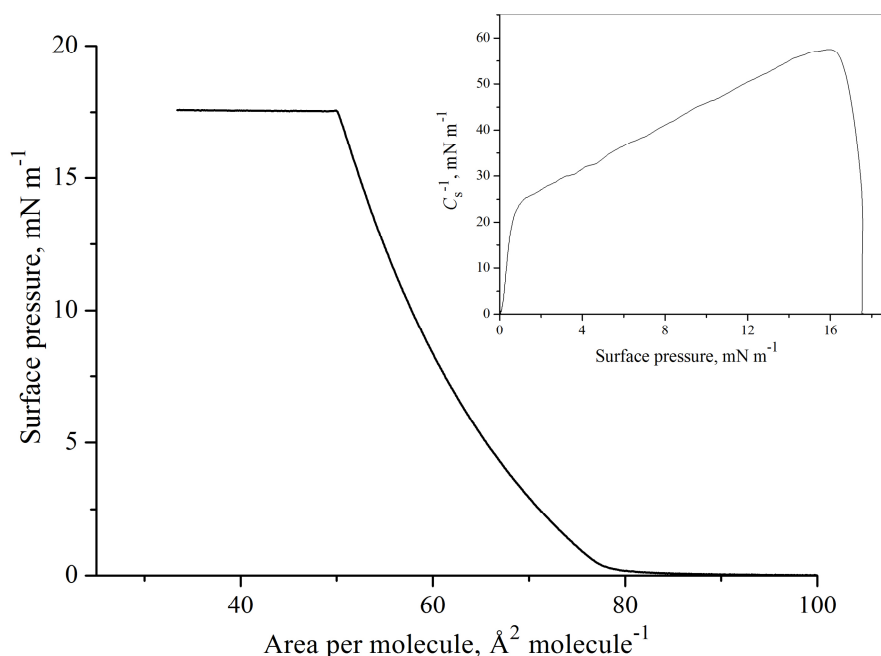


Figure 4.44. Surface pressure–area (Π - A) isotherm of VE monolayer on a 50 mM phosphate buffer pH 7 at 25 °C. The inset showed the C_s^{-1} as a function of surface pressure for VE.

As revealed in this study, most of the mixture consisting 2 mol % of PEGylated lipids with fatty acid may result in a favorable intermolecular interaction. Hence, this combination of mixture was applied for the study of their interaction with VE for comparison purpose.

The Π - A isotherms of fatty acid with different mole fractions of VE during the compression of monolayer were shown in figure 4.45. The presence of interaction between the components in a monolayer is reflected as dependency of the curve position and curve shape to the composition in a mixture. It shows that incorporation of VE does not cause a remarkable change in the shape of isotherms whereupon the monolayers maintain their liquid expanded properties. However, some of the isotherms are shifted towards smaller area per molecule. This may indicate that VE molecules were accommodated in the molecular cavities in the region of hydrocarbon chain through cohesive energy. Furthermore, the collapse pressure of the monolayer reduces as expected when the mole fraction of VE increases. Similar results were also observed in Π - A isotherms of ternary mixture consisting of fatty acid/DPPE-PEG2000/VE (Figure 4.46) and fatty acid/DPPE-PEG5000/VE (Figure 4.47).

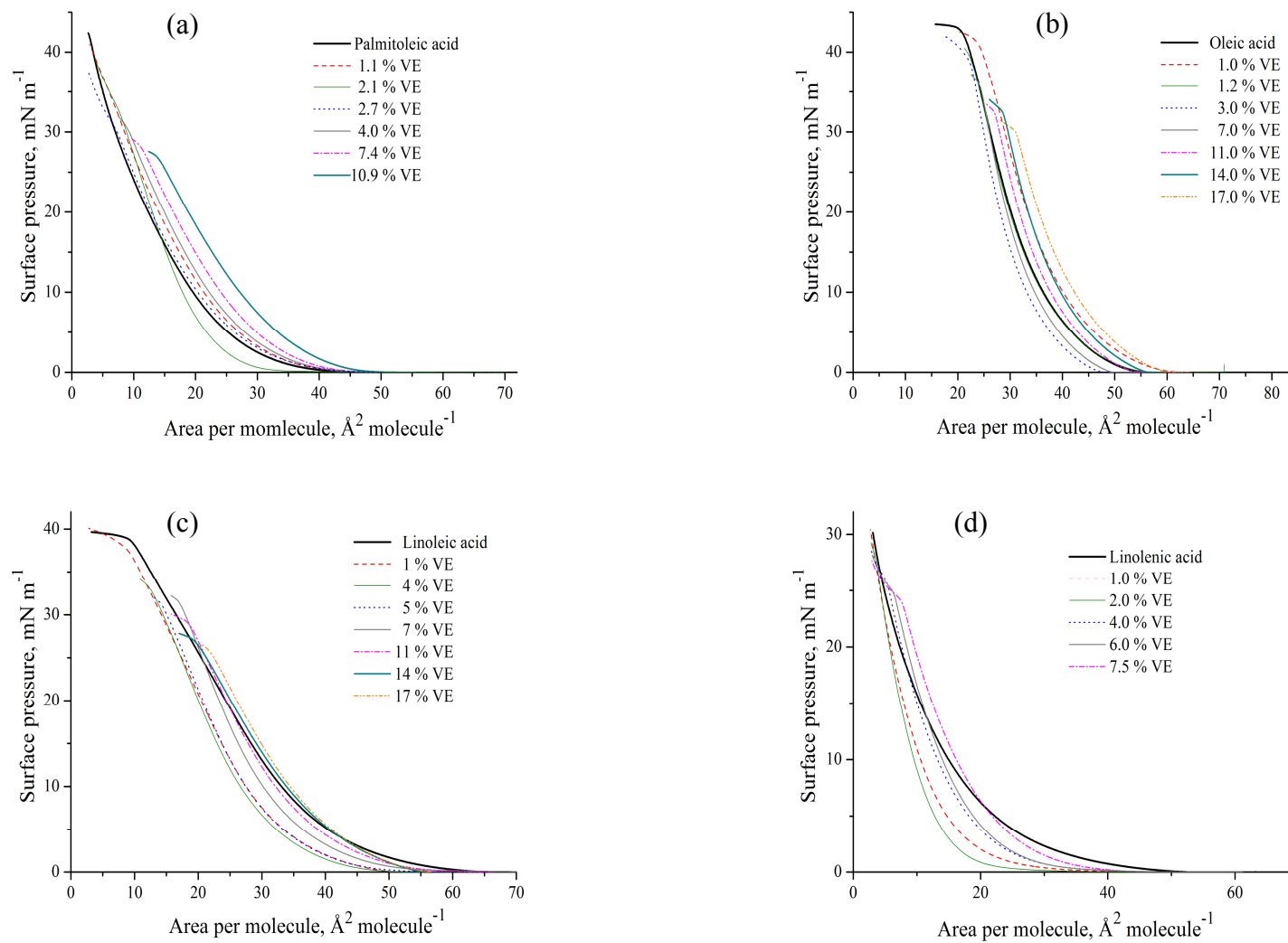


Figure 4.45. Surface pressure–area (Π – A) isotherms for mixed monolayer of VE with (a) palmitoleic acid, (b) oleic acid, (c) linoleic acid and (d) linolenic acid at air–aqueous interface at 25 °C.

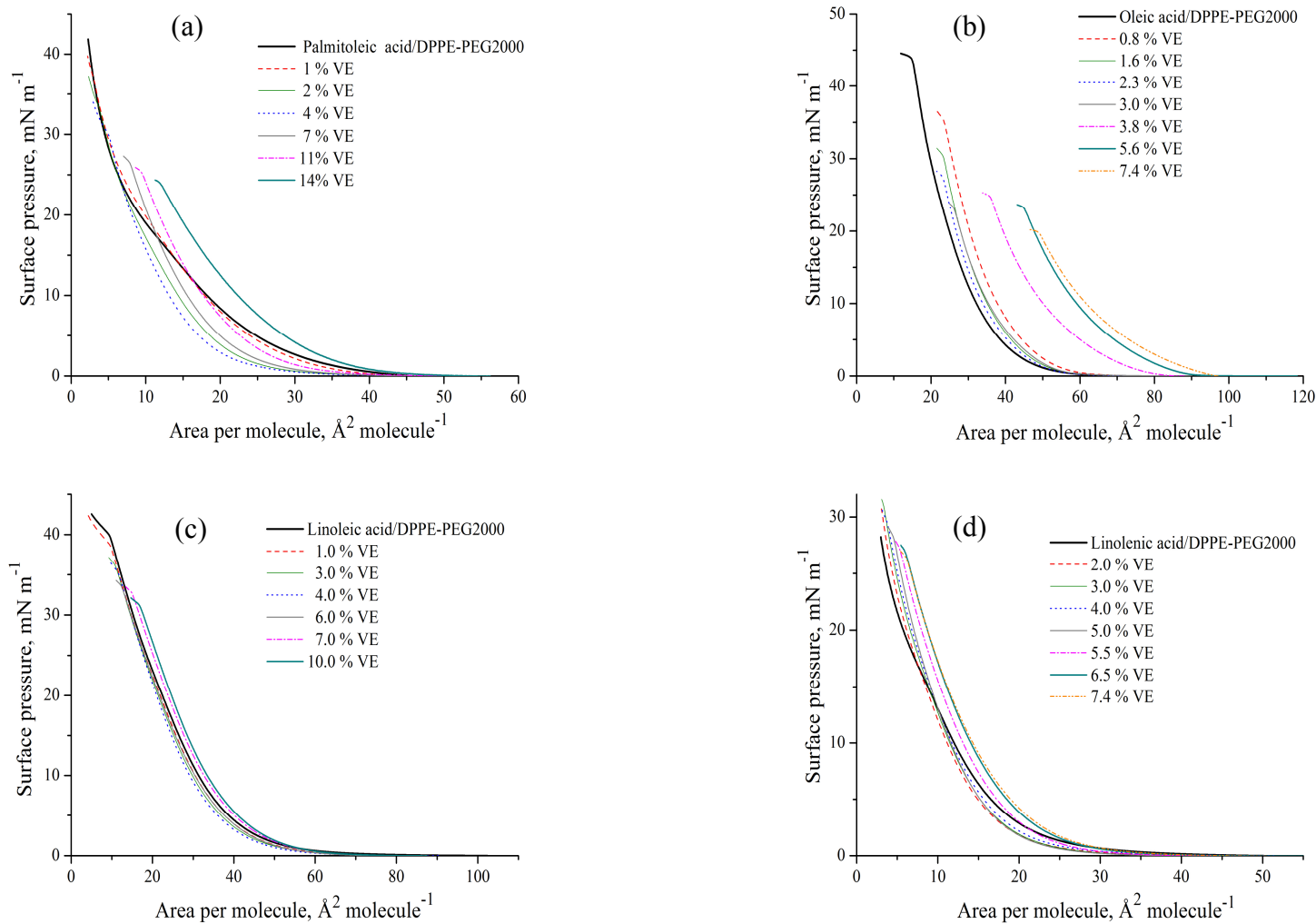


Figure 4.46. Surface pressure–area (Π – A) isotherms for mixed monolayer of VE/2 % DPPE-PEG2000 with (a) palmitoleic acid, (b) oleic acid, (c) linoleic acid and (d) linolenic acid at the air-aqueous interface at 25 °C.

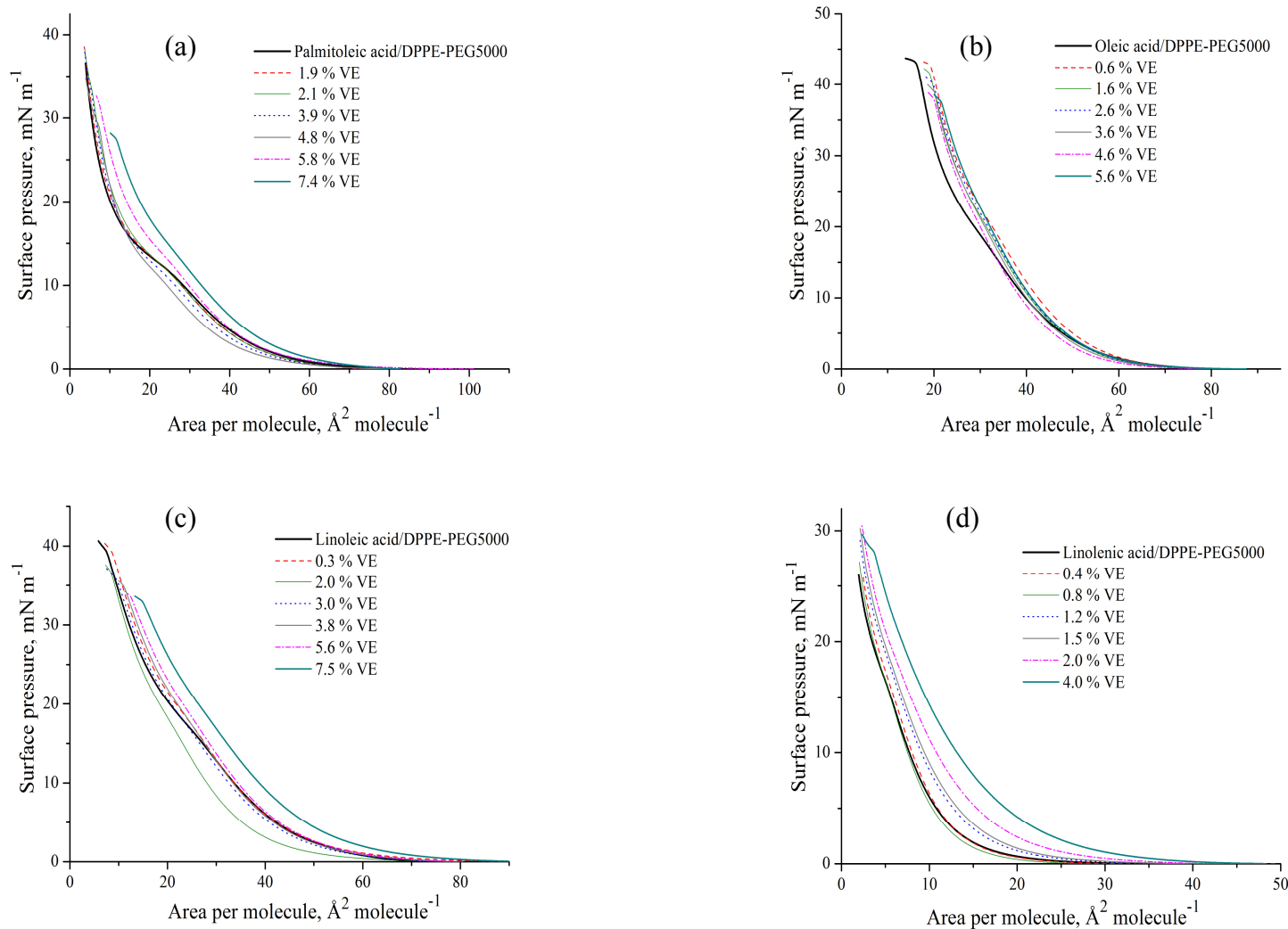


Figure 4.47. Surface pressure–area (Π – A) isotherms for mixed monolayer of VE/2 % DPPE-PEG5000 with (a) palmitoleic acid, (b) oleic acid, (c) linoleic acid and (d) linolenic acid at the air-aqueous interface at 25 °C.

C_s^{-1} of mixed monolayer with VE during the compression are shown in figure 4.48 for pure fatty acid. Figure 4.49 and figure 4.50 revealed the changes of compression modulus upon compression of the monolayer composing mixed fatty acid and DPPE-PEG2000 for the former and DPPE-PEG5000 for the latter. C_s^{-1} indicates the structural changes in the acyl chains upon the process of compression. The higher the value of C_s^{-1} , the more rigid the monolayer becomes. It is worth noting that addition of VE in the pure fatty acid as well as in mixed fatty acid/PEGylated lipids monolayers has imparted the formation of more rigid monolayers with higher C_s^{-1} . The variation of C_s^{-1} is more pronounced in mixed monolayer of fatty acid/VE compared to the monolayer of fatty acid/PEGylated lipid/VE whereupon the increment of C_s^{-1} in the fatty acid/VE monolayer is higher followed by fatty acid/DPPE-PEG2000/VE and fatty acid/DPPE-PEG5000/VE. As the amount of VE increased, the surface pressure rapidly decreased after the $C_{s,max}^{-1}$ which shows a similar characteristic to the plot of C_s^{-1} as a function of surface pressure for pure VE. A similar trend is also observed in the monolayer of fatty acid/PEGylated lipid/VE. In addition, the gradual disappearance of the two peaks is observed as the amount of VE increases indicating the monolayer is dominantly affected by VE.

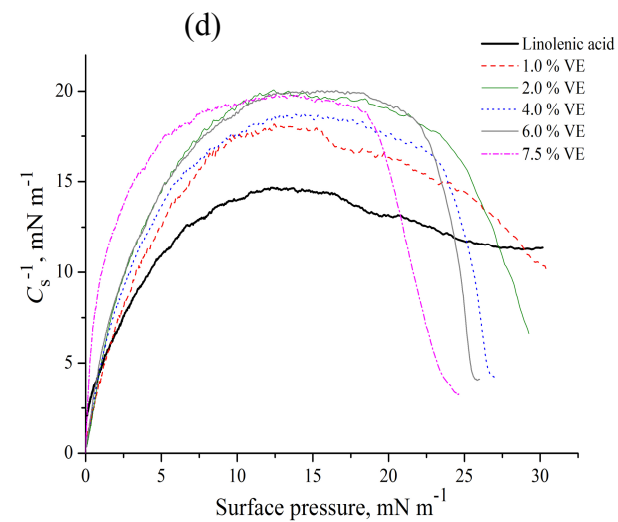
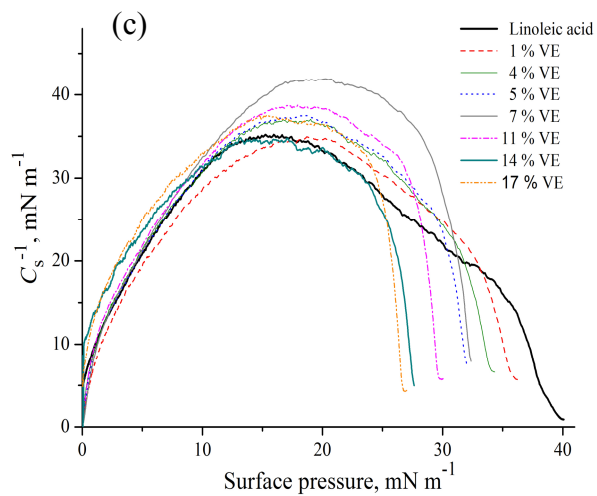
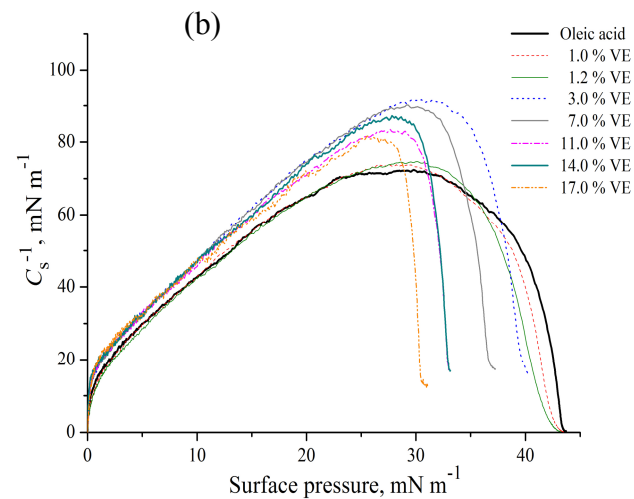
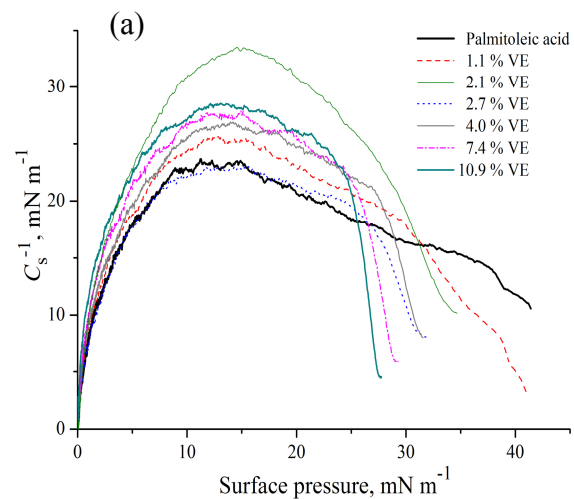


Figure 4.48. Compression modulus (C_s^{-1}) for mixed monolayer of VE with (a) palmitoleic acid, (b) oleic acid, (c) linoleic acid and (d) linolenic acid at air-aqueous interface at 25 °C.

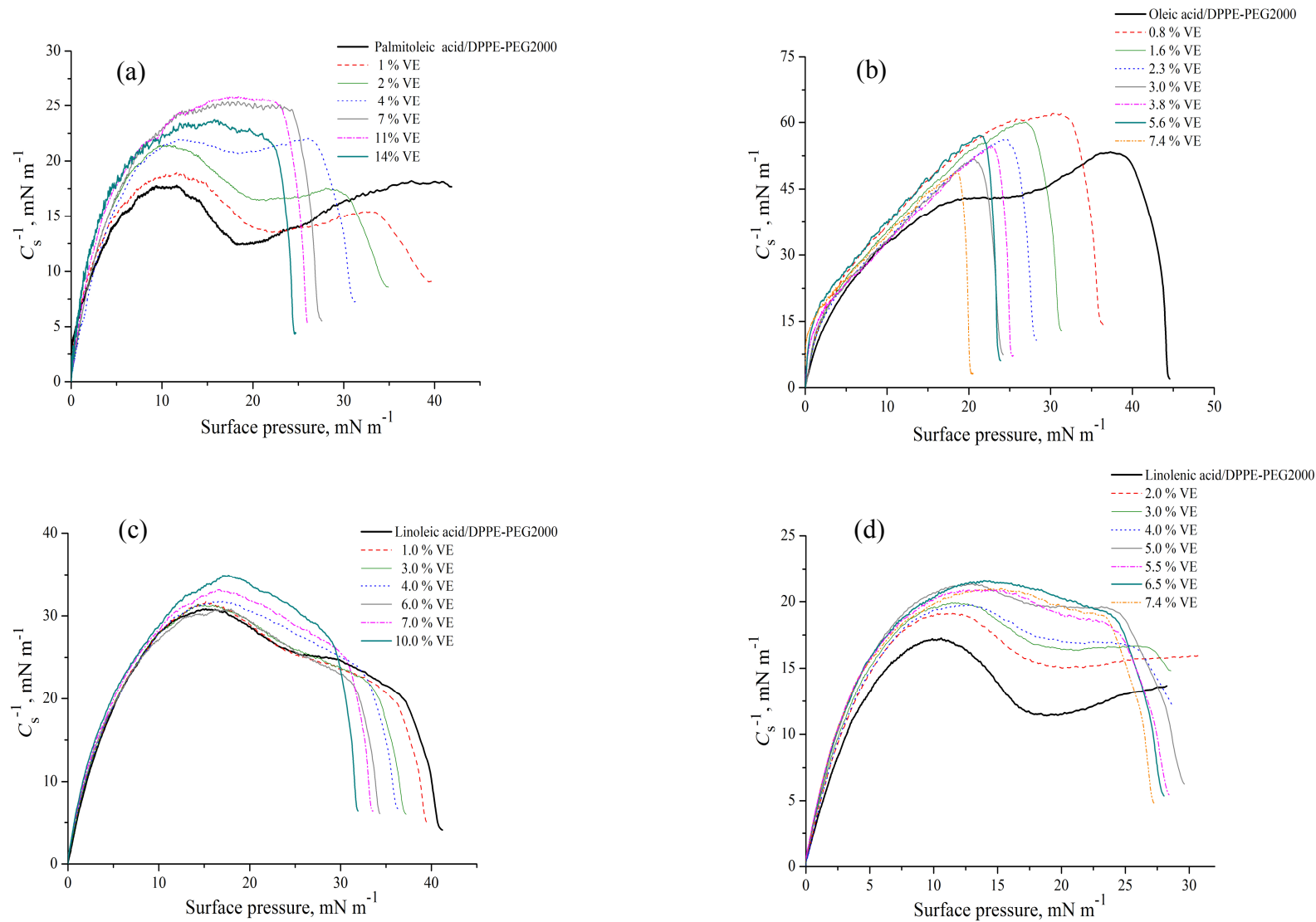


Figure 4.49. Compression modulus (C_s^{-1}) for mixed monolayer of VE/2 % DPPE-PEG2000 with (a) palmitoleic acid, (b) oleic acid, (c) linoleic acid and (d) linolenic acid at the air-aqueous interface at 25 °C.

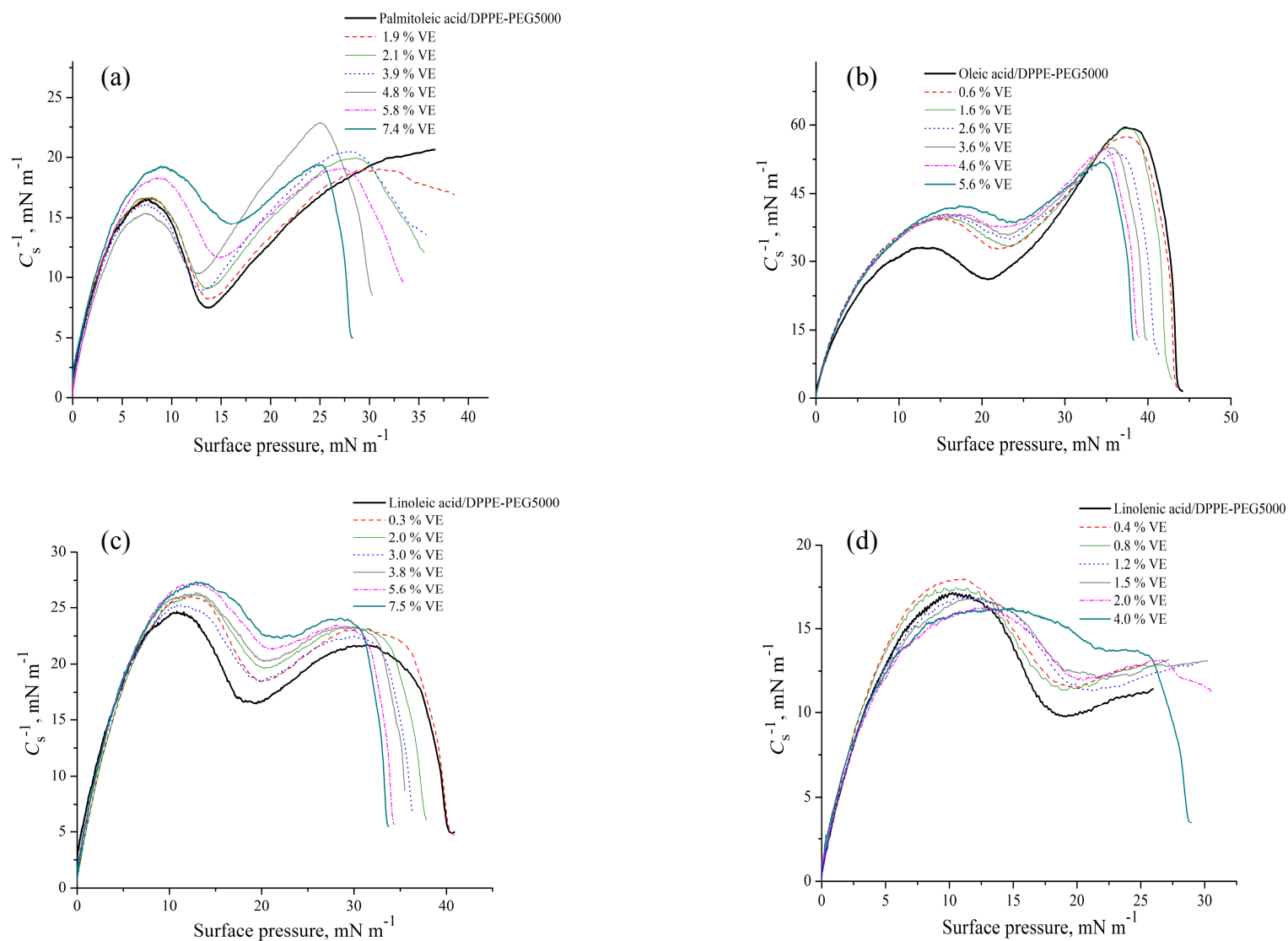


Figure 4.50. Compression modulus (C_s^{-1}) for mixed monolayer of VE/2 % DPPE-PEG5000 with (a) palmitoleic acid, (b) oleic acid, (c) linoleic acid and (d) linolenic acid at the air-aqueous interface at 25 °C.

For a better understanding on the degree of compatibility between these mixtures with two or more substances in a monolayer, the molecular areas at different surface pressure were analyzed as shown in figure 4.51 for fatty acid/VE monolayer, figure 4.52 for fatty acid/DPPE-PEG2000/VE monolayer and figure 4.53 for fatty acid/DPPE-PEG5000/VE monolayer. The dotted lines indicate the ideal area per molecule that varies linearly with the X_{VE} . Some general trends can be observed for the mixed monolayers. Apparently, the linear relationship between area per molecule and X_{VE} in a monolayer of fatty acid or fatty acid/PEGylated lipid is not observed. This indicates presence of intermolecular interaction and molecular compatibility between the substances in the mixture.

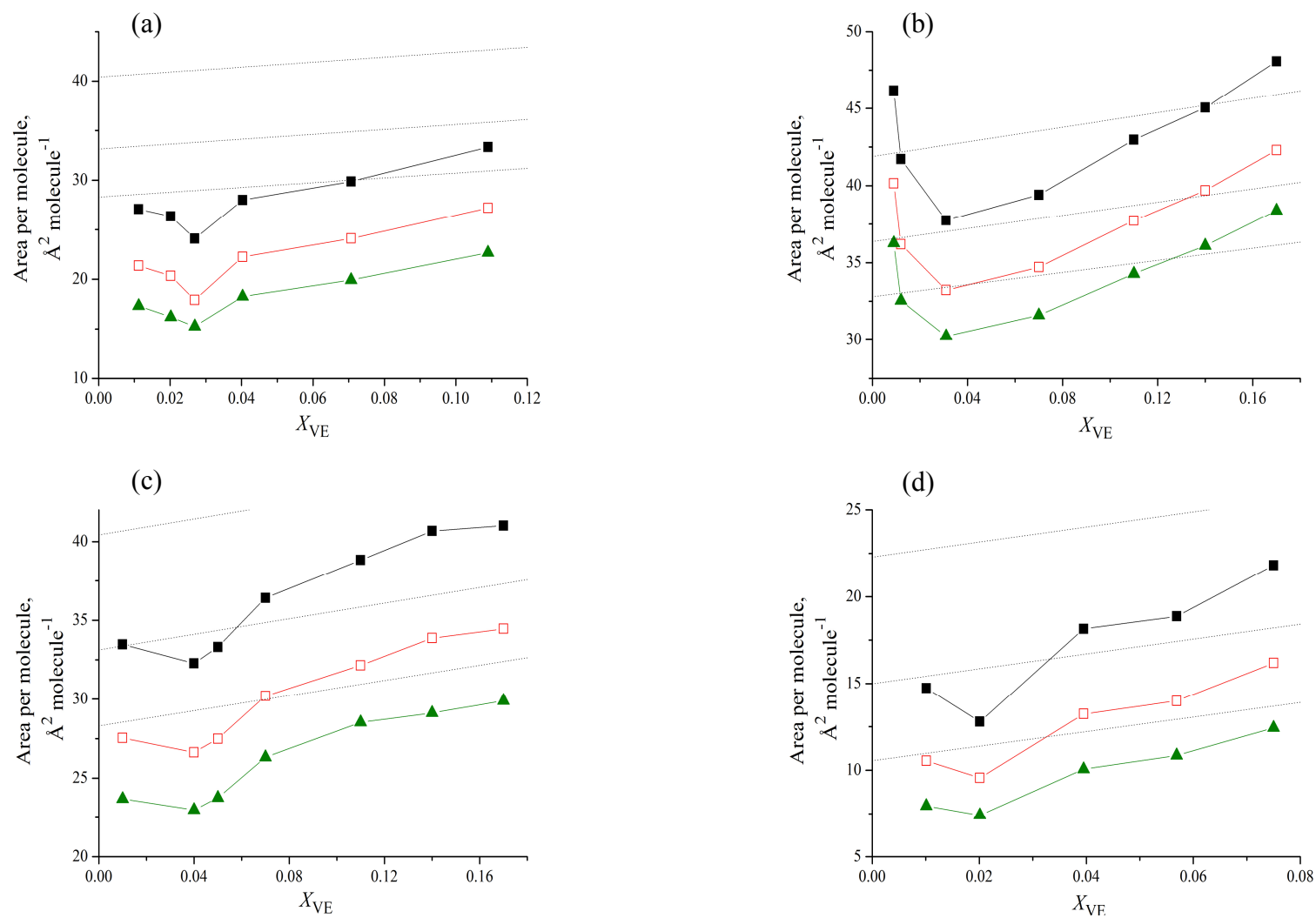


Figure 4.51. Area per molecule as a function of mole fraction X_{VE} in monolayer of (a) palmitoleic acid, (b) oleic acid, (c) linoleic acid and (d) linolenic acid at the air-aqueous interface at 25 °C and surface pressure \blacksquare = 5 mN m^{-1} , \square = 10 mN m^{-1} , \blacktriangle = 15 mN m^{-1} .

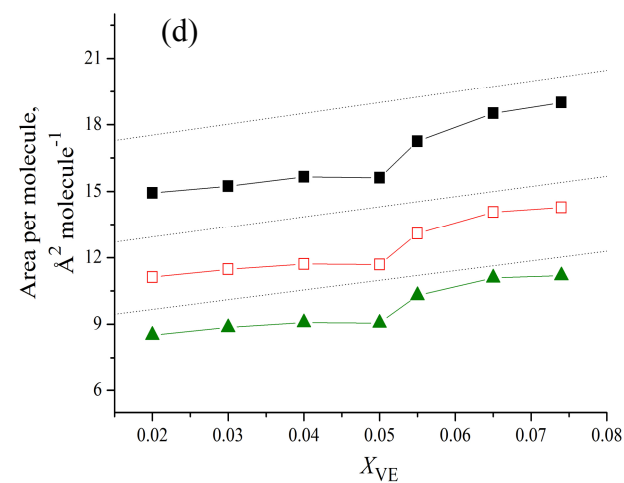
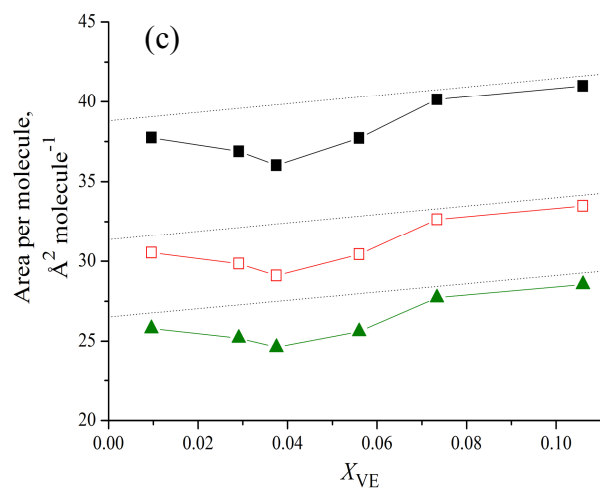
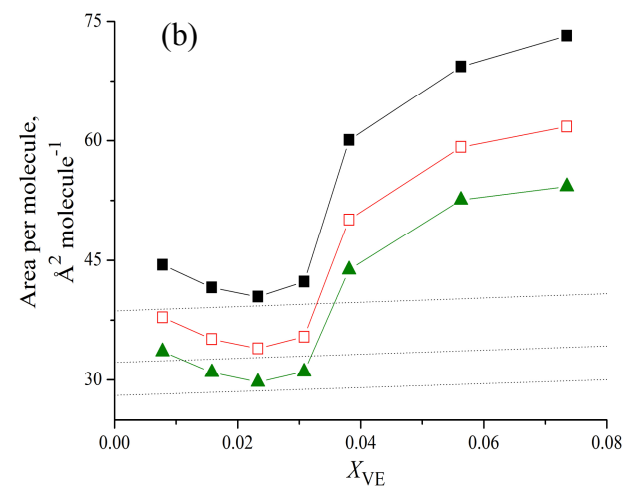
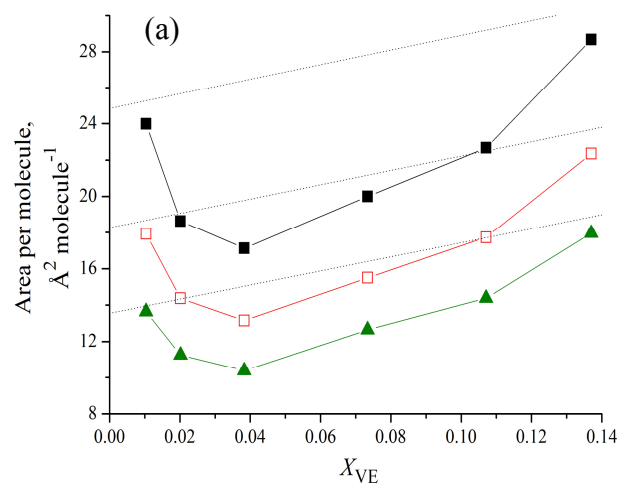


Figure 4.52. Area per molecule as a function of mole fraction X_{VE} in monolayer of 2 % DPPE-PEG2000 with (a) palmitoleic acid, (b) oleic acid, (c) linoleic acid and (d) linolenic acid at the air-aqueous interface at 25 °C and surface pressure ■ = 5 mN m⁻¹, □ = 10 mN m⁻¹, ▲ = 15 mN m⁻¹.

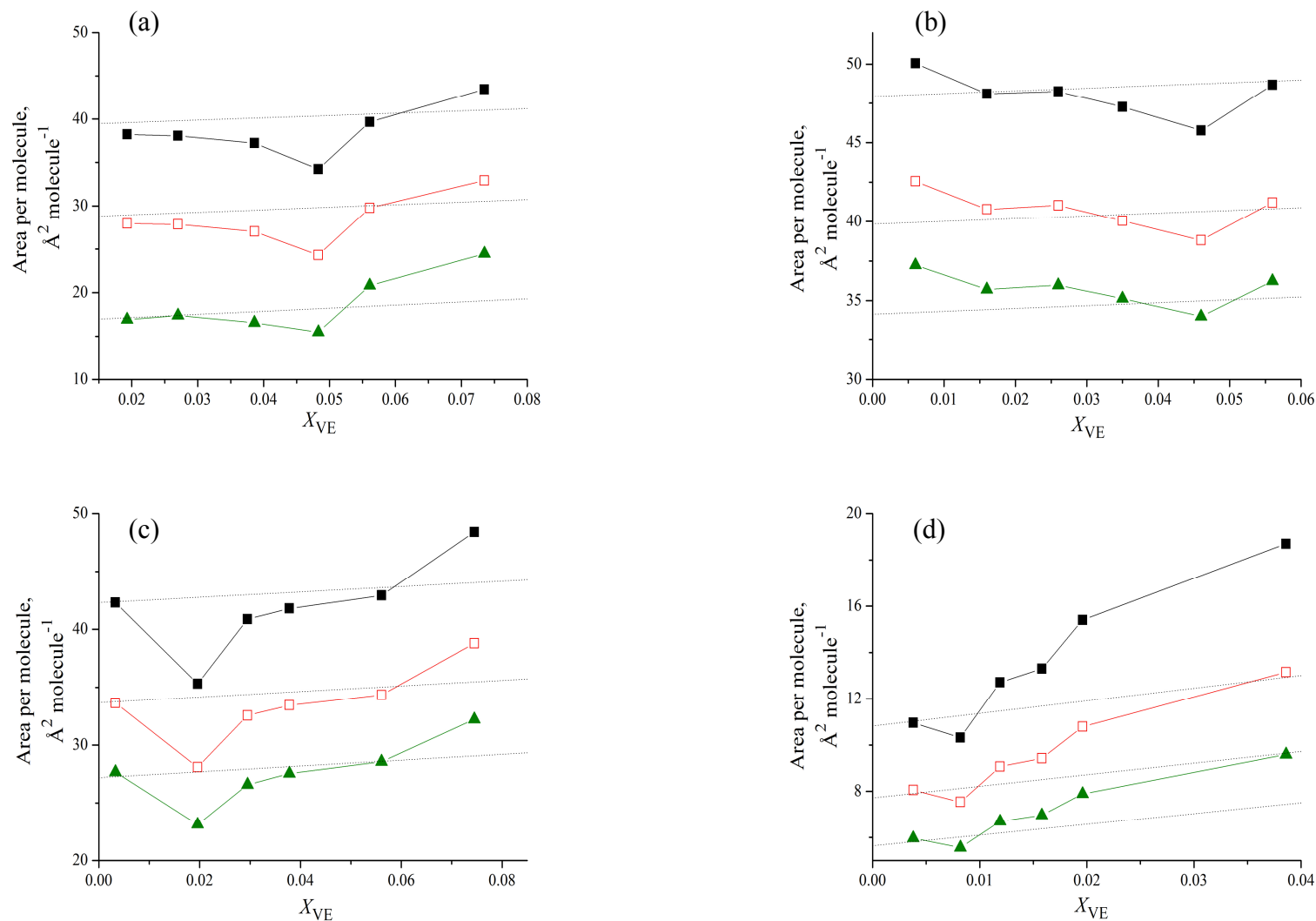


Figure 4.53. Area per molecule as a function of mole fraction X_{VE} in monolayer of 2 % DPPE-PEG5000 with (a) palmitoleic acid, (b) oleic acid, (c) linoleic acid and (d) linolenic acid at the air-aqueous interface at 25 °C and surface pressure ■ = 5 mN m^{-1} , □ = 10 mN m^{-1} , ▲ = 15 mN m^{-1} .

The plots of $A_{\text{exc}}/A_{\text{id}}$ at different surface pressure for mixed monolayer of palmitoleic acid, oleic acid, linoleic acid and linolenic acid as a function of X_{VE} were illustrated in figure 4.54. When the $A_{\text{exc}}/A_{\text{id}} \neq 0$, this is showing that the mixture in a monolayer deviates from ideality with the substances being partially or completely compatible. In addition, the deviation of $A_{\text{exc}}/A_{\text{id}}$ from 0 could be showing either positive or negative. Positive deviation may imply the substances occupy a larger area per molecule in a mixed monolayer than in the pure substance monolayer. This could be due to strong intermolecular repulsion between the molecules that caused the molecules to be unable to accommodate each other in the formation of monolayer. A negative deviation means net attractive interaction between the molecules and also indicates a reduction in the area per molecule of the substances in a mixed monolayer that is contributed by space filling or geometric accommodation into the hydrophobic region of the monolayer as suggested by Shah and Schulman [Shah and Schulman, 1968]. Presence of VE molecules in the hydrophobic region may interact with the hydrocarbon chain of fatty acid and reduce the distance in between two fatty acid molecules. Therefore, space filling or geometric accommodation by the VE may subsequently lead to changes in intermolecular hydrophobic interaction between the hydrocarbon tails of fatty acid molecules.

For all of the X_{VE} in this study, negative deviations of $A_{\text{exc}}/A_{\text{id}}$ in mixed monolayer of linoleic acid or linolenic acid with VE are observed that imply geometric accommodation or space filling of VE molecules in the hydrophobic region and cause an intermolecular hydrophobic interaction between the fatty acid and VE molecules. Negative deviations are also found in monolayer composed of VE with palmitoleic acid ($X_{\text{VE}} = 1.3 \% - 3.7 \%$) or oleic acid ($X_{\text{VE}} = 1.2 \% - 12.5 \%$). On the other hand, a maximum condensation effect is observed in all of the fatty acid monolayer. Monolayers of palmitoleic acid or linolenic acid mixed with 2 % of VE are found to

deviate to the most negative values from ideality. Similarly, mixture of 3 % and 4 % of VE with oleic acid for the former and linoleic acid for the latter, have recorded the most negative deviation.

Values of A_{exc}/A_{id} for mixture composed of fatty acid/DPPE-PEG2000 and various X_{VE} were shown in figure 4.55. Similar to mixed monolayer of fatty acid/VE, the variations of surface pressures do not have profound effect on the trend of deviation. In addition, negative values of A_{exc}/A_{id} are observed in this study for the entire mole fraction range of VE mixed with palmitoleic acid/DPPE-PEG2000, linoleic acid/DPPE-PEG2000 and linolenic/DPPE-PEG2000. In the same manner to monolayer of fatty acid mixed with VE, minimum value of A_{exc}/A_{id} is also found at 4.0 %, 3.8 % and 5 % of VE for palmitoleic acid/DPPE-PEG2000, linoleic acid/DPPE-PEG2000 and linolenic acid/DPPE-PEG2000, respectively. On the other hand, monolayer for mixture of oleic acid/DPPE-PEG2000/VE showed that A_{exc}/A_{id} deviate positively from ideality throughout the investigated mole fraction range. This suggested that intermolecular interaction between oleic acid/DPPE-PEG2000 and VE is weaker than the interaction between the molecules of oleic acid and DPPE-PEG2000 or pure VE molecules at the air-aqueous interface.

In accordance with mixture of fatty acid/VE, negative deviations of A_{exc}/A_{id} with addition of DPPE-PEG5000 are also limited to certain mole fraction range of VE and the most negative value is also found in each plot as shown in figure 4.56. The most negative A_{exc}/A_{id} values for mixed monolayer of DPPE-PEG5000 with palmitoleic acid, oleic acid and linoleic acid were observed at 4.8 %, 4.6 % and 2.0 % of VE, respectively. Only 0.8 % of VE can be accommodated in the mixed monolayer of linolenic acid/DPPE-PEG5000 to obtain the most negative A_{exc}/A_{id} . Further increase in the amount of VE beyond the most negative A_{exc}/A_{id} value induces packing constraint in between the hydrophobic region of the molecules at a monolayer. Consequently, the

molecules may strongly repel each other and result in a less negative deviation of $A_{\text{exc}}/A_{\text{id}}$.

Despite the fact that the deviation trend shown in figure 4.54 to figure 4.56 is not greatly affected by the surface pressure, the deviation of $A_{\text{exc}}/A_{\text{id}}$ in monolayer of fatty acid/PEGylated lipid/VE become less negative as surface pressure increases from 5 mN m⁻¹ to 15 mN m⁻¹ for most of the mixtures with an exception for the monolayer consisting mixture of linoleic acid/DPPE-PEG2000/VE and linolenic acid/DPPE-PEG5000/VE. This data suggest that availability of the area for each molecule is reduced as the surface pressure is increased. Hence, repulsive interaction between the mixed molecules is relatively stronger compared to pure molecules. On the other hand, deviations of $A_{\text{exc}}/A_{\text{id}}$ for monolayer of linoleic acid/DPPE-PEG2000 and linolenic acid/DPPE-PEG5000 become more negative although in a limiting available area. This indicates the arrangement of mixed molecules becomes more ordered and stronger attractive interaction is present among the mixed molecules system as the surface pressure increases.

We have discovered that addition of VE displayed a different effect on the behaviour of fatty acid and mixed fatty acid/PEGylated lipid monolayers. This is due to VE, being a water insoluble substance, mainly interacts with the hydrocarbon tail of fatty acid through hydrophobic interaction. It can further be viewed as insertion of VE in the space between the hydrocarbon tails of fatty acid molecules that imparts rigidity to the monolayers. However, all of the mixtures are found compatible within the investigated mole fraction range.

The compatibility sequence for monolayer consisting of pure fatty acid and VE, with the exception of linolenic acid, is in the order of linoleic acid > oleic acid > palmitoleic acid. The order can be explained from the effect of unsaturation degree in acyl chain of fatty acid molecules. Monolayer with higher degree of unsaturation is

loosely packed and this therefore provides a temporary void that can be used to accommodate VE molecules. It has been observed that palmitoleic acid with a shorter and more rigid hydrocarbon has a higher compressibility which therefore possesses lower packing efficiency than oleic acid which has a longer and more flexible hydrocarbon tail. As a result, pure palmitoleic acid is less compatible in accommodating VE in its monolayer. However, monolayer composed of palmitoleic acid/DPPE-PEG2000 displays a better compatibility with VE than linoleic acid/DPPE-PEG2000 and oleic acid/DPPE-PEG2000. This would be due to the presence of DPPE-PEG2000 with bulky polyethoxylated head group has effectively induces loose packing at the hydrocarbon tail and significantly increases the space in between the molecules for accommodation of VE molecules. However, addition of DPPE-PEG2000 into the monolayer of linoleic acid or oleic acid is found less compatible with VE compared to palmitoleic acid/DPPE-PEG2000. This can be explained as the presence of DPPE-PEG2000 promotes a higher packing efficiency at the hydrocarbon tail and disrupts the initially loosely packed acyl chains of the pure fatty acid in monolayers. Moreover, addition of DPPE-PEG5000 into fatty acid monolayer displays similar behaviour to those monolayers composed of fatty acid/DPPE-PEG2000 as observed from our results. Monolayers of palmitoleic acid/DPPE-PEG5000 and linoleic acid/DPPE-PEG5000 are found more likely to accommodate VE. Mixed monolayers of oleic acid/DPPE-PEG5000 and linolenic acid/DPPE-PEG5000 are relatively less compatible in occupying VE. This could be due to the presence of bulky polyethoxylate group that is 1.5 times longer in DPPE-PEG5000 than DPPE-PEG2000. Hence, compression of the mixed monolayer did not significantly affect the packing at hydrocarbon tails whereas a larger space is retained in between the hydrocarbon tails. Nevertheless, the larger condensing effect was observed for monolayer composing mixture of palmitoleic acid/DPPE-PEG5000/VE than oleic acid/DPPE-PEG5000/VE although both of the

molecules contain one unsaturated double bond. These results suggest that the same hydrocarbon chain length of palmitoleic acid and PEGylated lipid may promote stronger molecular attraction interaction with VE [Chen *et. al.*, 2000].

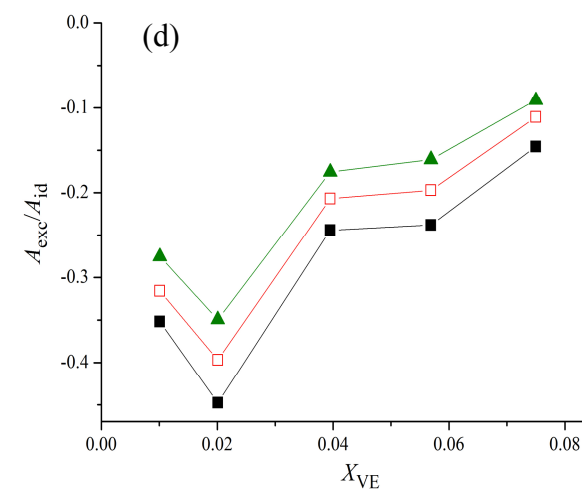
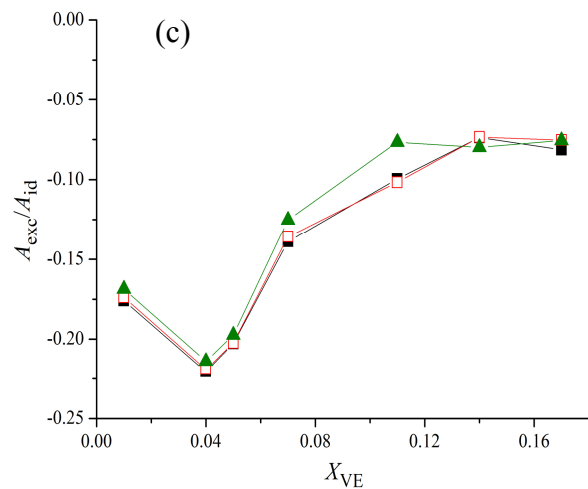
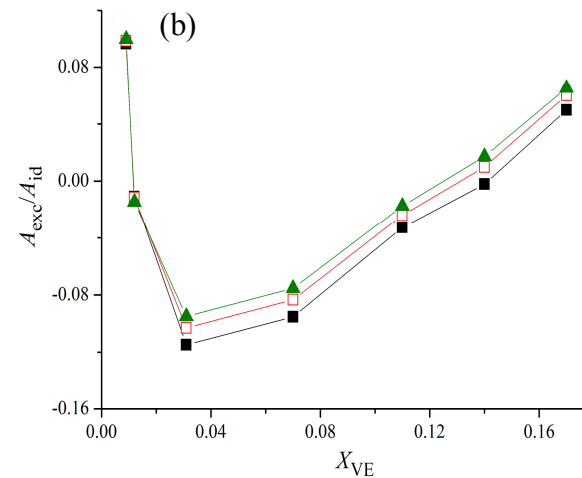
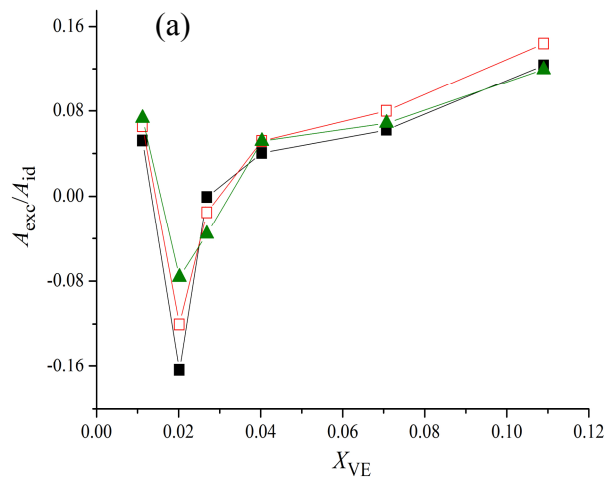


Figure 4.54. A_{exc}/A_{id} as a function of mole fraction X_{VE} in monolayer of (a) palmitoleic acid, (b) oleic acid, (c) linoleic acid and (d) linolenic acid at the air-aqueous interface at 25 °C and surface pressure $\blacksquare = 5 \text{ mN m}^{-1}$, $\square = 10 \text{ mN m}^{-1}$, $\blacktriangle = 15 \text{ mN m}^{-1}$.

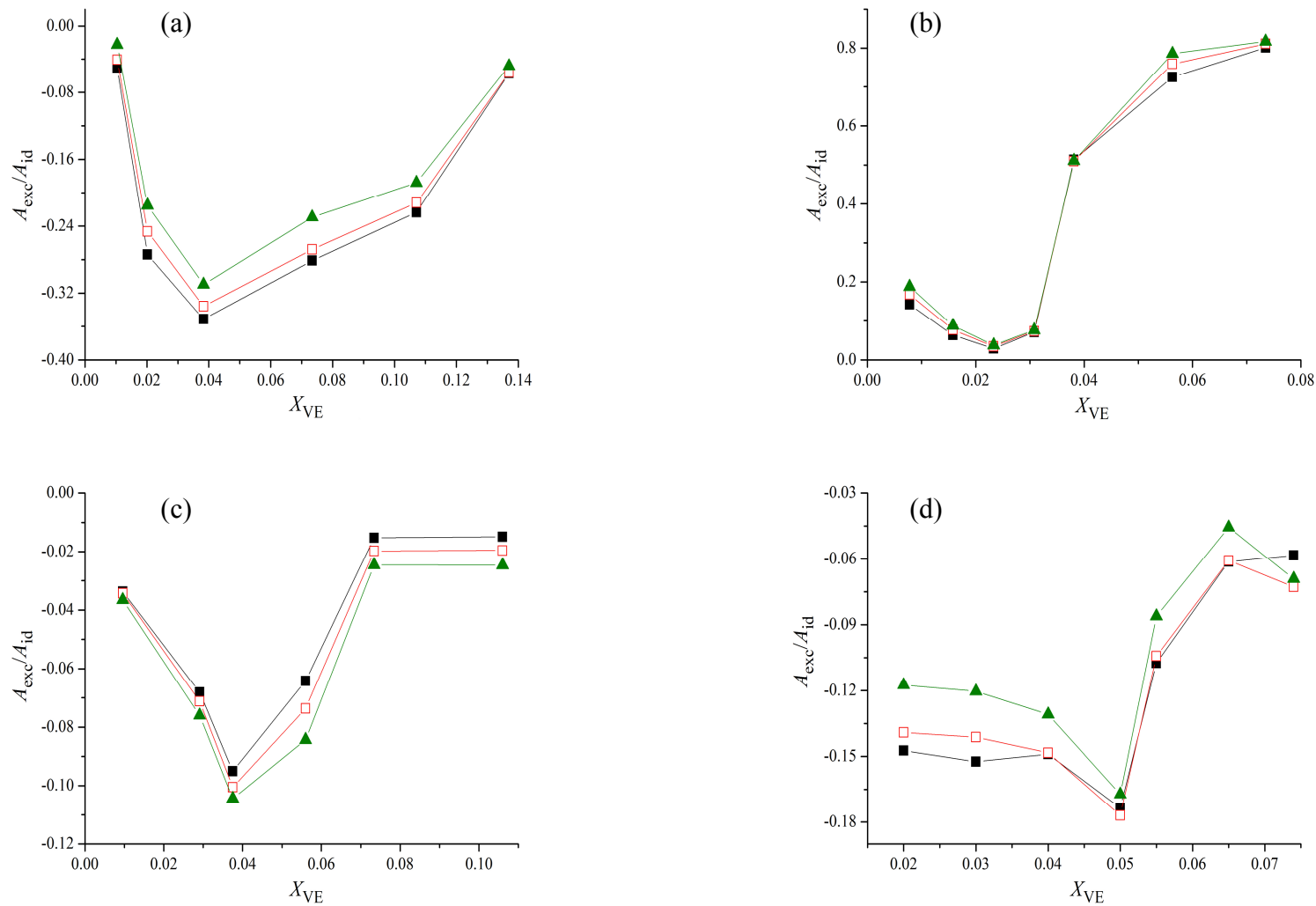


Figure 4.55. $A_{\text{exc}}/A_{\text{id}}$ as a function of mole fraction X_{VE} in monolayer of 2 % DPPE-PEG2000 with (a) palmitoleic acid, (b) oleic acid, (c) linoleic acid and (d) linolenic acid at the air-aqueous interface at 25 °C and surface pressure ■ = 5 mN m⁻¹, □ = 10 mN m⁻¹, ▲ = 15 mN m⁻¹.

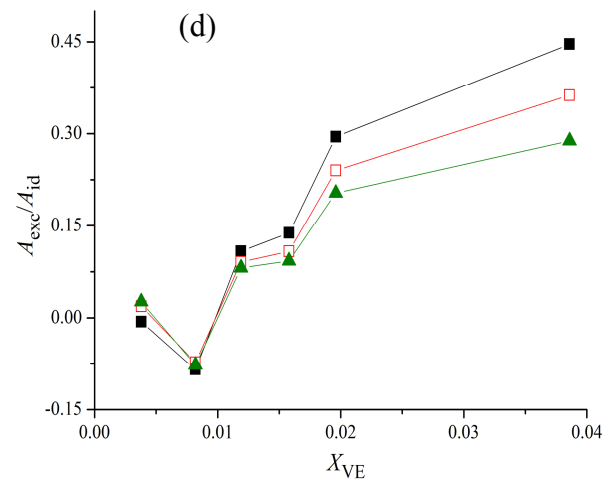
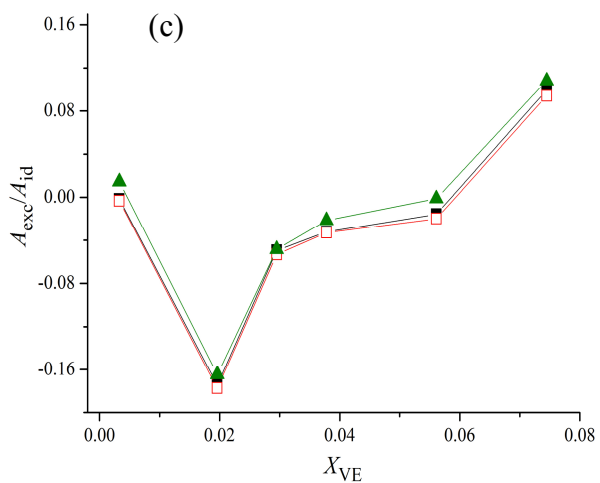
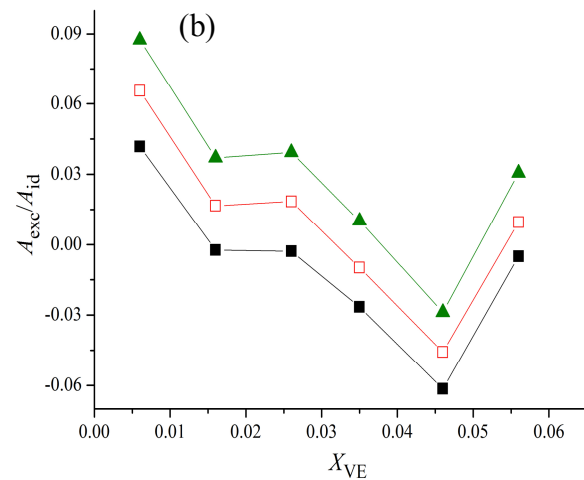
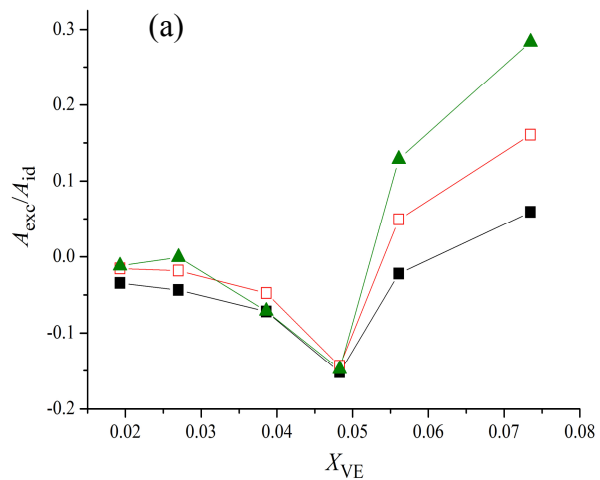


Figure 4.56. A_{exc}/A_{id} as a function of mole fraction X_{VE} in monolayer of 2 % DPPE-PEG5000 with (a) palmitoleic acid, (b) oleic acid, (c) linoleic acid and (d) linolenic acid at the air-aqueous interface at 25 °C and surface pressure ■ = 5 mN m⁻¹, □ = 10 mN m⁻¹, ▲ = 15 mN m⁻¹.

The influence of VE on the packing density of fatty acid and mixed fatty acid/PEGylated lipid monolayer can be analyzed in a more precise manner on the basis of C_s^{-1} . The values of C_s^{-1} as a function of mole fraction VE at various constant surface pressures were presented in figure 4.57, figure 4.58, and figure 4.59, for pure fatty acid, mixed fatty acid/DPPE-PEG2000 and mixed fatty acid/DPPE-PEG5000, respectively.

As revealed in the figures mentioned above, increasing the mole fraction of VE in the mixed monolayer has demonstrated various effects on the values of C_s^{-1} . A maximum C_s^{-1} value was found at $X_{VE} = 0.02$ for palmitoleic acid mixed monolayer while C_s^{-1} values rises from $X_{VE} = 0.012$ to 0.03 for oleic acid mixed monolayer and level off. Similar trend is also observed for mixed monolayer of linolenic acid at $X_{VE} = 0.01$ to 0.02. This implies addition of VE at mole fraction less than 0.02 for mixed monolayer of palmitoleic acid, 0.03 for oleic acid and 0.01 for linolenic acid may imparts rigidity at the acyl chain that result in a less flexible monolayer. This could be due to “cavity filling” of VE molecules in the space between hydrocarbon chains of fatty acid [Maggio *et. al.*, 1977]. Further addition of VE in palmitoleic acid monolayer induced their expansion that could be seen as a reduction of C_s^{-1} as a consequence of palmitoleic acid molecular arrangement becoming more closely packed. However, further increase of VE in oleic acid and linolenic acid mixed monolayer does not show any significant effect on the C_s^{-1} . This might be due to molecules in the monolayer are loosely packed therefore provide more empty space for VE molecules. Similar explanation is also applied to linoleic acid/VE mixed monolayer that demonstrates little changes in C_s^{-1} values.

On the other hand, C_s^{-1} value for monolayer of oleic acid mixed with VE is found significantly higher than linoleic acid. This could be due to packing efficiency of VE in single unsaturated hydrocarbon chain is higher than in linoleic acid with two double bonds. Nevertheless, monolayer of palmitoleic acid mixed with VE is shown

more compressible than oleic acid/VE. This might be caused by longer chain of oleic acid than palmitoleic acid that restricts the fluidity of monolayer. Hence it can be deduced that oleic acid/VE forms the most rigid monolayer. In addition, as the surface pressure increases, C_s^{-1} value also increases regardless the amount of VE and the type of fatty acid in a mixed monolayer. This implies the monolayers are in their expanded state at low surface pressures, and so interfacial elasticity is higher and the monolayers are more fluid like. As expected, condensation of the monolayers would occur as the monolayers were compressed.

The increase of X_{VE} in monolayer composed of palmitoleic acid/DPPE-PEG2000 and linolenic acid/DPPE-PEG2000 results in an increase of C_s^{-1} . On the other hand, a reduction of C_s^{-1} is observed for oleic acid/DPPE-PEG2000 from $X_{VE} = 0.016$. However, little effect of VE is observed in mixed linoleic acid/DPPE-PEG2000. This is possibly due to DPPE-PEG2000 has effectively conformed to a loosely packed arrangement at the acyl chain of palmitoleic acid monolayer than the other type of fatty acid monolayer owing to its shorter acyl chain length. Consequently, this provides an additional space for the filling of VE molecules that leads to enhancement in rigidity of the monolayer. On the other hand, insertion of VE molecules by filling the space in oleic acid acyl chain is only limited at $X_{VE} < 0.016$. Further increase in the amount of VE induces expansion of the monolayer that results in a more fluid monolayer. However, addition of DPPE-PEG2000 into monolayer of linoleic acid with two unsaturated bonds provides sufficient space for accommodation of VE molecules. Therefore, addition of VE does not display significant variation in interfacial elasticity of the monolayers.

In mixed monolayer composed of VE with oleic acid/DPPE-PEG5000 and linoleic acid/DPPE-PEG5000, little effect on C_s^{-1} have been observed as increasing the amount of VE in the mixed monolayer. This might be owing to the large and bulky

polyethoxylated group in DPPE-PEG5000 that inhibits close packing of the monolayer and hence provides an additional spacing in monolayer. However, reduction of C_s^{-1} is observed as X_{VE} increases in mixed monolayer of palmitoleic acid/DPPE-PEG5000/VE and linolenic acid/DPPE-PEG5000/VE that is not observed in the mixture of DPPE-PEG2000.

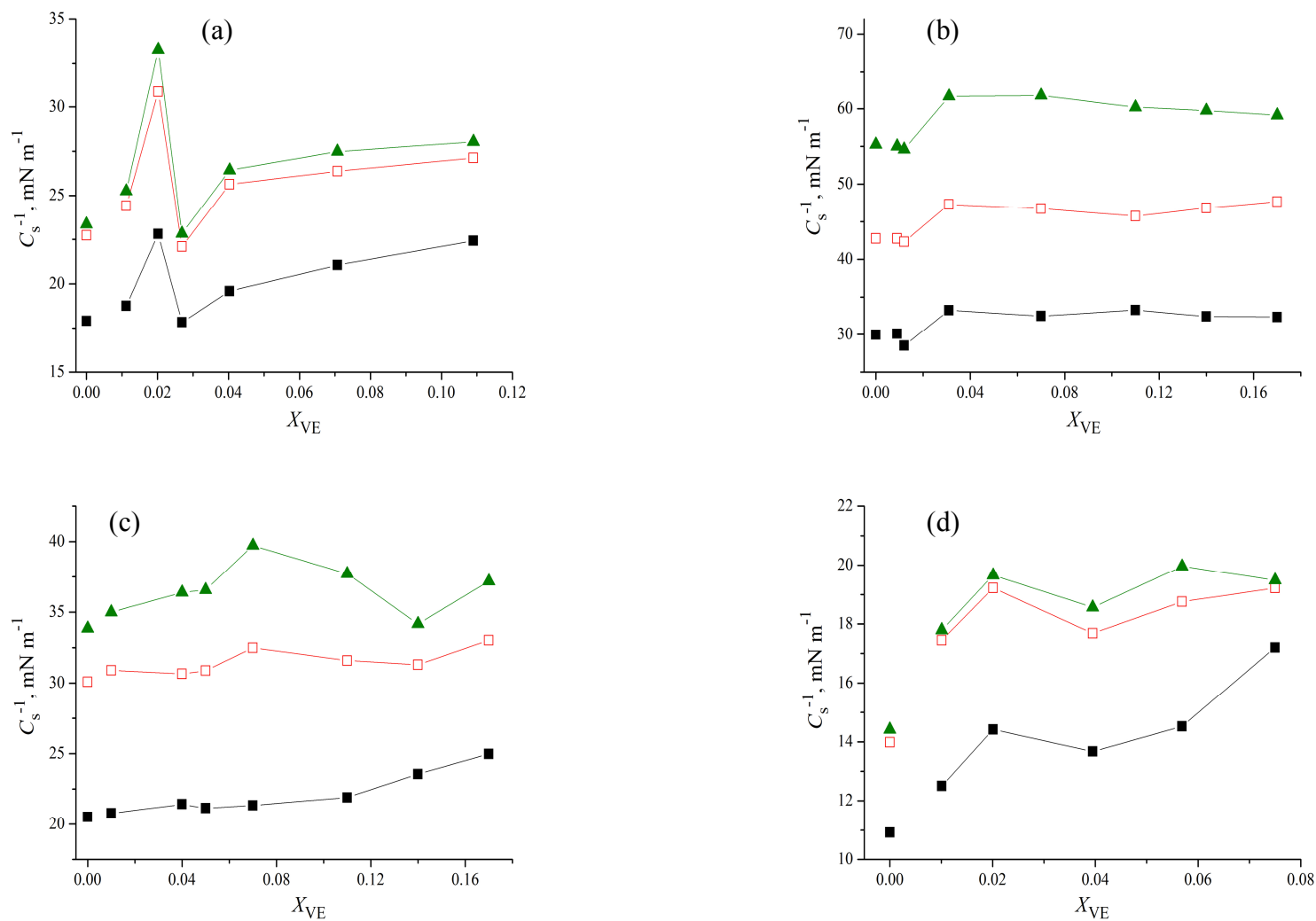


Figure 4.57. Compression modulus (C_s^{-1}) as a function of mole fraction VE (X_{VE}) in (a) palmitoleic acid, (b) oleic acid, (c) linoleic acid and (d) linolenic acid monolayer at the air-aqueous interface at 25 °C and surface pressure $\blacksquare = 5 \text{ mN m}^{-1}$, $\square = 10 \text{ mN m}^{-1}$, $\blacktriangle = 15 \text{ mN m}^{-1}$.

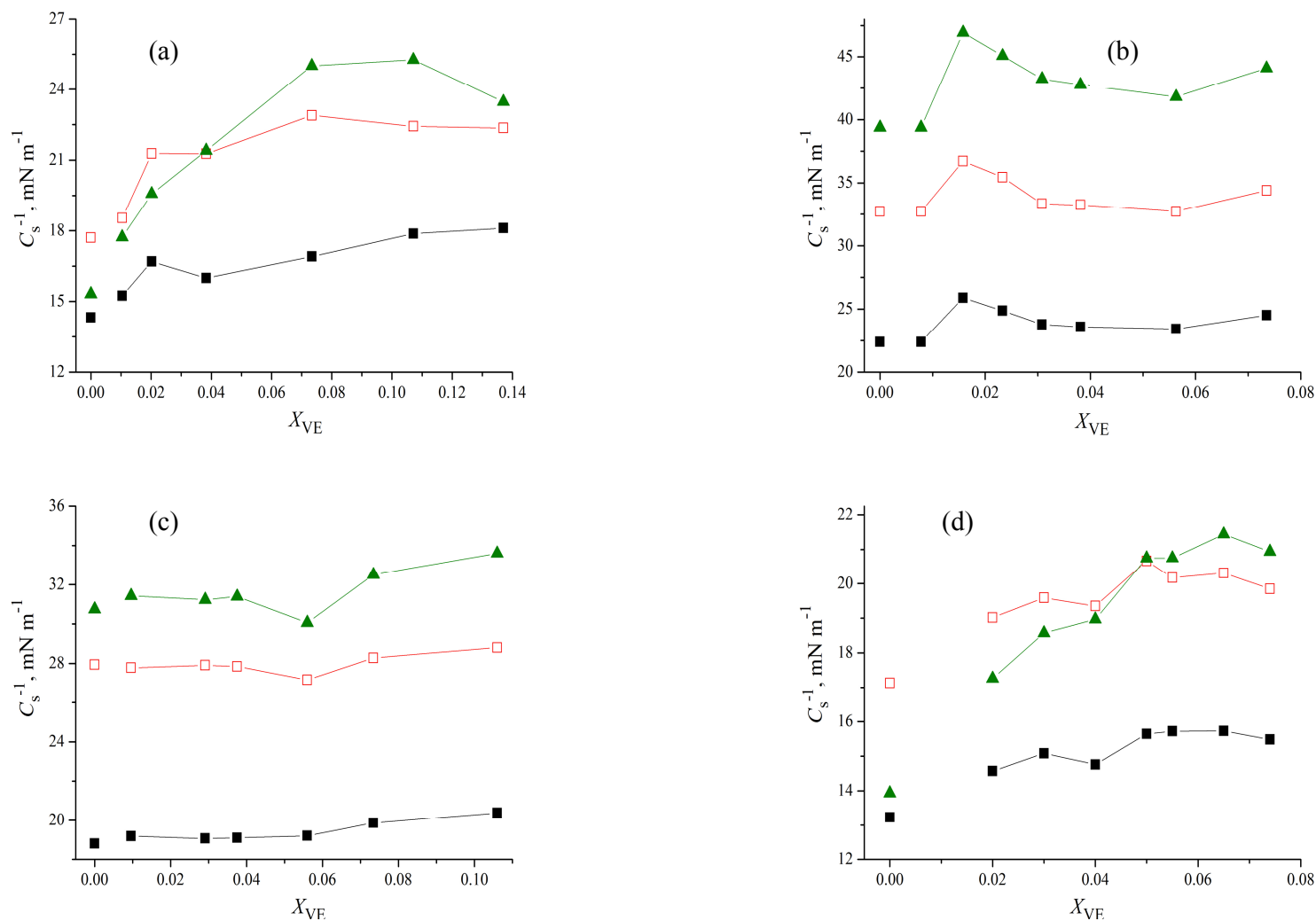


Figure 4.58. Compression modulus (C_s^{-1}) as a function of mole fraction VE (X_{VE}) in monolayer of 2 % DPPE-PEG2000 with (a) palmitoleic acid, (b) oleic acid, (c) linoleic acid and (d) linolenic acid at the air-aqueous interface at 25 °C and surface pressure ■ = 5 mN m^{-1} , □ = 10 mN m^{-1} , ▲ = 15 mN m^{-1} .

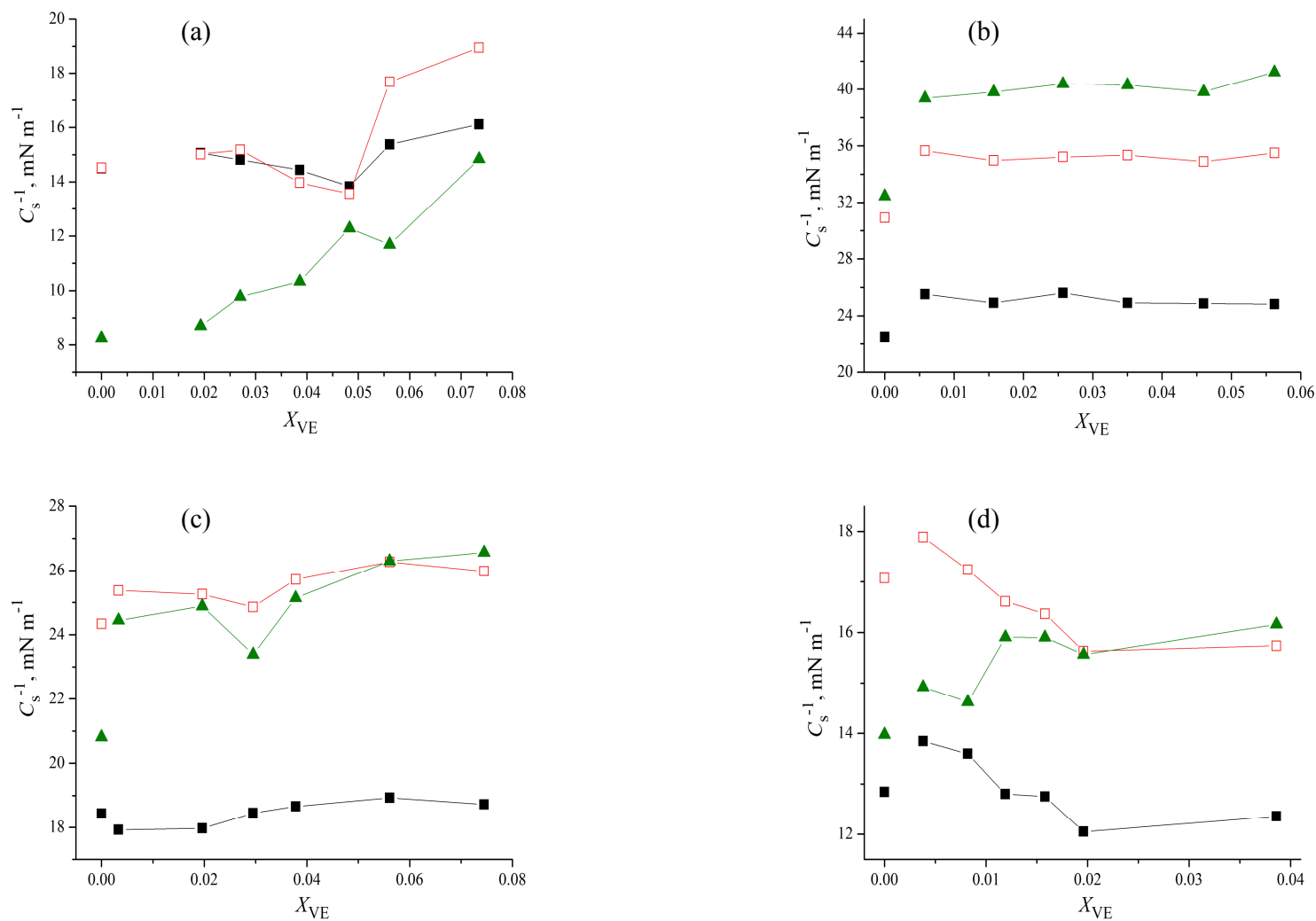


Figure 4.59. Compression modulus (C_s^{-1}) as a function of mole fraction VE (X_{VE}) in monolayer of 2 % DPPE-PEG5000 with (a) palmitoleic acid, (b) oleic acid, (c) linoleic acid and (d) linolenic acid at the air-aqueous interface at 25 °C and surface pressure \blacksquare = 5 mN m^{-1} , \square = 10 mN m^{-1} , \blacktriangle = 15 mN m^{-1} .

In addition to the mentioned parameter for determination of compatibility between the mixed substances, excess Gibbs free energy of the mixture, ΔG_{exc} is another parameter used for the same purpose. The strength of interaction between the substances can be directly evaluated from Π - A mixed monolayer isotherm. By applying equation 14 and equation 15, values for ΔG_{exc} for mixture of fatty acid and various compositions of VE were calculated at surface pressures 5 mN m⁻¹, 10 mN m⁻¹ and 15 mN m⁻¹ as illustrated in figure 4.60. ΔG_{exc} for mixture composing fatty acid/VE/DPPE-PEG2000 or DPPE-PEG5000 were shown in figure 4.61 and figure 4.61, respectively.

It is observed that ΔG_{exc} is dependent on X_{VE} in the mixture which induces changes in the molecular packing for both fatty acid/VE and fatty acid/PEGylated lipid/VE monolayers. In mixture of linoleic acid or linolenic acid with VE as shown in figure 4.60(c) and (d), ΔG_{exc} are negative in the whole range of studied X_{VE} regardless of surface pressure. However, similar result is only obtained for certain X_{VE} mixed with palmitoleic acid ($X_{\text{VE}} = 0.015 - 0.03$) and oleic acid ($X_{\text{VE}} = 0.012 - 0.14$) as displayed in figure 4.60(a) and (b), respectively. This implies intermolecular interaction between fatty acid and VE in the mixed monolayer at air-aqueous interface is stronger compared to the interaction among their pure molecules in a single component monolayer. In addition, the emergence of a minimum at each surface pressure studied in the plot of ΔG_{exc} as a function of mole fraction implies the most favorable composition with the strongest interaction between the mixed molecules at that particular composition. In other words, this is the most stable system that VE can be incorporated in the monolayer. The minimum ΔG_{exc} for mixed monolayer linoleic acid/VE is found at $X_{\text{VE}} = 0.04$, for oleic acid/VE at $X_{\text{VE}} = 0.03$ and for either palmitoleic acid or linolenic acid with VE, ΔG_{exc} is observed at $X_{\text{VE}} = 0.02$. Monolayer of linoleic acid/VE is found capable to accommodate higher amount of VE could be due to the higher degree of unsaturation in linoleic acid with two kinks in the acyl hydrocarbon tail that provides more space to

accommodate VE. Similarly, oleic acid with longer and more flexible tail than palmitoleic acid monolayer therefore can be allocated with more VE at the space in between the hydrocarbon tail. In addition, it is also revealed that ΔG_{exc} gradually becomes more negative as surface pressure is increased at this mole fraction. This could be due to shorter intermolecular distance upon compression of the monolayer that leads to stronger intermolecular interactions and in a more non-ideal and compact state. However, at higher X_{VE} , ΔG_{exc} increase progressively to less negative value with surface pressure as a consequence of space limitation that causes strong repulsion as the monolayer was compressed.

On the other hand, the result shows that at almost all the studied mole fractions of VE, positive ΔG_{exc} values are found for monolayer of oleic acid/DPPE-PEG2000/VE (Figure 4.61). This implies the intermolecular interaction between oleic acid/DPPE-PEG2000 and VE is weaker compared to oleic acid and DPPE-PEG2000 at air-aqueous interface. It can be presumed that DPPE-PEG2000 with two C16 hydrocarbon chains has significantly perturbed the molecular packing in the hydrophobic region that is more loosely pack in the pure oleic acid monolayer. Nevertheless, negatively ΔG_{exc} were calculated for mixture of palmitoleic acid/DPPE-PEG2000/VE (Figure 4.61(a)). This demonstrated that the molecules of palmitoleic acid and DPPE-PEG2000 interact strongly with VE. This could be owing to DPPE-PEG2000 with bulky head group at low surface pressure inhibit close packing and hence significantly induce spacing at the hydrocarbon tail of palmitoleic acid that is packed tightly in the pure (one component) monolayer. Hence, higher mole fraction of VE ($X_{\text{VE}} = 0.038$) can be accommodated in the hydrophobic region of the monolayer. Similarly, mixtures of linoleic acid or linolenic acid with DPPE-PEG2000/VE still remain the negative ΔG_{exc} values as illustrated in figure 4.61(c) and 4.61(d), respectively but with magnitude lower than those of palmitoleic acid/DPPE-PEG2000/VE. Hence, this again has shown that DPPE-

PEG2000 rather decreases the space at the hydrophobic region for fatty acid than enhances the space. This suggestion is also supported by less amount of VE is required to obtain the most negative ΔG_{exc} that was found at $X_{\text{VE}} = 0.038$ for all surface pressure.

The effect of VE amount present in the monolayer on ΔG_{exc} values for mixture of fatty acid/DPPE-PEG5000 monolayers are shown in figure 4.62. The most negative ΔG_{exc} value for palmitoleic acid/DPPE-PEG5000 was found at $X_{\text{VE}} = 0.047$, oleic acid/DPPE-PEG5000 at $X_{\text{VE}} = 0.046$, linoleic acid/DPPE-PEG5000 at $X_{\text{VE}} = 0.02$ and linolenic acid/DPPE-PEG5000 at $X_{\text{VE}} = 0.05$. X_{VE} are found higher in mixed monolayer of fatty acid/DPPE-PEG5000 than in fatty acid/DPPE-PEG2000 for palmitoleic acid oleic acid and linolenic acid. This implies that DPPE-PEG5000 has effectively increased the spacing in the monolayer to accommodate more VE molecules. On the contrary, that effect is not significant in linoleic acid/DPPE-PEG5000 monolayer hence less amount of VE can be loaded in order to form the most favorable mixed monolayer.

At higher surface pressure, ΔG_{exc} became more negative regardless the amount of VE in the monolayer for mixture of palmitoleic acid/PEGylated lipid and linoleic acid/PEGylated lipid. This indicates the formation of a more compatible mixed monolayer with stronger interaction between the molecules as the surface pressure increases. Whereupon the molecules at the air-aqueous interface are in a situation of closer packing after the surface pressure of 10 mN m^{-1} due to conformation change at the long polyethoxylate chain from mushroom-like to “extended” or coil conformation. However, this change has significantly affected the molecular packing in monolayer consisting ternary mixture of oleic acid/PEGylated lipid/VE to a state of stronger repulsion interaction by exhibiting a less negative ΔG_{exc} as the surface pressure increases.

On the other hand, further increase the amount of VE beyond X_{VE} results in less negative ΔG_{exc} as shown in figure 4.60 to figure 4.62. This suggests weak

intermolecular interaction between molecules. A plausible reason could be due to positioning of VE molecules near the polar head group of the fatty acid molecules in the aqueous region rather than occupying the space in the hydrophobic region. This could be explained from delocalization of π electron at the benzene ring creates a polar group moiety in VE molecules that allows it to be arranged at the air-aqueous interface as the amount of VE in the monolayer increases. The presence of VE molecules at the air-aqueous interface caused the molecular packing became less efficient and thus weaker intermolecular interaction among the molecules.

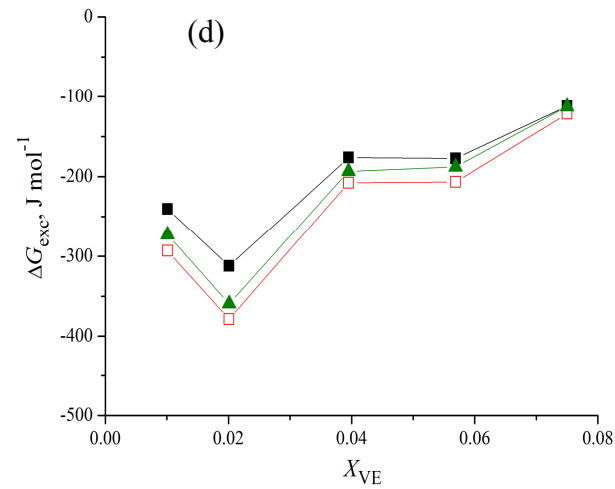
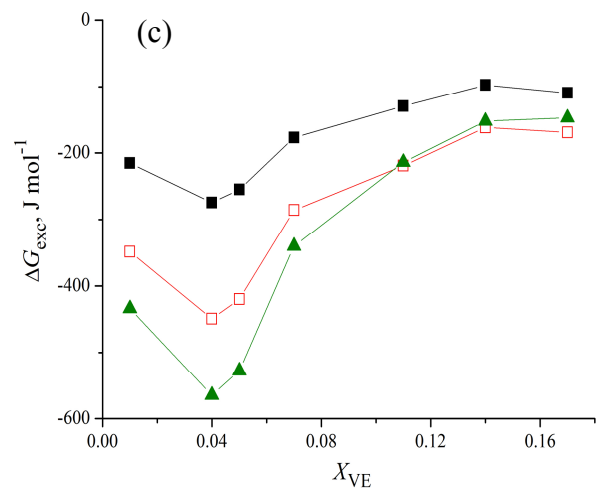
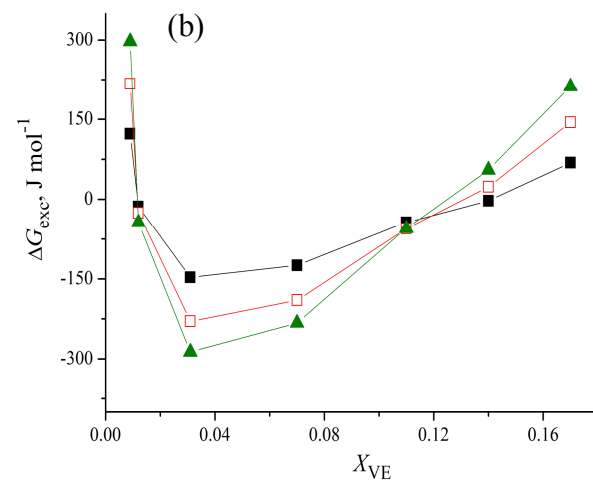
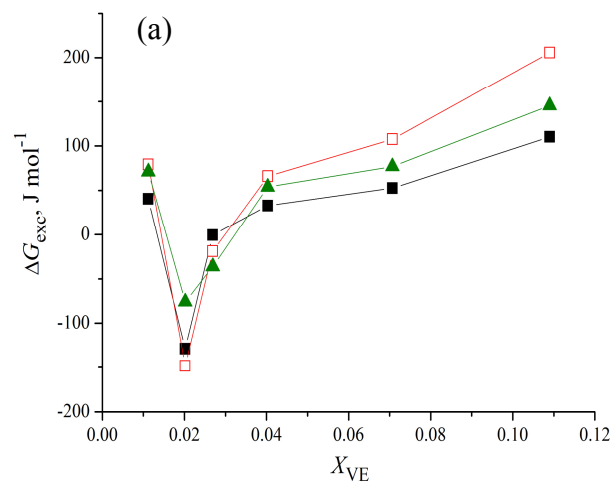


Figure 4.60. Surface excess energy (ΔG_{exc}) as a function of mole fraction VE (X_{VE}) in (a) palmitoleic acid, (b) oleic acid, (c) linoleic acid and (d) linolenic acid monolayer at the air-aqueous interface at 25 °C and surface pressure ■ = 5 mN m^{-1} , □ = 10 mN m^{-1} , ▲ = 15 mN m^{-1} .

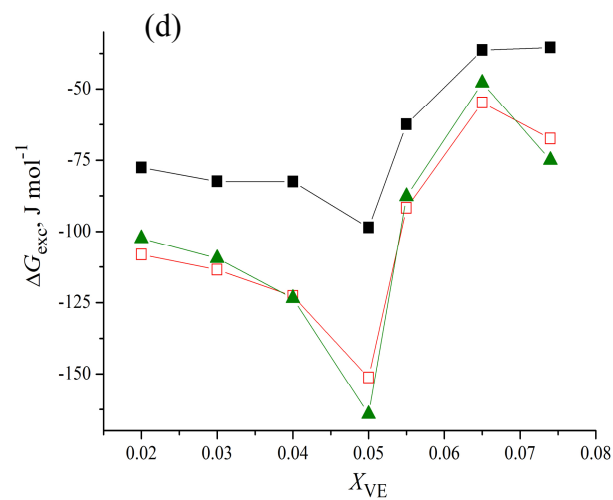
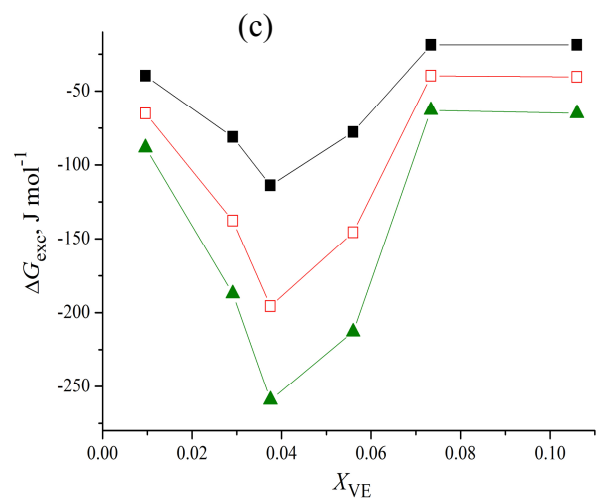
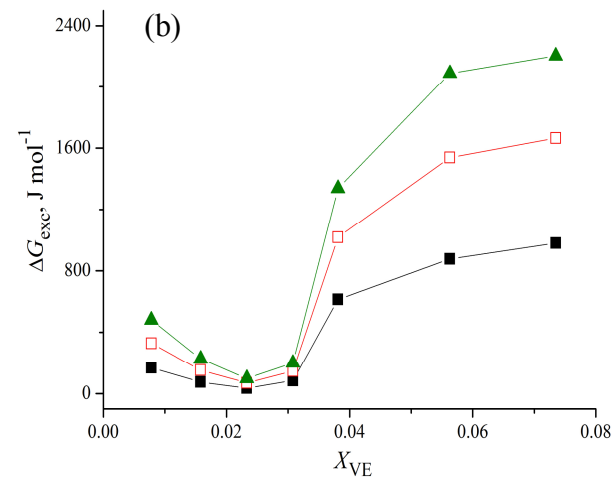
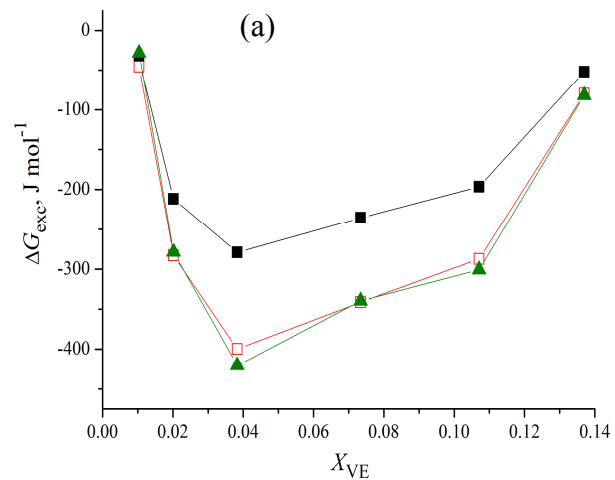


Figure 4.61. Surface excess energy (ΔG_{exc}) as a function of mole fraction VE (X_{VE}) in monolayer of 2 % DPPE-PEG2000 with (a) palmitoleic acid, (b) oleic acid, (c) linoleic acid and (d) linolenic acid at the air-aqueous interface at 25 °C and surface pressure ■ = 5 mN m⁻¹, □ = 10 mN m⁻¹, ▲ = 15 mN m⁻¹.

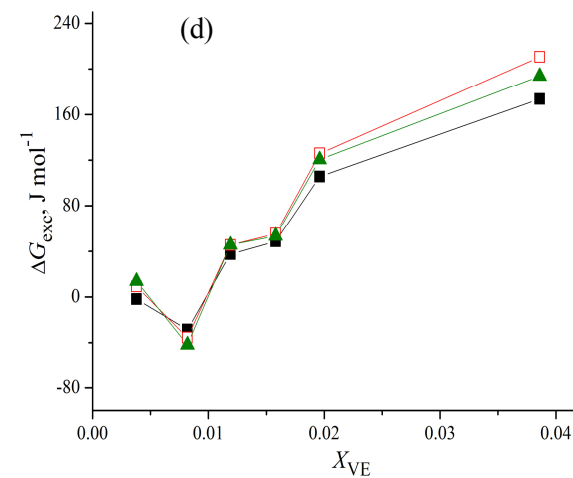
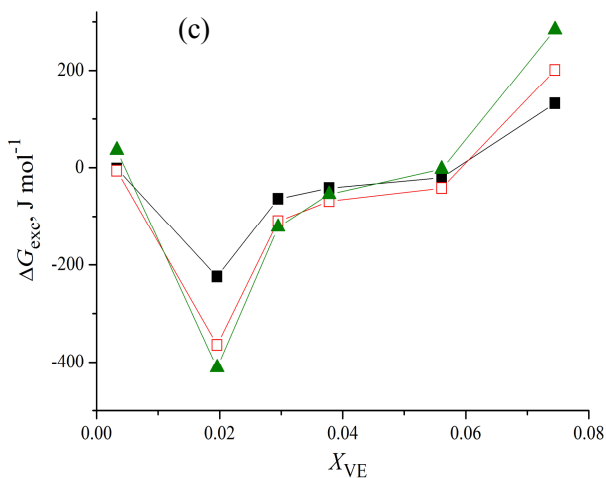
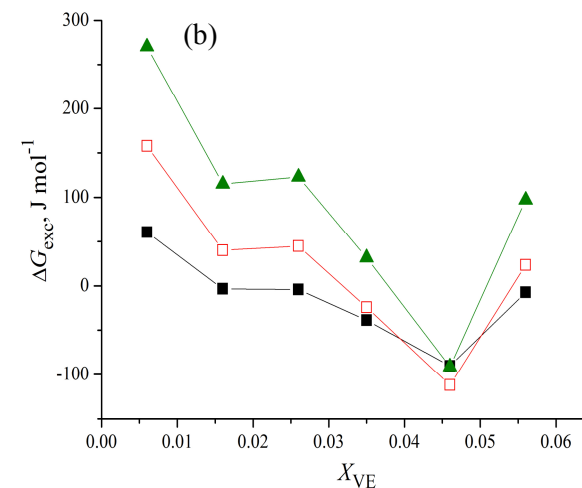
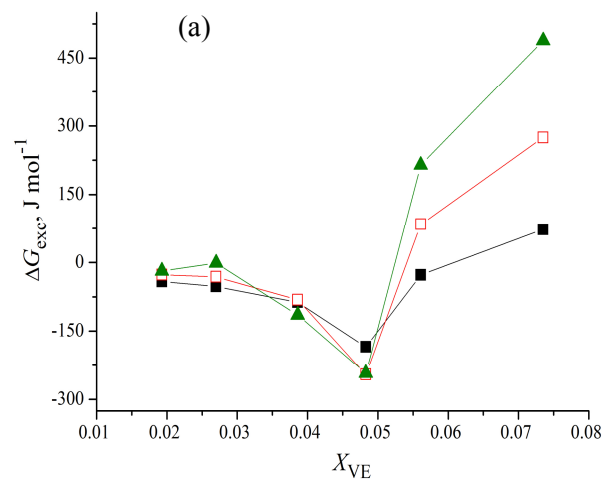


Figure 4.62. Surface excess energy (ΔG_{exc}) as a function of mole fraction VE (X_{VE}) in monolayer of 2 % DPPE-PEG5000 with (a) palmitoleic acid, (b) oleic acid, (c) linoleic acid and (d) linolenic acid at the air-aqueous interface at 25 °C and surface pressure ■ = 5 mN m^{-1} , □ = 10 mN m^{-1} , ▲ = 15 mN m^{-1} .

4.6.3 Application of monolayer studies in liposome formulation

Despite Langmuir monolayer being half a bilayer with their flat rather than curved structure, the findings can be extrapolated to liposome system. In fact, these studies can be highly informative, by giving insights into the packing of the molecules in a bilayer through the changes in molecular orientation or conformation, intermolecular interactions within the membrane bilayer, the factors controlling liposome formation and the stability of liposome. By using this method, not only the monolayer of pure substance can be investigated, the mixture of substances can also be used to form the monolayer. This in fact helps to study the best composition of mixed fatty acid/PEGylated lipid in the preparation liposome in order to obtain the most stable membrane bilayer and hence liposome system. Similar to the system containing VE, the most compatible composition is also identified that provides the information on the loading efficiency of VE in liposomes. Hence, Langmuir monolayer may save the cost of production, time and materials by knowing the optimum composition of a stable liposome system.

4.7 References

1. Bahiaa, C.O.A.P., Azevedoa, E.G., Ferreirab, A.M.L. and Frézarda, F. (2010). *European Journal of Pharmaceutical Sciences* **39**, 90.
2. Becher, P. and Schick, M.J. In Schick, M.J., (Ed.), Dekker, M (1987). *Nonionic Surfactants*, New York, 435.
3. Belsito, S., Bartucci, R. and Sportelli, L. (2001). *Biophys. Chem.* **93**, 11.
4. Centis, V. and Vermette, P. (2008). *Colloid and Surfaces B: Biointerfaces* **65**, 239.
5. Cevc, G. (1991). *Biochemistry*. **30**, 7186.
6. Chen, K.B., Chang, C.H., Yang, Y.M. and Maa, J.R. (2000). *Colloids and Surfaces A: Physicochemical and Engineering Aspects* **170**, 199.
7. Chou, T.H. and Chu, I.M. (2002). *Colloids and Surfaces A: Physicochem. Eng. Aspects* **211** 267.
8. Drost, W.H. (1965). *Ind. Eng. Chem.* **57**, 18.
9. Fan, X.J., Liu, Q., Zhen, P., Zhang, Y. and Hu, X. (2007). *Journal of Chinese Pharmaceutical Sciences*. **16**, 96.
10. Feng, S.S. (1999). *Langmuir* **15**, 998.
11. Gong, K., Feng, S.S. and Go, M.L. (2002). *Colloids Surf. A* **207**, 113.
12. Heurtault, B., Saulnier, P., Pech, B., Proust, J.E. and Benoit, J.P. (2003). *Biomaterials* **24**, 4283.
13. Hoke, B.C. and Chen J.C. (2001). *J. Chem. Eng. Data* **36**, 322.
14. Hoke, B.C. and Patton, E.F. (1992). *J. Chem. Eng. Data* **37**, 331.
15. Kanicky, J.R. and Shah, D.O. (2002). *J. Colloid and Interface Science* **256**, 201.
16. Keough, K.M., Giffin, B. and Kariel, N. (1987). *Biochim. Biophys. Acta.* **902**(1), 1.
17. Kuhl, T.L., Leckband, D.E., Lasic, D.D. and Israelachvili, J.N. in: Lasic, D.D and Martin, F. (Eds.) (1995). *Stealth liposomes Chapter 8*, CRC press, Boca Raton, Florida, 73.

18. Kulkarni, S.B., Betageri, G.V. and Singh, M. (1995). *J. Microencapsul.* **12**, 229.
19. Liu, N. and Park, H.J. (2010). *Colloids and Surfaces B: Biointerfaces* **76**, 16.
20. Liu, N. and Park, H.J. (2010). *Colloids and Surfaces B: Biointerfaces* **76**, 16.
21. Maggio, B., Diplock, A. and Lucy J.A. (1977). *Biochem. J.* **161**, 111-121.
22. Majewski, J., Kuhl, T.L., Gerstenberg, M.C., Israelachvili, J.N. and Smith, G.S. (1997). *J. Phys. Chem. B* **101** 3122.
23. Majewski, J., Kuhl, T.L., Wong, J.Y., Smith, S.G. (2000). *Reviews in Molecular Biotechnology* **74**, 207.
24. Manosroi, A., Wongtrakul, P., Manosroi, J., Sakai, H., Sugawara, F., Yuasa, M. and Abe, M. (2003). *Colloids and Surfaces B: Biointerfaces.* **30**, 129.
25. Marinova, K.G., Alargova, R.G., Denkov, N.D., Velev, O.D., Petsev, D.N., Ivanov, I.B. and Borwankar, R.P. (1996). *Langmuir* **12**, 2045.
26. Marsh, D. (1996). *BBA* **1286**, 183.
27. Memoli, A., Palermi, G. L., Travagli, V. and Alhaique, F. (1994). *J. Soc. Cosme. Chem.* **45**, 167.
28. Mohanty, A and Dey, J (2006). *Journal of Chromatography A* **1128**, 259.
29. Nagle, J.F. (1986). *Faraday Discuss. Chem. Soc.* **81**, 151.
30. Nii, T., Takamura, A., Mohri, K. and Ishii, F. (2003). *Colloids and Surfaces B: Biointerfaces* **27**(4), 323.
31. Risselada, H.J and Marrink, S.J. (2009). *Phys Chem Chem Phys.* **11**(12), 2056.
32. Rogerson, M.L. Robinson, B.H., Bucak, S. and Walde, P. (2006). *Coll. Surf. B: Biointerfaces* **48**, 24.
33. Safran, S.A., Pincus, P.A. and Andelman, D. (1990). *Science* **248**, 354.
34. Sakai, H., Masada, Y., Takeoka, S. and Tsuchida, S. (2002). *J. Biochem.* **611**.
35. Seoane, R., Dynarowicz-tstka, P., Miñones, Jr. J. and Rey-Gómez-Serranillos, I. (2001). *Colloid & Polymer Science* **279**(6), 562.

36. Shah, D.O. and Schulman, J. (1968). *Adv. Chem. Ser.* **84**, 189.
37. Sriwongsitanont, S. and Ueno, M. (2004). *Colloid Polym. Sci.* **282** 753.
38. Stubbs, C.D., Kouyama, T., Kinoshita, K. and Ikegami, A. (1981). *Biochemistry* **20**, 4257.
39. Tirosh, O., Barenholz, Y., Katzhendler, J. and Priev, A. (1998). *Biophys. J.* **74** 1371.
40. Woodle, M. C., Collins, L.R., Sponsler, E., Kossovsky, N., Papahadjopoulos, D. and Martin, F. J. (1992). *Biophys. J.* **61**, 902.

5.0 Conclusions

In this study different type of liposomes prepared from unsaturated fatty acids, palmitoleic acid, oleic acid, linoleic acid and linolenic acid were investigated. Since the formation of liposome is highly affected by pH change, therefore, the appropriate pH for the preparation of fatty acid liposomes was determined by titration of the alkali fatty acid solution using 0.1 M HCl solution and found that liposome could be observed at pH in between 8.0 to 9.0. At this pH region, the mean particle size is in the range of 140 nm – 290 nm and zeta potential is in the range of -70 mV – -110 mV.

Presence of PEGylated lipids and/or double chain saturated lipid (Lecinol S-10) in the bilayer composition dramatically enhanced their stability and reduced the liposome sizes to below 100 nm. All of the liposomes were prepared by using dry lipid hydration method. Two types of PEGylated lipids (DPPE-PEG2000 and DPPE-PEG5000) that are only different on the degree of polymerization at polyethoxylate group were used in this study. The addition of DPPE-PEG2000 and DPPE-PEG5000 into fatty acid solutions did not significantly change the trend of the equilibrium curve. However, addition of DPPE-PEG5000 and Lecinol S-10 into fatty acid solution results in a drastic change in pH as HCl was added into the solution as observed in the equilibrium titration curve. We found that the pH suitable for the formation of liposome is not influenced by the type of PEGylated lipid and all of the mixture may form liposome at pH 8.0 – pH 9.0. Hence, pH 8.5 was selected in the preparation of liposome in this studies. CVC values are higher in the presence of DPPE-PEG2000 and DPPE-PEG5000 compared to those liposomes prepared from pure fatty acid. This clearly suggested that the bulky head group of PEGylated lipids has a significant influence in molecular self-assembly. Therefore, the increase in CVC is more pronounced for mixture of fatty acid and DPPE-PEG5000 compared to DPPE-PEG2000. CVC for fatty

acid liposomes containing PEGylated phospholipid and Lecinol S-10 were found comparably lower than those liposome system of fatty acid/PEGylated lipid.

The size of fatty acid liposomes has been dramatically reduced to nanosize in the presence of PEGylated lipid in the system. DPPE-PEG5000 with bulkier polyethoxylate group tends to form smaller size liposomes compared to DPPE-PEG2000. Similar results were observed for mixture of fatty acid/DPPE-PEG2000/Lecinol S-10. On the contrary, mixture of C18 fatty acid/DPPE-PEG5000/Lecinol S-10 demonstrated a larger size liposome compared to those in their mixed system of C18 fatty acid/DPPE-PEG5000.

The presence of DPPE-PEG2000 in fatty acid liposome has effectively promoted stabilization in fatty acid liposome to a certain extent. However, limited stability was also observed in linoleate-linoleic acid/DPPE-PEG2000 liposomes system. Similar results were obtained in the mixture of fatty acid/Lecinol S-10. Particle size of liposome with incorporation of DPPE-PEG5000 in oleate-oleic acid liposomes, linoleate-linoleic acid liposomes and palmitoleate-palmitoleic acid liposomes remained stable for limited duration of storage period. Surprisingly, changes in liposome size with time in mixed system of linoleate-linoleic acid/DPPE-PEG5000 was not as dramatic as those in linoleate-linoleic acid/DPPE-PEG2000. Particle size for all of the fatty acid liposomes containing DPPE-PEG5000/Lecinol S-10 were found to increase gradually during the storage period.

Liposomes containing PEGylated lipid have less negative zeta potential than the pure fatty acid liposomes from -100 mV to -60 mV. This is a good indication of successful incorporation of PEGylated lipid into the liposome bilayer whereby the polyethoxylate group is adsorbed or coated on the surface of liposome and shielded the negatively surface charge. From the result of zeta potential, we concluded that addition of DPPE-PEG2000 or Lecinol S-10 into the formation of fatty acid liposome helps in

the stabilization of the liposome system. On the other hand, addition of DPPE-PEG5000 into the liposome system may render destabilization of the liposome.

Loading efficiency of calcein and VE in liposome with inclusion of PEGylated lipid is lower compared to the pure fatty acid liposomes or mixed fatty acid/Lecinol-S10 liposomes. However, the loading efficiency for mixture of fatty acid/DPPE-PEG2000 liposomes were found slightly higher than those of fatty acid/DPPE-PEG5000. It is understood that fatty acid liposome is formed via convolution of bilayer as a result of different localized pressure exerted on the surface of the bilayer. In a liposome system consisting of pure fatty acid, the pressure exerted on the bilayer surfaces is almost equal as compared to mixed fatty acid-lipid system. Hence, the stability of the liposome will also be greatly affected depending on the mixture composition. Therefore, the intermolecular interaction and compatibility of the molecules in a mixture can be studied via Langmuir monolayer that is half of the bilayer. Information from the Langmuir isotherm such as deviation of excess area per molecules indicates the participation of PEGylated lipid molecules in the monolayer. This study also revealed that addition of PEGylated lipid in the fatty acid monolayer results in a more compressible monolayer as indicated by compression modulus of the monolayer. The most compatible composition between the PEGylated lipid and fatty acid for the preparation of liposome has also been obtained from this study. Table 5.1 shows the most thermodynamically favourable mixture or the optimum composition for fatty acid and PEGylated lipid.

Table 5.1 The optimum composition of mixed fatty acid and PEGylated lipid.

Fatty acid	DPPE-PEG2000		DPPE-PEG5000	
	X_{opt}	ΔG_{exc} , J mol ⁻¹	X_{opt}	ΔG_{exc} , J mol ⁻¹
Palmitoleic acid	0.02	-1250	0.04	-1500
Oleic acid	0.022	-2500	0.010	-1350
Linoleic acid	0.0135	-500	0.02	-2000
Linolenic acid	0.012	-550	0.003	-600

X_{opt} = mole fraction for optimum ΔG_{exc}

VE is used to be loaded in the liposome in this study, their interaction with fatty acid molecules has also been investigated by using Langmuir monolayer. From the monolayer study, the inclusion of VE is found to be accommodated in the cavities formed by fatty acid monomer within the lipid bilayer of liposome. As evident by monolayer study, addition of VE in the pure fatty acid as well as mixed fatty acid/PEGylated lipids monolayer has imparted the formation of a more rigid monolayer with higher C_s^{-1} . The variation of C_s^{-1} is more pronounced in mixed monolayer of fatty acid/VE compared to the monolayer of fatty acid/PEGylated lipid/VE whereupon the increment of C_s^{-1} in the fatty acid/VE monolayer is higher followed by fatty acid/DPPE-PEG2000/VE and fatty acid/DPPE-PEG5000/VE. In addition, a maximum condensation effect is observed in all of the fatty acid monolayer. The ability of VE to be “solubilized” in the hydrophobic region of the bilayer and induce membrane stability is thought to occur via an interaction between the rigid hydrophobic chromanol ring structure of VE molecules and the acyl chain of the fatty acid molecules. This strongly suggests the interaction between fatty acid and VE molecules as evidence from the ΔG_{exc} . The “condensing effect” of VE molecules within the bilayer is attributed from the accommodation of VE molecules in the molecular cavities. The cavities are generated from assembling of fatty acid molecules into liposomes. The optimum composition in order to attain the most

negative ΔG_{exc} is shown in table 5.2. Although the loading efficiency of VE in liposome is related to this composition and varied according to the type of fatty acid and their mixture with PEGylated lipids, the factor of particle size of the liposome may also play an important role in determining the loading efficiency. This is due to VE being forced to accommodate in the monolayer during the compression of Langmuir monolayer. This process is different compared to self-assemble of fatty acid monomer into liposomes whereby VE molecules move freely in the system.

The aim of this study is partly achieved due to the many factors that contribute to the variation of results. However a better understanding of the fatty acid liposome system is disclosed in this work.

Table 5.2 The optimum composition of fatty acid and mixed fatty acid/PEGylated lipid with VE

Substance	VE	
	X_{opt}	$\Delta G_{\text{exc}}, \text{J mol}^{-1}$
Palmitoleic acid	0.02	-150
Palmitoleic acid/DPPE-PEG2000	0.04	-400
Palmitoleic acid/DPPE-PEG5000	0.05	-250
Oleic acid	0.03	-300
Oleic acid/DPPE-PEG2000	0.03	~ 0
Oleic acid/DPPE-PEG5000	0.046	-125
Linoleic acid	0.04	-600
Linoleic acid/DPPE-PEG2000	0.04	-250
Linoleic acid/DPPE-PEG5000	0.02	-400
Linolenic acid	0.02	-400
Linolenic acid/DPPE-PEG2000	0.05	-175
Linolenic acid/DPPE-PEG5000	0.01	-50

X_{opt} = mole fraction for optimum ΔG_{exc}

5.1 Future works

This study has developed many unexplored thoughts or new path ways for fatty acid liposomes. Although the presence of PEGylated lipid in liposome may enhance the stability of liposome, the rate of liposome formation or breakdown with the presence of PEGylated lipid is not clear. Whereupon this information may help in identifying the factor that contributes to stabilization or destabilization of the liposome. In addition to PEGylated lipid, another stabilizer as an example that can be anchored to the membrane bilayer is chitosan attached to a long hydrocarbon chain which may also promotes stabilization in fatty acid liposome.

In view of the ability of fatty acid liposome to encapsulate active ingredients, this may render them to be applied in the field of cosmetics and pharmaceuticals. However, further investigation has to be carried out as the optimum amount to be encapsulated is highly dependent on the type of active ingredients as revealed in this study.

Application of fatty acid liposome in cosmetic products is promising as they are natural, non-toxic, biological with functional activities similar to phospholipid. The investigation on addition of fatty acid nanoliposome in cosmetic cream should be carried out. Therefore the effectiveness of delivery active ingredients deep into the skin rather than blocked by the stratum corneum layer can be attained.

APPENDIX

Effect of Unsaturation on the Stability of C₁₈ Polyunsaturated Fatty Acids Vesicles Suspension in Aqueous Solution

Yin Yin Teo,* Misni Misran, Kah Hin Low, and Sharifuddin Md. Zain

Department of Chemistry, Faculty of Science, University of Malaya, 50603, Kuala Lumpur, Malaysia

*E-mail: yinyinteo@um.edu.my

Received June 18, 2010, Accepted October 21, 2010

Degree of unsaturation in fatty acid molecules plays an important role in the formation of vesicles. Vesicle formation from C₁₈ fatty acids with different amount of double bonds such as oleic acid, linoleic acid and linolenic acid with the incorporation of 1,2-dipalmitoyl-*sn*-glycerol-3-phosphoethanolamine-*N*-[methoxy(polyethylene glycol)-2000] (DPPE-PEG2000) have been examined by TEM. Critical vesicular concentrations (CVC) of the vesicle suspension are determined by turbidity and surface tension methods. The CVC of fatty acids increases when the amount of unsaturation in the alkyl chain increases. On the other hand, stability of vesicle suspension has been examined by using particle size and zeta potential at 30 °C. There was a dramatic decrease in particle size measurement from mono-unsaturation to tri-unsaturation which could be due to the effect of fluidity in the membrane bilayer caused by different degree of unsaturation. The values of zeta potential for vesicles that were formed without the incorporation of DPPE-PEG2000 were in the range of -70 mV to -100 mV. It has been observed that the incorporation of DPPE-PEG2000 to the vesicle reduces the magnitude of zeta potential. However, this phenomenon does not obviously seen in fatty acid vesicles formed by linoleate-linoleic acid and linolenate-linolenic acid. We therefore conclude that the addition of DPPE-PEG2000 does not effectively improve the stability of the linoleate-linoleic acid and linolenate-linolenic acid vesicle at pH 9.0 after the evaluation of their particle size and zeta potential over a period of 30 days. Although the vesicles formed were not stable for more than 10 days, they have displayed the potential in encapsulating the active ingredients such as vitamin E and calcein. The results show that the loading efficiencies of vitamin E are of encouraging value.

Key Words: Stability, Unsaturated fatty acid, Vesicles, Zeta potential

Introduction

Vesicle is an artificial microscopic lipid bilayer membrane separating inner aqueous compartment from outer aqueous environment. It is capable in encapsulating drugs and active ingredients. This capability of vesicle provides a promising technology for protection of loads during storage and delivery to the target site. Dialkyl phospholipids are commonly used in the preparation of vesicles. However, single chain fatty acids have also been reported to be able to form vesicles.^{1,2} As phospholipids are relatively more expensive compared to amphiphilic fatty acids, therefore, amphiphilic fatty acids maybe a better replacement for phospholipids.

There are several techniques for the preparation of vesicle. The most common technique to prepare vesicle is dry lipid film hydration. It involves evaporation of solvent from amphiphilic solution which produces a thin surfactant films on the wall of the container. These thin films will be hydrated when they come into contact with warm aqueous environment that later lead to the formation of vesicles.³ There are reports which suggested that vesicles can be spontaneously produced from surfactant solution without the application of any external stimuli. One of the methods that induce the formation of fatty acid vesicles spontaneously is by changing the pH of fatty acid solution through acid-base titration or by pH-jump technique.^{4,5} The kinetics of spontaneous formation and breakdown of the vesicle when subjected to a pH-jump perturbation were rapid over a time scale of a few seconds.¹ However, fatty acid vesicles

are kinetically stable but thermodynamically unstable. Hence, the vesicles formed are polydispersed and their sizes may be varied from small to giant oligolamellars. As reported elsewhere, vesicles of laurate-lauric acid as a saturated short chain fatty acid were found in emulsion². On the other hand, formation of unsaturated long chain fatty acid vesicle from *cis*-9-octadecenoic acid, *cis,cis*-9,12-octadecadienoic acid and docosahexaenoic acid in dilute aqueous solution have also been reported recently.⁶⁻⁸

The inherent problem of vesicle suspension is its instability during prolonged storage and thermodynamically sensitive to the surrounding. This will hinder the appropriateness and effectiveness of vesicles in their applications such as in drug delivery systems. Therefore, the incorporation of bulky hydrophilic molecule such as polyethylene glycol, polysaccharides and protein to the vesicle has been studied extensively to increase the stability of vesicle.⁹⁻¹¹ In general, stability can be considered as the ability of vesicles to maintain their particle size and remain suspended in solution with no agglomeration or flocculation during storage time. Thus, by monitoring the particle size and zeta potential of vesicle suspension over a period of time could determine the stability of vesicle. Other factors such as molecular structure of the amphiphilic molecule, molecular rigidity, head group type, hydrocarbon chain length and degree of unsaturation may well contribute to the variation in the vesicle suspension stability during the storage time. Only little works have been reported on the stability of unsaturated fatty acids vesicle. For this paper, we have studied, firstly, the effect of

unsaturation on the stability of the vesicle in aqueous solution namely oleic acid (*cis*-9-octadecenoic acid), linoleic acid (*cis*, *cis*-9,12-octadecadienoic acid) and linolenic acid (*cis*, *cis*, *cis*-9,12,15-octadecatrienoic acid). Secondly, we have also studied the effects after the incorporation of 1,2-dipalmitoyl-*sn*-glycerol-3-phosphoethanolamine-*N*-[methoxy(polyethylene-glycol)-2000](DPPE-PEG2000) on the stability of vesicle. Lastly, the loading efficiency studies of calcein as a hydrophilic substance and DL- α -tocopherol acetate as a hydrophobic substance have been evaluated.

Methods and Materials

Materials. Oleic acid (*cis*-9-octadecenoic acid, $\geq 99.0\%$), linoleic acid (*cis*, *cis*-9,12-octadecadienoic acid, $\geq 99.0\%$) and boric acid minimum 99.5% were purchased from Fluka (Buchs, Switzerland). Alpha-linolenic acid (*cis*, *cis*, *cis*-9,12,15-octadecatrienoic acid) and DL- α -tocopherol acetate were from Sigma (St. Louis, USA) with purity $\geq 99.0\%$ and 96%, respectively. 1,2-dipalmitoyl-*sn*-glycerol-3-phosphoethanolamine-*N*-[methoxy(polyethyleneglycol)-2000] (DPPE-PEG2000) was from Avanti Polar Lipids Inc. (Alabama, USA). Hydrochloric acid, sodium hydroxide 98% and chloroform of analytical grade were purchased from HMBG Chemicals. Calcein and solvent for HPLC which are methanol, ethanol and acetonitrile of HPLC grade were from Merck. The above mentioned chemicals were used as received. Deionized water with $18.2 \mu\text{S cm}^{-1}$ was obtained from Barnstead NANO pure[®] Diamond[™] ultrapure water system. Deionized water was further distilled and deaerated under nitrogen gas prior to use.

Preparation of Stock Solution. A stock solution of 12.62 mM oleic acid and 27.81 mM NaOH was prepared by mixing 0.90 g of oleic acid into NaOH (0.5000 mL 1.3905 M) solution. Thereafter, the mixture was stirred for 2 hours. The procedure for preparation of stock solution for linoleic acid and alpha-linolenic acid are essentially the same, except that the concentration for each of them has to be adjusted accordingly. On the other hand, preparation of vesicle solution containing DPPE-PEG2000 had been prepared by firstly mixing fatty acid with DPPE-PEG2000 in the mole ratio of 50 to 1 in small amount of chloroform. Secondly, the mixture solution was sonicated in order to dissolve DPPE-PEG2000. It was followed by the removal of the chloroform under reduced pressure by using rotary evaporator. Gel liked mixture was obtained and rehydrated with warm deionised water (50 °C) and NaOH solution to form the colourless solution.

Titration of the Stock Solution with HCl (1 M). A series of samples with fixed amount of fatty acid at various pH were prepared by mixing 1.50 mL of stock solution with the appropriate amount of 0.7725 M HCl and deionised water. The mixture was left to vortex for a minute by using Uzusio VTX 3000L vortex mixer before the pH measurement was carried out by a Mettler Toledo pH meter which had been pre-calibrated at the titration temperature with buffer pH 4.01, 7.00 and 9.21. An average of 3 measurements was recorded.

Transmission Electron Microscopy. The vesicle images were obtained by using Hitachi H-7100 transmission electron microscope through negative-staining method. The samples were pre-

pared by immersing the formvar-coated copper grid into a drop of the vesicle solution. Thereafter, it was allowed to stand for 10 minutes. The excess of vesicle solution was blotted with filter paper before staining process by using 3% (w/v) phosphotungstic acid. The grid was allowed to stand for another 10 minutes and air-dried. The specimens were viewed and photographed with a transmission electron microscope operating at accelerating voltage of 100 kV.

Critical Vesicular Concentration (CVC) Determinations. A series of solutions with different concentration of fatty acid at pH 9.0 in 50 mM borate buffer were prepared. Borate buffer solution was prepared in the manner as mentioned elsewhere.⁷ The solutions were filtered through a 25 mm diameter 0.2 μm pore size Minisart[®] NY nylon filter (Germany) prior to measurements. The CVC determinations were carried out at 30.0 °C by *via* tensiometer balance from KRUSS with K12 tensiometer processor *via* Du nuoy ring method. The CVC value obtained was double confirmed by turbidity measurement at the chosen wavelength of 350 nm by employing Varian Cary 50 UV-vis spectrophotometer at same temperature. The cell housing was thermostated by the VARIAN Cary single cell peltier unit with a water circulator water bath.

Particle Size and Zeta Potential Measurement. The hydrodynamic diameter of the vesicle was measured by the dynamic light scattering (DLS) method. The mean size of the vesicle and zeta potential were estimated by Malvern Nano ZS particle size analyzer from Malvern Instruments Ltd. UK at 30 °C. The solutions were first extruded through 100 nm pore diameters polycarbonate Whatman membranes filter using Lipex Bio-membrane extruder prior to the size measurement.

Studies of Loading Efficiency.

Encapsulation of DL- α -Tocopherol Acetate: Fatty acid and DL- α -tocopherol acetate in the mole ratio of 25 to 4 were mixed in CHCl_3 and subsequently dried under rotor evaporator to remove the CHCl_3 . This mixture was then blown with stream of N_2 gas to ensure total removal the trace amount of CHCl_3 followed by rehydrated with 50 mM borate buffer pH 9.0. The pH of the solution was adjusted to 9.0 by 0.5 M sodium hydroxide and 0.5 M hydrochloric acid.

Encapsulation of Calcein: Calcein (0.5 mM) was dissolved in 50 mM borate buffer pH 9.0 then added into a CHCl_3 solution with 25 mM fatty acid. The mixture solution was kept stirring until all of the CHCl_3 was eventually evaporated. The resulting mixture was then adjusted to pH 9.0 by NaOH and HCl solution.

Determination of Loading Efficiency: Separation of loaded/unloaded species for calcein and DL- α -tocopherol acetate were achieved by gel permeation chromatography technique. The solid phase consists of Sepharose 4B that pretreated with fatty acid solution just above the CVC (mobile phase); which was packed in a glass column of 30 cm \times 1 cm. For sample introduction, 200 μL of the mixture solution was applied. Subsequently every 2 mL of eluent was collected and each fraction was diluted with ethanol to a total volume of 5 mL. Ethanol was applied instead of Triton-X to overcome the self-quenching effect especially for calcein as proposed by Ishii and Nagasaka (2001).¹² In fact, addition of ethanol addresses disruption of the vesicles and fully release those encapsulated species as a consequence.¹³ For the determination of calcein concentrations,

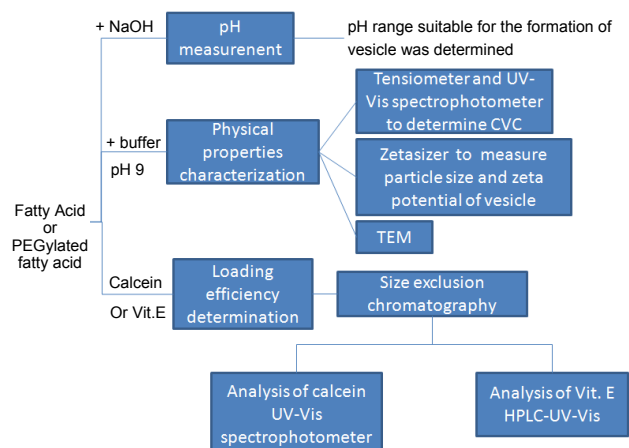


Figure 1. Schematic figure for vesicle preparation and characterization.

spectrophotometric measurement at 496 nm was employed as suggested by Namani *et al.*⁸ On the other hand, the amount of DL- α -tocopherol acetate was analysed by Shimadzu LC-20AT HPLC coupled with an UV detector. A sample of 20 μ L was injected into C18 reverse phase Purospher[®] Star column (dimension 4.6 mm \times 250 mm and the particle diameter of 5 μ m) and separated under isocratic flow of mobile phase (10% acetonitrile, 45% ethanol and 45% methanol). The flow rate is 1.0 mL min⁻¹ and the eluent was monitored at 287 nm. The loading efficiency (%) was calculated as stated in equation 1.

$$\text{Loading efficiency (\%)} = \frac{\text{Absorbance or area of encapsulated material}}{\text{Absorbance or area of amount material}} \times 100 \quad (1)$$

A schematic flow of the current study is illustrated as in Figure 1.

Results and Discussion

Titration Curve. The equilibrium curve of fatty acids as a function of HCl concentration (Figure 2) shows the transparent micellar solutions of deprotonated fatty acid at pH greater than pH 9.5. The presence of vesicles for oleate-oleic acid and linoleate-linoleic acid were observed at pH of the solution between pH 8.0 - pH 9.5 while for linolenate-linolenic acid solution was between pH 7.5 - 9.0. The results obtained were in agreement with those reported elsewhere for vesicle formation by oleic acid and linoleic acid.⁷ Nevertheless all of these three types of fatty acids are having almost the same buffering capacity. However, formation of vesicles from linolenic acid has not been studied. On the other hand, incorporation of DPPE-PEG2000 to the vesicle seems did not show significant effect on the trend of equilibrium curve.

The pH region at which vesicles was observed is approximately equal to the pK_a of fatty acid. According to Kanicky and Dinesh, pK_a for oleic acid is 9.85, for linoleic acid and linolenic acid are 9.24 for the former and 8.25 for the latter.¹⁴ At these pH,

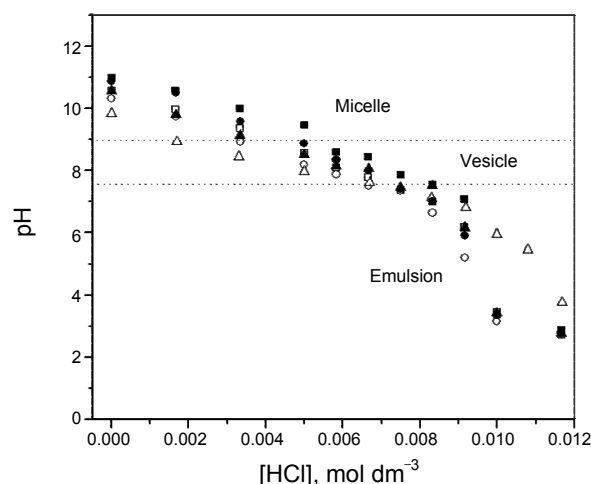


Figure 2. Equilibrium curve of fatty acid as a function of added HCl at room temperature (28 °C), (■) 12.5 mM oleic acid, (●) 12.5 mM linoleic acid and (▲) 12.5 mM linolenic acid. Fatty acid with DPPE-PEG2000 were represented by opened symbol.

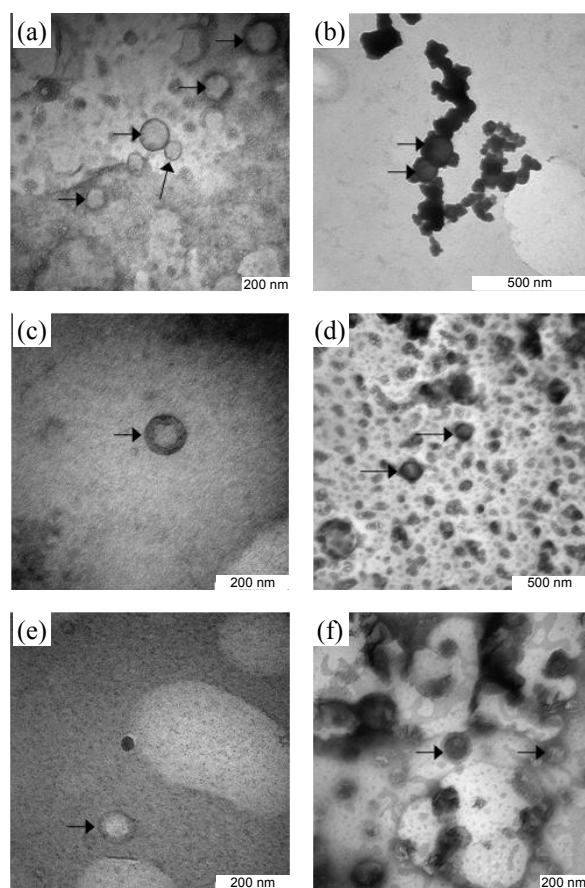


Figure 3. Transmission electron micrograph of (a and d) oleate-oleic acid, (b and e) linoleate-linoleic acid and (c and f) linolenate-linolenic acid at pH 9.0. Figure (a-c) without incorporation of DPPE-PEG2000 while (d-f) with incorporation of DPPE-PEG2000. The presences of vesicles are indicated by arrow.

about half amount of the corresponding acid are ionized. The ionic pair interaction from the ionized and non-ionized single

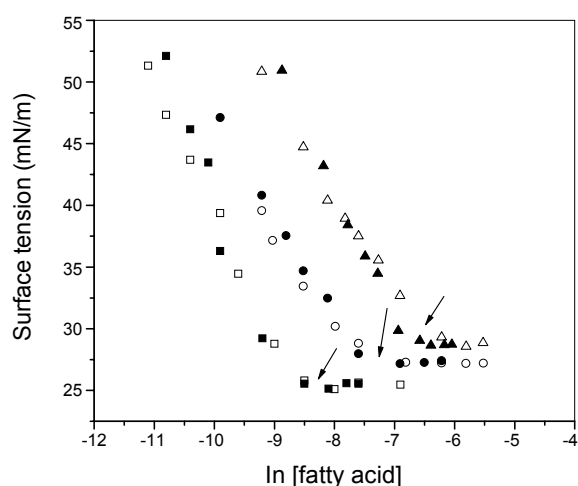


Figure 4. Surface tension as a function of fatty acid concentration, (■) oleate-oleic acid, (●) linoleate-linoleic acid and (▲) linolenate-linolenic acid at 30 °C. Opened symbol indicates the respective fatty acid with DPPE-PEG2000. The arrows in the curve show the CVC of the fatty acids.

Table 1. Summary of CVCs measured by different methods at 30 °C

Fatty acid	CVC, mM	
	By surface tension method	By turbidity method
Oleate-oleic acid	0.13	~ 0.2
DPPE-PEG2000 -oleate-oleic acid	0.17	~ 0.4
Linoleate-linoleic acid	0.51	~ 0.5
DPPE-PEG2000-linoleate-linoleic acid	0.84	~ 1.0
Linolenate-linolenic acid	1.23	~ 1.2
DPPE-PEG2000-linolenate-linolenic acid	1.48	~ 1.6

chain fatty acid molecules brings about an increase in the packing parameters that induced the vesicle formation.

Transmission Electron Micrograph. The presence of vesicles in a solution has been confirmed by using TEM. As revealed in Figure 3, negatively stained electron micrographs of the samples prepared from fatty acids mentioned above confirms the formation of vesicles with average diameter of 100 - 250 nm. The vesicle size determined from TEM images are consistent with the size distributions acquired from DLS measurement. Notwithstanding the numerical differences between both measurements, the deviations were not significant.

CVC Determinations. CVCs for C₁₈ polyunsaturated fatty acids include oleic acid, linoleic acid and linolenic acid were determined at pH 9 for comparison purposes. All CVC values were determined at the inflection point of a plot of surface tension as a function of fatty acid concentration as shown in Figure 4. CVC for oleic acid is the lowest whereas linolenic acid has the highest value of CVC as mentioned in Table 1. In general, hydrophobicity of the aliphatic chain will be weaker if the number of unsaturation is higher. Therefore, oleic acid molecules possess only one double bond in the aliphatic chain has stronger hydrophobicity property, hence they are less soluble

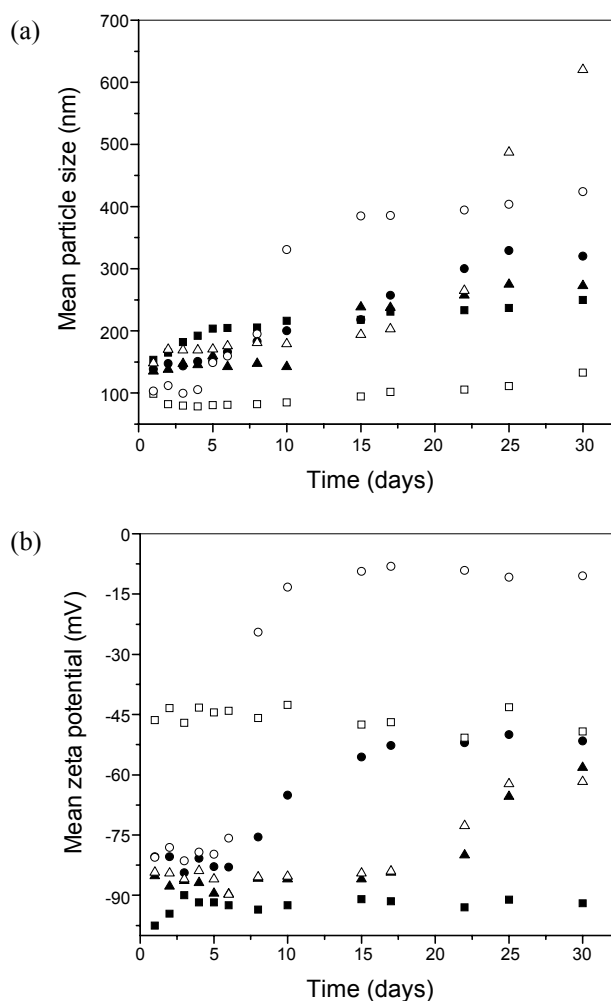


Figure 5. (a) Mean particle size and (b) mean zeta potential of (■) oleate-oleic acid, (●) linoleate-linoleic acid and (▲) linolenate-linolenic acid as a function of incubation time in 50 mM aqueous borate buffer solution at pH 9.0 at room temperature (28 °C). Opened symbol indicates the respective fatty acid with DPPE-PEG2000.

in aqueous solution. This further explains why oleate-oleic acid solution indicated the lowest CVC value. On the contrary, linolenate-linolenic solution that corresponds to three unsaturations has the highest CVC value owing to the fact that it has the weakest hydrophobicity property. The similar results were observed for vesicles with incorporation of DPPE-PEG2000. However, CVC values are higher with the present of DPPE-PEG2000 compared to those without DPPE-PEG2000. This is due to the present of DPPE-PEG2000 as anionic molecules in the solution increase the ratio of ionized to non-ionized molecules and hinder the formation of vesicle. Therefore, the higher amounts of fatty acid molecules are required to uphold the ratio. It can be achieved by increase the concentration of fatty acid meanwhile pH of the solution is maintained.

Particle Size and Zeta Potential of Vesicles. Particle size of a fatty acid vesicle is affected by the fatty acid chain length and degree of unsaturation. Fatty acid with shorter chain length tends to form a larger vesicle than the longer chain fatty acid. This may be due to shorter aliphatic chain length is more rigid, consequently forming larger vesicle with less curvature. With

Table 2. Loading efficiency of fatty acids' vesicle

Fatty acid	Loading efficiency, %	
	Calcein	DL- α -tocopherol acetate
Oleate-oleic acid	4.4	61.2
DPPE-PEG2000 -oleate-oleic acid	3.1	47.2
Linoleate-linoleic acid	2.3	44.1
DPPE-PEG2000-linoleate-linoleic acid	2.0	39.0
Linolenate-linolenic acid	2.3	44.8
DPPE-PEG2000-linolenate-linolenic acid	2.2	32.3

this idea in mind, it is expected that the higher the number of unsaturation in the hydrocarbon chain, the smaller the vesicle will be formed. The plausible explanation could be owing to the nature of intermolecular interaction that caused more stacking in the membrane as the number of unsaturation is less, thus leading to formation of "flatter" bilayer. Therefore, by increasing the degree of unsaturation in the lipid acyl chain, the more bends and kinks are present and hence membrane fluidity will also be increased that resulting in the formation of vesicle with higher curvature or smaller in particle size.¹⁵⁻¹⁷

The mean particle size and zeta potentials of fatty acid vesicle solutions with and without DPPE-PEG2000 were monitored for a period of 30 days at fatty acid concentration of 5 mM which is well above their CVC values as presented in Figure 5a. The particle size of all three types unsaturated fatty acid vesicles without DPPE-PEG2000 are larger than 100 nm as a result of polydispersity nature of the vesicle dispersion with polydispersity index values ranging from 0.1 - 0.6. The mean size for oleate-oleic acid vesicles found to be the largest whilst linolenate-linolenic acid vesicles showed markedly smaller than the others. By comparing the three fatty acids, oleic acid with only one unsaturation is considered to be less flexible, higher stacking and less curvature leading to larger vesicles. On the other hand, molecules with two or more unsaturations are more flexible and therefore have higher lateral diffusion coefficient than the monounsaturated. The dynamics nature of the monomers in the bilayer membrane and more fluidic nature of the bilayer for higher unsaturation lead to higher membrane stability and curvature. This explains linolenate-linolenic suspension was dominated with smaller size vesicles. Nevertheless, the particle size of linoleate-linoleic acid and linolenate-linolenic acid vesicles were increased drastically after 7 days of storage at room temperature (28 °C) as a result of aggregation. However, there is no apparent change in the size of the DPPE-PEG2000-oleate-oleic acid vesicle solutions which indicates the stability of the vesicles. Although lots of works had been reported on improving the stability of phospholipid vesicles through incorporation of stealth into the vesicles, unfortunately, it was not totally applicable on fatty acid vesicles as revealed from our finding. Obviously, Figure 5b demonstrates that only oleate-oleic acid vesicles promote significantly reduce in zeta potential to a less negative value after the incorporation of DPPE-PEG2000 to the vesicles. This is probably due to the long and bulky polyoxyethylene group wrapping around the vesicles that reduced mobility of vesicles, and hence the zeta potential. This observa-

tion also implicates the interaction form between the oleate-oleic acid and DPPE-PEG2000 is the strongest among the acids. In contrast, vesicles forming from linoleic acid and linolenic acid with the incorporation of DPPE-PEG2000 did not display any significant change on the zeta potential. In other words, DPPE-PEG2000 is unlikely to interact with linoleic acid and linolenic acid in the formation of vesicles at pH 9.0. Therefore, these vesicles were not as stable as in the case of oleate-oleic vesicles. Hence, explanation for the increase in zeta potential to a less negative value for linoleate-linoleic acid vesicles and linolenate-linolenic acid vesicles after day seven was due to aggregation effect. These results are in agreement with the increase of vesicle size after day seven.

Loading Efficiency of Calcein and DL- α -Tocopherol acetate.

There are several factors affect the loading efficiency of vesicles, which include the concentrations and chemical properties of corresponding substances and also the preparation method.^{18,19} The loading efficiencies of calcein and DL- α -tocopherol acetate on C₁₈ unsaturated fatty acid vesicles were calculated by applying Eq. 1 and are listed in Table 2. In general, all vesicles prepared via current method show different capability in encapsulation of the above mentioned substances. It is also observed that DL- α -tocopherol acetate associated with remarkably higher loading efficiency under our working conditions. The plausible explanations are DL- α -tocopherol acetate that behaves as a hydrophobic substance tends to be embedded in between the bilayer. On the other hand, the loading efficiency of calcein encountered in this study is considerably low (2 to 4%) regardless of the vesicle size. Yet, as revealed by other researchers, the calcein loading efficiencies may vary from 0.1% to 39.5% subjected to the factors mentioned above.^{8, 19-22}

Conclusion

The present work reports the effect of vesicle stability as a function of unsaturation degree in fatty acid molecules. The membrane become more fluid liked as the degree of unsaturation increase, therefore thickness of membrane will be reduced. As a consequence the membrane will become more flexible. Thus, the particle size of the vesicles is expected to be smaller. It has also been observed that vesicles prepared from mono-unsaturated fatty acid are the most stable suspension for at least 30 days compared to fatty acid with two unsaturations and three unsaturations. Lastly, the incorporation of DPPE-PEG2000 does not always exhibit its ability on improving the stability of vesicles as revealed in this study.

Acknowledgments. This research work was supported by the Ministry of Science, Technology and Innovation Malaysia (MOSTI) under the eScienceFund 03-01-03-SF0316 and Postgraduate Research Grant (PPP) P0267-2007A from University Malaya.

References

- Morigaki, K.; Walde, P.; Misran, M.; Robinson, B. H. *Colloids Surf. A: Physiochem. Eng. Aspects.* **2003**, 213, 37.
- Boris, B. N.; Tjong, N. S.; Misran, M. *Coll. Surf. A: Physiochem.*

- Eng. Aspects*. **2004**, 236, 7.
3. Bangham, A. D.; Sandish, M. M.; Watkins, J. C. *J. Mol. Biol.* **1965**, 13, 239.
4. Gebicki, J. M.; Hicks, M. *Nature* **1973**, 243, 232.
5. Hargreaves, J. W.; Deamer, D. W. *Biochemistry* **1978**, 17, 3759.
6. Gebicki, J. M.; Hicks, M. *Chem. Phys. Lipids* **1976**, 16, 142.
7. Rogerson, M. L.; Robinson, B. H.; Bucak, S.; Walde, P. *Coll. Surf. B: Biointerfaces* **2006**, 48, 24.
8. Namani, T.; Ishikawa, T.; Morigaki, K.; Walde, P. *Coll. Surf. B: Biointerfaces*. **2007**, 54, 118.
9. Alben, N. K.; Malcom, N. J. *Biochimica et Biophysica Acta* **1996**, 1304, 120.
10. Minakshi, G.; Tathagata, D.; Narendra, K. J. *AAPS PharmaSciTech*. **2007**, 8(2), E1.
11. Klibanov, A. L.; Maruyama, K.; Torchillin, V. P.; Huang, L. *FEBS Lett.* **1990**, 268, 235.
12. Ishii, F.; Nagasaka, Y. *Journal of Dispersion Science and Technology* **2001**, 22, 97.
13. Nii, T.; Takamura, A.; Mohri, K.; Ishii, F. *Colloids and Surfaces B: Biointerfaces* **2002**, 27, 323.
14. Kanicky, J. R.; Dinesh, O. S. *J. Colloid and Interface Science* **2002**, 256, 201.
15. Cevc, G. *Biochemistry* **1991**, 30, 7186.
16. Keough, K. M.; Giffin, B.; Kariel, N. *Biochim. Biophys. Acta* **1987**, 902(1), 1.
17. Stubbs, C. D.; Kouyama, T.; Kinoshita, K.; Ikegami, A. *Biochemistry* **1981**, 20, 4257.
18. Liu, N.; Park, H. J. *Colloids and Surfaces B: Biointerfaces* **2010**, 76, 16-19.
19. Bahia, C. O. A. P.; Azevedo, E. G.; Ferreira, A. M. L.; Frézarda, F. *European Journal of Pharmaceutical Sciences* **2010**, 39, 90-96.
20. Memoli, A.; Palermi, G. L.; Travagli, V.; Alhaique, F. *J. Soc. Cosme. Chem.* **1994**, 45, 167-172.
21. Manosroi, A.; Wongtrakul, P.; Manosroi, J.; Sakai, H.; Sugawara, F.; Yuasa, M.; A. M. *Colloids and Surfaces B: Biointerfaces* **2003**, 30, 129-138.
22. Fan, X. J.; Liu, Q.; Zhen, P.; Zhang, Y.; Hu, X. *Journal of Chinese Pharmaceutical Sciences* **2007**, 16, 96-100.
-

Effect of pH on Physicochemical Properties and Encapsulation Efficiency of PEGylated Linolenic Acid Vesicles

YIN YIN TEO*, MISNI MISRAN AND KAH HIN LOW

Department of Chemistry, Faculty of Science,
University Malaya 50603 Kuala Lumpur, Malaysia
yinyinteo@um.edu.my

Received 29 September 2011; Accepted 9 November 2011

Abstract: The preparation of vesicle from a mixture of linolenic acid and 1,2-dipalmitoyl-*sn*-glycerol-3-phosphoethanolamine-N-[methoxy-(polyethylene glycol)-2000] (DPPE-PEG2000) has been successfully carried out by using dry lipid hydration method. The effect of pH on particle size, zeta potential, encapsulation efficiency and critical vesiculation concentration (CVC) of the prepared vesicle suspensions in aqueous were studied. Macroscopic stability of the vesicles was also evaluated through their particle size and zeta potential for a period of 30 days. We found that CVC vary according to the pH, with higher pH of the bulk solution, CVC is higher. Vesicles formed at pH 8.5 were the most stable suspension throughout a period of 30 days compared to those at pH 7.5 and pH 9.0. Addition of DPPE-PEG2000 into the preparation of vesicle at pH 8.5 caused a reduction of the vesicle size to the scale of nanometer which is an advantage to their application. On the other hand, encapsulation of calcein and vitamin E were carried out. Certain amount of these compounds could be successfully loaded into the resulting liposomes under this experimental condition.

Keywords: linolenic acid, Vesicle, pH, DPPE-PEG2000.

Introduction

Vesicles are bilayer spherical aggregates of amphiphilic molecules with the basic matters are commonly consisting of a hydrophilic head group and double hydrocarbon tailed such as phospholipid. Vesicles have long been used as a tool for the delivery of vaccines, enzymes and drugs in the body because it can direct a drug to the target. At the same time vesicles also act as a reservoir in release of the drug at a slower rate. Therefore healthy cells are shielded from the drug's toxicity, especially at the vulnerable tissues such as kidneys and liver. In addition, vesicles are biocompatible, low risk of toxicity, commercially available and the preparation methods are not too complicated¹.

Amphiphiles with single hydrocarbon tail such as fatty acids have also been used to prepared vesicles. Oleate-oleic acid vesicles were the first single chain fatty acid vesicle

successfully prepared by Gebicki and Hicks in 1973^{2,3}. Later, vesicles were also prepared from polyunsaturated fatty acid such as linoleic acid (*cis,cis*-9,12-octadecadienoic acid)^{4,5} and *cis*-4,7,10,13,16,19-docosahexaenoic acid⁶. Besides, short chain saturated fatty acids such as octanoic acid and decanoic acid⁷ have also been reported to form vesicles successfully.

Fatty acids are selected instead of phospholipids because they are less expensive, easily hydrolyzed, simple molecular structure and present in the membrane naturally. However, the formation of fatty acid vesicles is restricted to certain range of pH, type of ionic composition in the buffer solution and concentration of the fatty acid⁸. For a solution at pH approximately to the pKa of the fatty acid, concentration ratio of the ionized to non-ionized fatty acid molecules are ≈ 1 . Hence, pseudo-double-chain surfactant can be formed through hydrogen bonding where a proton from the non-ionized carboxylic acid is shared by the adjacent ionized carboxylated molecule that has the appropriate geometry to induce the formation of bilayer and hence vesicle.

Nevertheless, fatty acid vesicles encounter a challenge like other colloidal system which is stability. They are facing trouble on retain their physical particle size with no agglomeration or flocculation during time of storage. Environment of the fatty acid dispersing medium such as pH and ionic concentration play an important role in maintaining the stability of vesicle suspension. Hence, lots of works have been carried out in order to improve the stability of vesicles suspension.

One of the successful works that enhanced the stability of fatty acid vesicle was by extending the pH range of vesicle formation. In order to form vesicle in a more acidic region, addition of amphiphilic molecule with headgroup of sulphonate, sulphate or oligo(ethylene oxide) unit intercalated between the hydrocarbon chain and the carboxylate were found to be effective⁹. On the other hand, addition of long chain linear alcohol has successfully shifted the pH for vesicle formation towards alkaline region¹⁰. To our knowledge, no literature work has been reported regarding the effect of pH on PEGylated fatty acid vesicle solution. Although fatty acid vesicles can be formed in a narrow range of pH, evaluation on the physicochemical properties of the vesicles within that range of pH are still not clear. It is vital to open a new path way of application with additional information about the changes occurred as the pH change slightly although still within the pH range for vesicle formation. Another alternative that has been proven to enhance the stability of the vesicle is through steric stabilization by modifying the surface of the vesicle¹¹⁻¹³. In this regard, a bulky hydrophilic head group is introduced to the vesicle. This can be done by incorporation of either natural or synthetic substances such as glycolipid, glycoprotein, polysaccharides, lectins and synthetic polymer. Nevertheless, less attention has been paid to the relevancy of synthetic polymer in stabilization of the fatty acid vesicle.

In the present study, investigation of pH effect on the stability of linolenate-linolenic acid vesicle was carried out through evaluation of the data from particle size and zeta potential over a storage period of 30 days. Furthermore, synthetic polymer covalently bonded to phospholipid; 1,2-dipalmitoyl-*sn*-glycerol-3-phosphoethanolamine-*N*-[methoxy (polyethylene glycol)-2000] (DPPE-PEG2000) was added to the formation of vesicle and the effect of this substance with respect to pH on the physicochemical properties of vesicle was also studied. The efficiency of vesicle to encapsulate water soluble and water insoluble materials will also be explored.

Experimental

Alpha-linolenic acid (*cis,cis,cis*- 9, 12, 15- octadecatrienoic acid) was from Sigma (St. Louis, USA) with purity $\geq 99.0\%$, 1,2-dipalmitoyl-*sn*-glycerol-3-phosphoethanol-

amine-N-[methoxy(polyethylene glycol)-2000] (DPPE-PEG2000) sodium salt was purchased from Avanti polar lipids (Alabaster, AL), boric acid with minimum 99.5% was from Fluka (Buchs, Switzerland), hydrochloric acid, sodium hydroxide 98 % and chloroform (distilled) were from HMBG Chemicals, sodium dihydrogen phosphate dehydrate $\geq 99.0\%$ and disodium hydrogen phosphate $\geq 98\%$, DL- α -tocopherol acetate $\sim 98\%$ and calcein $\geq 93\%$ were from Fluka. All chemicals were used as received. Deionized water with resistivity $18.2 \text{ M}\Omega \text{ cm}$ was obtained from Barnstead NANOpure[®] Diamond[™] ultrapure water system. Deionised water was doubly distilled and deaerated with dried nitrogen gas prior to use.

Investigation of the effect of pH on vesicles' size and zeta potential

Preparation of stock solution

A stock solution of 12.5 mM alpha-linolenic acid in 27.5 mM NaOH was prepared by mixing both chemicals. The solution was stirred until a transparent solution was obtained. Stock solution of alpha-linolenic acid containing DPPE-PEG2000 was prepared by first dissolving 12.5 mM alpha-linolenic acid and 0.25 mM DPPE-PEG2000 in 2 ml Chloroform. The mixture was then placed into a rotary evaporator at 40 °C to remove all of the chloroform. Warm distilled water at 50 °C and 27.5 mM NaOH solution were slowly added. The solution was then sonicated for 5 minutes.

Acid-base titration of the stock solution with HCl (0.125 M)

A stock solution of 1.500 mL was pipetted into a 14.5 ml sample vial followed by addition of $(1.500 - x)$ mL deionised water and x mL HCl (0.125 M). The solution was mixed for 1 minute by vortex mixer Uzusio VTX 3000L then the pH of the solution was measured by a Mettler Toledo pH meter. Calibration was performed at the titration temperature with buffer of pH 4.0, 7.0 and 9.2. An average of 3 measurements was carried out. A similar procedure was repeated for alpha-linolenic acid containing DPPE-PEG2000.

Light microscopy observation

The formations of vesicle in the solutions were observed with LEICA DMRXP Germany made light polarizing microscope. Images were focused by bright field and dark field mode between cross polarizers using oil immersion technique. This system consists of a high voltage beam source, a polarizing unit and a detector unit. The detector unit is interface with a personal computer equipped with image analysis software (Leica Qwin Standard version 2.6) that helps capture and import images from the microscope.

Transmission electron microscopy

The vesicle images at 40 mM were obtained by using Hitachi H-7100 transmission electron microscope with the negative-staining method. The sample was prepared by immersed the formvar-coated copper grid into a drop of the vesicle solution and allowed to stand for 10 minutes. The excess vesicle solution was blotted with filter paper and followed by staining process with 3% phosphotungstic acid. The grid was allowed to stand for another 10 minutes and air dried. The specimens were viewed and photographed with a transmission electron microscope operating at accelerating voltage 100 kV.

Particle size and zeta potential measurement

The hydrodynamic size and zeta potential of the vesicles with various pHs were determined by dynamic light scattering (DLS) Malvern particle size analyzer, Model Nano ZS (Worcestershire, UK). All particle size and zeta potential measurements were made at the scattering angle of 175° and 17°, respectively. The measurements were carried out at

temperature of 30 °C. The mean value is obtained from three measurements. Similar method was applied on the evaluation of vesicles' stability.

Determinations of CVCs for alpha-linolenic acid solutions

A series of solutions with various concentration of alpha-linolenic acid at pH 7.5, pH 8.5 and pH 9.0 were prepared. Borate buffer pH 8.5 or pH 9.0 of 50 mM after make up to the volume was added to the solution at desired pH. Similarly, 50 mM of phosphate buffer pH 7.5 was used to prepare vesicle solution of pH 7.5. The solutions were then filtered by use of a 0.45 µm nylon filter from (Minisart®) prior to measurements. PEGylated vesicle solutions of alpha-linolenic acid containing DPPE-PEG2000 were prepared by the similar procedure. The CVC determinations were carried out at 30 °C employing du Nouÿ ring tensiometer balance from KRUSS with K12 tensiometer processor.

Evaluation of stability

Vesicle solutions with concentration of 2 mM at pH 7.5, pH 8.5 and pH 9.0 were prepared as mentioned in the determination of CVC and stored at 28 °C for a period of 30 days. Measurement of particle size and zeta potential for the vesicle solutions were carried out by using the similar method as stated above during that period of time.

Encapsulation of calcein and vitamin E

A mixture of 25 mM fatty acid and 0.5 mM calcein in chloroform was dried under a rotor evaporator at 40 °C. Similarly, the PEGylated vesicle was prepared in the same manner but this time 0.5 mM of DPPE-PEG2000 was added. Warmed deionized water at 50 °C was then slowly added to the dried lipid followed by addition of buffer solution at the desired pH with make up final concentration of 50 mM. The solution was then placed in a bath sonicator (JAC Ultrasonic 1505) at 30 °C for 5 minutes. Similar method was applied for the encapsulation of vitamin E. The encapsulated and non-encapsulated substances were separated by using mini-column method¹⁴. Pretreatment of Sepharose 4B with mobile phase for swelling purpose was used as a stationery phase. A small piece of cotton was placed at the bottom of the barrel of a 5 mL plastic syringe prior to packing with Sepharose 4B in order to prevent leakage of sepharose 4B. Then the column was inserted into a centrifugal tube so that it was securely supported at the top of the test tube by the finger grips of the syringe. A volume of 50 µL vesicle solution containing entrapped and free solute was applied to the Sepharose 4B bed followed by 3 × 0.5 mL of mobile phase. The column was spun at knob 4 for 2 minutes in an MSE centrifuge with swinging buckets. The first separation that comes out into the centrifugal tube was the encapsulated vesicle solution that latter was diluted to 5 mL with distilled ethanol. The remaining solute retained by the Sepharose was recovered by washing the column with the mobile phase and eluted by centrifugation at the similar speed for three times followed by dilution to 10 mL with distilled ethanol. Both solutions of encapsulated and non-encapsulated vitamin E were then analyzed using Shimadzu LC-20AT High Performance Liquid Chromatography coupled with SPD-20A prominence UV/Vis Detector. The isocratic mobile phase system composed mixture of all HPLC grade solvents; ethanol/methanol/acetonitrile (45:45:10 by volume) was delivered to the column at a flow rate of 1 mL min⁻¹. A sample of 20 µL was injected into the C18 reverse phase Purospher® Star column with dimension 4.6 mm × 250 mm and the particle diameter of 5 µm. The eluent was monitored at 287 nm, and the detector temperature was set at 25 °C. Analysis of calcein concentration was carried out by Cary 50 UV-Vis Spectrophotometer at 496 nm. The encapsulation efficiency was calculated from the percentage value of absorbance for encapsulated calcein at 496 nm or the area under peak at retention time 9.2 min for encapsulated vitamin E over the absorbance or area for total amount of solute.

Results and Discussion

The equilibrium titration curve of linolenic acid and PEGylated-linolenic acid as a function concentration HCl added is illustrated in Figure 1. A transparent solution composes of all ionized fatty acid molecules were observed at pH above 9.5. Further addition of HCl into the alkaline solution resulted in protonation of some anionic linolenate molecules. Hence, addition of HCl may increases the amount of non-ionized fatty acid molecules. The coexistence of ionized and non-ionized molecules in the solution leads to the formation of pseudo-double-chain surfactant between the head groups of COO^- and COOH via hydrogen bond. From our studies, linolenic acid is found to form vesicles in the pH range of solution from 7.5 to 9.0. As can be seen from figure 1, the pH of mixed fatty acid and DPPE-PEG2000 is lower compared to solution with only fatty acid. The presence of DPPE-PEG2000 with a long hydrophilic polyethylene glycol head group moiety would coat around the surface of spherical vesicle and hence promotes steric stabilization to the vesicles. It has also been agreed that PEG promotes the formation of vesicle and inhibits the aggregation of the vesicle through the long ethoxylate hydrophilic chains that extended out to at least 5 nm from the surface of bilayer^{15,16}. This hydrophilic chain also plays a role in shielding the ionized fatty acid molecules from react with proton. As a result, concentration of free proton in the bulk solution is normally higher, therefore the pH is lowered.

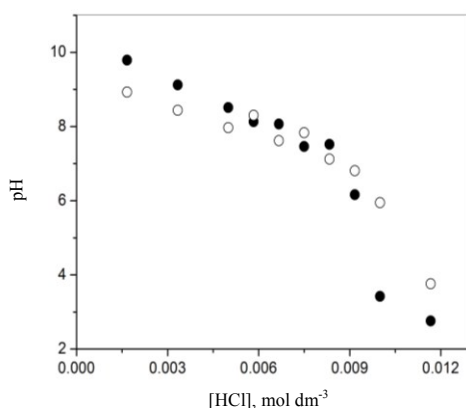


Figure 1. Equilibrium titration curve of linolenic acid (●) 12.5 mM and PEGylated linolenic acid (○) 12.5 mM at 28 °C as a function concentration HCl.

The mean particle size and zeta potential for both linolenate-linolenic acid vesicles and PEGylated linolenate-linolenic acid vesicles at pH range from 3.5 to 10.0 were displayed in figure 2 and figure 3, respectively. Both of the figures show a drastic change in particle size and zeta potential values at the pH region about 7.5 to 9.0. The addition of DPPE-PEG2000 into linolenic acid promotes the formation of smaller size vesicles. Furthermore, the magnitude of zeta potential for mixture of DPPE-PEG2000-linolenate-linolenic acid vesicles was also significantly smaller than those of linolenate-linolenic acid vesicle solution.

A plausible explanation for the formation of smaller size vesicle with incorporation of DPPE-PEG2000 is due to the presence of long PEG chain that is more dynamic in an aqueous solution¹⁷. As a result, the effective head group area is larger with addition of DPPE-PEG2000 that lead to a smaller value of packing parameter compared to the packing parameter in vesicle composing only linolenate-linolenic acid. A smaller value of packing parameter that still within the value greater than 0.5 but smaller than 1 may favors the formation of particles with higher curvature which promote the molecules to pack tightly.

Therefore, particle size for PEGylated linolenate-linolenic acid vesicle is smaller compared to linolenate-linolenic acid vesicles. This observation supports the theory of successful insertion of DPPE-PEG2000 into the bilayer of vesicle.

A further confirmation on insertion of DPPE-PEG2000 into the membrane bilayer was revealed from the measurement of zeta potential as indicated in Figure 3. The decrease in magnitude of zeta potential is due to the presence of long ethoxylate polymer chain in DPPE-PEG2000 that coated around the surface of vesicles and hidden the negatively charge underneath the polymer layer. As a consequence, the mobility of the vesicles was reduced and the zeta potential becomes less negative.

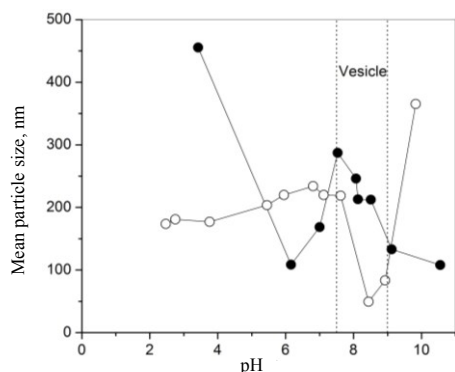


Figure 2. Mean particle size of 12.5 mM linolenic acid (●) and 12.5 mM PEGylated linolenic acid (○) at various pH.

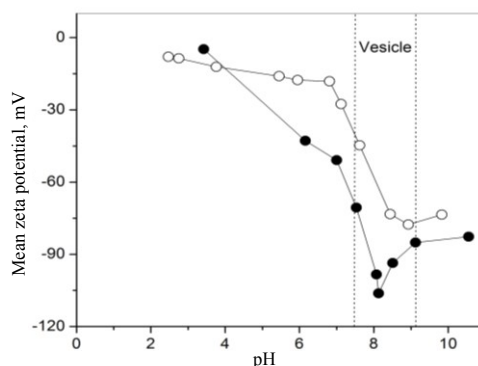


Figure 3. Mean zeta potential of 12.5 mM linolenic acid (●) and 12.5 mM PEGylated linolenic acid (○) at various pH.

The presence of vesicle was authenticated by appearance of cross-maltese images that showing the lamellar structure of the spherical vesicle suspension using light polarizing micrograph. In fact, Figure 4 confirmed the formation of vesicles at pH 7.5, 8.5 and 9.0.

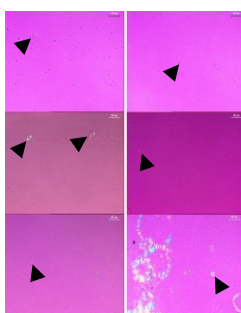


Figure 4. Polarizing micrograph of (1) linolenate-linolenic acid vesicle and (2) PEGylated linolenate-linolenic acid vesicle at pH (A) 7.5, (B) 8.5 and (C) 9.0.

In this regard, the minimal concentration of linolenic acid required to form stable membrane bilayer which is known as critical vesiculation concentration (CVC) was also determined via surface tension method. As indicated in Table 1, CVC of linolenic acid and PEGylated linolenic acid at pH 7.5 is the lowest with assumption that emulsion was not

formed. The formation of fatty acid vesicle is dominated as the ionized carboxylate and non-ionized carboxylic are co-exist. As mentioned elsewhere, pKa of linolenic acid is 8.28¹⁸. Therefore, at pH approximately 8.28, concentration of linolenate and linolenic acid are almost equimolar and the formations of pseudo-double-chain surfactant via hydrogen bonds that can be analogue to phospholipid are encouraged. Thus, it leads to engender of bilayer vesicle. However, at the pH higher than pKa, CVC of the solution is the highest due to considerable increase amount of linolenate monomer in the solution. Thus at pH 9.0, the overall hydrophilicity in the solution is higher that results in a weaker driving force for self aggregation. As a consequence, higher amount of non-ionized linolenic acid is required and resulting in a higher CVC. In contrary, despite the amount of linolenate anion is less at pH 7.5, the concentration of linolenic acid is sufficient for vesicle formation through the hydrophobic interactions and hydrogen bonds. Similar trend was found for linolenic acid with incorporation of DPPE-PEG2000 where we observed CVC raised as pH increased. Yet, CVC for the solution of linolenate-linolenic acid with incorporation of DPPE-PEG2000 is found significantly different compared to the pure linolenate-linolenic acid solution. The result indicates that at pH 8.5 and pH 9.0, addition of DPPE-PEG2000 to linolenic acid increased the CVCs. In general, DPPE-PEG2000 with negatively charge causes an additional concentration of anion in the solution. Therefore, at pH 8.5 and pH 9.0, concentration of anion in the solution is higher compared to the non-ionized linolenic acid. In order to achieve the formation of vesicle, much more non-ionized linolenic acid molecule is required and this leads to an increase in CVC. In other words, addition of DPPE-PEG2000 destabilized the formation of bilayer at pH 8.5 and pH 9.0. In contrast, CVC for linolenic acid-DPPE-PEG2000 solution at pH 7.5 is lower than CVC of linolenic acid. This can be explained by lower amount of linolenate anion is required due to the availability of anionic DPPE-PEG2000. The results obtained here are consistent with the findings reported by Charles *et. al.*. They found that formation of nonanoate-nonanoic acid vesicle was stabilized by addition of nonanol and reported a lower CVC (20 mM) compared to vesicle prepared from only nonanoic acid (85 mM)¹⁰.

Table 1. Critical vesiculation concentration (CVC) of linolenate-linolenic acid vesicle and PEGylated linolenate-linolenic vesicle at various pH.

pH	Critical vesiculation concentration, mM	
	Linolenic acid	DPPE-PEG2000-linolenic acid
7.5	0.24	0.15
8.5	0.88	0.91
9.0	1.23	1.48

A colloidal system is considered stable if the particles do not aggregate into clusters at a significant rate. As illustrated from Figure 5, mean particle size of linolenate-linolenic acid vesicles and vesicles consist of DPPE-PEG2000 at pH 7.5 increase gradually. The plausible explanation for this is due to the hydrophobic nature of the non-ionized linolenic acid. In contrast, it is observed from figure 6 that zeta potential becomes less negative for PEGylated vesicle with time. This phenomenon implicates the aggregation of vesicles which lead to slower mobility and thus the magnitude of zeta potential. Similarly, vesicles formed at pH 9.0 from both pure linolenic acid and PEGylated lipid mixed with linolenic acid only manage to maintain their particle size for about 7 days. This is also revealed by a decrease in magnitude of the zeta potential. An important feature discovered from these results is DPPE-PEG2000 did not play a significant role in stabilization of the vesicle suspension at pH 7.5 and pH 9.0 as expected.

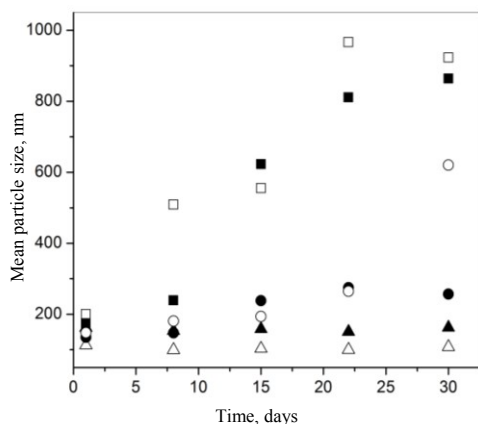


Figure 5. Mean particle size at pH 7.5 (■, □), 8.5 (▲, △) and 9 (●, ○) of linolenate -linolenic acid vesicle (filled symbol) and PEGylated linolenate-linolenic acid vesicle (empty symbol).

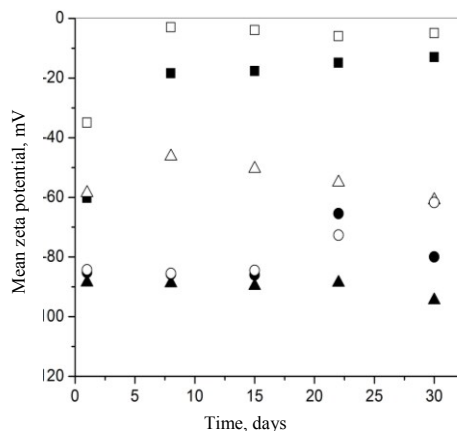


Figure 6. Mean zeta potential at pH 7.5 (■, □), 8.5 (▲, △) and 9 (●, ○) of linolenate -linolenic acid vesicle (filled symbol) and PEGylated linolenate-linolenic acid vesicle (empty symbol).

On the other hand, our results suggested that the most stable vesicle suspension can be formed at pH 8.5 as their mean vesicle size and zeta potential were almost consistent regardless the incorporation of DPPE-PEG2000. Nevertheless, it is observed that vesicles incorporated with DPPE-PEG2000 were smaller with particle size around 100 nm at pH 8.5. This might be due to the presence of bulky hydrophilic PEG chain at the bilayer surface promoting the molecules to pack tightly with higher curvature. Therefore, this has proven the effectiveness of DPPE-PEG2000 participates in the formation of vesicles as to enhance the stabilization of vesicle suspension in an aqueous solution. An additional transmission electron micrograph for linolenic acid and PEGylated linolenic acid at pH 8.5 were shown in Figure 7.

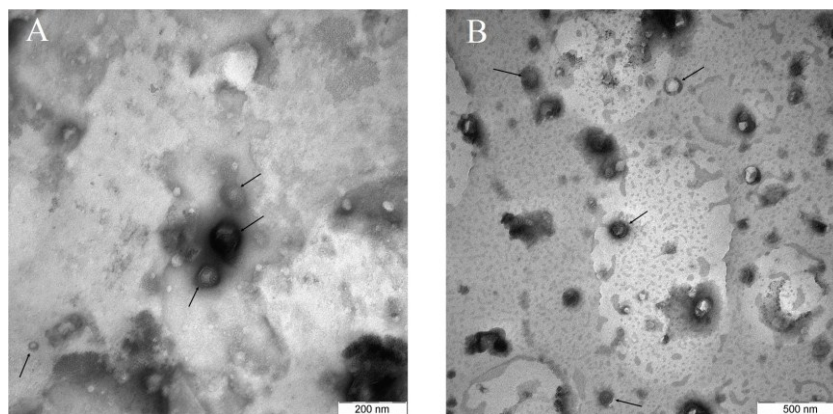


Figure 7. TEM micrograph of 40 mM linolenate-linolenic acid vesicle (A) and PEGylated linolenate-linolenic acid vesicle (B) at pH 8.5. The presences of vesicles are indicated by the arrow.

Since the stability of the vesicle has been identified, encapsulation of water soluble and water insoluble materials such as calcein for former and vitamin E for latter were also studied. From table 2, it is found that the encapsulation efficiency of vitamin E in the vesicle is at least 10-fold higher than the encapsulation efficiency of calcein under our experimental condition. One of the plausible explanations for this observation is due to hydrophobicity nature of vitamin E which shows higher preferences to be embedded in the membrane bilayer. In contrary, calcein is water soluble especially at high pH, so they have a higher tendency of escaping in to the bulk solution during the process of bilayer convolution. As a result, the entrapped calcein that attribute to the percent of loading may be either from calcein entrapped at the hydrophilic layer of the membrane or those within the multilamellar structure. This explains the low percentage of calcein encapsulation by the vesicles. Similar reason also applicable to the vesicles with insertion of DPPE-PEG2000.

As the pH increase, the encapsulation of vitamin E decrease. This could be due to higher surface polarity and stronger electron density at the head group that inhibit permeation of vitamin E into the membrane. On the other hand, the encapsulation efficiency of vitamin E in PEGylated vesicle was found lower than linolenic acid that probably due to their smaller particle size. In addition, another possible explanation is the number of lamellae is reduced with incorporation of PEG as reported by Belsito *et al.*¹⁹. Therefore, limited amount of vitamin E can be loaded into to bilayer.

Table 2. Percentage encapsulation efficiency of linolenate-linolenic acid vesicle and PEGylated linolenate-linolenic acid vesicle at pH 7.5, 8.5 and 9.0.

pH	% Encapsulation Efficiency			
	Vitamin E		Calcein	
	Linolenate-linolenic acid vesicle	PEGylated linolenate-linolenic acid vesicle	Linolenate-linolenic acid vesicle	PEGylated linolenate-linolenic acid vesicle
7.5	83±5	65±5	0.3±0.1	0.9±0.4
8.5	55±6	39±6	3.4±0.5	3.0±0.8
9.0	45±4	32±6	2.3±0.3	2.5±0.9

Conclusion

Physico-chemical properties of linolenate-linolenic acid vesicle can be altered by pH and/or addition of DPPE-PEG2000. Although vesicles can only be formed at a narrow range of pH as reported elsewhere, their physico-chemical properties deviate significantly in that region. In general, CVC vary according to the pH, higher pH associated with higher CVC and vice versa. In this study, vesicles formed at pH 8.5 are the most stable suspension regardless the incorporation of DPPE-PEG2000. The incorporation of DPPE-PEG2000 in the preparation of vesicles at pH 8.5 promotes the formation of nano size particles that broaden their field of application. Moreover, the encapsulation efficiencies of calcein and vitamin E display encouraging values.

Acknowledgment

This research work was supported by the Ministry of Science, Technology and Innovation Malaysia (MOSTI) under the eScienceFund 03-01-03-SF0316 and Postgraduate Research Grant (PPP) P0267-2007A from University Malaya.

References

1. Gregoriadis G, Liposome Technology; 2nd Ed., Vol 1; CRC Press: Boca Raton Florida United States, 1993, 2.
2. Hargreaves W R and Deamer D W, *Biochem.*, 1978, **17**, 3759.
3. Gebicki J M and Hicks M, *Nature*, 1973, **243**, 232.
4. Gebicki J M and Hicks M, *Chem Phys Lipids.*, 1976, **16**, 142.
5. Rogerson M L, Robinson B H, Bucak S and Walde P, *Colloids Surfaces B: Biointerfaces.*, 2006, **48**, 24.
6. Namani T, Ishikawa T, Morigaki K and Walde P, *Colloids Surfaces B: Biointerfaces.*, 2007, **54(1)**, 118.
7. Namani T and Walde P, *Langmuir.*, 2005, **21**, 6210.
8. Haines T H, *Proc Natl Acad Sci U.S.A.*, 1983, **80**, 160.
9. Renoncourt A, Bauduin P, Nicholl E, Touraud D, Verbavatz J M and Dubois M, *Chem Phys Chem.*, 2006, **7**, 1892.
10. Apel C L, Deamer D W and Mautner M N, *Biochimica et Biophysica Acta*, 2002, **1559**, 1.
11. Kohno S, Miyazaki T, Yamaguchi K, Tanaka H, Hayashi T, Hirota M, Saito A, Hara K, Sato T and Sunamoto J, *J Bioact Compat Polym.*, 1988, **3**, 137.
12. Liautard J P, Vidal M and Philipott J R, *Cell Biol Int Rep.*, 1985, **2**, 1123.
13. Blume G and Cevc G, *Biochim Biophys Acta*, 1993, **1146**, 157.
14. Fry D W, White J C, Goldman I D, *Anall Biochem.*, 1978, **90**, 809.
15. Needham D, McIntosh T J and Lasic D D, *Biochim Biophys Acta*, 1992, **1108(1)**, 40.
16. Bedu-Addo F K and Huang L, *Adv Drug Deliv Rev.*, 1995, **16**, 235.
17. Xu H, Deng Y H, Chen D W, Hong W W, Lu Y and Dong X H, *J Controlled Release.*, 2008, **130**, 238.
18. Kanicky J R, Shah D O, *J Colloid Interface Sci.*, 2002, **256(1)**, 201.
19. Belsito S, Bartucci R and Sportelli L, *Biophys Chem.*, 2001, **93**, 11.